NSF/RA-800215

CALIFORNIA INSTITUTE OF TECHNOLOGY

EARTHQUAKE ENGINEERING RESEARCH LABORATORY

FULL-SCALE EXPERIMENTAL INVESTIGATION OF A MODERN EARTH DAM

BY

A. M. ABDEL-GHAFFAR, R. F. SCOTT

AND M. J. CRAIG

REPORT NO. EERL 80-02

A Report on Research Conducted under Grants from the National Science Foundation and the Earthquake Research Affiliates Program at the California Institute of Technology

PASADENA, CALIFORNIA

FEBRUARY, 1980

EAS INFORMATION RESOURCES
NATIONAL SCIENCE FOUNDATION

This report is based on research conducted under Grant No. PFR77-23687 from the National Science Foundation with support from the Earthquake Research Affiliates of the California Institute of Technology. Any opinions, findings, and conclusions or recommendations expressed in this publication are those of the authors and do not necessarily reflect the views of the National Science Foundation.

50272-101

REPORT DOCUMENTATION PAGE	1. REPORT NO. NSF/RA-800215	2.	3. Recipient's Accession No. PB81 123788
4. Title and Subtitle: Full-Scale Experimental Investigation of a Modern Earth Dam			5. Report Date: February 1980 6.
7. Author(s): A. M. Abdel-Ghaffer, R. F. Scott, M. J. Craig			8. Performing Organization Rept. No. EERL-80-02
9. Performing Organization Name and Address: California Institute of Technology Earthquake Engineering Research Laboratory Pasadena, CA 91125			10. Project/Task/Work Unit No. 11. Contract(C) or Grant(G) No. (C) (G) PFR7723687
12. Sponsoring Organization Name and Address: Engineering and Applied Science (EAS) National Science Foundation 1800 G Street, N.W. Washington, D.C. 20550			13. Type of Report & Period Covered 14.

15. Supplementary Notes

16. Abstract (Limit: 200 words)

Extensive investigation of a modern earth dam's behavior during relatively intense shaking is reported. The study utilized records on full-scale dynamic tests recovered from the Santa Felicia Dam in Southern California. These records provided information on the dynamic characteristics of the dam which was instrumented with motion sensors. The project gathered experimental data used for testing and developing various analytical and numerical methods for computing the natural frequencies and mode shapes of dams and, particularly, for predicting earthquake response. Data on the dam's responses indicate the following: Analytical or finite models are needed to represent the prototype realistically in vertical and longitudinal directions and to include coupling of these directional motions; More than two sets of strong-motion instruments should be deployed on and in the vicinity of the structure to obtain reliable information on a dam's three-dimensional behavior during an earthquake. Suggestions are made for the appropriate location of instruments.

17. Document Analysis a. Descriptors

Earth dams
Earthquakes
Soil dynamics
Earth movements
Forecasting
Seismographs
Dynamic tests

b. Identifiers/Open-Ended Terms

Santa Felicia Dam
Southern California
Earthquake Hazards Mitigation

c. COSATI Field/Group

18. Availability Statement	19. Security Class (This Report)	21. No. of Pages
NTIS	20. Security Class (This Page)	22. Price

CALIFORNIA INSTITUTE OF TECHNOLOGY

EARTHQUAKE ENGINEERING RESEARCH LABORATORY

FULL-SCALE EXPERIMENTAL INVESTIGATION OF A MODERN EARTH DAM

by

Ahmed M. Abdel-Ghaffar
Assistant Professor
Civil Engineering Department
Princeton University

Ronald F. Scott
Professor of Civil Engineering
Division of Engineering & Applied Science
California Institute of Technology

Michael J. Craig
Research Engineer
Union Oil Company of California

Report No. EERL 80-02

A Report on Research Conducted under Grants from
the National Science Foundation and
the Earthquake Research Affiliates Program at
the California Institute of Technology

Pasadena, California

February, 1980

TABLE OF CONTENTS

TABLE OF CONTENTS (Cont'd.)

ABSTRACT

An extensive investigation has been made based on the results of full-scale dynamic tests performed on a modern earth dam, Santa Felicia Dam in Southern California. This dam was chosen for the experimental studies because it had been subjected to strong shaking during two earthquakes: the strong, 6.3 local Richter magnitude San Fernando earthquake of 1971, and a 1976 earthquake of magnitude 4.7. The records recovered from these two earthquakes provided usable information on the dynamic characteristics of the dam which was instrumented with motion sensors to yield data on the structural response as well as the input ground motion at the site.

In the test programs, various types of dynamic excitations were used including mechanical vibration, ambient vibration, hydrodynamically generated forces, and the two strong seismic ground motions; thus, the imposed dynamic forces varied greatly in their time-history characteristics, spatial distributions, and intensities. For the forced vibration tests, the dam was excited into resonance in the upstream-downstream direction and in the longitudinal direction by a coupled pair of mechanical vibration generators (200 feet apart) capable of producing force up to 10,000 lbs. Symmetric and antisymmetric vibrations were separated by synchronizing the two shakers to run in-phase and 180° out-of-phase, respectively, with the aid of control units. During the ambient vibration tests, the naturally occurring vibrations of the dam caused by strong wind and the spilling of the reservoir were measured. The test of dam response to hydrodynamic forces involved the use of pressure waves (to impinge upon the upstream face of the dam) originating from a controlled,

submerged release of gas under pressure in the reservoir water. During the dynamic tests, three-dimensional measurements of the motions of approximately 25 stations along the crest and seven stations on the downstream slope were recorded and then analyzed in both time and frequency domains. Modes of vibrations and associated natural frequencies as well as damping ratios were determined in the frequency range from 0.0 to 6.0 Hz. The reliability of the existing analytical techniques for earth dams, which are restricted to horizontal shear deformation in the upstream-downstream direction, was examined. Finally, in order to reveal any change in the dynamic properties of the dam, the dam's natural frequencies, mode shapes, dynamic shear moduli and damping factors (the latter two as functions of the induced strains) estimated from the measured responses to the two earthquakes were compared with those determined from the full-scale dynamic excitation tests.

I. INTRODUCTION

An extensive investigation has involved the results of full-scale dynamic tests performed on Santa Felicia Dam, a modern earth dam in Southern California. This dam was chosen for the experimental studies because it not only typifies many earth dams in seismic areas, but it also has been subjected to strong shaking during two earthquakes: the strong, 6.3 local Richter magnitude San Fernando earthquake of February 1971, and a 1976 (April) earthquake of local magnitude 4.7. During the earthquakes, the dam was instrumented with motion sensors which indicated its structural response as well as the input ground motion at the site. Thus the records recovered from these two earthquakes offered an unusual opportunity for analysis of a dam's behavior during relatively intense shaking by providing usable information on the dynamic characteristics of the dam such as natural frequencies, mode shapes, dynamic shear moduli and damping factors (the latter two as functions of the induced dynamic strains). The purpose of the full-scale experimental work was not to investigate Santa Felicia Dam itself, but rather to gather experimental data concerning its dynamic characteristics which could then be used to test and develop various analytical and numerical methods for computing the natural frequencies and mode shapes of dams in general, particularly for predicting earthquake responses. It was intended also to gather information about the amount of damping, at low levels of excitation, in an earth dam. For more details about the analyses of the dam's earthquake response during the two earthquakes, see Ref. 2.

In the test programs reported below, various types of relatively low level dynamic excitations were used including mechanical (or forced)

vibration, ambient vibration (unique in earth dam research), hydraulic actuator ("popper") forces, and the two strong seismic ground motions; thus, the imposed dynamic forces varied greatly in their time-history characteristics, spatial distributions, and intensities. For the forced vibration tests, the dam was excited into resonance in the upstream-downstream direction and in the longitudinal direction by a coupled pair of eccentric-mass vibration generators, located on the central part of the crest (200 ft apart) capable of producing force up to 10,000 lbs. Symmetric and antisymmetric vibrations were separated by synchronizing the two shakers to run in-phase and 180° out-of-phase, respectively, with the aid of control units.

During the ambient vibration tests, the naturally occurring vibrations of the dam caused by strong wind and the spilling of the reservoir were measured, The test of dam response to hydraulic actuator forces involved the use of pressure waves(hitting the upstream face of the dam) originating from a controlled, submerged release of gas under pressure into the reservoir water (popper tests). During the dynamic tests, three-dimensional measurements of the motions of twenty-five stations along the crest and seven stations on the downstream slope were recorded and then analyzed in both time and frequency domains. From these measurements, which are more extensive than in previous full-scale tests of this type (Refs. 4, 13, 14, 15 and 17), modes of vibrations and associated natural frequencies as well as damping ratios were determined in the frequency range from 0.0 to 6.0 Hz. It was possible to determine frequencies and mode shapes of about 14 upstream-downstream symmetric modes, 11 up-stream-downstream antisymmetric modes, and 18 longitudinal modes.

Full-scale experimentally determined dynamic characteristics are required both to improve the techniques by which such properties are calculated for purposes of analysis and design, and to permit interpretation of the measured response of earth dams in the event of a strong earthquake. In order to reveal any change in the dynamic properties of the dam due to the type of excitation, its dynamic characteristics estimated from the measured responses to the two earthquakes were compared with those determined from the full-scale tests. Also, the measured frequencies and modes of upstream-downstream vibrations resulting from the forced, ambient and popper vibration tests were compared with those predicted by some existing 2-D shear-beam theories. The results of these comparisons are presented in this report. As information on the dynamic characteristics of dams and their earthquake response accumulates, it should be possible to develop better procedures for determining the appropriate levels of earthquake loading for design.

In this study, shear strains and shear moduli were estimated from the full-scale tests and, in addition, were plotted along with those estimated from the earthquake response analysis. Then the combined results were interpolated and extrapolated to give informative material to both the earthquake and the geotechnical engineers. The same procedure was followed for damping versus shear strains at different levels.

The full-scale vibration tests are especially important to understanding the behavior of earth dams, because soil is a nonlinear, hysteretic, and widely varying substance. Measurement of the properties of the soil in a dam is extremely difficult: samples taken for laboratory measurements have necessarily been disturbed and may not reflect actual properties of the soil in place. Also, laboratory measurements on a soil sample of only

a fraction of a cubic foot may not reflect the soil properties throughout the structure. Studies of the total performance of full-scale structures like dams could enable engineers to determine which laboratory tests best reflect large-scale soil dynamics.

II. OBJECTIVES OF THE EXPERIMENTAL INVESTIGATION

The principal objectives of these field measurements on Santa Felicia Dam were:

1. To interpret the full-scale dynamic test results in terms of the structural performance under the two real seismic conditions.
2. To reveal any change in the dynamic characteristics of the dam by studying both the nonlinearity associated with various levels of response and modal coupling and interference. For example, from the forced vibration tests, where the level of displacements induced in the dam was low, the fundamental frequency of the upstream-downstream mode was found to be 1.635 Hz, while in the 1971 earthquake, which induced larger displacements, the fundamental frequency was found (by spectral analysis of the observed response) to be 1.45 Hz, lower than that of the tests. This type of behavior is representative of a softening dynamic system composed of soil.
3. To test and improve the existing earth dam analytical techniques which are restricted to horizontal shear deformation in the upstream-downstream direction, and to facilitate development of mathematical modelling intended to represent realistically the prototype behavior in both longitudinal and vertical directions.
4. To recommend improvements in the existing, low-strain, full-scale experimental techniques for use in future testing.
5. To enable improvement of seismic-resistant designs for earth dams, and thus provide adequate levels of safety for such important structures.

Finally, it is believed that these data sets obtained from the full-scale dynamic tests (including the two earthquake records) offer an unusual opportunity of learning in a general way about the dynamic response characteristics of earth dam structures.

III. DESCRIPTION OF THE DAM

Santa Felicia Dam (Fig. 1) is located on Piru Creek 65 km north-west of Los Angeles, It is owned by the United Water Conservation District of Ventura County and was completed in December 1955. The dam consists of a rolled-fill embankment, a low-level outlet works, and an ungated chute spillway. It is about 273 ft high above its lowest foundation and 200 ft above the original stream bed; it is 450 ft long across the valley at the base and approximately 1,275 ft long at the crest (Fig. 2). An impervious core of silty clays and clayey sands and gravels, with 0.33:1 slopes, is carried up from bedrock. Gravelly materials excavated from the core trench and those available from other excavations were placed on the upstream and downstream faces. The bedrock consists of sandstone strata of varying degrees of hardness interlayered with shale seams of varying thickness. The geological profile across the site was utilized to provide a sound, watertight and economical section and to assure a firm seal between the bedrock and the core throughout the dam's length. The impervious core and pervious shell materials are basically of an alluvial nature; the alluvium consists of clay, sand, gravel, and boulders. Table 1 indicates design values assumed to be representative of the typical soils as determined from field and laboratory testing before and during construction.

During the tests the reservoir was full, as shown in Fig. 3.

In 1967 the dam was equipped with two accelerographs which recorded the earthquakes of 1971 and 1976; one instrument was located at the central section of the crest and the other was placed at the right abutment on the downstream side. A more complete description of the dam and permanent strong-motion instrumentation is given in Ref. 2.

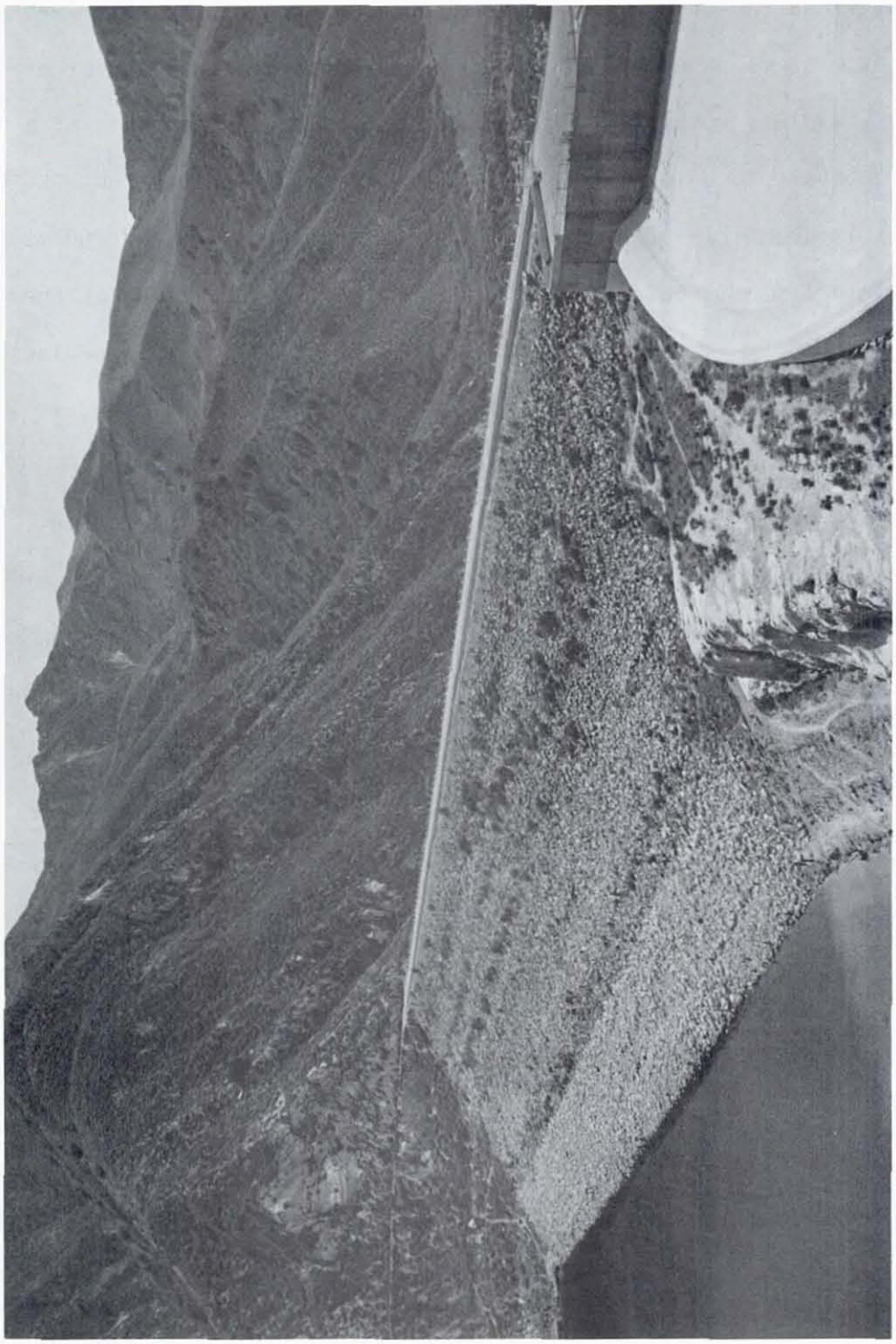

Fig. 1. General view showing the upstream side of Santa Felicia Dam and part of the spillway at the right (western) abutment (one week before the tests).

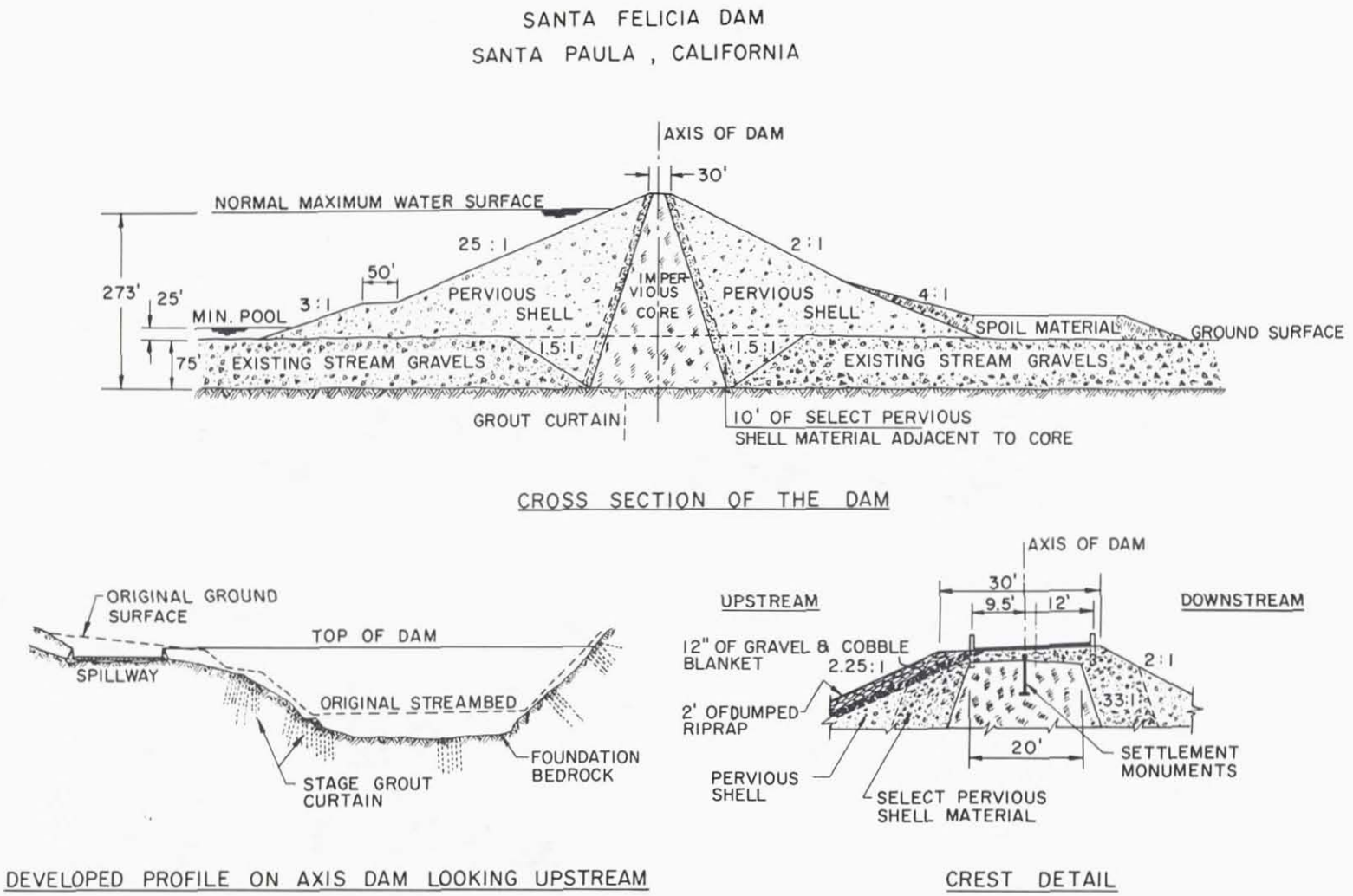

Fig. 2. Structural details of Santa Felicia Dam.

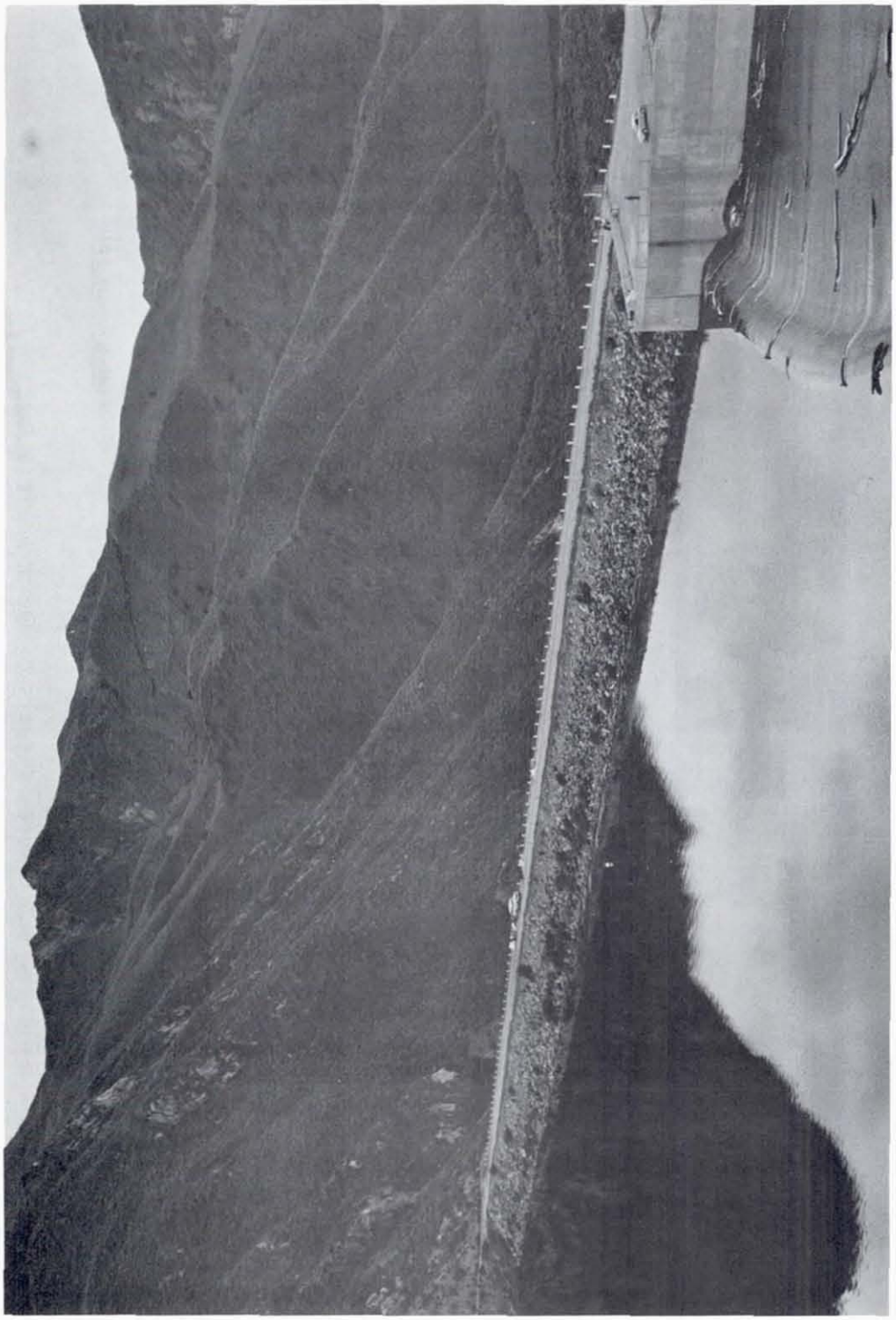

Fig. 3. General view showing the upstream side of Santa Felicia Dam during the tests. Reservoir is full and spilling. Test vehicle and equipment can be seen at the center of the crest.

Table 1

Characteristics of Santa Felicia Dam Materials (during construction)

(Ref. 2)

Property	Core	Shell	Foundation
Dry unit weight	114 pcf	125 pcf	116 pcf
Moist unit weight	131 pcf	131 pcf	122 pcf
Saturated unit weight	134 pcf	141 pcf	135 pcf
Submerged unit weight	73 pcf	79 pcf	73 pcf
Permeability	0.001 ft/day	20 ft/day	150 ft/day
Specific gravity	2.68	2.69	2.69

(Note: 1 ft = 0.305 m and 1 pcf (lb/ft^3) = 16.02 Kg/m^3)

IV. DESCRIPTION OF THE INSTRUMENTATION

The essential features of the instrumentation are substantially the same as those used in previous full-scale tests and have been described in detail in other reports (Refs. 6 to 13, and Ref. 15); only a brief summary is given here.

IV-1. Vibration Pick-ups (motion-sensing transducers)

The vibrations of the dam during forced, ambient, and popper tests were picked up by eight Kinemetrics SS-1 Range seismometers (velocity-type transducers with natural period close to one second) manufactured and supplied by Kinemetrics Inc. of Pasadena, California. Due to the difficulty of making absolute calibrations of the velocity-sensing Rangers in the field, they were used only to measure relative motion and phase between stations. Figure 4 shows three of the Range seismometers mounted on an aluminum plate in such a way that three orthogonal components of motion (upstream-downstream or U-D, longitudinal or L, and vertical or V) at any point on the crest could be measured.

IV-2. Recording Instruments

2-1. Signal Conditioners

Two four-channel Kinemetrics SC-1 signal conditioners were used during the tests to amplify, filter, and simultaneously control the eight outputs from the seismometers. Each channel of the signal conditioner is adjustable to provide displacement, velocity or acceleration outputs. The signal conditioners also provide optional low-pass filters which are continuously adjustable between 1.0 and 100.0 Hz. The power for the two signal conditioners was provided by a motor-driven electric generator

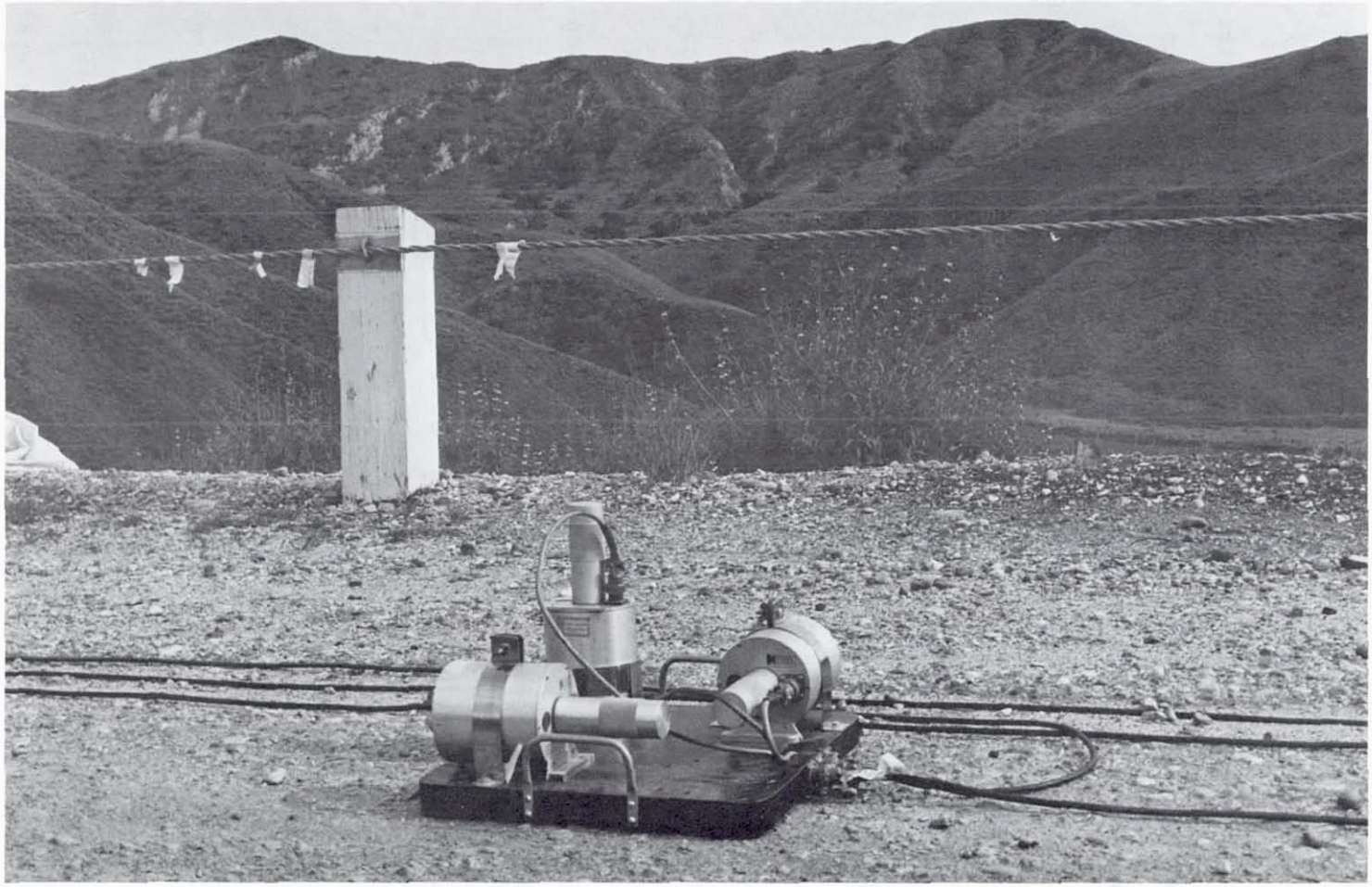

Fig. 4. Three Ranger seismometers mounted on an alunimum plate to measure upstream-downstream, longitudinal and vertical responses at one measurement station.

placed at the central region of the dam's crest (Fig. 5).

2-2. Oscillograph Recorder

The measurements taken during the dynamic tests were monitored on an eight-channel Hewlett-Packard 7418A oscillograph recorder. This enabled an immediate visual inspection of the vibrational motion at the seismometer locations to be made during each measurement. It was also used for calibrating the seismometers by monitoring their outputs and adjusting the attenuation of the signal conditioners.

2-3. Instrumentation Tape Recorders

During the tests, the amplified and filtered signals (sinusoidal and random) were recorded on two four-channel Hewlett-Packard 3960A instrumentation tape recorders. The electrical outputs of this type of recorder can be digitized for computer processing by means of an analog-digital converter. Figure 6 shows the recording instruments including (from left to right) the oscillograph recorder, the two signal conditioners, and the tape recorders.

IV-3. Shaking Machines (force generating systems)

A VG vibrational generating system (manufactured by Kinemetrics Inc.) having two mechanical shakers (described in Refs. 7, 8, 9, and 10) was used to excite the dam sinusoidally. The shakers were provided with a precise and stable control system, capable of imposing and holding a frequency in the range 0.0 to about 10.0 Hz within 0.1%.

Each machine comprises two counter-rotating (about a vertical axis), wedge-shaped baskets so arranged that they provide an oscillating lateral force (varying sinusoidally with time). The direction and magnitude of the periodic force can be selected by adjusting the baskets and their

Fig. 5. The electric generator used for instrument operation.

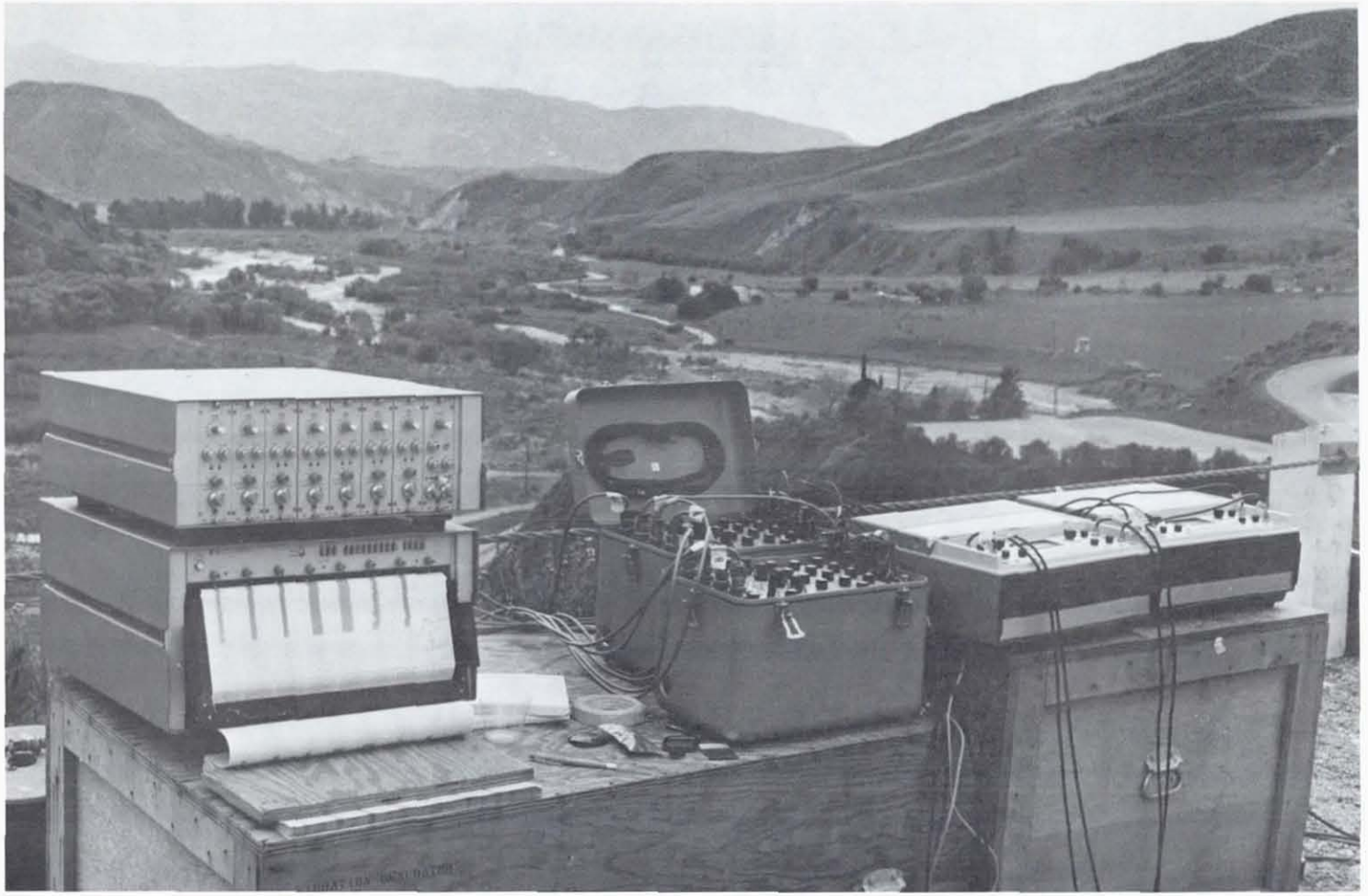

Fig. 6. The recording instruments: Oscillograph Recorder, two Signal Conditioners and two Tape Recorders.

lead weight contents. Since, in a particular test sequence, the frequency is changed at intervals to cover a certain range including a resonance peak or peaks, the actual force level, which depends on the square of the angular velocity, varies. The maximum frequency of about 9.5 Hertz is limited by the stress in the shakers. Consequently, for each interval of frequencies studied over the entire frequency range, different lead weights are placed in the basket, greater weights at the lower frequencies. In this way the force level is maintained relatively constant over the whole frequency range, although it varies in any one test sequence. Each shaker generates a peak force in the range 1000 to 5000 pounds, depending again on the lead weights used and the exciting frequency.

To couple the shaking machines to the dam, two reinforced concrete blocks (8' by 8' by 20" thick) were cast in place in excavated areas on the crest as shown in Figs. 7 and 8. The two blocks were 200 ft apart (each one about 100 ft from the crest midpoint) and were positioned slightly to one side of the center line of the crest to allow sufficient clearance for traffic on the crest. Although this arrangement was fairly satisfactory, there was still a substantially enhanced local displacement field in the vicinity of the machine and block (see "Experimental analysis and results"); better coupling would have been desirable. Also, it was not possible to form concrete foundations on other portions of the crest more amenable to the generation of nonsymmetrical mode shapes.

Finally, the two shakers ran simultaneously at the same frequency; they were synchronized to run in-phase (for symmetric vibration) and 180° out-of-phase (for antisymmetric vibration) with the aid of the control units. Figure 9 shows one of the two shakers mounted on its concrete

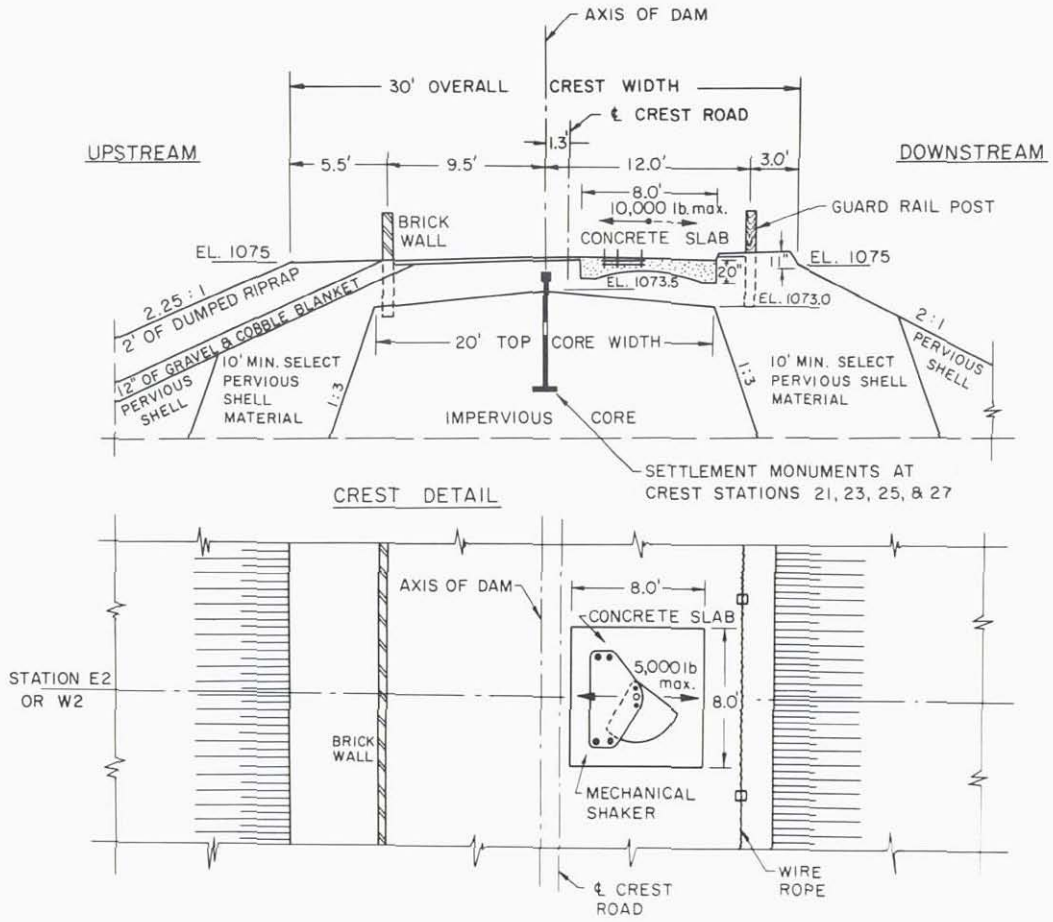

LOCATION OF MECHANICAL SHAKER AND ITS FOUNDATION SLAB ON THE CREST

Fig. 7

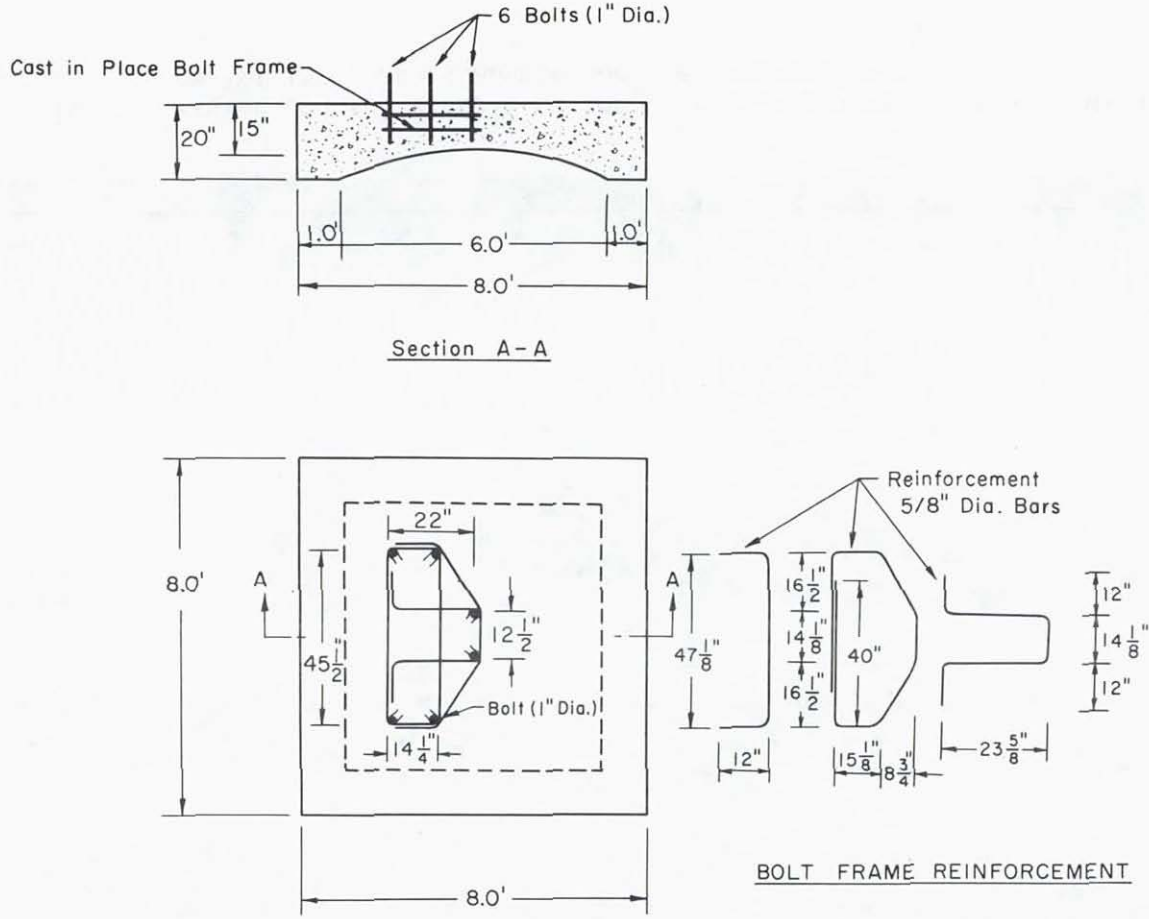

STRUCTURAL DETAILS OF THE CONCRETE SLAB

Fig. 8

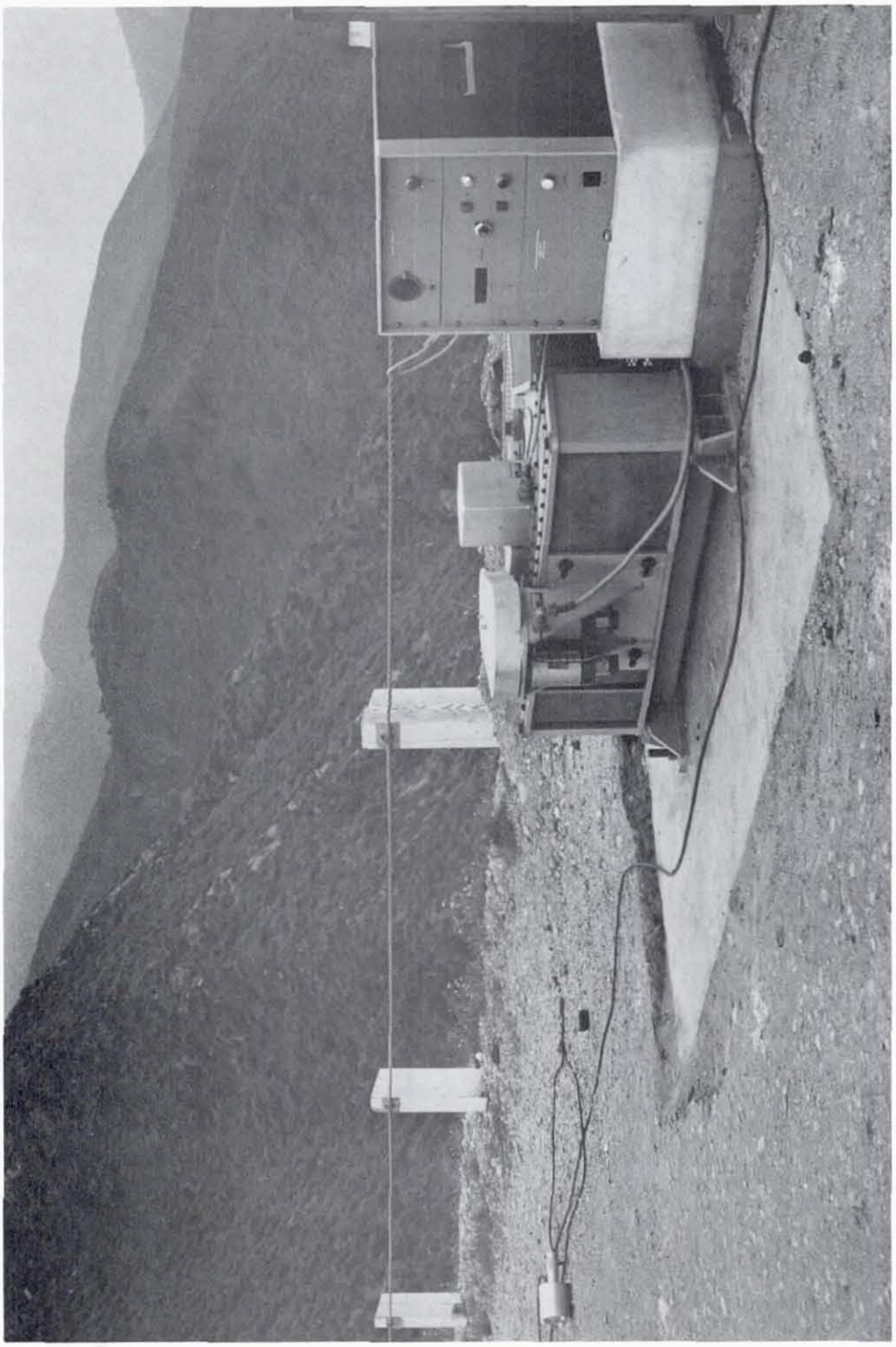

Fig. 9. Master control console of the vibration generating system with one of the shakers mounted on the concrete block.

block; it also shows the master control console of the vibration generating system.

IV-4. Data Processing Instruments

1. Electronic Analog-Digital Converter

The recorded tapes from all the tests (forced, ambient, and popper) were taken to the Caltech Vibration Laboratory where the recorded analog signals were digitized using the Kinemetrics DDS-1103 electronic analog-digital converter.

2. Digital Signal Processor

The phase information between different measurement stations for the forced, ambient and popper tests was obtained, in the Vibration Laboratory, by using a digital signal processor (model SD360 manufactured by Spectral Dynamics Corporation). The signal processor was used to calculate and display the Fourier transforms, the cross-correlation functions, and the cross-spectral functions of the digitized and recorded responses.

The SD360 is a hard-wired FFT (Fast Fourier Transform) analyzer that provides complete signal analysis from 0.01 to 150,000 Hz. It combines the capabilities of two real time spectrum analyzers, a transform function analyzer, analog signal conditioners, and a computer; it employs the FFT method for processing raw data signals into finalized information that can be reviewed and used immediately. The DSP conditions and analyzes two signals, correlates the mutual properties, and displays results in a broad variety of forms and formats. Instant selection is provided for 12 distinct data analyses, from simple signal averaging and single- or dual-channel FFT to transfer function analysis, correlation, cross-spectrum, coherence, and coherent output power.

Figure 10 shows the DSP, the digital converter, the oscillograph recorder and the two tape recorders during the data reduction in the Vibration Laboratory.

IV-5. The Popper Test Instruments

The popper test utilized, as the loading mechanism, pressure waves in the dam reservoir induced by single or low-frequency, multiple-pulse P-wave impingements on the upstream face (for more details see Ref. 16). This provides a small pressure over a large area of the dam so that a relatively large load is applied. The pressure waves (which vary approximately with the inverse of the distance) originated from a controlled submerged release of high pressure gas from a differential pressure piston-driven mechanism. This release of gas was accompanied by an audible thump. Figure 11 shows all the popper test instruments which were operated from a small boat in the reservoir. There were no dynamic pressure transducers mounted on the upstream face to measure the pressure (or the force) applied to the dam.

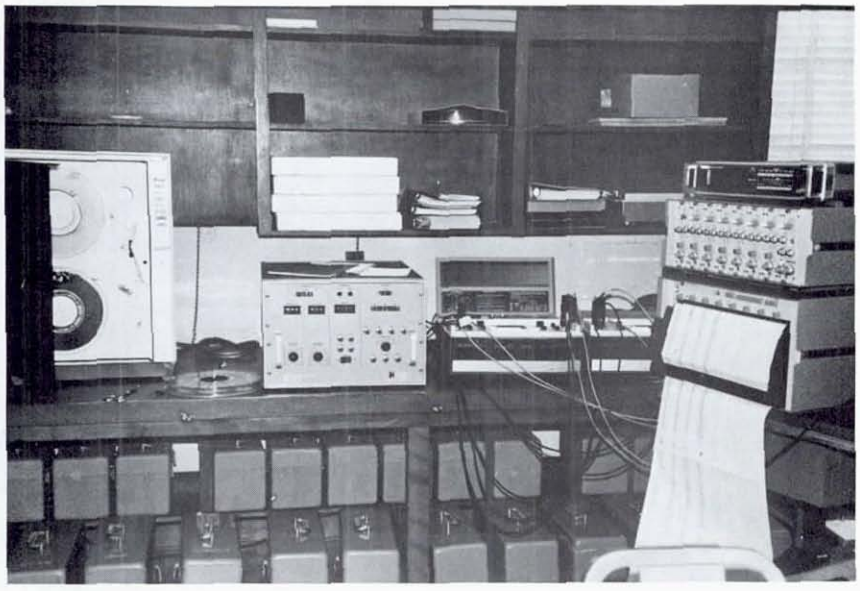

(a) Digitization of the recorded analog signals.

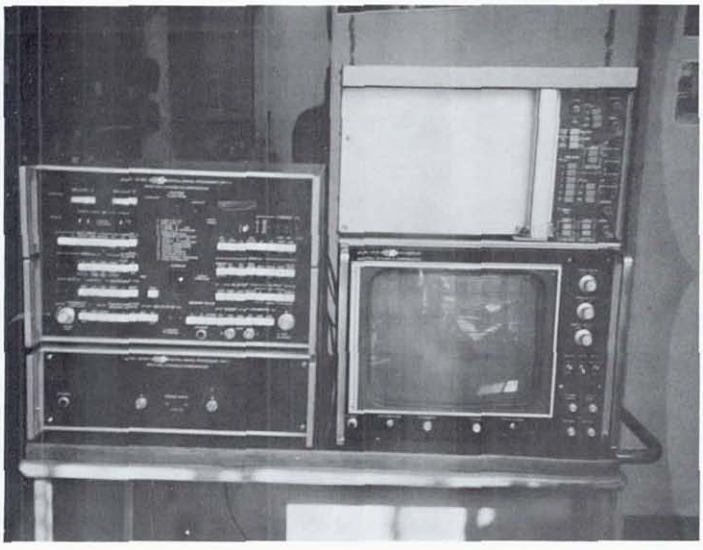

(b) The spectrum analyzer

Fig. 10. Data processing in the Vibration Laboratory.

Fig. 11. Popper test instruments.

V. EXPERIMENTAL PROCEDURE

The on-site work encompassed a ten-week period from the beginning of February until mid-April 1978. The work involved installation of the concrete blocks and the instruments, operation of these instruments, and taking measurements. The greatest time was spent on measurement of the forced vibration; measurements of the ambient vibrations were taken when wind combined with the spilling water downstream to give a more significant level of excitation.

V-1. Installation

The crest was apportioned 25 measurement stations at intervals of approximately 50 ft (see Fig. 12); these stations were designated by E1 to E12 for the eastern half and W1 to W12 for the western half, with the center station designated 0. There were two arrays of measurement stations on the downstream slope (Figs. 12 and 13). Each array consisted of 7 stations (at intervals of approximately 50 ft along the slope); one array was along the mid-point cross section, for measurements of symmetric modes, while the other was even with station E4, for measurements of anti-symmetric modes. One vibration generator was mounted at station E2 which was about 100 ft east of the midpoint of the dam's crest (station 0), and the other was placed at station W2, about 100 ft west of the midpoint (Figs. 12 and 14).

The recording instruments, consisting of the signal conditioners, the tape recorders, and the oscillograph recorder were placed in the central region of the crest between the two shakers.

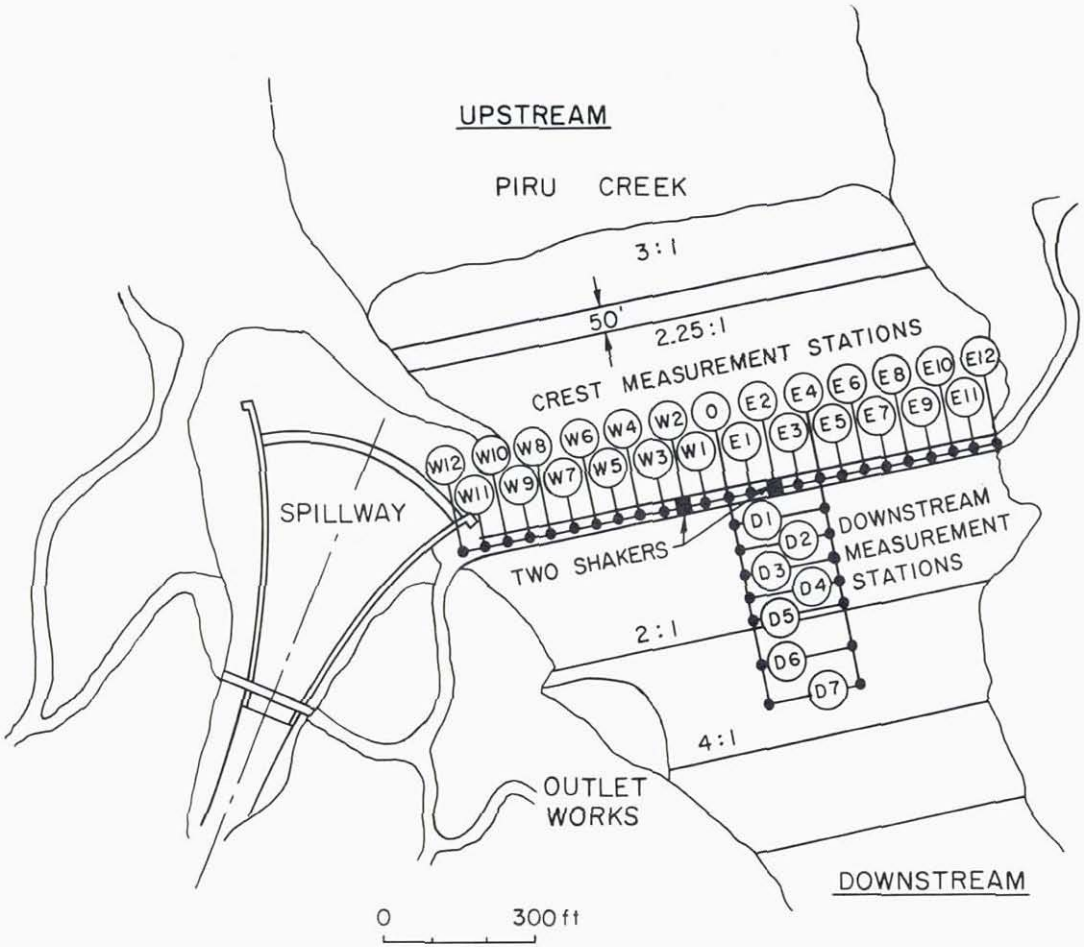

PLAN VIEW SHOWING MEASUREMENT STATIONS

Fig. 12

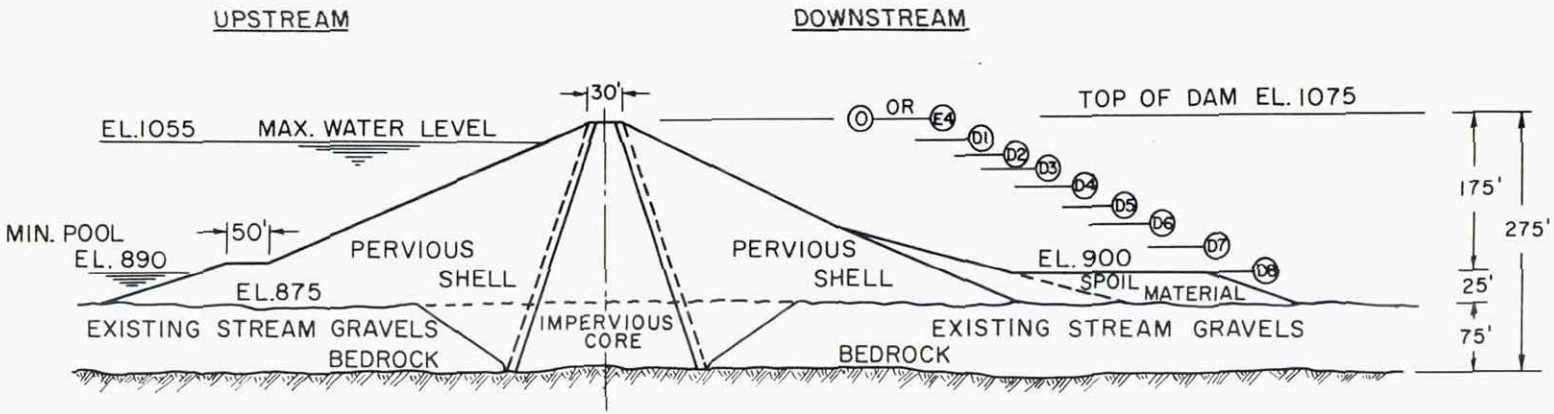

MEASUREMENT STATIONS ACROSS THE DAM

Fig. 13.

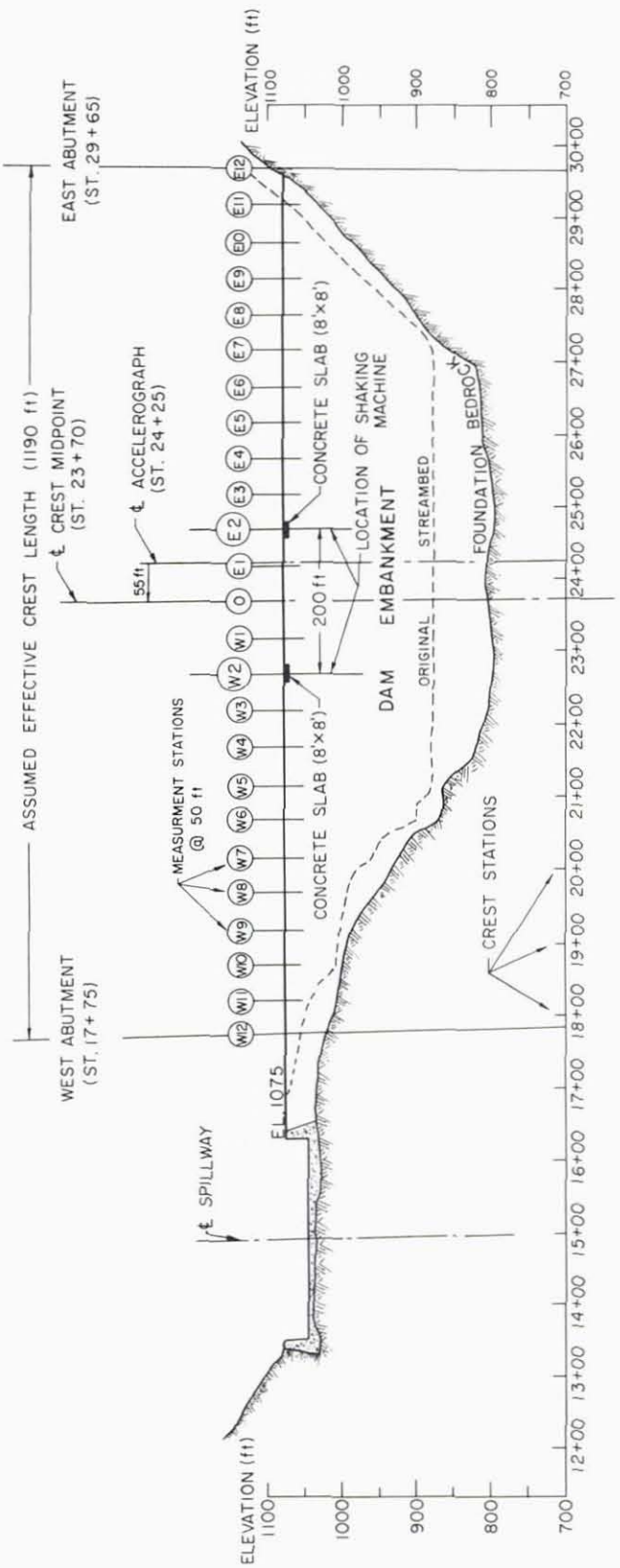

PROFILE ALONG AXIS OF DAM SHOWING MEASUREMENT STATIONS

Fig. 14.

V-2. Operation

V-2-1. Calibration

The first procedure in any measurement involved the relative dynamic calibration of the seismometers at frequencies of interest; this was accomplished by aligning them side by side in the same direction and by measuring their motion (as shown in Fig. 15 for the longitudinal direction). For the forced vibration calibration the dam was excited at a known frequency, and the outputs of all the seismometers were measured; the necessary adjustment of the signal conditioners' attenuation was made in order to obtain the same amplitudes. For the ambient vibration, relative calibration was performed at all of the frequencies of interest by comparing the discrete peaks of the Fourier amplitude spectra of the recorded 10-minute motion. In this manner the differences in output between the transducers for a particular frequency could be determined. The dynamic calibrations were particularly useful for determining the preliminary as well as the three-dimensional mode shapes; this only requires relative values of response at different stations.

V-2-2. Forced Vibration Tests

The first stage of the forced vibration testing program involved a series of preliminary frequency sweeps using sinusoidal excitation. After calibrating the eight seismometers, they were placed at the initial stations selected for a particular frequency range, and were oriented in the direction of the exciting force; then the dam was excited at a specific frequency until steady-state response was attained, at which time the responses at selected stations on the crest and on the downstream slope were recorded. The frequency of excitation was then increased (at intervals

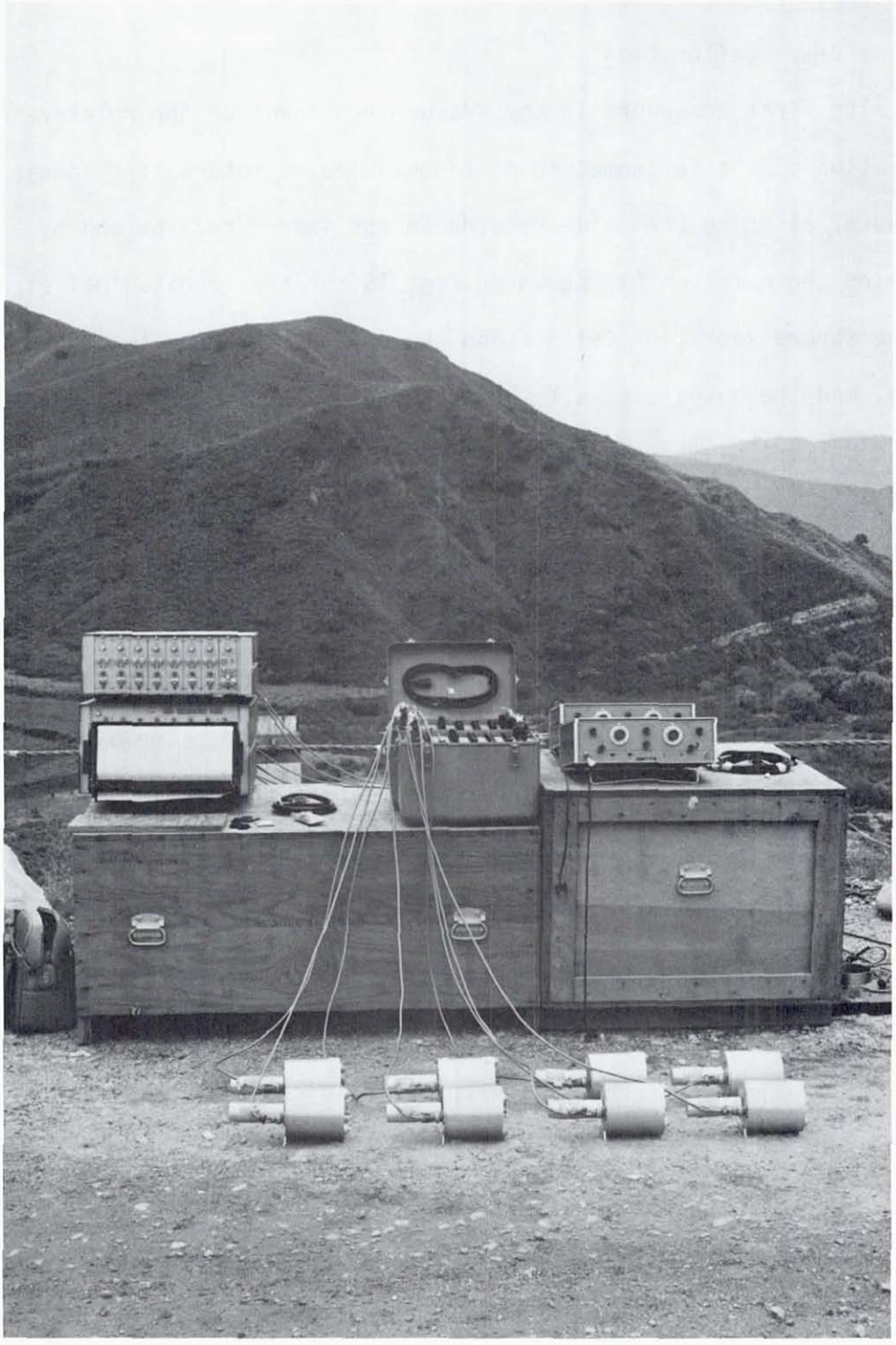

Fig. 15. Typical calibration set-up for Ranger seismometers (in longitudinal direction).

between 0.01 and 0.05 Hz) and the process repeated. At each frequency change, the shakers were held at constant frequency long enough for all transient effects to decay, so only steady-state response was recorded. The transient effect was a problem (particularly on windy days) for the low modes, for which the exciting forces were very low,as shown in Fig. 16 for f = 1.2 Hz; it was also a problem for seismometers located close to the spillway (see Fig. 17). To get rid of this transient effect, a very narrow bandpass filter around the exciting frequency was used; in addition, the spectral and time analyses by the Fourier analyzer helped a great deal in determining amplitudes and phases.

The response of the dam in the frequency range 1.0 to 6.0 Hz was explored in this manner, both in the horizontal plane by stations along the crest and (for some preliminary modes) in the vertical plane by stations arrayed down the downstream slope. This stage of testing enabled the natural frequencies and preliminary mode shapes to be determined. In order to clearly identify some of the unclear resonating mode shapes (in the shaking direction) more detailed measurements were taken at other selected stations to cover a greater portion of the dam.

The second stage of the testing involved measuring the more important modes of vibration determined from the frequency sweeps. The dam was excited at a specific frequency corresponding to one of these modes until steady-state response of the dam was attained. Then the dam's three-dimensional response was measured using six seismometers. Three were mounted on an aluminum plate in such a way that three orthogonal components (U-D, L and V) of motion at one point could be measured. This package was placed at a reference point at station W1 (Figs. 12 and 13) where it

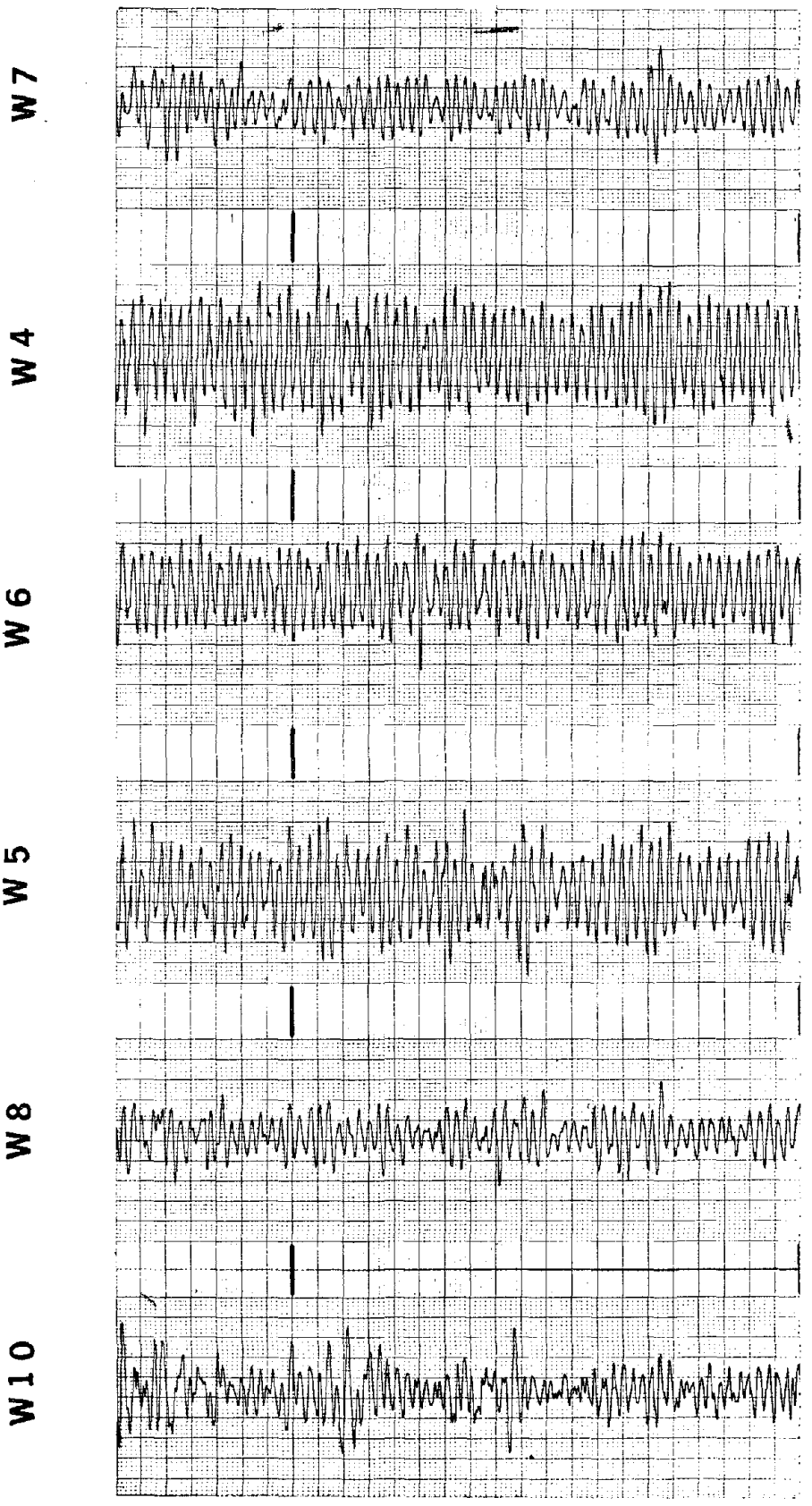

Fig. 16. Transient effect of wind at (low) exciting frequency of 1.2 Hz.

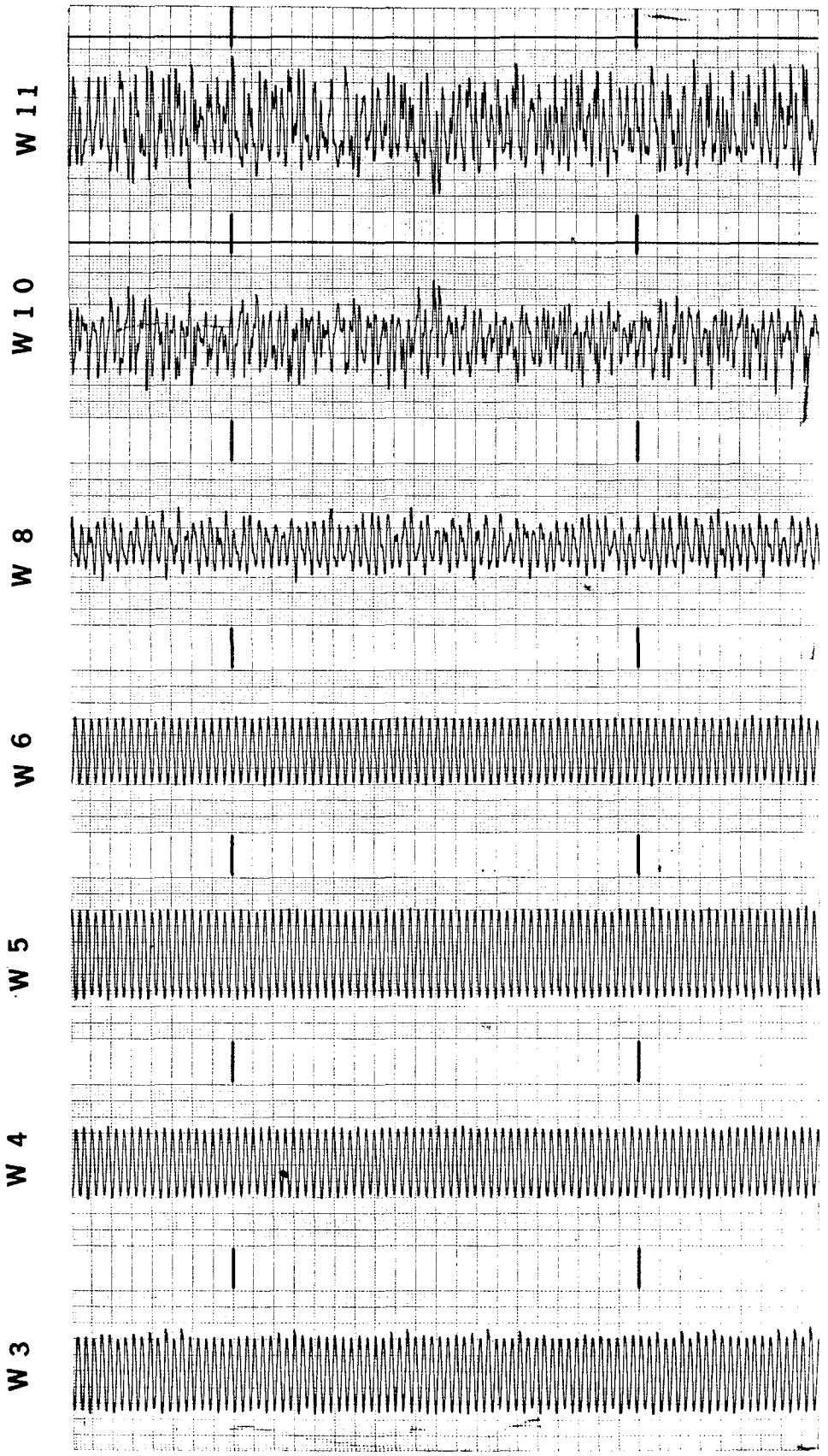

Fig. 17. Transient effects, under steady sinusoidal force input, for seismometers located close to the spillway (W8, W10 and W11).

remained throughout all the mode-measuring tests. Another package of three transducers was then moved from station to station to measure the 3-D motion during steady-state response. In order to discriminate among the vertical profiles of the mode shapes, the instruments were also installed at vertical intervals on the downstream slope of the dam, as shown in Figs. 12 and 13. Eight modes of the upstream-downstream (U-D) vibration were measured in this way.

To study the interaction between the foundation slab (the concrete block of the shaker) and the surrounding soil, two other seismometers were used during the 3-D measurements of the modes; one was placed permanently (as a reference) on the slab and the other was placed at different points surrounding the block on the crest (see Fig. 18).

During the longitudinal shaking, which was the last stage of the whole testing program, one of the two shakers was malfunctioning so the other one was used alone.

Some technical difficulties arose when adding an additional stationary synchro (to the circuit which maintains the relative phase between two shakers) to measure the phase between the excitation and response, and it was eventually decided to dispense with it, although this feature would have permitted a marked increase in the information gained from the tests.

Also, because of the constant high water level in the reservoir at the time of the tests, it was not possible to determine the effect of the reservoir level on the behavior of the dam. Nor was it possible to take measurements on the upstream face which would have enabled a comparison of the upstream and downstream displacements as a check on the assumption of equal displacement predicted by shear-beam theories.

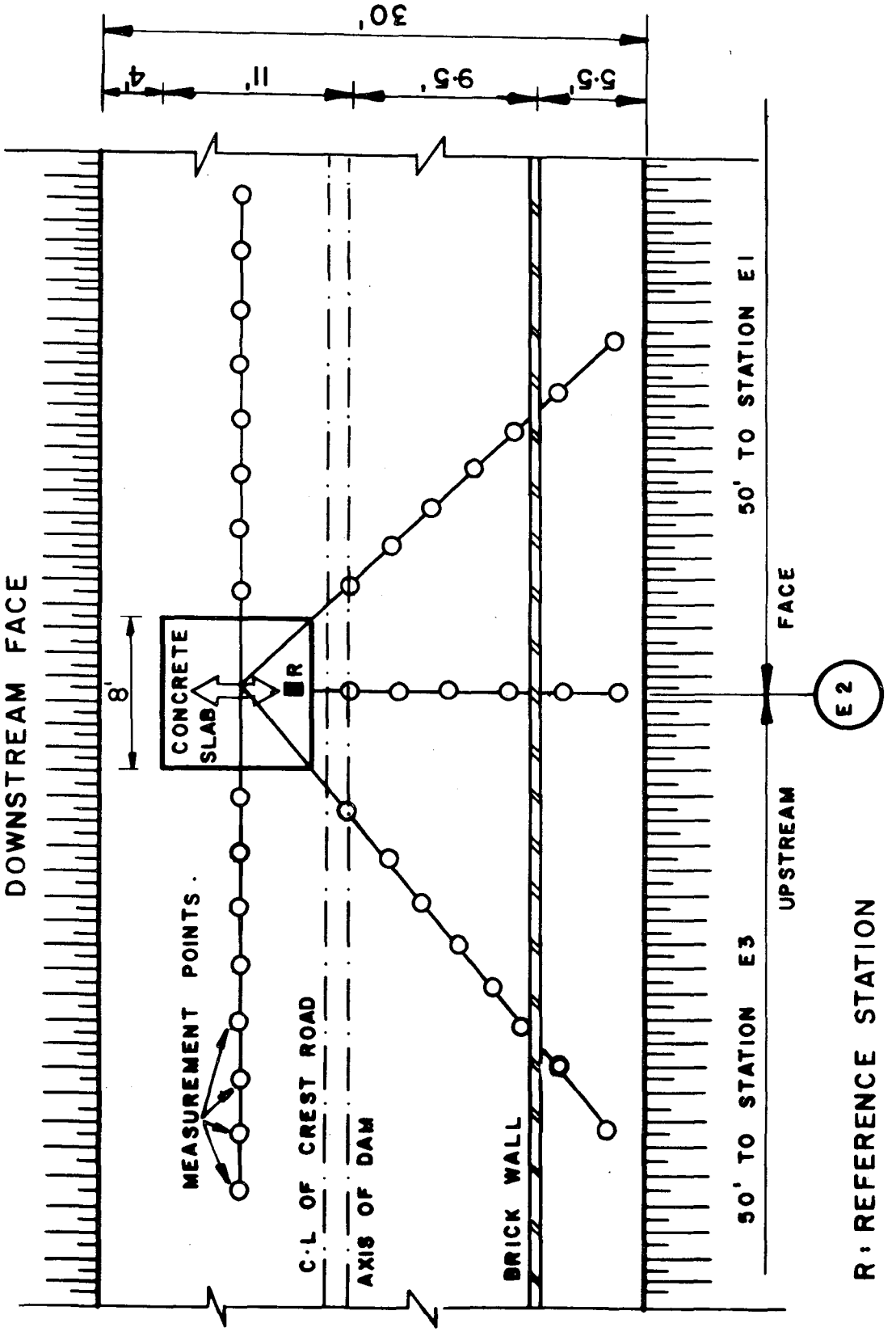

Fig. 18. Measurement stations for study of the interaction between the shaker slab and the surrounding soil.

Figure 19 summarizes the instrumentation used in the tests, the measuring procedures, and the experimental set-up of the frequency sweeps as well as the 3-D mode measurements on Santa Felicia Dam.

V-2-3. Ambient Vibration Tests

The naturally occurring vibrations of the dam caused by strong winds (of speed ranging from 10 to 40 mph), spilling of the reservoir, microtremors, and other environmental factors were measured during ambient tests to yield dynamic properties of the dam. The principal exciting force was the wind, the strength of which was easily monitored by noting the gradual rise and fall of the level of the seismometers' recording. Average wind speeds on different days were recorded based on the meteorological reports broadcast by radio stations. On most days it was observed that the amount of energy imparted to the dam by the spilling of the reservoir was less than that produced by the wind.

Measurements of the upstream-downstream (U-D) as well as the three-dimensional motions of a large number of stations on the crest and the downstream slope were taken on seven different days under varying conditions.

V-2-4. Popper Tests

The test of the dam response to small hydraulic actuating forces was accomplished by use of pressure waves, impinging upon the upstream face of the dam and generated from a controlled, submerged release of gas under pressure in the reservoir water. The purposes of this test were: (1) to determine the feasibility of the popper method of testing a relatively large earth dam, and (2) to obtain more information on the dam's low-strain dynamic characteristics. By loading mostly the central portion

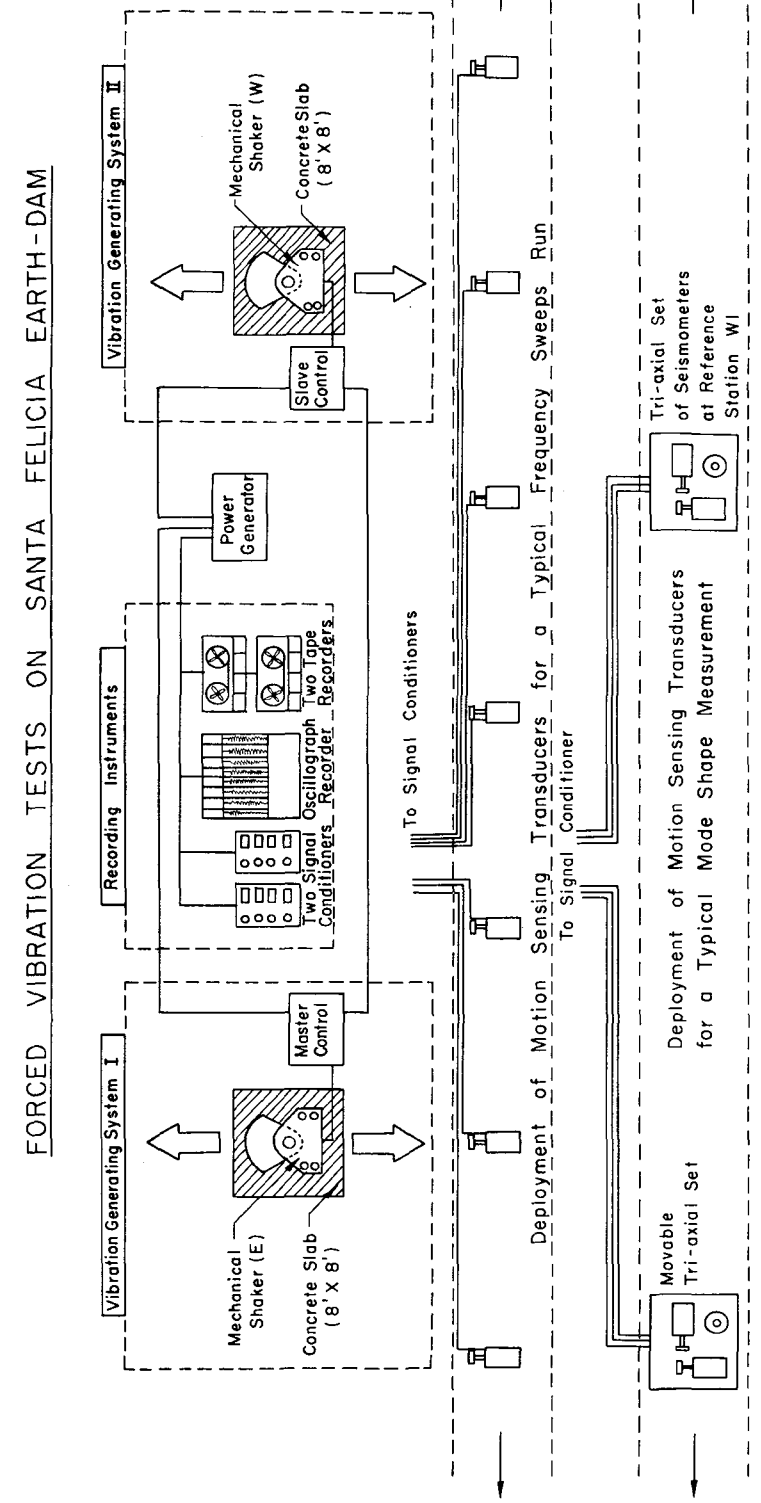

Schematical Diagram Showing the Experimental Set-up

Fig. 19

of the dam, it was intended to excite the first shear mode exclusive of all other modes. Theoretically, to excite any mode exclusively, the distance from the source of the P-wave to the dam must be adjusted such that the pressure distribution would approximate the mode shape to be excited (Ref. 16).

Three sets of popper tests were performed on March 17, 1978; each set lasted about 20 minutes. In popper test I the source of energy release was placed relatively close to the dam, in the central region (in this manner several symmetric modes were excited with each release of energy). In popper test II, the source was moved closer to the dam (about 10-20 ft) along a line perpendicular to the dam's longitudinal axis. In popper test III, the boat which released the popper traversed half of the dam length (starting from the east abutment) and energy was released at every other measurement station (additional modes could be excited by varying the location of the popper with respect to distance along the crest). During all popper tests some seismometers were oriented (at selected stations) in the upstream-downstream direction only, to gain the maximum amount of information about the U-D modal configurations.

V-3. Recording

Recording was begun after several minutes of visual monitoring of the vibration (on the oscillograph recorder), during which fine adjustments were made. In all tests, the velocity circuits of the two signal conditioners were used to measure the motion due to both lower and higher modes (particularly in the ambient vibration tests) since the velocity responses enhance the higher frequencies of the motion. The recording time for the steady-state vibration was about 4 to 5 minutes, while random

responses of ambient vibration were recorded for about 10 to 15 minutes during each run. All vibrations were recorded on the tape recorder as well as on the oscillograph. Sample traces from the oscillograph recorder made during the forced vibration tests and during the ambient vibration tests are shown in Figs. 20 and 21, respectively.

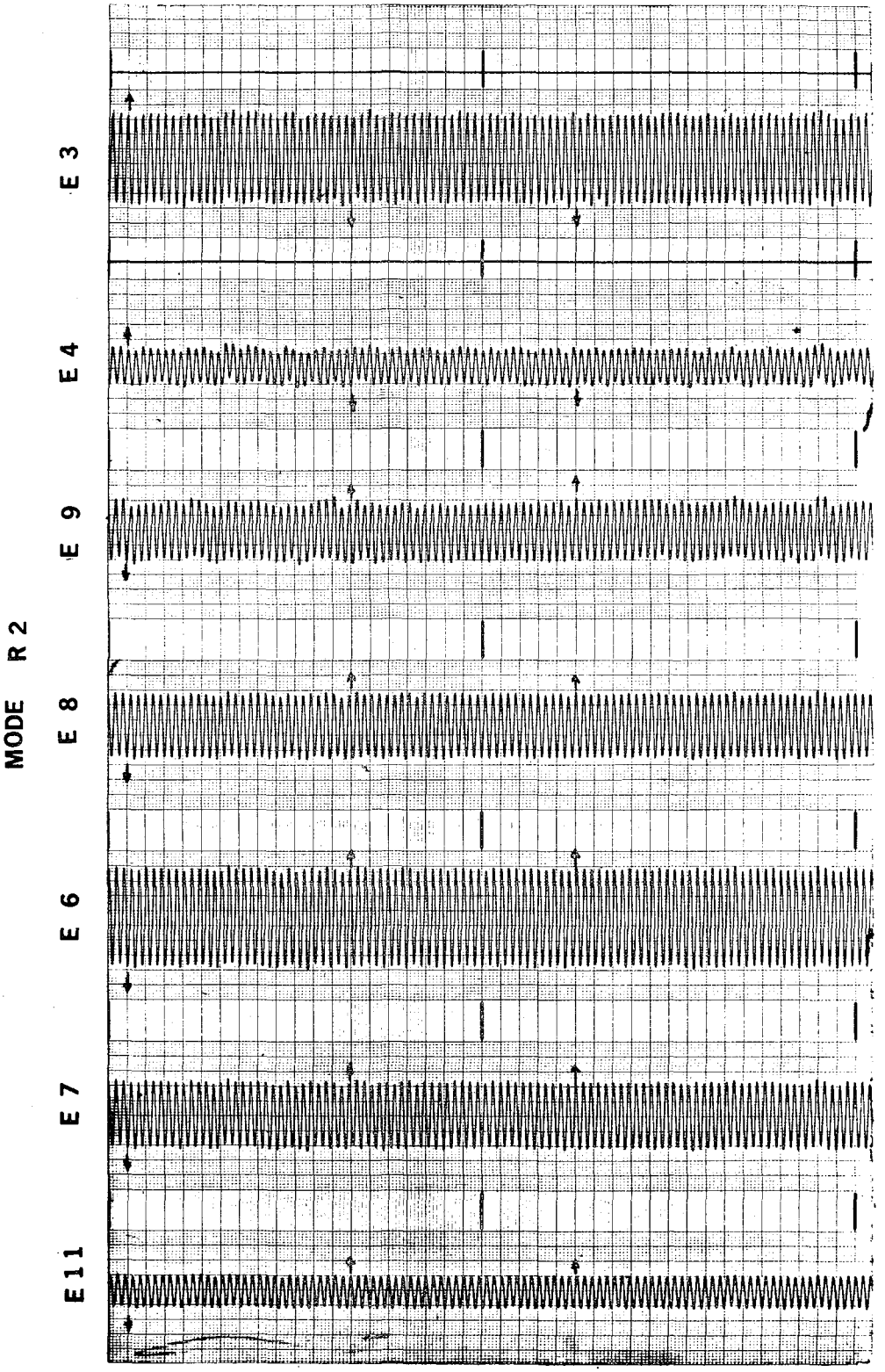

Fig. 20. Sample traces from the oscillograph recorder made simultaneously during the forced vibration tests (frequency sweep at f = 2.270 Hz). (The arrows show the in-phase and out-of-phase motions.)

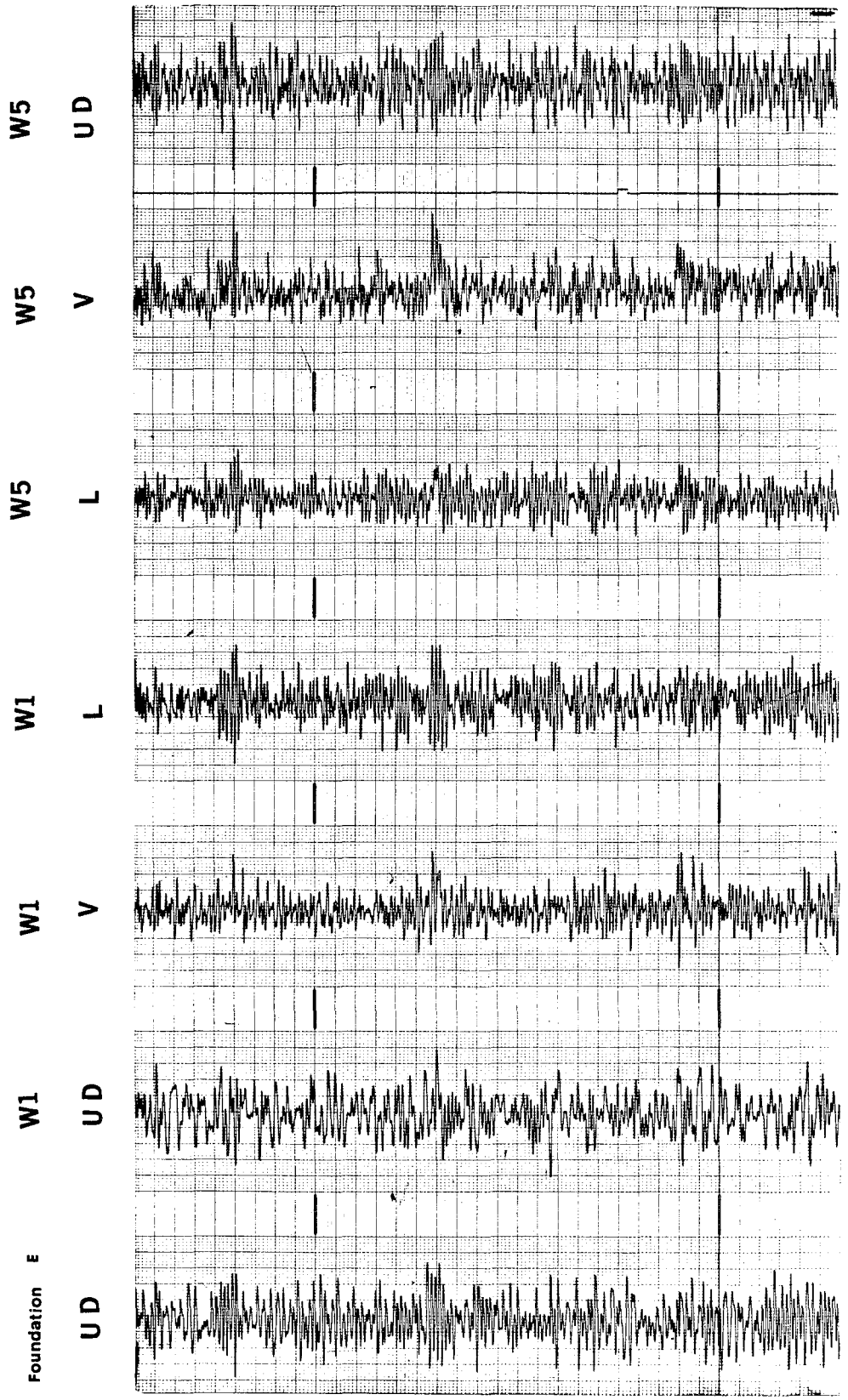

Fig. 21. Sample traces from the oscillograph recorder made simultaneously during the ambient vibration tests (taken on 3/14/78). Note: Amplitude scale of this figure is different from that of Fig. 20.

VI. EXPERIMENTAL ANALYSIS AND RESULTS

VI-1. Forced Vibrations

VI-1-1. Resonance Curves

Some results of the frequency sweep tests for selected stations are shown as resonance curves in Figs. 22 through 24 for upstream-downstream (U-D) symmetric shaking, in Figs. 25 through 27 for U-D antisymmetric shaking, and in Figs. 28 through 30 for longitudinal (L) shaking (using only one shaker). In most of these figures there are four frequency sweeps (from 1.0 to 2.5, 2.0 to 3.0, 2.5 to 5.0, and 4.5 to 6.0 Hz) recorded at every station. Discontinuities in these curves resulted when changes were made in the weight combinations used in the shakers. Other resonance curves (also results of frequency sweep tests) can be found in Appendix A. The force level (weight combinations in the shakers) for each segment of the curves is indicated in the figures. Since the seismometers were used as the motion-sensing transducers, again, no absolute calibration was made. Therefore, for these tests, the magnitude of the double-amplitude of the response was normalized (divided by the largest response obtained for each set of weights, then divided by the square of the exciting frequency, as shown in part b of all curves) and plotted versus frequency.

It is seen in Figs. 22 through 30 that the response at this stage reaches peaks at the same frequencies for various measurement stations and in various vibration runs. In addition, the resonance curves of Santa Felicia Dam contain many closely-spaced resonance peaks. In several instances, the resonance peaks overlap to the extent that the values of

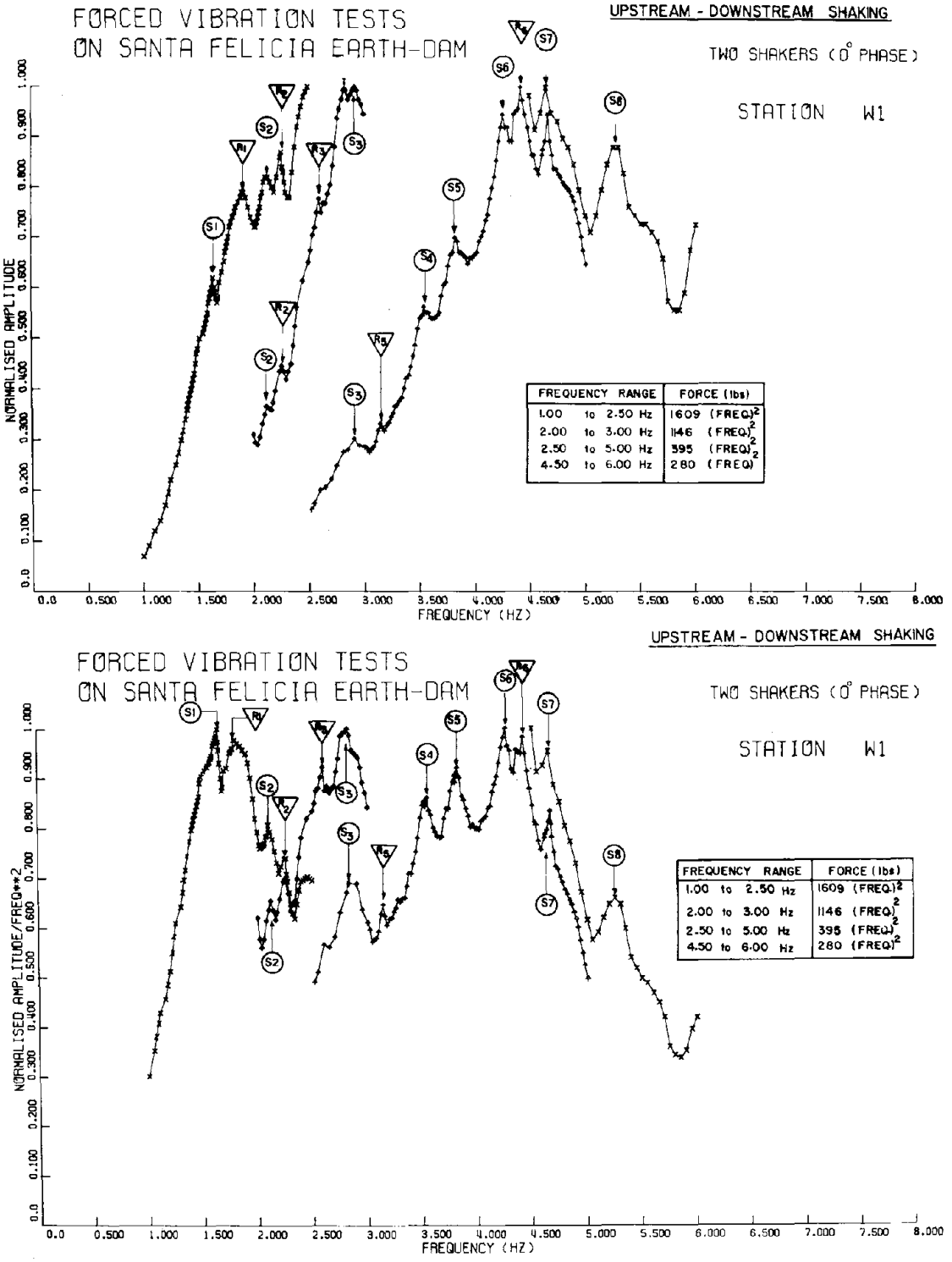

Fig. 22. Response curves of symmetric upstream-downstream shaking (seismometer at Station W1). Note: In each following figure, through Fig. 30, the amplitude has been normalized by the frequency squared in the lower picture.

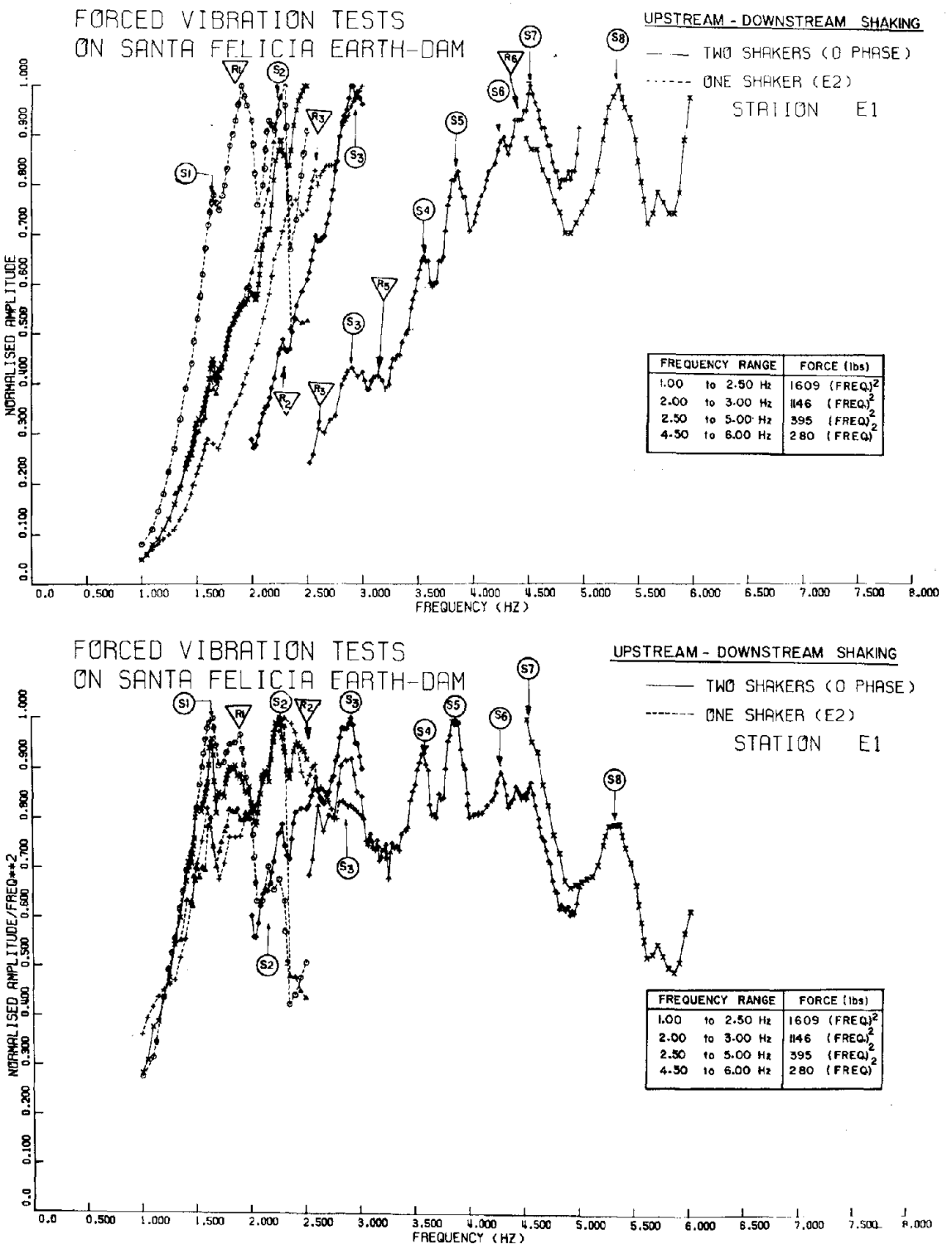

Fig. 23. Response curves of symmetric upstream-downstream shaking (seismometer at Station E1).

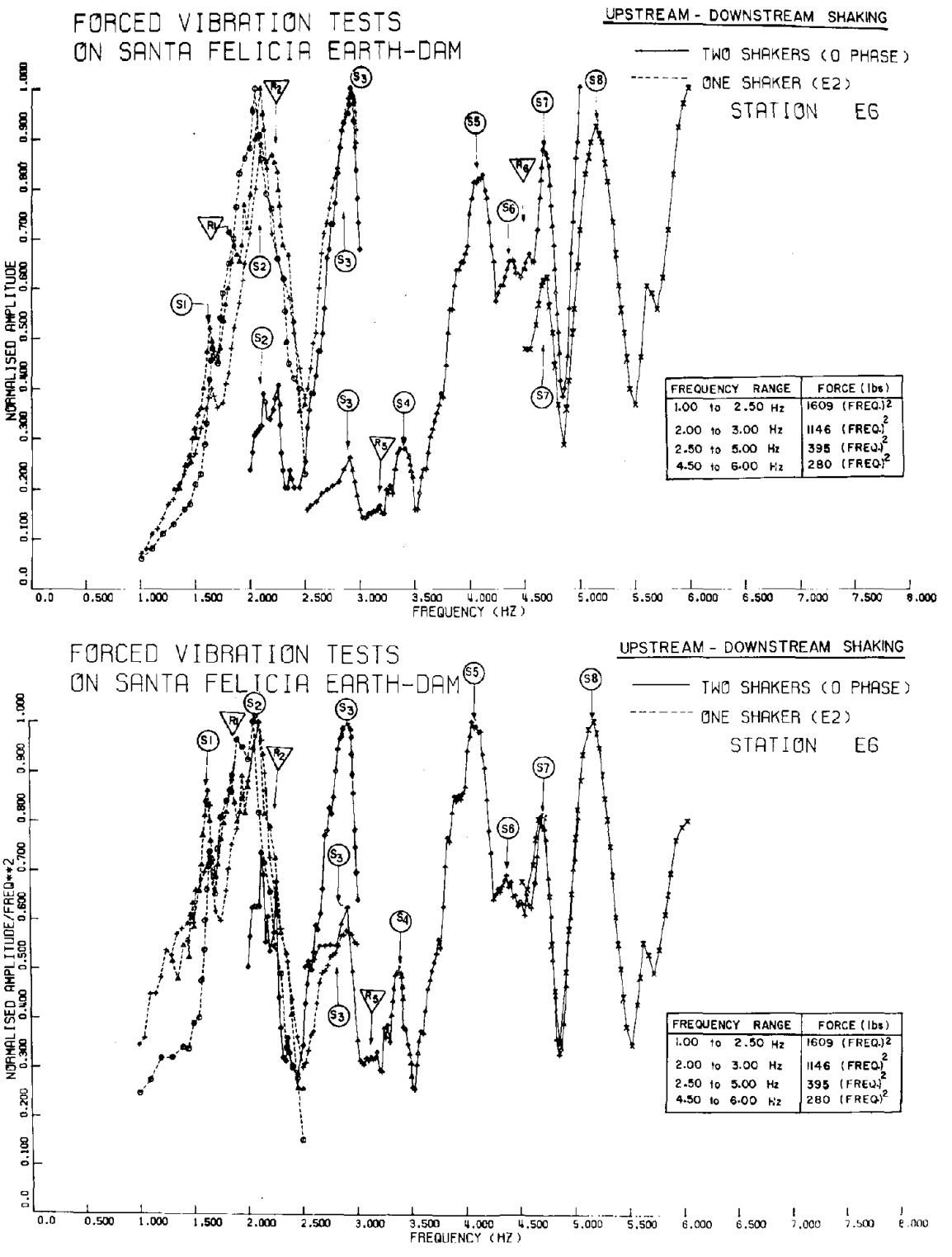

Fig. 24. Response curves of symmetric upstream-downstream shaking (seismometer at Station E6).

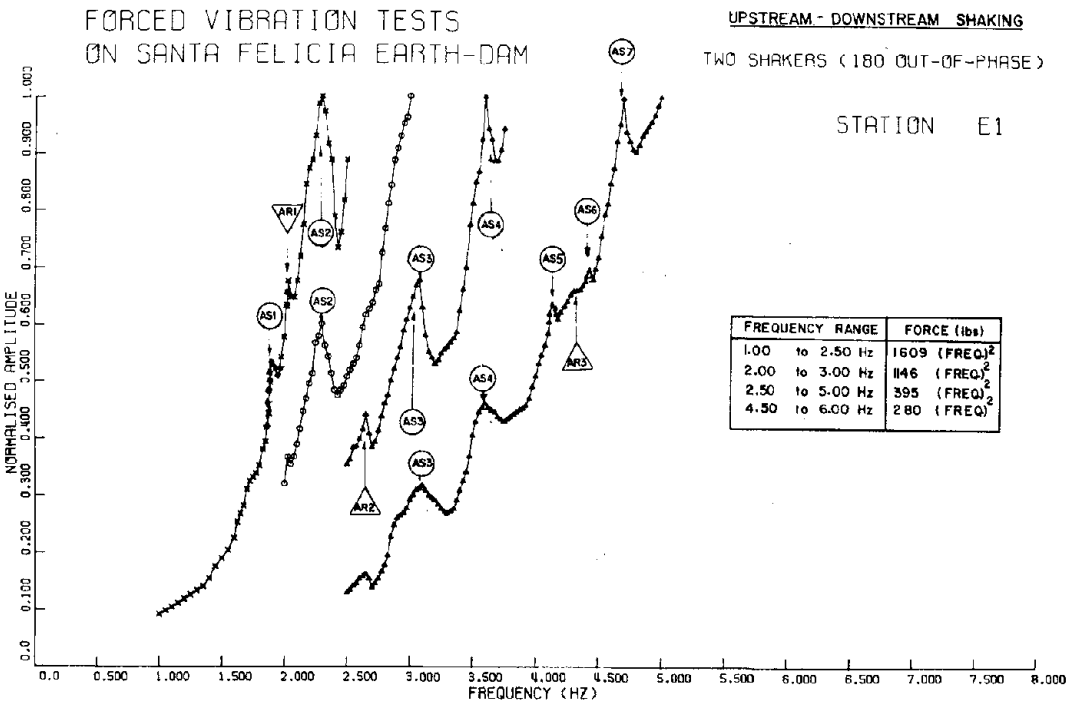

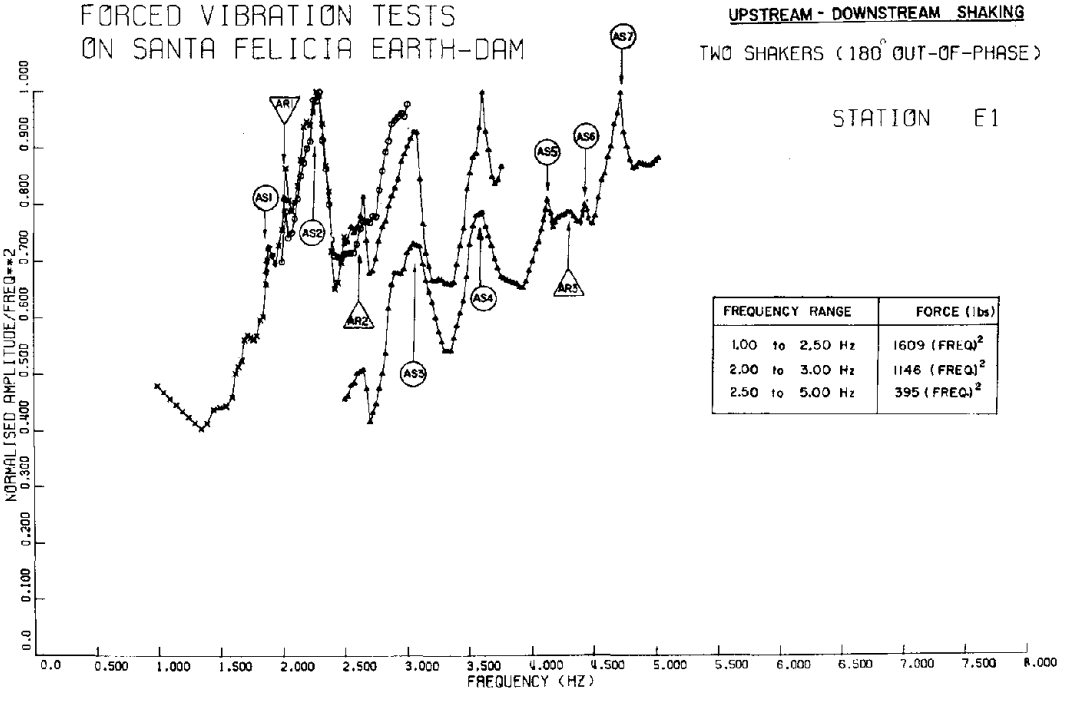

Fig. 25. Response curves of antisymmetric upstream-downstream shaking (seismometer at Station E1).

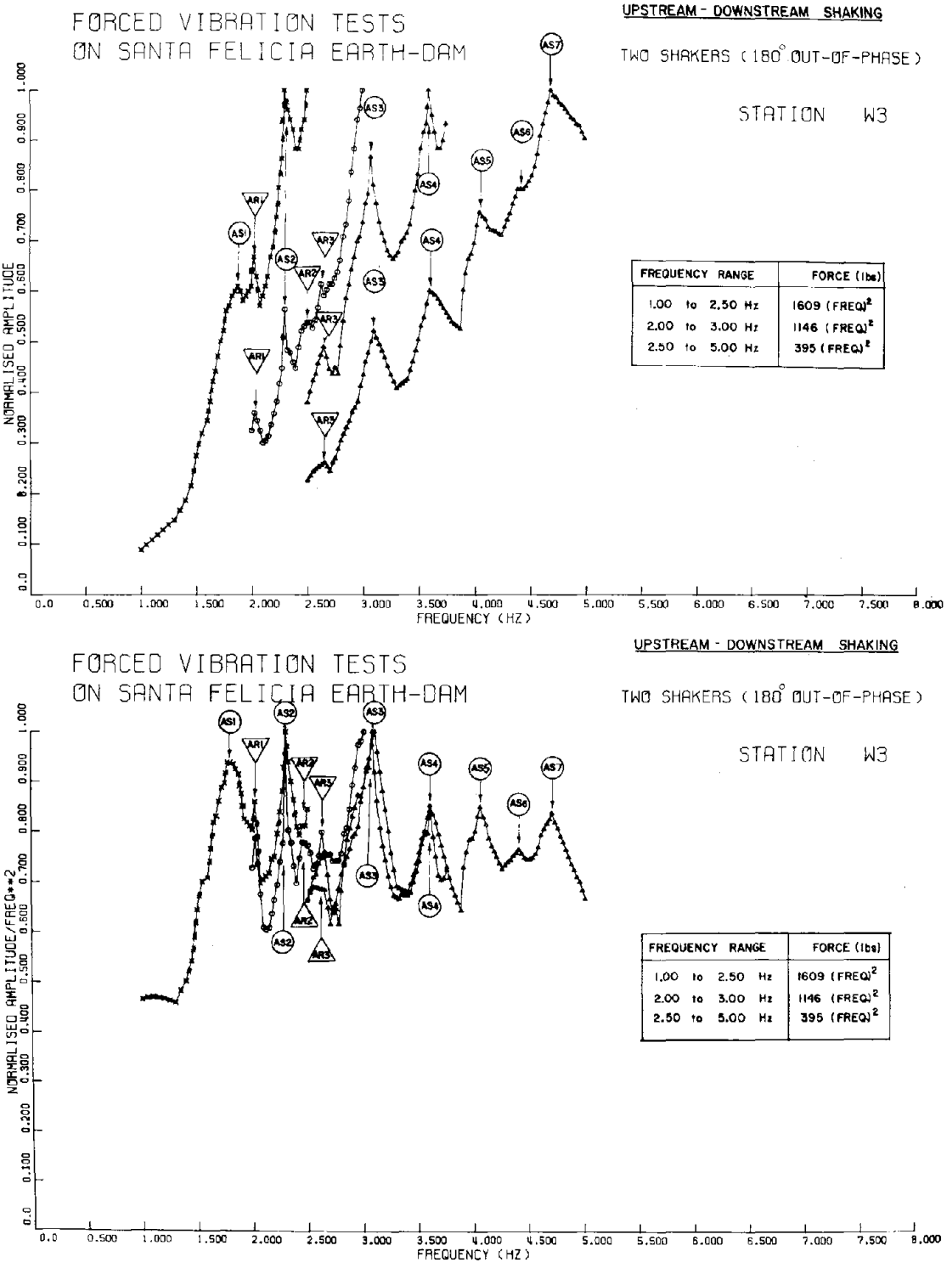

Fig. 26. Response curves of antisymmetric upstream-downstream shaking (seismometer at Station W3).

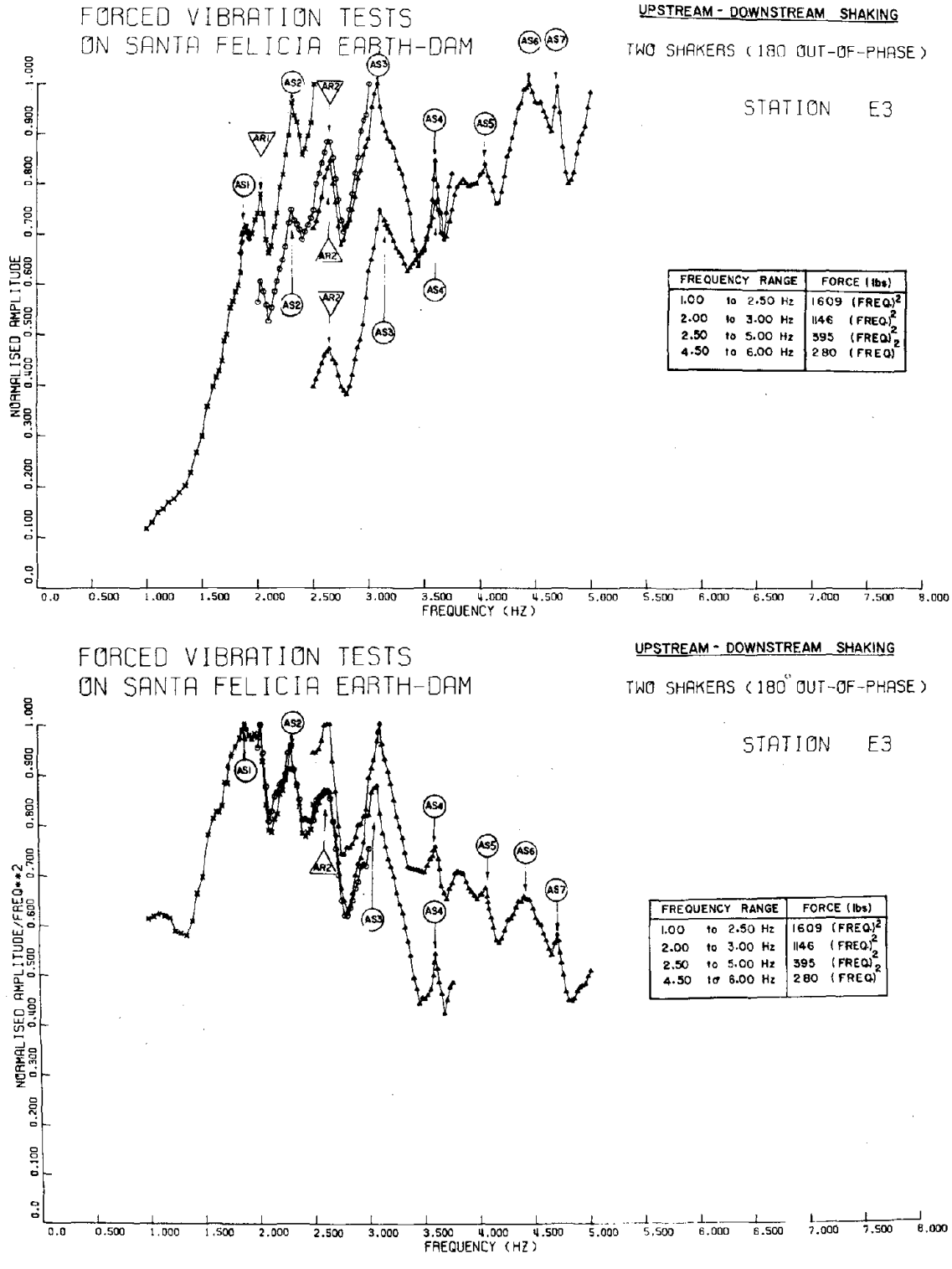

Fig. 27. Response curves of antisymmetric upstream-downstream shaking (seismometer at Station E3).

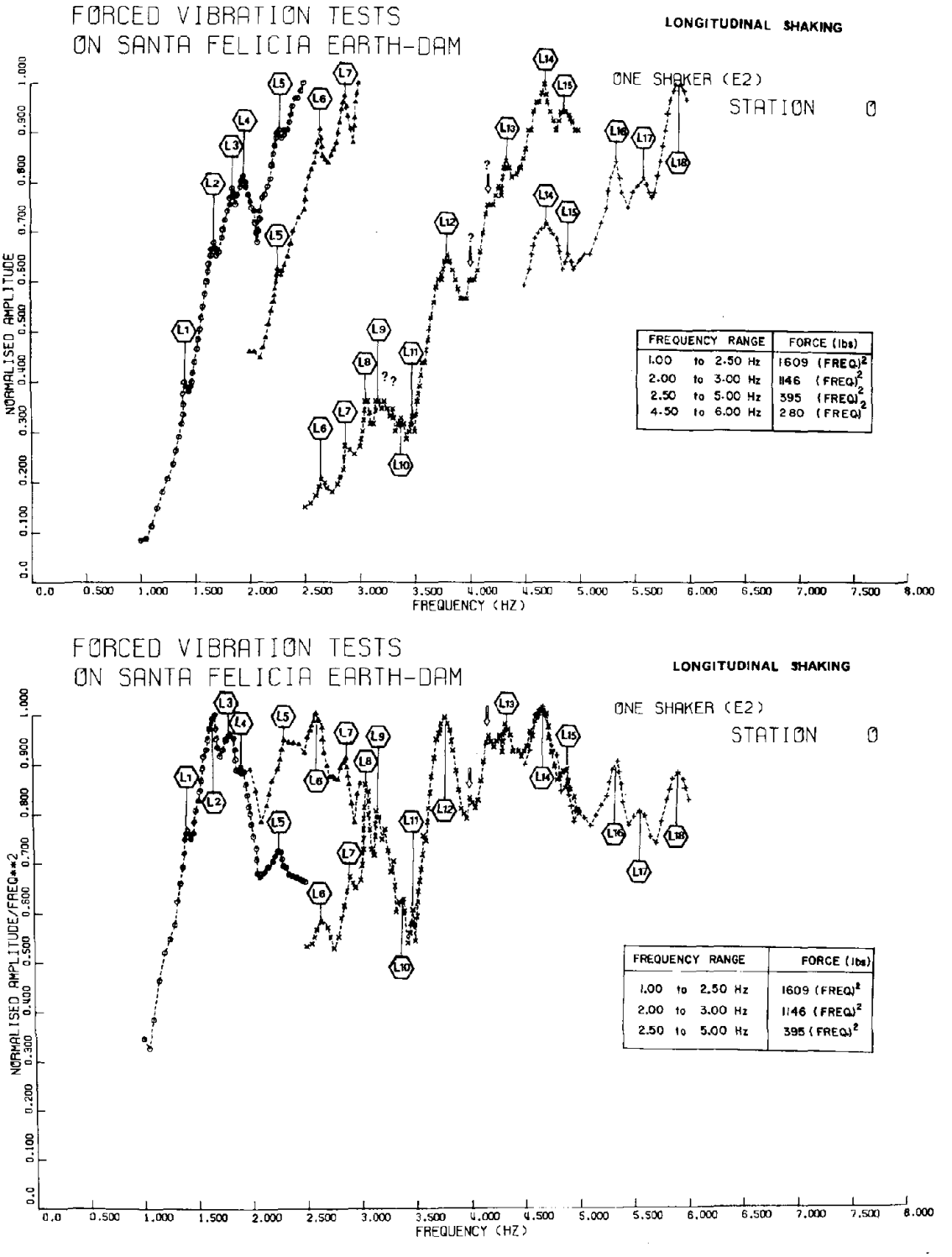

Fig. 28. Response curves of longitudinal shaking (seismometer at Station 0).

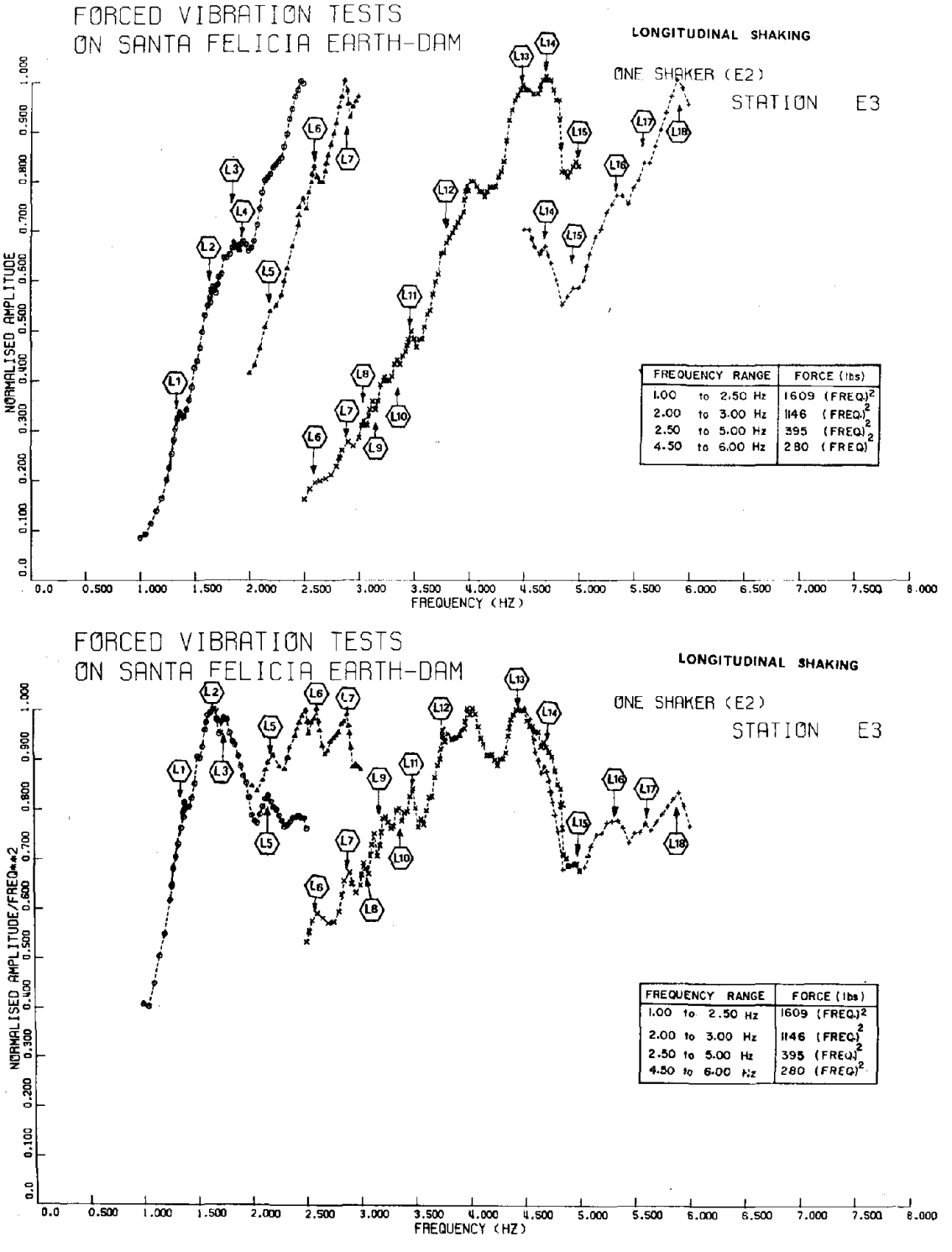

Fig. 29. Response curves of longitudinal shaking (seismometer at Station E3).

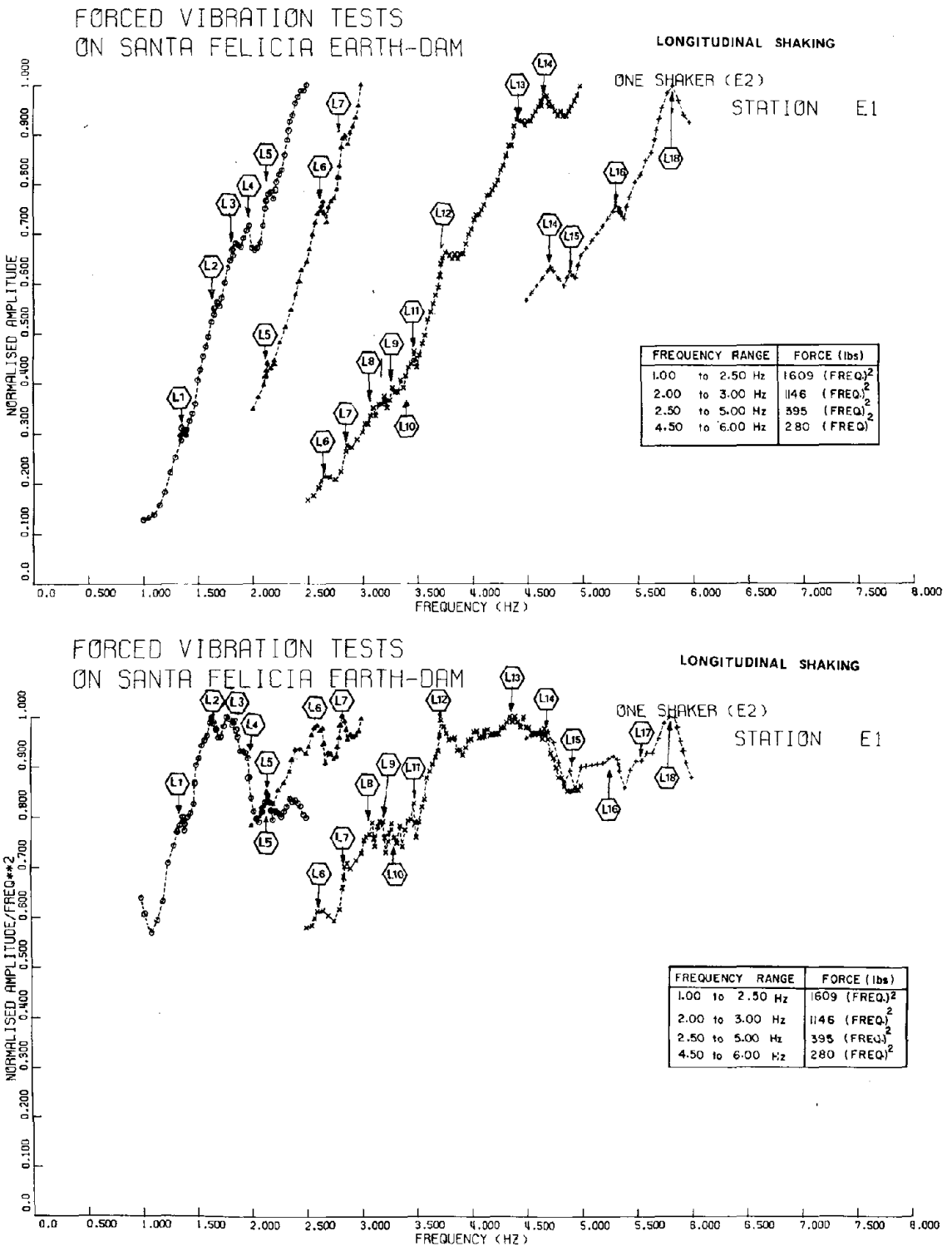

Fig. 30. Response curves of longitudinal shaking (seismometer at Station E1).

the resonant frequencies cannot be accurately determined.

Some structural properties can be found from analysis of the resonance curves of Figs. 22 through 30 and similar curves of Appendix A, but the interpretation is difficult because of two factors. First, the resonant frequencies and damping values cannot be determined accurately from the figures for some lower as well as higher modes because:

(1) The force level used to excite this massive structure (it weighs about six million tons), particularly at low frequencies, is very low. This would make very desirable the development and use of a new larger vibration generator capable of producing very large forces (preferably up to 100,000 lbs at frequencies of 0.3 to 2.0 Hz) for full-scale testing of dams, nuclear reactors, and other massive structures.

(2) The peaks of some modes are not well defined because of the interfering response of other modes of the structure. This difficulty would have been largely overcome by measuring the phase between the excitation and the response. The measured phase allows the response to be separated into its in-phase and 90° out-of-phase components, and if the latter is plotted versus frequency, each resonance of the structure becomes much more sharply defined, and frequencies, dampings, and modes are more readily determined.

Second, as mentioned previously, the resonant frequencies of the structure are often too closely spaced, sometimes overlapping, to permit identification of every mode (Refs. 6 and 11).

VI-1-2. Upstream-Downstream Modes of Vibration

As seen in Figs. 22 through 24, the first peak from symmetric shaking occurred at a frequency of 1.635 Hz, which is the fundamental U-D shear mode of the dam at this excitation level. The 2-D shear-beam concept of the deflection shape of the dam in this first mode is shown schematically in Fig. 31. It is obvious that a centrally-located instrument station is the best place to pick up this particular vibration, since the displacement peaks are at a maximum in that vicinity.

Tables 2 and 3 summarize all frequencies of major peaks recorded at selected stations for the symmetric and antisymmetric U-D shakings. The frequencies in these tables were determined by observing the frequencies where a peak occurred at different measurement stations, and by judging the degree to which the peaks were free from the influence of adjacent resonances. It is not possible to identify with confidence the related mode shapes without obtaining the output for pick-ups located horizontally across the entire crest and at vertical intervals on the downstream slope. The best estimates of the mode shapes of the crest vibrations at peak amplitudes obtained from the seismometer records are shown in Figs. 32 and 35 for the three-dimensional response, and Figs. 34 and 37 for the upstream-downstream response. The shapes of the downstream vibrations at frequencies corresponding to those of Figs. 32 and 35 are shown in Figs. 33 and 36. The mode shapes were obtained by dividing the response at a given station by the simultaneously recorded response at the reference station. In this way, an amplitude was obtained proportional to the mode shape amplitude at that station for the exciting frequency. The phase of the response was compared with that of the reference instrument to deter-

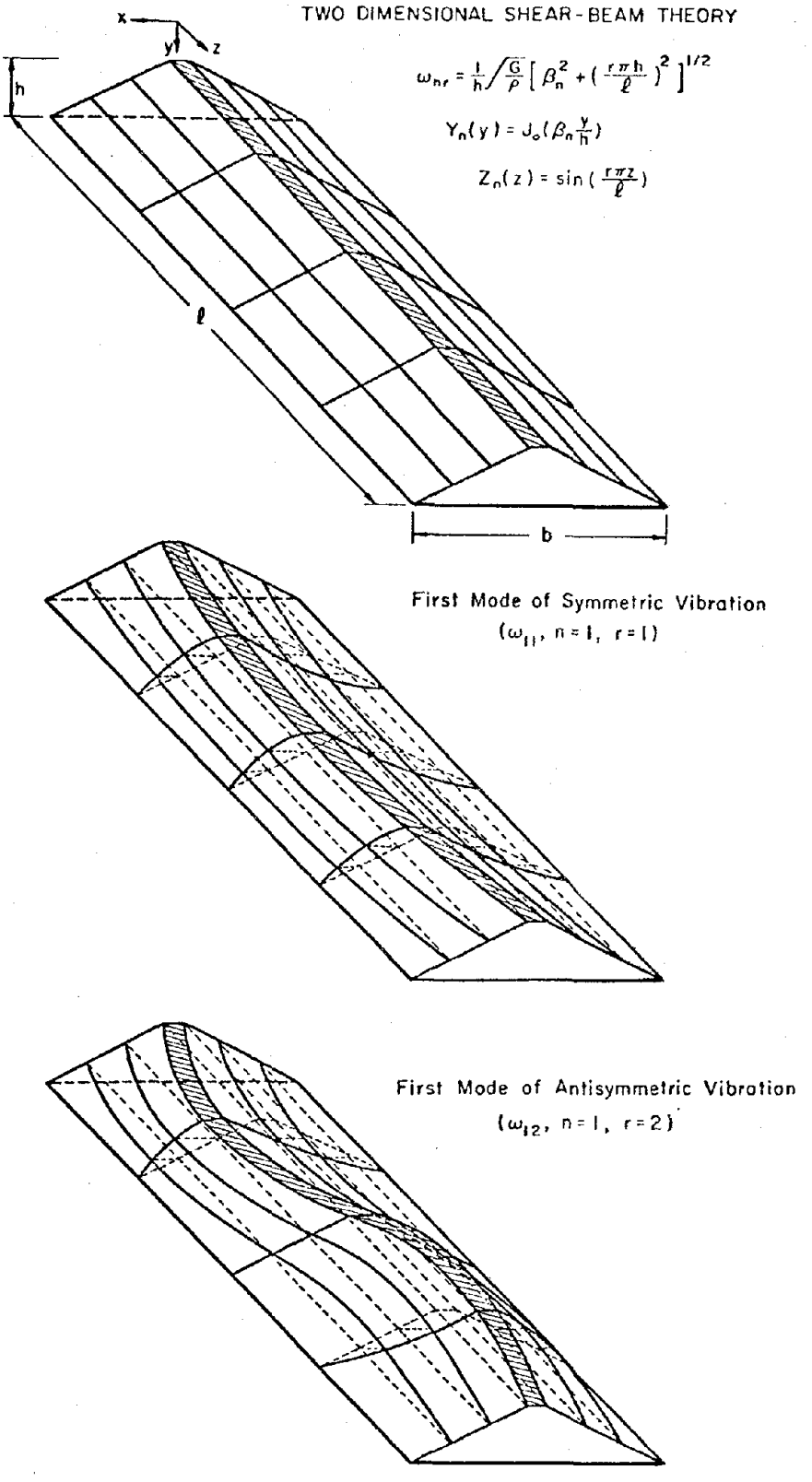

Fig. 31. Schematic diagram showing the first symmetric and the first antisymmetric shear modes as predicted by the 2-D shear-beam theory.

Table 2

RESONANT FREQUENCIES (in Hz) OBSERVED IN THE UPSTREAM-DOWNSTREAM DIRECTION (SYMMETRIC SHAKING)
SANTA FELICIA EARTH DAM

Measurement Station											Representative Natural Frequency	Modal Designation
W1	0	E1	E2	E3	E4	E5	E6	E7	E8	E9		
1.641	1.632	1.641	1.651	1.631	1.632	1.651	1.635	1.651	1.632	1.630	1.635	S1
1.850	1.851	1.851	1.901	1.841	1.851	1.901	1.851	1.855	1.851*	1.855	1.850	R1
2.122	2.100	2.119	2.000	2.100	2.102	2.049	2.122	2.142	2.101	2.122	2.100	S2
2.260	2.272	2.270*	2.302	2.275**	2.363*	-	2.261	2.261	2.201	2.301	2.270	R2
2.600*	2.606	2.604**	-	2.581	2.600	-	2.605*	2.640*	2.575*	2.581*	2.600	R3
2.821	2.820	2.821	-	2.809*	2.821	-	2.859	2.780	2.751	2.761	2.840	S3
2.906**	2.906**	2.906**	-	2.906**	2.881**	-	2.920**	2.941**	-	2.920	2.920	R4
3.142*	3.162**	3.081*	-	3.010**	3.301*	-	3.181**	-	-	-	3.150	R5
3.542	3.542	3.561	-	3.542	3.580	-	3.485	-	-	-	3.550	S4
3.820	3.860	3.879	-	3.901*	3.921	-	3.875	-	-	-	3.870	S5
4.259	4.301	4.301	-	4.221	4.160	-	4.359	-	-	-	4.300	S6
4.420	4.481	4.540**	-	4.439**	4.460*	-	4.480**	-	-	-	4.450	R6
4.665	4.665	4.665	-	4.665	4.665	-	4.665	-	-	-	4.665	S7
5.252	5.351**	5.351	-	5.302	5.401	-	5.255	-	-	-	5.257	S8
-	5.751	5.704	-	5.851	5.751	-	5.701	-	-	-	-	-

Most reliable data (No asterisk)
Less reliable data (*)
Least reliable data (**)

Note: S indicates symmetric shear modes while R indicates symmetric rocking modes.

Table 3

RESONANT FREQUENCIES (in Hz) OBSERVED IN THE
UPSTREAM-DOWNSTREAM DIRECTION (ANTISYMMETRIC SHAKING)
SANTA FELICIA EARTH DAM

Measurement Station								Representative Natural Frequency	Modal Designation
W5	W4	W3	W1	E1	E3	E5	E7		
1.875	1.875	1.875	1.900	1.900	1.875	1.875	1.875	1.875	AS1
2.025	2.025	2.025	2.025	2.025	2.025	2.025	2.050	2.025	AR1
2.300	2.300	2.300	2.300	2.300	2.300	2.300	2.300	2.300	AS2
2.750	2.650**	2.650	2.675	2.650	2.625	2.650	2.600	2.650	AR2
3.100	3.100	3.075	3.100	3.075	3.100	3.100	3.100	3.100	AS3
3.600	3.600	3.600	3.600	3.600	3.600	3.600	3.600	3.600	AS4
4.050	4.050	4.050	4.200	4.150	4.050	4.100	4.100	4.100	AS5
-	-	-	-	4.275**	-	4.225**	4.225**	4.225	AR3
4.425	4.425	4.425*	4.600**	4.420*	4.450	-	4.420*	4.420	AS6
4.700	4.700	4.700	4.700	4.700	4.700	4.700	4.700	4.700	AS7
-	-	-	4.900	-	-	4.900	-	4.900	AR4

Most reliable data (No asterisk)
Less reliable data (*)
Least reliable data (**)

Note: AS indicates antisymmetric shear modes, while AR indicates antisymmetric rocking modes.

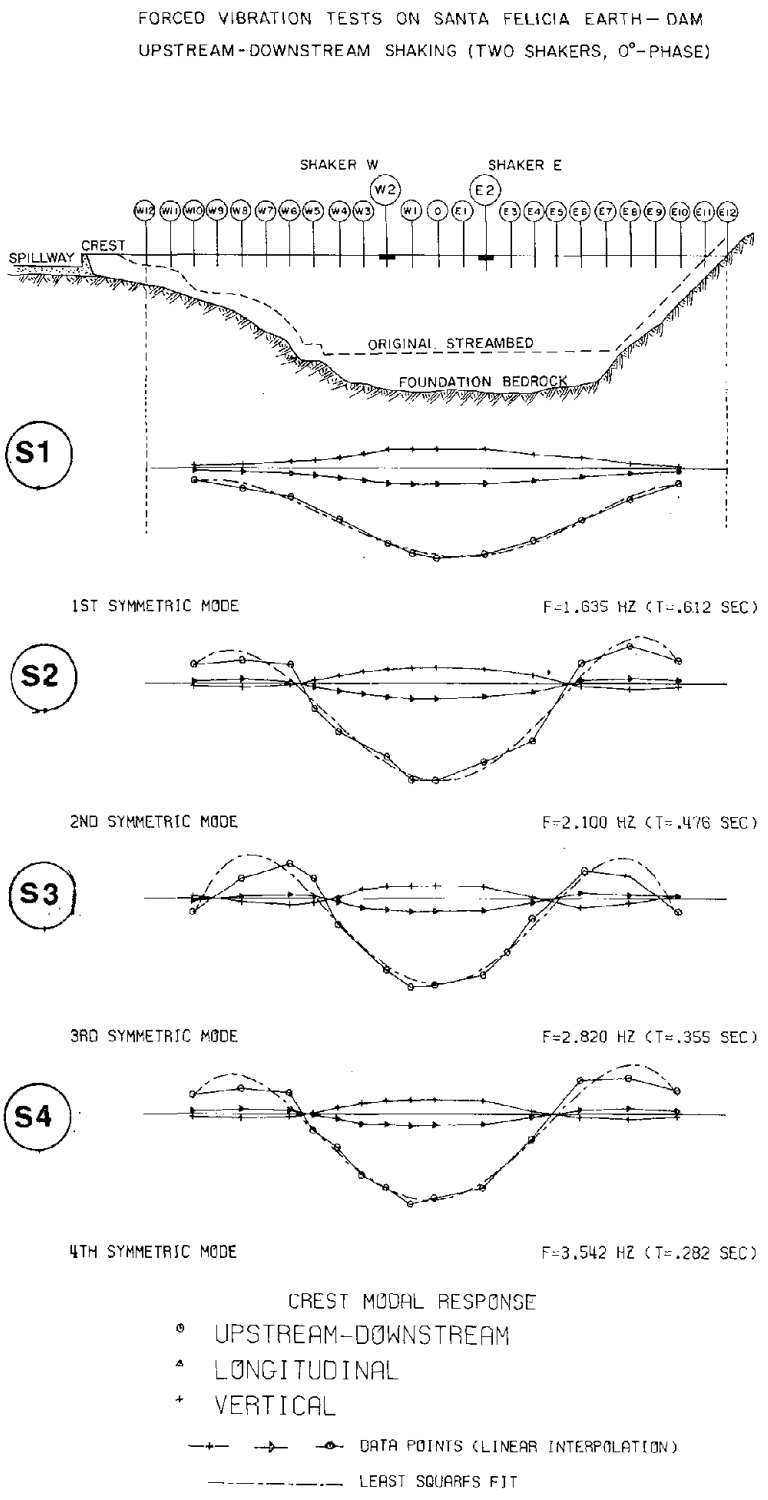

Fig. 32. The first four measured symmetric shear mode shapes. (Three dimensional measurements along the crest.) (Note: Mode S2 has two nodes along the crest, while mode S3 has four nodes along the crest.)

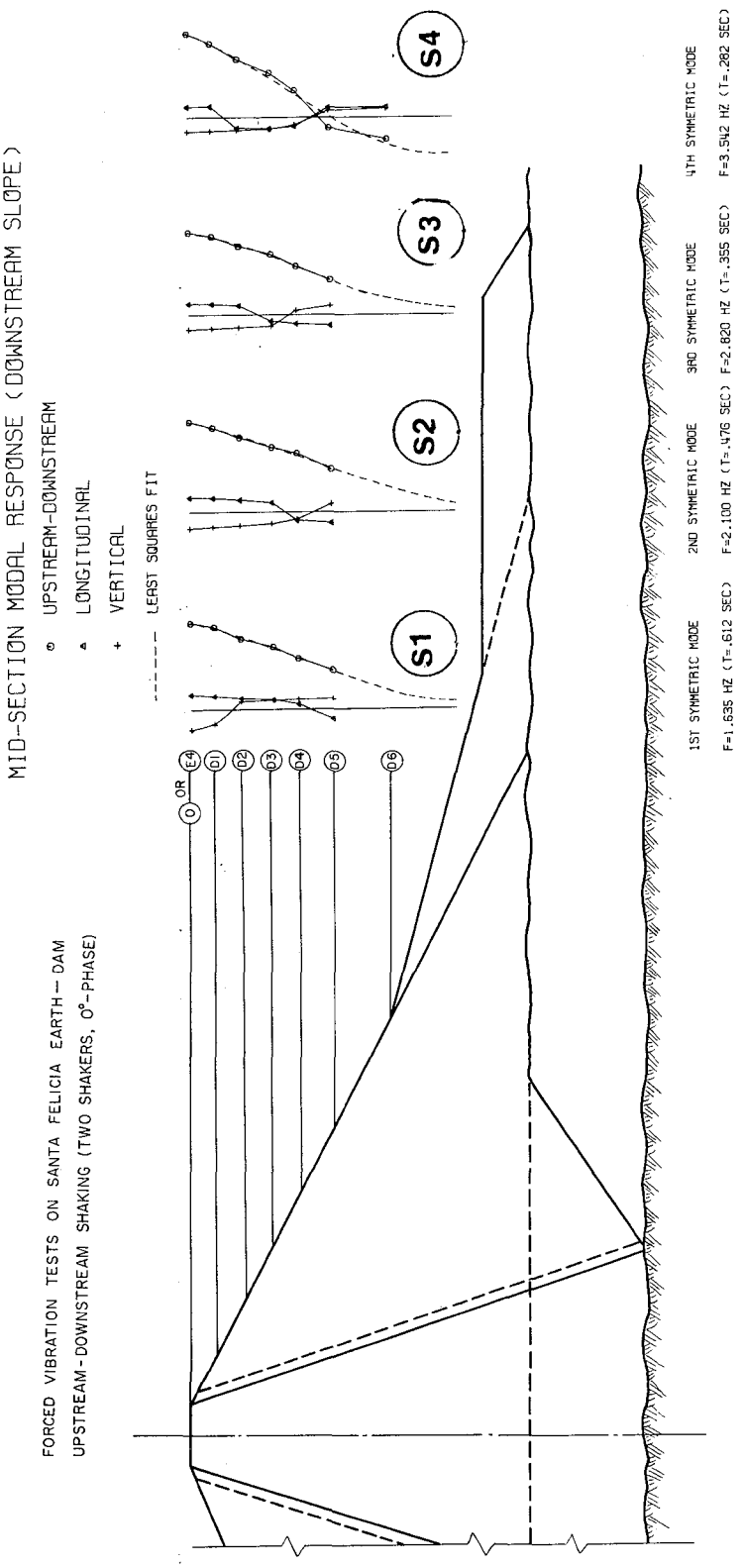

Fig. 33. The first four measured symmetric shear mode shapes. (Three-dimensional measurements along the downstream face.)

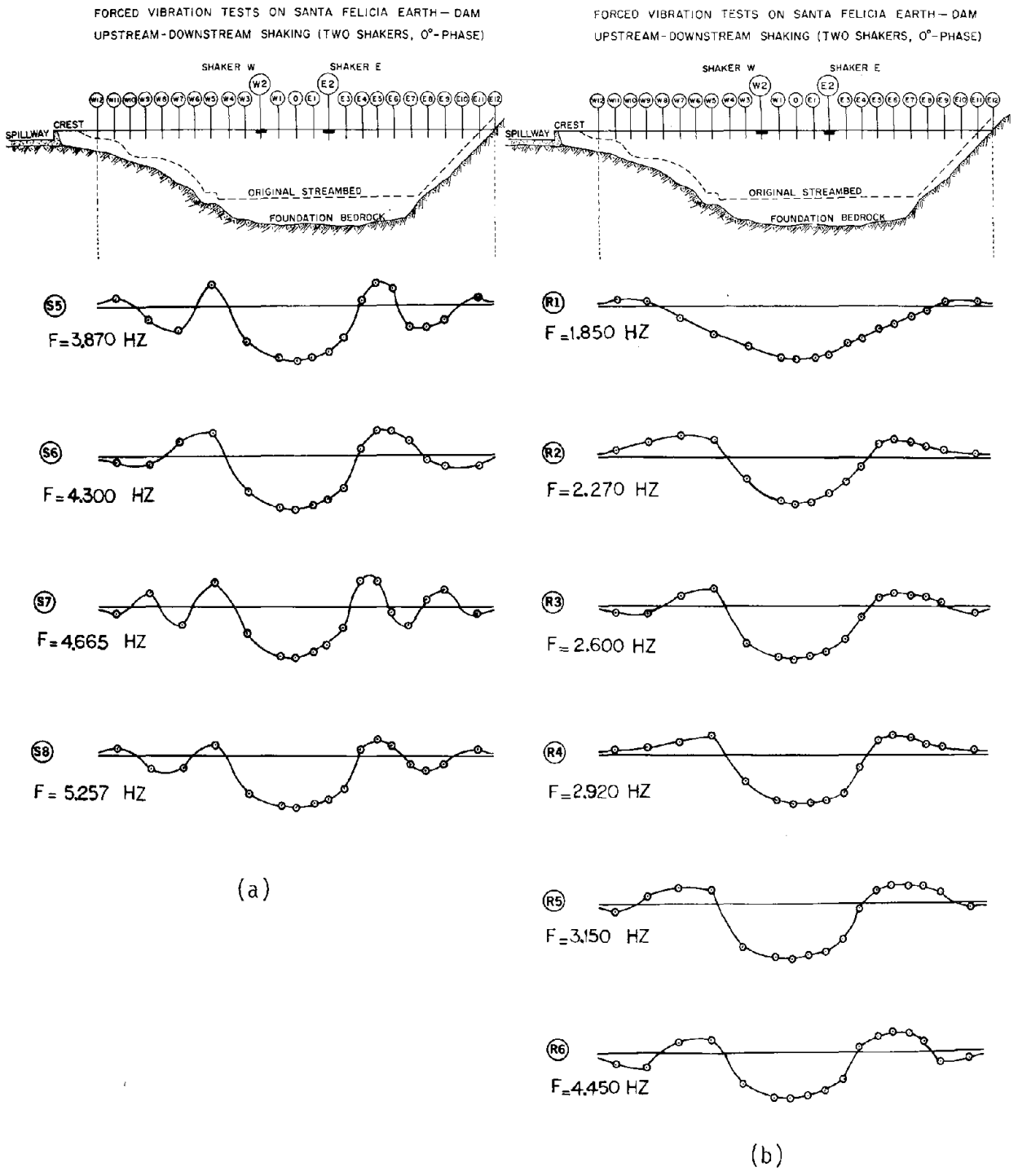

Fig. 34. Measured symmetric mode shapes determined during the frequency sweep tests. (a) Some shear modes. (b) Rocking modes.

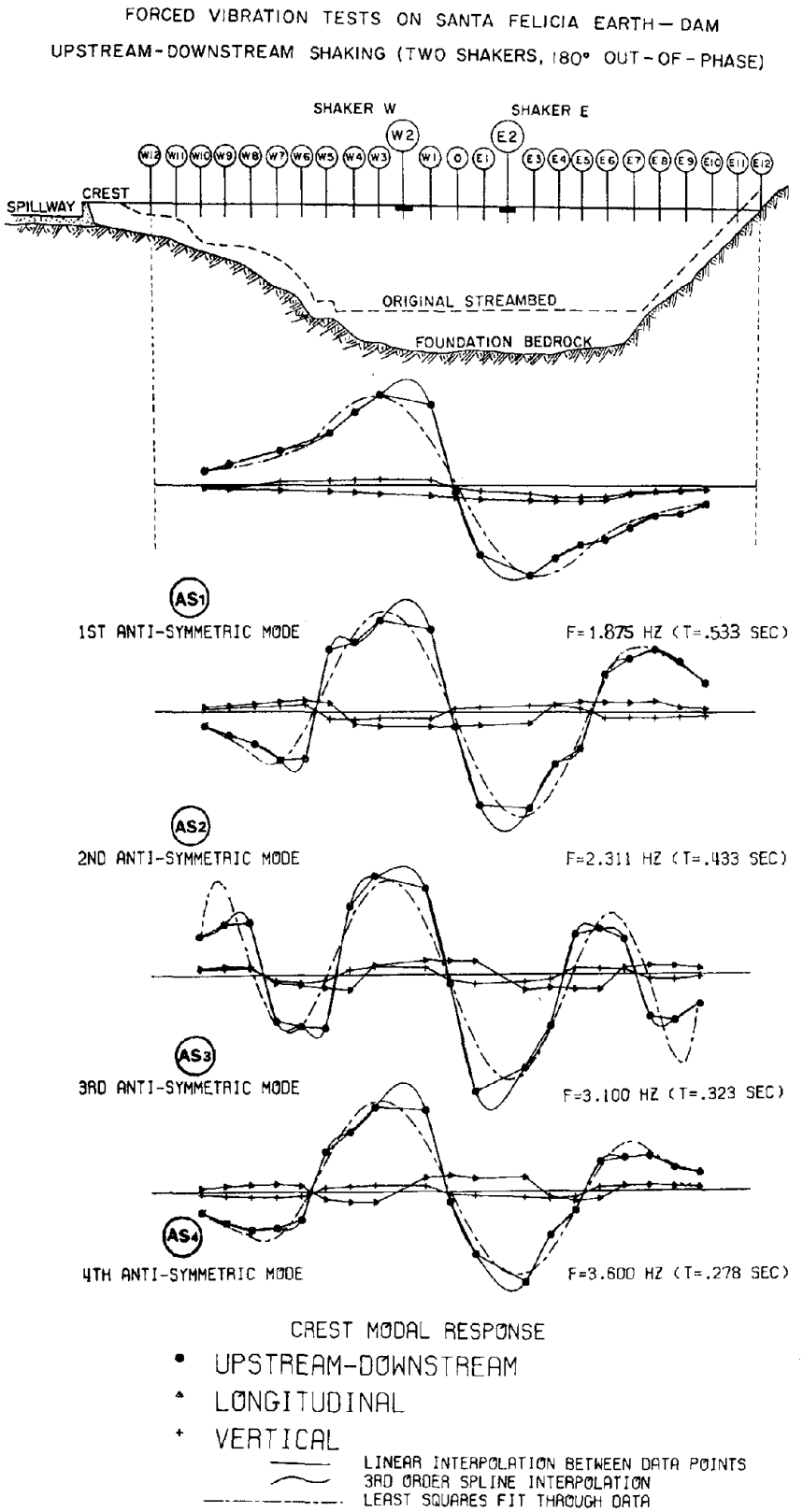

Fig. 35. The first four measured antisymmetric shear mode shapes. (Three-dimensional measurements along the crest.)

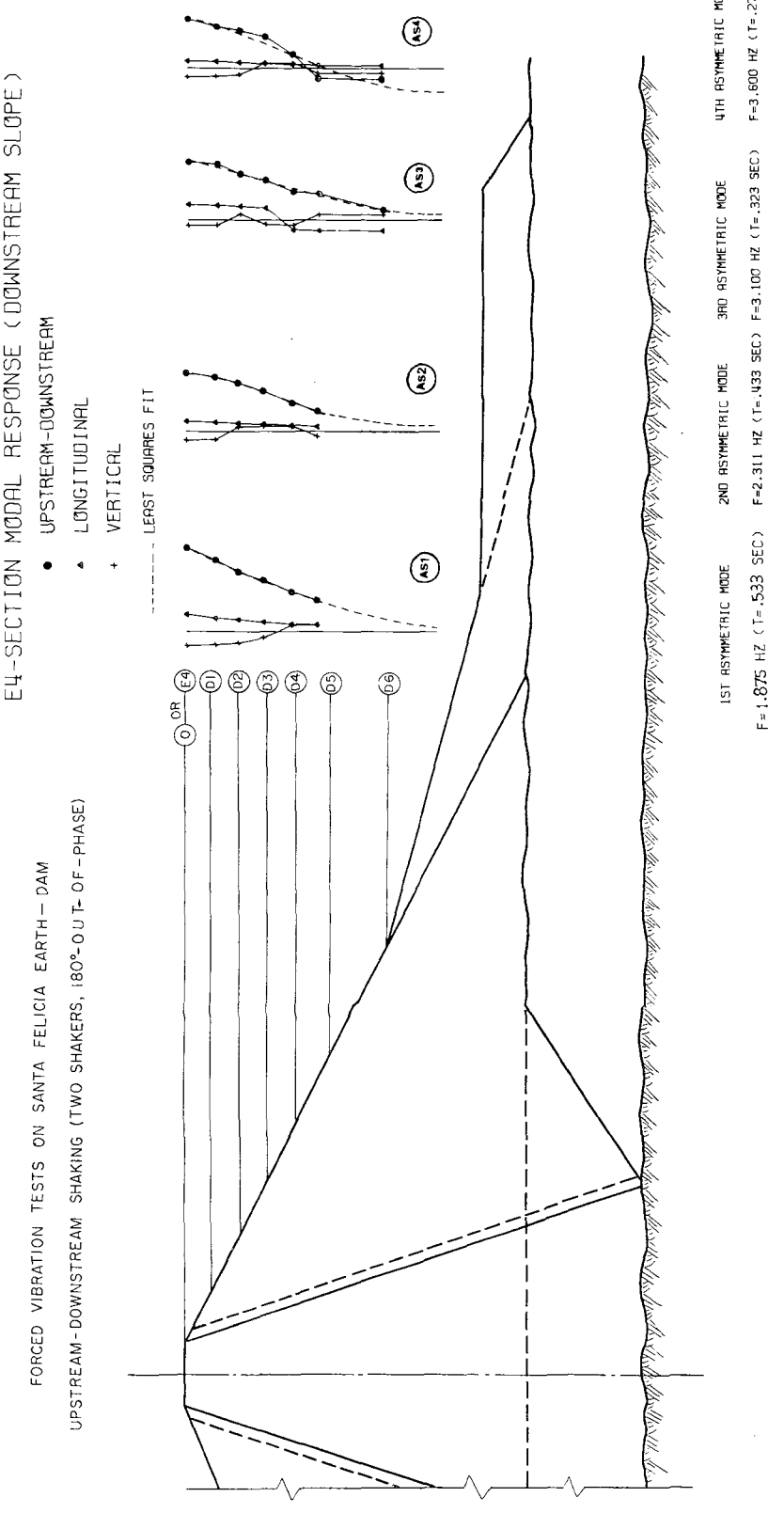

Fig. 36. The first four measured antisymmetric shear mode shapes. (Three-dimensional measurements along the downstream face.)

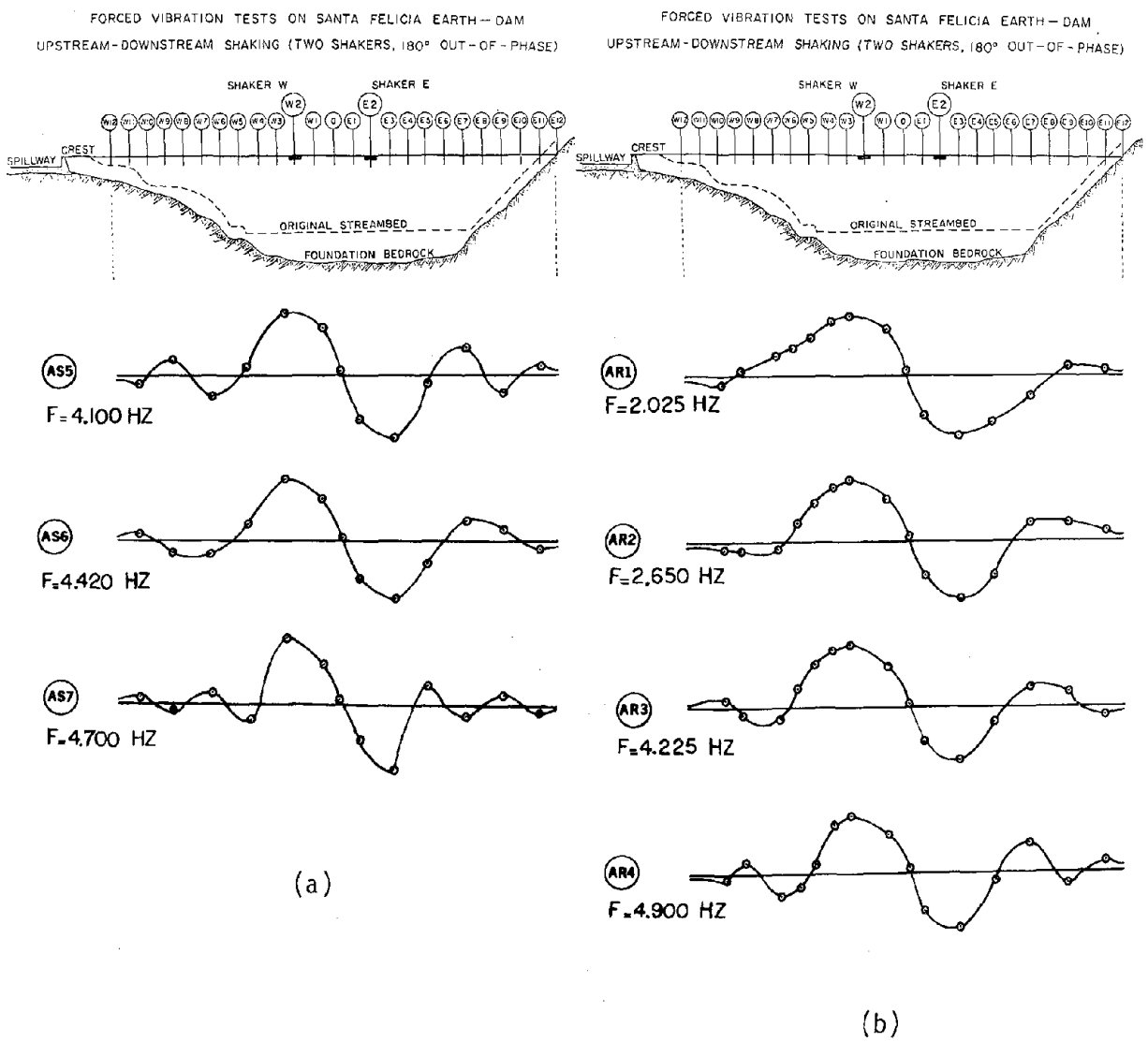

Fig. 37. Measured antisymmetric mode shapes determined during the frequency sweep tests. (a) Some shear modes. (b) Rocking modes.

mine the signs of the modal displacements. Repeating this procedure for all stations where measurements were made, the mode shape amplitudes were determined.

These shapes do not correspond to ideal versions of the mode shapes (sinusoidal shapes) because of the varying width of the valley in which the dam is built, and the nonhomogeneous nature of the construction material. The importance of recording at a number of stations will be recognized from these diagrams, since at some nodal points in a particular mode, essentially no movement occurred. The peak displacement response in the first symmetric shear mode at the center of the dam in this investigation is about 0.0034 mm (this estimate is discussed in Appendix B), which corresponds to an acceleration of 0.0037% g. The spectral analyzer was of great help in determining the phase and amplitudes of some of the contaminated recorded sinusoidal signals (motion with varying amplitudes), particularly the U-D motions recorded from stations close to the two abutments and the longitudinal and vertical recorded responses of most of the stations. These were determined by computing and displaying (in the Vibration Laboratory) the cross-correlation function (or cross-power spectrum) and the Fourier amplitude spectrum of any affected station and the reference station.

It is important to mention that during the frequency sweep tests the shapes of the residual shear modes (of Figs. 34a and 37a) and the shapes of the rocking modes (of Figs. 34b and 37b) were obtained from the recorded upstream-downstream motions. In some instances, the resonance curves of a certain vibration run were examined, and the resonant frequency of an unclear mode was determined; then, before conducting any additional

sweeps, the dam was excited into this unclear mode, and a different deployment of the seismometers on the dam was made to cover the entire dam. By so doing, a very clear idea of the modal configurations in the U-D direction was obtained, as indicated by Figs. 38, 39, and 40 for modes S6, AS2, and AR2, respectively. This shows the importance of performing some analysis simultaneously with the field tests. If only the field results at selected field stations had been determined before terminating the field work, such modes would have remained indistinct.

It should also be noted that the forced vibration tests indicated that the magnitude of the interaction between the shaker concrete-block and the surrounding soil in the dam crest was such that modal amplitude measurements in the vicinity of the two shakers were distorted. Consequently, the modal amplitudes of Figs. 32 through 37 at shaker stations E2 and W2 were modified (reduced) by comparing the measured amplitude in the vicinity of the shaker to those from later measurements on the downstream slope and at other adjacent stations on the crest, where the influence of the block-soil interaction was negligible. It will be seen in this report (Section VI-1-5) that the measured displacements of the shaker block, which reflect the local response of the block and the surrounding soil superimposed on the response of the dam as a whole, are considerably larger than the estimated displacements for the dam alone; measurements taken at distances greater than 20 to 30 ft from the vibration generators did not appear to be influenced by the block-soil interaction.

The peaks in Figs. 22 through 27 can be identified by reference to symmetrical and antisymmetrical mode shapes of Figs. 32 through 37.

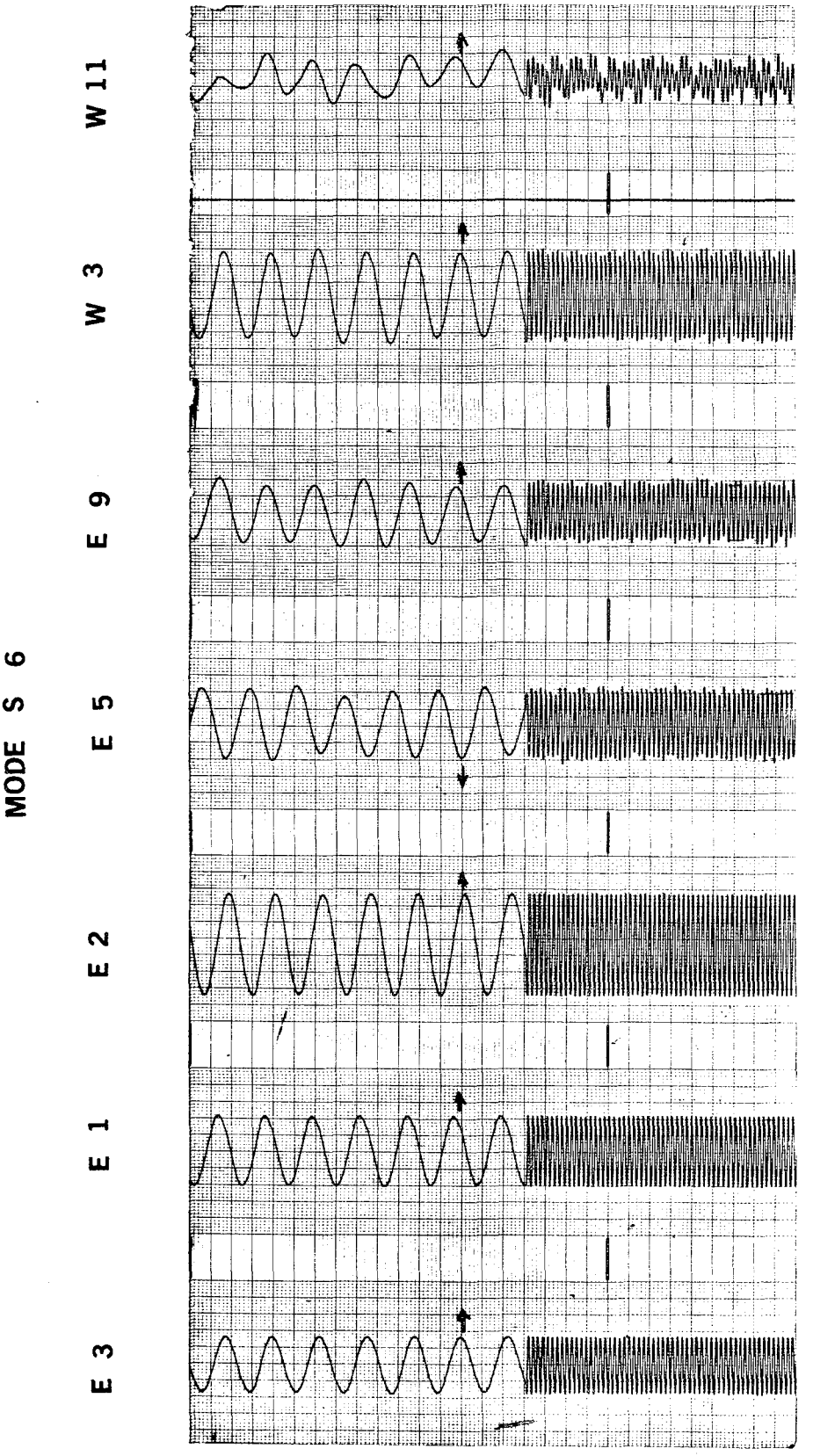

Fig. 38. Preliminary mode shape determination from the frequency sweep tests. (Note: The arrows show the in-phase and the out-of-phase motions.)

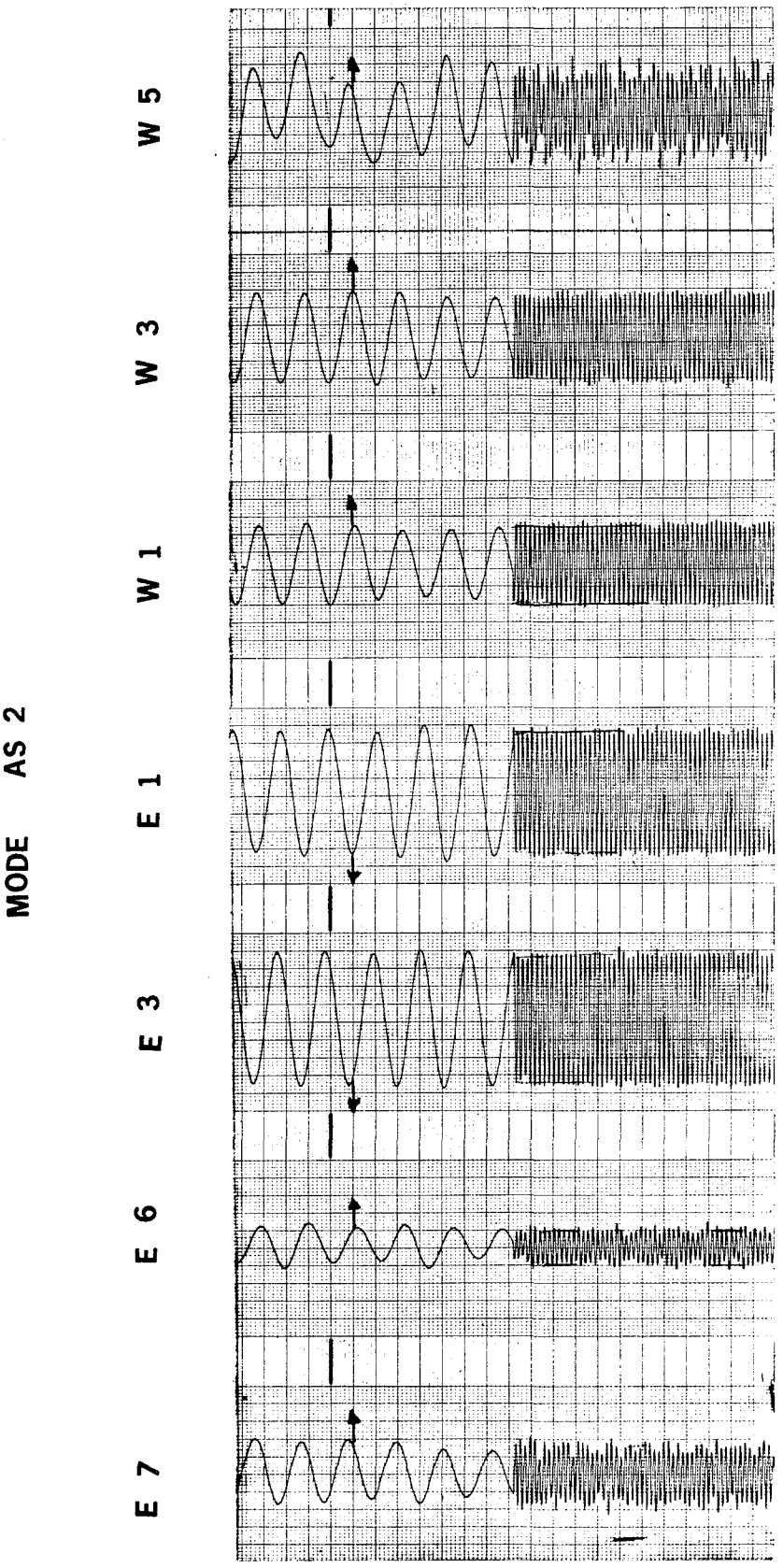

Fig. 39. Preliminary mode shape determination from the frequency sweep tests. (Note: The arrows show the in-phase and the out-of-phase motions.)

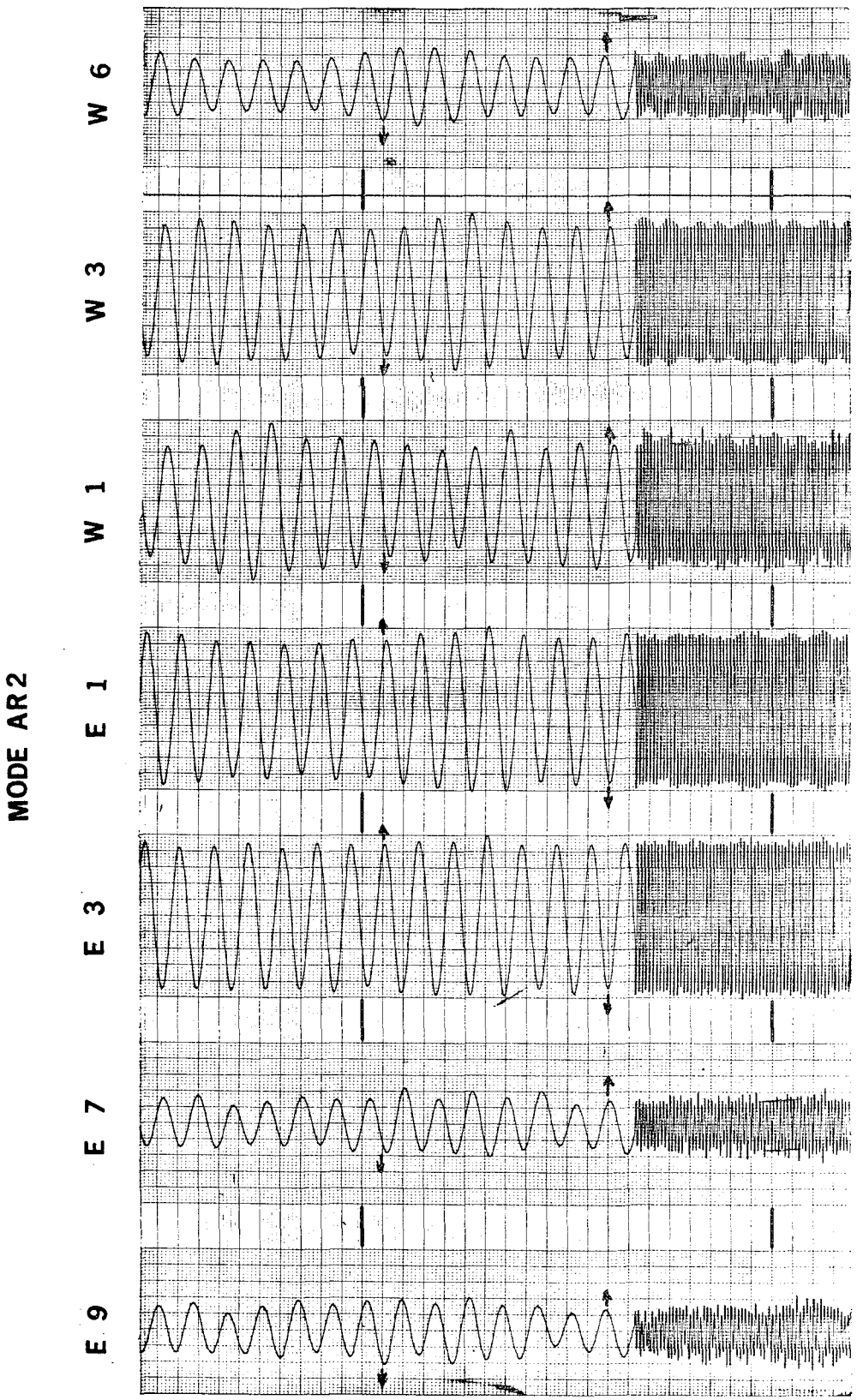

Fig. 40. Preliminary mode shape determination from the frequency sweep tests. (Note: The arrows show the in-phase and the out-of-phase motions.)

Peaks designated by S (or AS) correspond to symmetric (or anti-symmetric) shear modes. The term "shear" mode is defined as a mode whose deformation pattern resembles that predicted by the 2-D shear-beam theories for a triangular wedge in a rectangular canyon as shown in Fig. 31 for the first symmetric and antisymmetric modes. The shear-beam (wedge or slice) theory is popularly used and has been presented in more detail elsewhere (Refs. 3, 13, 14, and 15). Also, more discussion of the shear-beam theory and the results of these tests will be presented in the next section (VI-1-3) of the analysis.

Peaks designated by R (or AR) are believed to be either rocking modes (Ref. 15) as shown schematically in Fig. 41 for the first measured-symmetric mode (R1), or indications of upstream-downstream motion associated with longitudinal or vertical vibrations. Rocking modes could be a result of the vibrational moments generated by the horizontal sinusoidal forces from the shaking machines; each peak is between 2000 and 5000 lbs and has a moment arm of about 20 inches which produces a maximum moment at the crest of 80,000 to 200,000 lb-in. The recorded motion for the so-called rocking modes, along the downstream side, was more complicated than the motion resulting from the predominantly shear modes. These rocking modes have never shown up in previous full-scale measurements of earth dams (Refs. 4, 13, 14, 15, and 17), but the finite element idealization developed by Clough and Chopra (Ref. 5) and by Martin (Ref. 15) has predicted this kind of upstream-downstream rocking mode.

Examination of the resonance curves of Figs. 22 through 27 shows that, except for the first few modes (R1, R2, AR1, and AR2), the peaks of

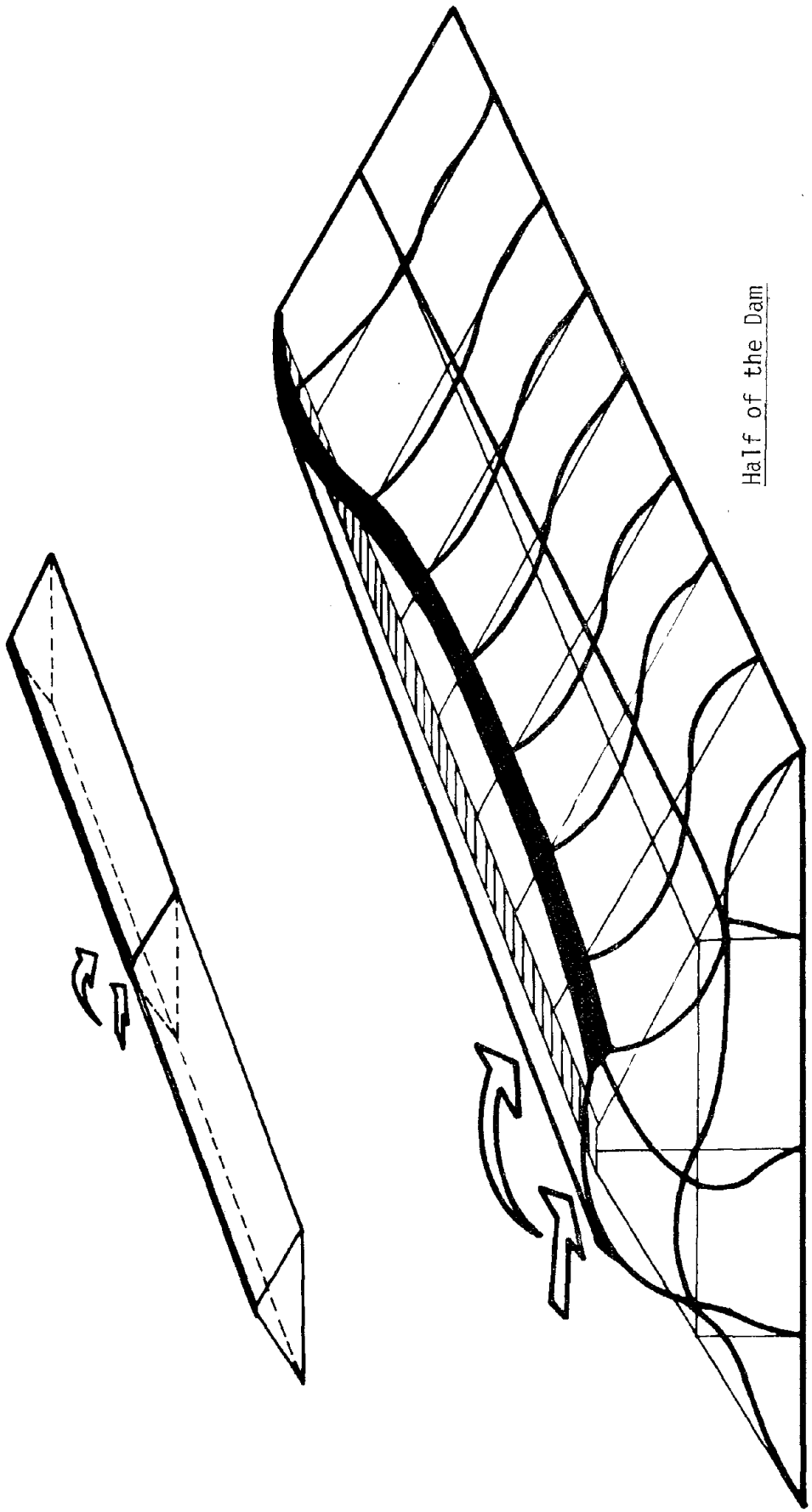

Fig. 41. Schematic diagram showing the first rocking mode of an earth dam.

the higher rocking modes are not as sharp and clear as those for the shear modes. The rocking modes' configurations (associated with frequencies listed in Tables 2 and 3) appear almost as transitions from the preceding to the following shear modes, as shown in Figs. 34 and 37. Examples of this are:

a - Mode R1 as a transition from S1 to S2

b - Mode R3 as a transition from S2 to S3

c - Mode AR1 as a transition from AS1 to AS2, ... etc.

Finally, an interesting feature of the data in Tables 2 and 3 is the closeness of each symmetric resonant frequency to a corresponding antisymmetric one. For example, the following modes are very closely spaced in the frequency domain:

R1 and AS1	S2 and AR1
R2 and AS2	S3 and AR2
R5 and AS3	R5 and AS3
S4 and AS4	R6 and AS6
S7 and AS7	

Experimentally, a structure with such close or repeated natural frequencies would be expected to exhibit a variety of mode shapes at the same frequency. Later in the analysis, another type of frequency similarity is found between the upstream-downstream frequencies and the longitudinal resonant frequencies.

Table 4 illustrates the amplitude of sinusoidal forces related to the U-D natural frequencies; it also shows the frequency differences among all the U-D resonating modes.

Table 4

Amplitude of Sinusoidal Forces Needed to Excite the U-D Natural Frequencies

Upstream-Downstream Direction Santa Felicia Earth Dam

Symmetrical Shaking				Antisymmetrical Shaking				Freq. Difference of U-D
Mode	Measured Freq. (Hz)	Freq. Difference	Total Force (lb)	Mode	Measured Freq. (Hz)	Freq. Difference	Force/ Shaker (lb)	
S1	1.635	0.000	4301	-	-	-	-	0.000
R1	1.850	0.215	5507	-	-	-	0	0.215
-	-	-	-	AS1	1.875	0.000	2829	0.025
-	-	-	-	AR1	2.025	0.150	3299	0.150
S2	2.100	0.250	7096	-	-	-	-	0.075
R2	2.270	0.170	8291	-	-	-	0	0.170
-	-	-	-	AS2	2.300	0.275	4256	0.030
R3	2.600	0.330	7747	-	-	-	-	0.300
-	-	-	-	AR2	2.650	0.350	4024	0.050
S3	2.840	0.240	9243	-	-	-	-	0.190
R4	2.920	0.080	9771	-	-	-	-	0.080
-	-	-	-	AS3	3.100	0.450	1898	0.080
R5	3.150	0.230	3919	-	-	-	-	0.050
S4	3.550	0.400	4978	-	-	-	-	0.400
-	-	-	-	AS4	3.600	0.500	2555	0.050
S5	3.870	0.320	5915	-	-	-	-	0.270
-	-	-	-	AS5	4.100	0.500	3320	0.230
-	-	-	-	AR3	4.225	0.125	3526	0.125
S6	4.300	0.430	7304	-	-	-	-	0.075
-	-	-	-	AS6	4.420	0.195	3859	0.120
R6	4.450	0.150	7822	-	-	-	-	0.030
S7	4.665	0.215	8578	-	-	-	-	0.215
-	-	-	-	AS7	4.700	0.280	4363	0.035
-	-	-	-	AR4	4.900	0.200	4742	0.200
S8	5.257	0.592	7738	-	-	-	-	0.357

VI-1-3 Comparison with Results of 2-D Shear-Beam Theory

To estimate the shear wave velocity within the dam material from the observed resonant frequencies and to check the values of the measured resonant frequencies, a two-dimensional homogeneous medium shear beam theory was used. The natural frequencies and modes of shear vibration determined by this theory are given by (Refs. 3, 12, 13, 14, and 15):

$$\omega_{n,r} = \frac{\sqrt{s}}{h}\left[\beta_n^2 + \left(\frac{r\pi h}{\ell}\right)^2\right]^{1/2} \quad , \quad n,r = 1,2,3,\cdots \qquad (1)$$

and

$$\phi_{n,r}(y,z) = J_o(\beta_n \frac{y}{h}) \sin(\frac{r\pi z}{\ell}) \quad , \quad n,r = 1,2,3,\cdots \qquad (2)$$

where $\omega_{n,r}$ is the $(n,r)^{th}$ natural frequency (circular), v_s is the shear wave velocity within the dam ($v_s = \sqrt{G/\rho}$, G is the shear modulus of the dam material, and ρ is its mass density), h is the height of the dam, β_n ($n = 1,2,3,\cdots$) are the roots of the Bessel function of zero order of the first kind, $J_o(\beta_n)$, [e.g., $\beta_1 = 2.4048$, $\beta_2 = 5.5201$, $\beta_3 = 8.653$, etc.], ℓ is the length of the dam (a rectangular canyon), y is the depth coordinate, and z is the length coordinate.

For symmetric modes, $n = 1,2,3,4,\cdots$ and $r = 1,3,5,7,\cdots$, while for antisymmetric modes, $n = 1,2,3,4,\cdots$ and $r = 2,4,6,8$. For this 2-D theory of a triangular wedge in a rectangular canyon, the trapezoidal canyon of Santa Felicia Dam (Fig. 3) is represented by an equivalent rectangle of length ℓ equal to the average of the crest length and the length of the base of the trapezoidal section, i.e., $\ell = 0.5\ (1275 + 450) = 912.5$ ft. Substituting values $h = 236.5$ ft and $f_{1,1} = \omega_{1,1}/2\pi = 1.635$ Hz (measured natural frequency of first U-D shear mode) and $\ell = 912.5$ ft, in Eq. (1), gives a value of v_s equal to 957 ft/sec. This is fairly close to the

value obtained by in situ wave-velocity measurements on the dam (Ref. 2) which show that there is a shear-velocity variation as the depth changes, but a range of v_s between 850 ft/sec and about 1070 ft/sec is a representative range for the dam material. Also, by substituting the value of the measured first antisymmetric shear frequency $f_{1,2} = \frac{\omega_{2,1}}{2\pi} = 1.875$ Hz in Eq. (1), the resulting v_s is equal to 959 ft/sec which is very close to the one from the first symmetric mode.

The values of higher frequencies ($> f_{1,1}$ or $> f_{1,2}$) were therefore computed by substituting the value of $v_s = 958$ ft/sec in Eq. (1); these computed natural frequencies are listed in Table 5 where they have also been compared with those observed from symmetric and antisymmetric shakings. The only measured shear modes (taken from Tables 2 and 3) which have been shown in Table 5 are similar in configuration to those predicted by Eq. (2) (which are also shown in Table 5).

On the basis of the information contained in the resonance curves (Figs. 22 through 27), the plots of U-D mode shapes (both shear and rocking modes of Figs. 34 and 37), the plots of 3-D components of shear modes (Figs. 32, 33, 35, and 36), and Tables 2, 3, 4, and 5 of upstream-downstream modes of vibration obtained for measurements involving different seismometer locations and orientations, the following conclusions may be drawn:

1. Values of the observed resonant (shear) frequencies vary slightly from those predicted by Eq. (1) (the measured resonant frequencies are lower than the computed frequencies by from 3 percent to 17 percent), but overall it is fair to say that the correspondence between the observations and Eq. (1) is good over the entire frequency range evaluated. The computations were based on the

Table 5

Comparison Between Observed Resonant Frequencies (From the Uperstream-Downstream Shaking)

and Those Computed by the 2-D Shear-Beam Theory

Santa Felicia Earth Dam

SYMMETRIC VIBRATION							ANTISYMMETRIC VIBRATION						
2-D SHEAR-BEAM THEORY (Based on the Observed First Frequency 1.635 Hz)		Symmetric Shaking		Error Percent	Mode Shape as Predicted by the 2-D Shear-Beam Theory		2-D SHEAR-BEAM THEORY (Based on the Observed First Frequency 1.635 Hz)		Antisymmetric Shaking		Error Percent	Mode Shape as Predicted by the 2-D Shear-Beam Theory	
Mode n,r	Frequency $f_{n,r}$	Measured Frequency (Hz)	Desig-nation		Along the Crest	Along the Downstream Side	Mode n,r	Frequency $f_{n,r}$	Measured frequency (Hz)	Desig-nation		Along the Crest	Along the Downstream Side
1,1	1.635	1.635	S1(1,1)	0.0	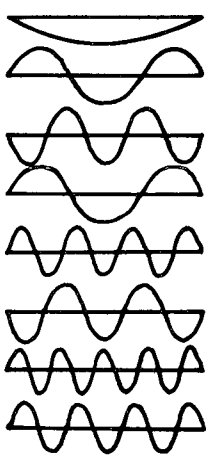		1,2	1.872	1.875	AS1(1,2)	0.2	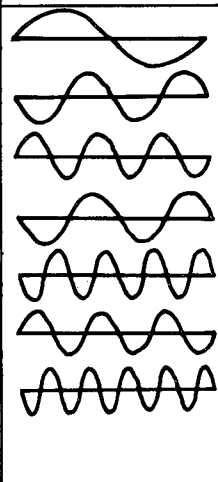	
1,3	2.209	2.100	S2(1,3)	5.2			1,4	2.610	2.300	AS2(1,4)	13.5		
1,5	3.048	2.840	S3(1,5)	7.3			1,6	3.510	3.100	AS3(1,6)	13.2		
2,1	3.595	NO?	NO?				2,2	3.710	NO?	NO?	NO?		
2,3	3.891	3.550	S4(2,3)	9.6			2,4	4.131	3.600	AS4(2,4)	14.8		
1,7	3.987	3.870	S5(1,7)	3.0			1,8	4.476	4.100	AS5(1,8)	9.2		
2,5	4.421	4.300	S6(2,5)	2.8			2,6	4.752	4.420	AS6(2,6)	7.5		
1,9	4.971	4.665	S7(1,9)	6.6			1,10	5.470	4.700	AS7(1,10)	16.4		
2,7	5.115	5.257	S8(2,7)	2.7									

assumption of a rigid foundation for the dam, a rectangular canyon, an average value for the shear wave velocity of 958 ft/sec, and only elastic shear (low strain level) deformations in the horizontal direction (U-D). If the flexibility of the foundation and abutments (end restraints) were taken into account, the computed values would decrease.

2. Because of the selected deployment of the two shakers, it was possible to excite pure first (1,1) modal response (response characterized by all points in the dam moving in the same phase). Several trials were made in the field to measure modes (2,1) and (2,2) which have similar configurations to the first symmetric mode (1,1) and the first anti-symmetric mode (1,2) along the crest, and have a node along a vertical section like modes (2,3) and (2,4)). Unfortunately, these modes were never excited or measured during the forced vibration tests. Nor have these modes ever been measured and reported in the literature (Refs. 4,13,14,15, and 17). Instrumentation which would accurately (and less laboriously) measure the phase between the excitation and the response would be a welcome addition to the experimentalist's equipment and would be of great help in exploring these unmeasured modes.
3. If the total measured amplitude at each station is resolved into two components, one in phase with the exciting force, and one at 90° out-of-phase to the exciting force, and if the dam were to behave as a linear structure, then all of the response of the resonating mode would appear in the component at 90° out-of-phase to the exciting force. However, as a result of damping, all of the other modes of the dam would respond at phase angles other than 0° or 180° to the exciting force, and hence they would appear to some extent in the component

of response at 90° out-of-phase, depending on the amount of damping, the spacing of the natural frequencies, and the location of the exciting force on the dam.

4. The shear-beam theory (low levels of strain), although in reasonably good agreement with predominantly shear-like modes, does not predict all upstream-downstream motion modes, hence indicating the inadequacy of the theory for earthquake response (high levels of strain) computations. In order to achieve agreement between the computed and all of the observed frequencies, it appears that a representation of the dam more sophisticated than that provided by shear-beam (or wedge) theory is needed, and possibly a more accurate knowledge of the physical properties of the soil in the dam is also required. A possible improvement of the 2-D shear beam theory with constant soil properties along the dam depth, may be attained by assuming, for instance, that the shear modulus G varies with depth (say, $G \propto y^{1/3}$ or $G \propto y^{2/5}$); this has not been tried in this investigation.

5. From the shapes of the first four measured symmetric (and antisymmetric) shear modes at peak amplitudes, obtained from the simultaneously-recorded three components (U-D, L, and V), it is seen that the upstream-downstream modal motions are accompanied by contributions from the longitudinal as well as the vertical motions; these contributions range between 10% and 25%, as shown in Figs. 32, 33, 35, and 36. Sample traces from the oscillograph recorder made simultaneously during the antisymmetric shaking of mode AS1 at stations W1 and W6 are shown in Fig. 42. For the symmetric vibration, along the crest the longitudinal and vertical motions are similar to the U-D

configuration (Fig. 32), while along the downstream slope there are some disagreements (Fig. 33). For the antisymmetric vibration the configuration of the longitudinal component is similar to that of the U-D but the vertical component is completely different along the crest. And again, there are disagreements among the three components along the downstream face. This leads to the conclusion that although a three-dimensional representation of the dam is costly, it will surely provide the most information description of the dam's vibrations.

VI-1-4. Damping Values

Although the response curves from the forced vibration tests would probably yield the most reliable values of damping belonging to each mode of vibration, modal damping values for all the measured U-D modes (S's, AS's, R's, and AR's) were determined by the logarithmic decrement method, applied to recordings of the damped free vibration of each mode of the dam. This was done because the width of the modal peaks of the response (resonance) curves determined from the shaker excitations of the structure were generally not suitable for the determination of modal damping values as is obvious from Figs. 22 through 27. However, modal damping for a few modes (where the spectral or modal peaks were well defined at the 0.707 points) were calculated on the basis of the width of the modal peaks of the response curves (as shown in Table 6).

The last measurements for every modal determination involving a sinusoidal shaker excitation were made by recording the damped free vibrations of the dam immediately after discontinuing the power to the vibration generating system. Simultaneous recordings were made in the U-D direction, usually at the reference station (W1) and at some other station

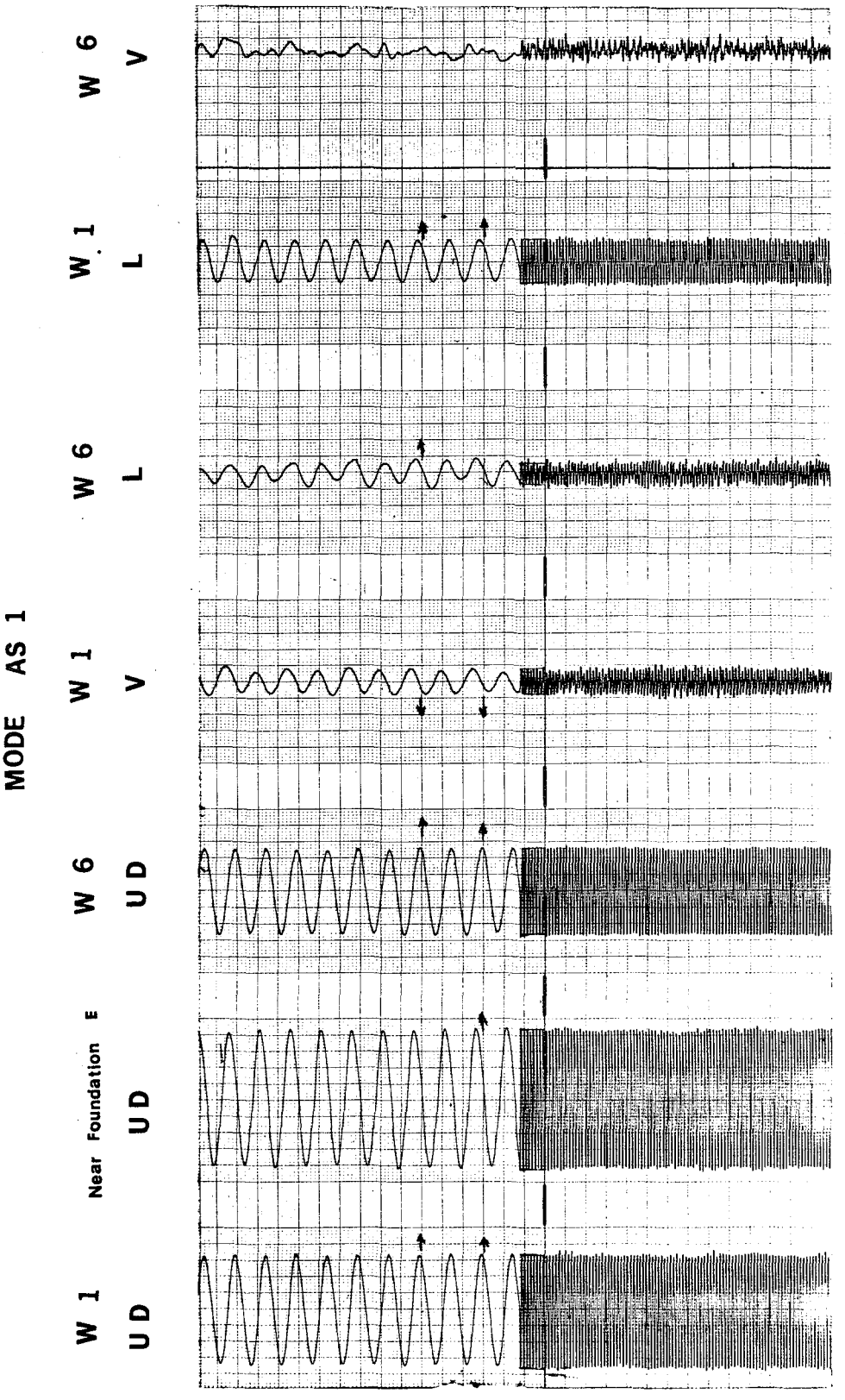

Fig. 42. Sample traces from the oscillograph recorder made simultaneously, during the antisymmetric shaking of mode AS1, at Stations W1 and W6. (Note: The arrows show the in-phase and the out-of-phase motions.)

(usually the location of the last test run). Recordings were made for each identifiable natural frequency, and care was taken to record as many cycles of the decaying sine wave as could be accurately described (see Fig. 43). The upper trace of Fig. 43 shows a case where the point at which the shaker stopped is included (note that the recording speed during the free vibration is different from the speed during the steady-state vibration). In most cases, the time it took the shaker to coast down was not recorded.

Damping is calculated from damped free vibrations by comparing the relative values of successive peaks of the damped sinusoid (Fig. 43). Unfortunately, this comparison may only be made by assuming that the system is basically linear. In order to estimate the damping of a nonlinear dam-type structure, the exciting force should be plotted against the structural displacement of the dam to produce the hysteretic response at the modal frequency of interest; the area inside the resulting hysteretic loop is proportional to the energy dissipated by the structure.

In most cases, the damped sinusoids measured exhibit contamination from nearby modal resonances, as seen in Fig. 43. Even though the energy from the contaminating frequencies may be small compared to the energy in the mode of interest, the effect on the damping calculation may be quite significant. The effect usually recorded by the interference of another mode is a mild modulation (or beating effect) caused by the contaminating frequency periodically occurring in phase and out of phase with the principal frequency of interest. This periodic modulation of the exponential envelope of the sinusoidal decay results in an equivalent periodic fluctuation in the damping values calculated from successive peaks of the decay. Such periodic modulations of the calculated damping values complicates the

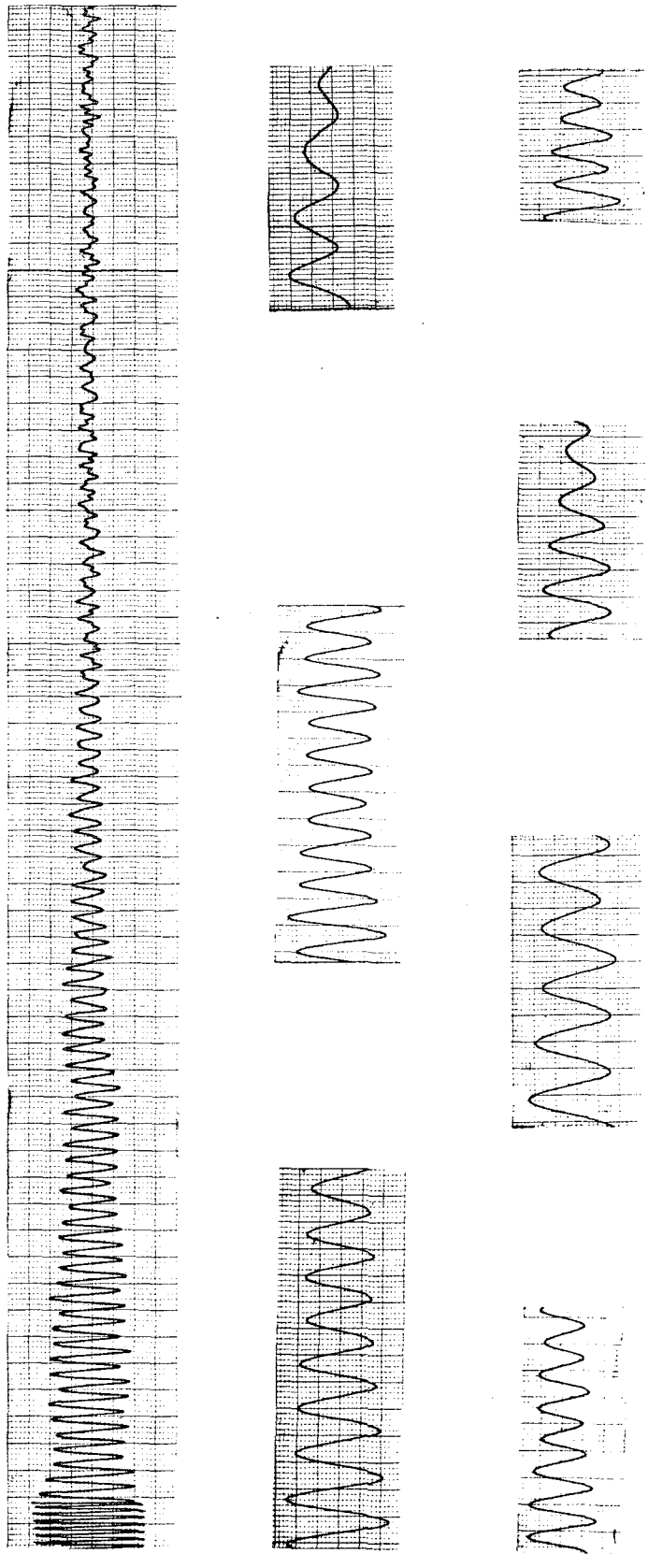

Fig. 43. Sample traces from the oscillograph recorder made separately during recordings of the damped free vibrations of the dam (immediately after discontinuing the power to the shakers.)

identification of the unique damping value for a given mode. In Table 6 the damping determined by averaging the values achieved for every possible number of cycles per record is presented.

It is seen from Table 6 that the modal damping values determined from the width of the modal peaks of the response curves are higher than those determined from the logarithmic decrement method. The damping values determined from the latter are seen to vary from 1.8% to 3.2% of critical damping, and the maximum shear strains in the dam, computed by the 2-D shear-beam theory (Appendix B) were correspondingly small (for example, for the first U-D symmetric shear mode, S1, they were only in the order of 0.72×10^{-5}%).

In addition, damping values which were determined from resonances at one station on the dam showed in some instances good agreement and in other instances disagreement with damping values determined at other stations. In addition to the two above observations, the impossibility of measuring the phase relationship between the exciting force and the response of the dam (mentioned previously) made damping values determined from the logarithmic decrement method more reliable than those determined from the response curve (half-power bandwidth method). In addition, it will be shown in the ambient vibrations section that the damping values determined from the logarithmic decrement method are close to those determined from the Fourier amplitude spectra of the ambient excitations.

Finally, the measurements did not permit determination of the actual mechanism of energy dissipation in the dam. Some of the energy imparted to the dam by shaking was dissipated by radiation into the foundation and abutments, and some was consumed by hysteretic damping in the dam material

Table 6

Estimated Damping Ratios from Both the Free Damped Vibration and the Response Curves of the Upstream-Downstream Shaking

Santa Felicia Earth Dam

Mode	Measured Damping Ratio (Percent)		Measured Frequency (Hz)
	Average from Damped Free Vibration	Average from Response Curves	
S1	3.2	-	1.635
R1	3.1	-	1.850
AS1	3.0	-	1.875
AR1	3.1	-	2.025
S2	2.9	4.5	2.100
R2	3.0	-	2.270
AS2	2.9	4.9	2.300
R3	2.7	-	2.600
AR2	2.8	4.7	2.650
S3	2.6	4.8	2.840
R4	2.7	-	2.920
AS3	2.7	4.8	3.100
R5	2.6	-	3.150
S4	2.5	3.5	3.550
AS4	2.4	3.8	3.600
S5	2.3	3.9	3.870
AS5	2.5	-	4.100
AR3	2.3	-	4.225
S6	2.2	-	4.300
AS6	2.1	-	4.420
R6	2.2	-	4.450
S7	2.0	2.7	4.665
AS7	1.8	2.7	4.700
AR4	2.0	-	4.900
S8	1.9	3.8	5.257

itself, but the relationship between the two could not be determined.

A final note: the estimated damping values for the dam are somewhat higher than those usually encountered for steel and concrete building structures for the same low levels of excitation. Moreover, it was found, for most steel and concrete building structures, that the damping values, estimated from full-scale tests, tend to increase from lower fundamental modes (where they range from 0.5 to 2%) to higher, say fourth to sixth modes (where they range from 3 to 6%) and that the change is less pronounced for values estimated from recorded earthquake responses. Because of the nonlinear behavior of building structures, close agreement between the full-scale tests and earthquake values is generally not expected. Unlike these building structures, Table 6 shows that the dam damping values are not mode-dependent (for a wide range of modes); the low-strain damping was 2.5-3.0% for all important modes.

VI-1-5. Interaction of the Shaker Block and Surrounding Soil

There is a scarcity of field data in the complex soil-structure interaction problem, making the corroboration of the varied analytical solutions all the more difficult.

The opportunity arose, during the course of the investigation of the dynamic characteristics of the dam, to measure surface ground motions (on the crest) in the vicinity of one of the concrete blocks (slabs) that supported the shaking equipment.

As can be seen from Figs. 7, 41, and 43, the spinning baskets of the shakers develop an oscillating shear force and moment on the concrete block, which in turn can cause local perturbations in the soil. The total exciting force acting on the dam is equal to the inertia force created by

the mass of the block and the shakers, plus the shaking force.

The object of this section of the report is to examine the effect of the magnification of the local displacements in the vicinity of the shakers upon the mode shapes. It also presents a simple comparative study of recorded ground motions and an analytical solution to the soil-structure interaction problem, using much of the data on the material and dynamical properties of the dam derived from the earthquake response of the dam (Ref. 2) and from the full-scale dynamic tests.

Unfortunately, no absolute measurements of displacements were taken, only the relative motions recorded by the seismometers. In order to quantify these motions, the 2-D shear-beam theory was used to define a central crest displacement due to point loads applied to the dam; the equation of motion and solution can be found in Appendix B. The horizontal displacement at the crest midpoint (station 0) was estimated using the 2-D shear-beam theory and much of the data of the material and dynamical properties of the dam derived from its earthquake responses (Ref. 2). It was assumed that the whole width of the crest at station 0 had the same upstream-downstream displacement; there was no evidence of local displacement effects of the two shakers at this station. Then the single-seismometer displacement output at station 0 was correlated with the estimated displacement to find how many divisions on the oscillograph paper will give, say, an inch displacement for a given sensitivity and attenuation (i.e., to find approximate calibration values). The seismometer measurement of the surface ground motions (on the crest) in the vicinity of one of the concrete blocks (where the local displacements were dominant) that supported the shaking equipment scaled accordingly.

A discussion of difficulties and approximations involved in the analyses is given in this section too.

1. Shaker Interaction

With one shaker operating and the other stationary, horizontal displacements in the vicinity of the redundant shaker caused by the active shaker proved to be negligible. With both shakers active, displacement measurements around the east shaker (station E2) were assumed to be caused by that shaker alone, with no influence from the west shaker (station W2).

2. Shaker-Soil Interaction

a. Quantifying field measurements

The 2-D shear-beam theory was used to define a horizontal central crest displacement in the upstream-downstream direction. This was matched to the appropriate seismometer output recorded at known sensitivity and attenuation.

The output for the horizontal displacements around the east shaker block, recorded at various sensitivities and attenuations, were then appropriately scaled, and quantified by the known match of the central displacement record.

Using the results of Appendix B, the generalized displacement (for the first symmetric shear mode) at the central part of the dam can be written as

$$q_{1,1}(t) = 3.185 \times 10^{-8} \sin(\omega_{1,1} t - \tfrac{\pi}{2}) \text{ inches per lb force} \qquad (3)$$

The output amplitude a, recorded at frequency f, attenuation A, and sensitivity S, can be scaled to an equivalent amplitude a_o at f_o, A_o, and

S_o, through the general relation

$$a_o = a \times \frac{10^{A/20}}{10^{A_o/20}} \times \left(\frac{f_o}{f}\right)^2 \times \frac{S}{S_o} \qquad (4)$$

Through Eq. (4) and the force expression of Figs. 22, 23, and 24, quantitative values of horizontal displacements were determined at each measurement location around the east shaker (see Fig. 18).

b. Elastic half space analysis

No exact solution exists for the problem of a flexible embedded rectangular slab resting on the surface of a homogeneous semi-infinite mass, subjected to oscillating simultaneous tangential and vertical loading.

As a first approximation, the solution derived was that of the summation of the solutions to the tangential and vertical point loading of the surface of an elastic half-space (the Cerruti and Boussinesq problems, respectively).

(i) Dynamics: The dimensionless frequency for a rigid disk of radius r resting on the surface of a homogeneous half-space, excited at a frequency ω, is given by

$$f^* = r\omega\left(\frac{\rho}{G}\right)^{1/2} \quad , \qquad (5)$$

where ρ and G are the density and shear modulus of the half-space, respectively. For low values of f^* it has been shown that the compliances of the dynamic solution tend to unity, and so the problem reduces to the static solution for a point load (Ref. 19).

This principle is assumed to apply to rectangular footings also, and substitution into Eq. (5) of realistic values gives a maximum value for f^* of 1.3×10^{-2}. A static solution was therefore assumed to be a valid

approach.

(ii) Contact pressures: The relative flexibility of the slab with respect to that of the adjacent medium strongly influences the distribution of tangential and vertical pressures on the underside of the slab, due to point shear and moment forces on the upper side, respectively.

Considering the relative crudeness of the analysis, as a first approximation the distribution of contact pressures was assumed uniform for the tangential shear forces resulting from the horizontal shaker force, and linear for the vertical forces resulting from the applied moment.

The distributions of force acting on the underside of the discretized surface of the slab are illustrated in Figs. 44c and d. The relative magnitudes of force are to scale, for a unit applied horizontal shear force.

The influence of the moment-induced vertical forces on the local horizontal displacements is obviously small (but as it turns out, not insignificant).

c. Horizontal displacements

The horizontal surface displacements are given by

$$U(X,Y) = \sum_{i=1}^{N} \left\{ p_{H_i}(1+\nu_s)[1 + \frac{x_i^2}{r_i^2} + (1-2\nu_s)(1 - \frac{x_i^2}{r_i^2})] / 2\pi E_s r_i \right.$$
$$\left. - p_{V_i}(1+\nu_s)(1-2\nu_s)x_i / 2\pi E_s r_i^2 \right\} , \qquad (6)$$

where the lower-case x,y coordinates refer to the loaded surface, and the upper case X,Y coordinates refer to the zone outside the loaded area. N is the total number of points on the discretized surface, p_{H_i} and P_{V_i} are point horizontal and vertical forces, respectively, and

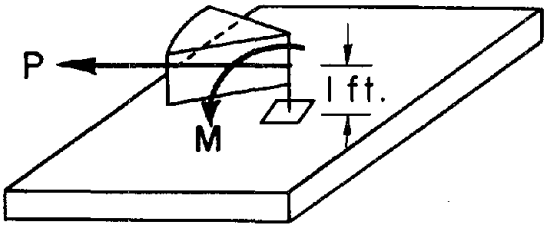

(a) Idealized Loading

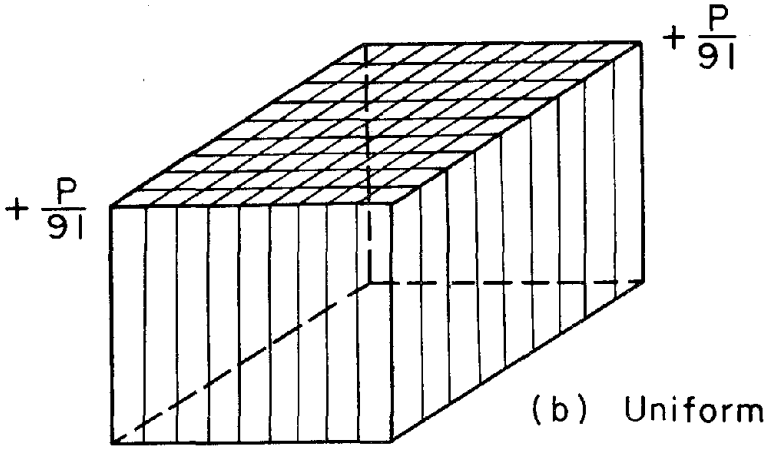

(b) Uniform Shear Forces

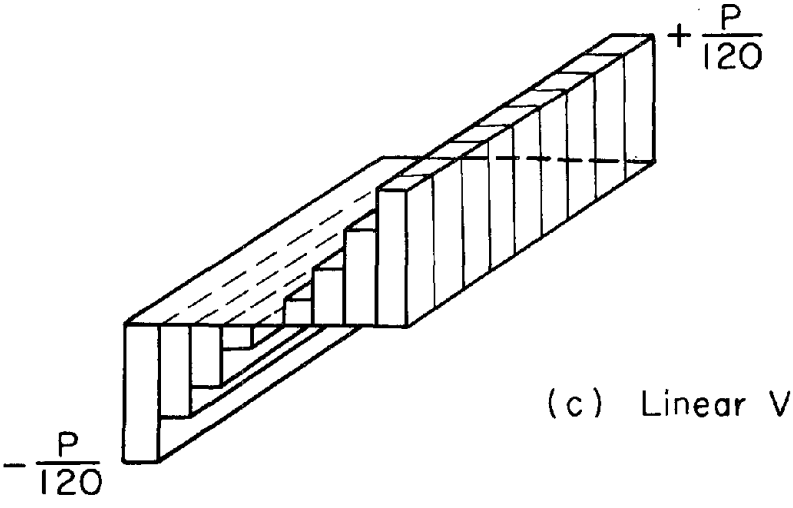

(c) Linear Vertical Forces

Fig. 44

$r_i = \sqrt{x_i^2 + y_i^2}$. The result of this approximate elastic solution is shown in Fig. 45.

For illustrative purposes, the infinite theoretical displacements under each of the point loads are cut off at a magnitude comparable with measured field motions of the block and surrounding soil.

3. Comparison of Results

Figure 46a shows the location where recorded seismometer measurements of horizontal crest motions were taken and shows their magnitudes as derived by the 2-D shear-beam theory. It also shows a topographic plot of the theoretical horizontal displacements as derived from the approximate elastic solution.

The decay of displacements, computed by both methods, perpendicular to and along the line of action of the shaking force, is shown in Figs. 46b and c, respectively.

The agreement between the two methods is remarkably good.

In the zone directly behind the shaker where the displacement gradients are highest (as might be expected), the discrepancy between the methods is largest. The rapid decay of the displacements during the field measurements at these higher strains emphasizes the nonlinear nature of the soil. In general, at points farther from the slab at lower strains, the rates of decay of the two solutions are similar.

4. Modal Amplitude Correction

As can be seen from Figs. 46b and c, the influence of the shaker-block interaction is negligible at distance ranges of from 20 to 30 ft (from the center of the block). At this distance the upstream-downstream

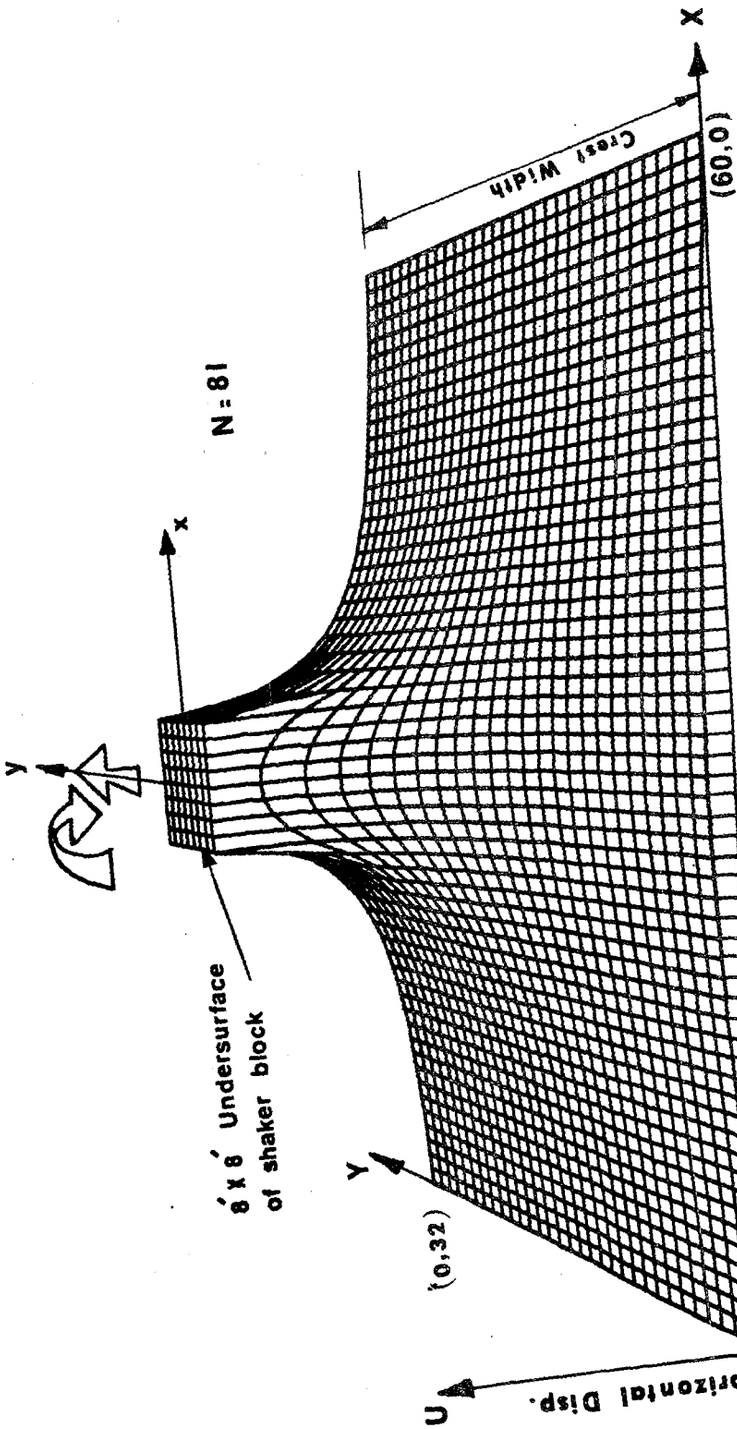

Fig. 45. Horizontal displacement distribution. (Scale: Each small block is 1 ft by 1 ft.)

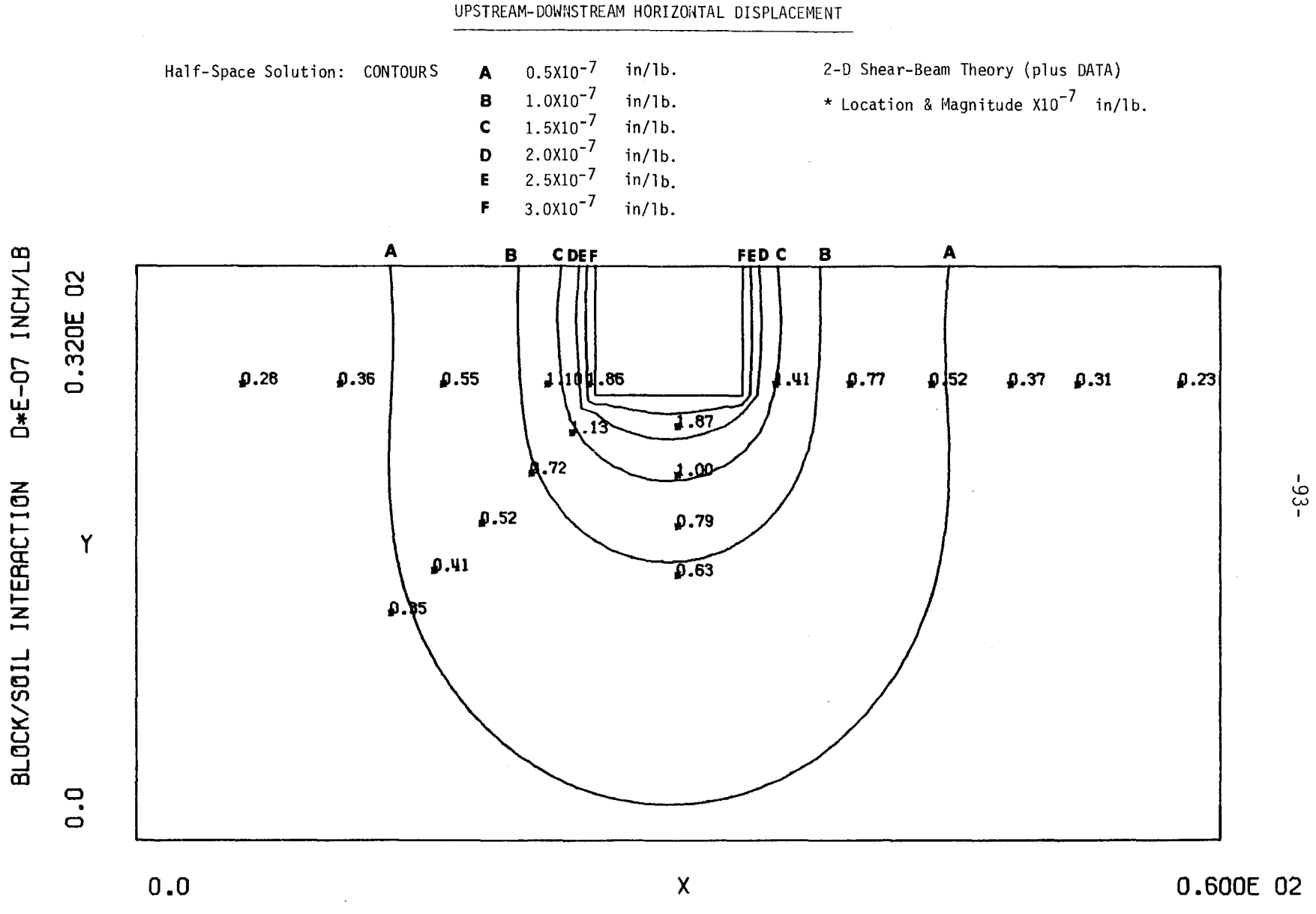

Fig. 46(a). Topographic plot of the U-D horizontal displacements.

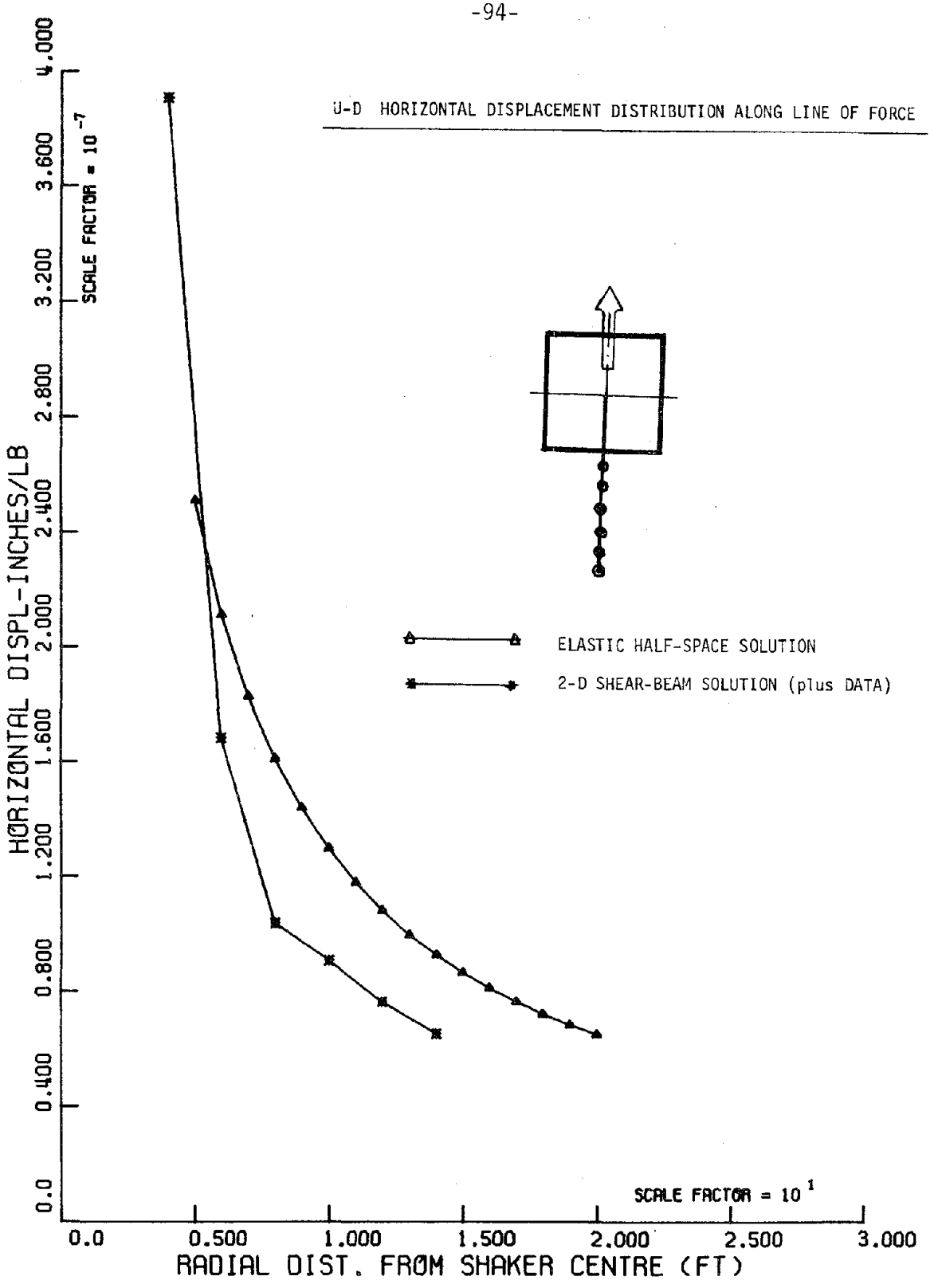

Fig. 46(b). (a) The 2-D theory was used to estimate the horizontal crest displacement (at Station 0); this was matched to the single seismometer output recorded at Station 0. Then the seismometers outputs around the shaker were appropriately scaled, and quantified by the known match.

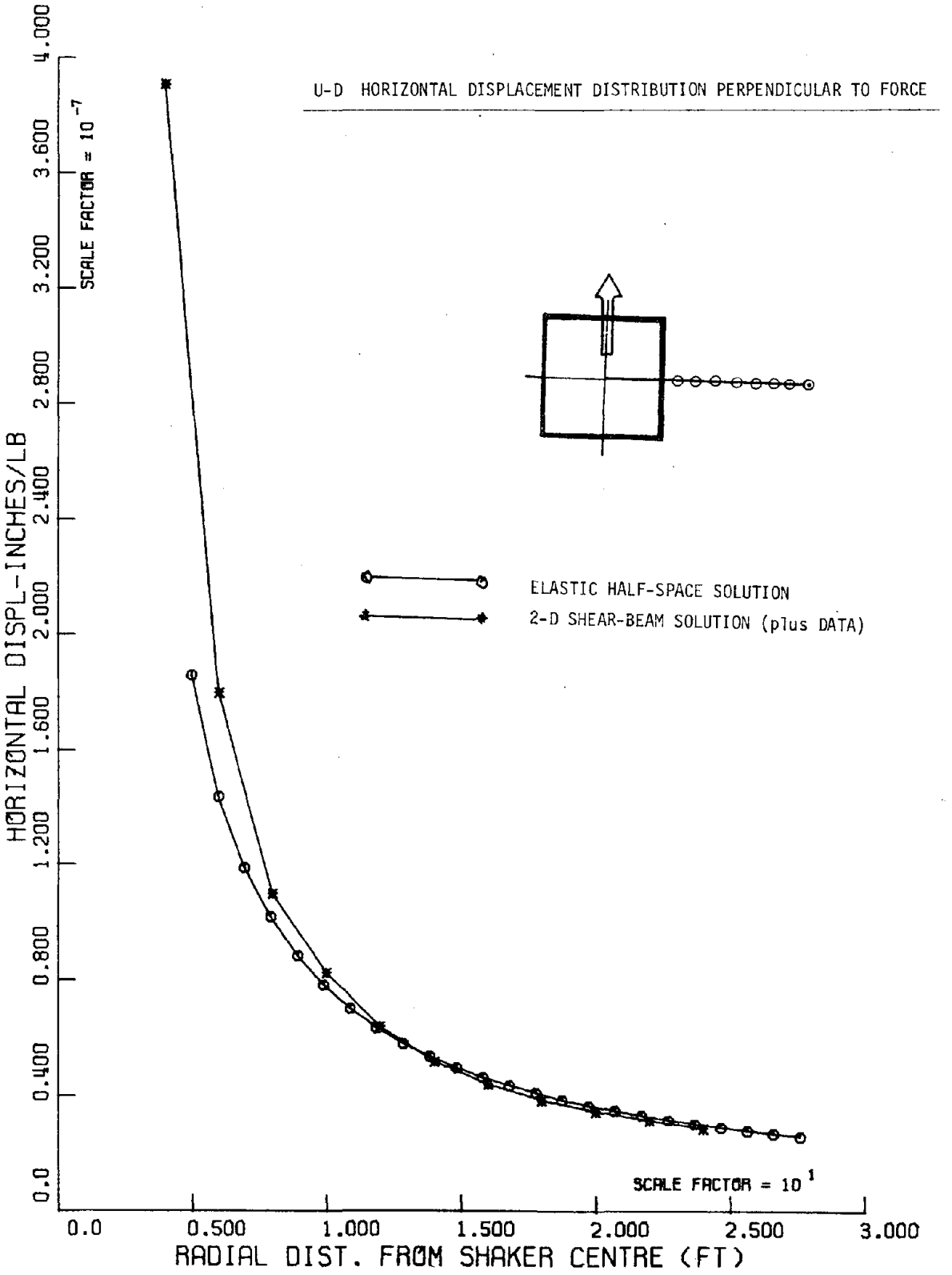

Fig. 46(c). The 2-D theory was used to estimate the horizontal crest displacement (at Station 0); this was matched to the single seismometer output recorded at Station 0. Then the seismometers outputs around the shaker were appropriately scaled, and quantified by the known match.

displacement of the crest is in the same order of magnitude as that estimated (from Eq. 3) for the central portion of the dam crest (3.185×10^{-8} inches per lb force). But, because the modal amplitude measurements in the neighborhood of the two shakers were considerably distorted, a correction of the measured mode shapes was made by comparing the measured amplitudes (as mentioned previously) in the vicinity of the shakers to those at distances of 20 to 30 ft from the shakers.

5. Evaluation of the Results

Sources of potentially important errors in both analyses are outlined below.

a. Shear-beam theory

(i) The canyon containing the Santa Felicia Dam is more trapezoidal than rectangular in cross section. The importance of choosing suitable dimensions of an equivalent rectangle are obvious. Nonetheless, relative to other dams in California, the Santa Felicia canyon has one of the best-suited sections for an equivalent rectangle analysis, in the sense that it is closer to a steep-sided parallelogram than to a trapezoid (Ref. 15).

(ii) The dam itself is a zoned dam with a large central impervious core flanked by two pervious shells, all of which are heterogeneous mixtures of clay, sands, and gravels. Consequently, to define suitable elastic material constants (that is, Young's modulus, Poisson's ratio, and the dam's density) is difficult, but was made easier by extensive in situ measurements of shear and compression wave velocities (see Ref. 2), and by knowledge of the densities of the different construction materials (see Table 1). The value of the shear modulus used comes from the frequency

equation (Refs. 2, 3, and 15)

$$J_o(\omega_n \sqrt{\frac{\rho}{G}}\, h) = 0 \quad , \tag{7}$$

which, with the fundamental natural shear frequency found by the frequency sweeps ($f_1 = \omega_1/2\pi = 1.635$ Hz) gives the value $G = 4.10 \times 10^6$ lb/ft^2. This is consistent with the results of Ref. 2 where the "assumed representative region" for G includes values derived from earthquake excitation (more discussion on values of G resulting from different excitation will be presented in a later section). At the level of excitation of interest here, the mean dam response should be somewhat more stiff than that expected in response to an earthquake.

(iii) The primary objective of this work was to define the dynamic characteristics of the dam under forced vibrations. Knowledge of the dynamic characteristics made the estimation of suitable values for the force/displacement phase lag and the damping factors possible.

Although not explicitly measured, the phase lag between the exciting force and resulting displacements was taken as $\pi/2$ radians. Inspection of the fundamental resonant peaks recorded at various stations during the symmetric forced vibration frequency sweeps and the recorded damped free vibration gave (as mentioned previously) an approximate modal damping ratio of 3% in the fundamental mode. This is a little bit lower than the value obtained in past experimental results (Refs. 4, 12, 13, 14, 15, and 17) on similar structures (about 5% of critical damping).

(iv) Having matched the computed central crest displacement to the recorded seismometer measurement, there is room for slight recording equipment errors in extrapolating to the soil measurements adjacent to

the block at different signal attenuations and sensitivities.

b. Elastic half-space analysis

(i) There is a geometric difference between a theoretical half-space and the crest, especially in the plane parallel to the direction of shaking, due to the sloping faces of the dam. The upstream slope (unlike the downstream face) has little effect, since the displacements are very small so far from the shaker, as shown by the contour plot in Fig. 46a.

Measured displacements for a medium with the geometry of the dam crest would obviously be larger than those computed from an elastic half-space analysis, assuming the same force and material properties, since the presence of the slope constitutes removal of a "wedge" of material, reducing the stiffness of the medium in the direction of the force.

This geometrical discrepancy can be compensated for by choosing softer elastic material properties. However, the medium surrounding the shaker block is by no means homogeneous, and the problem of choosing suitable elastic material properties remains, independent of any geometric dissimilarities.

(ii) From the in situ measurements presented in Ref. 2, as a first approximation Poisson's ratio was assumed independent of depth and was taken as the mean computed value of 0.45. However, the shear modulus (and therefore the Young's modulus) is assumed to be depth-dependent from the field evidence presented in Ref. 2. The shear-beam theory attempts to simulate the dynamic behavior of the complete dam, and the value of the shear modulus used in the analysis reflects this. However, the response of the soil on the crest surface due to vibrations of the shaker slab is a function of "local" shear moduli; therefore, the value of 1.45×10^6

lb/ft^2 for an elastic shear modulus, considerably lower than the one used in the shear-beam theory, is assumed to be a realistic approximation for use in the elastic half-space solution.

(iii) Further discretization of the loading surface, or more complex load distributions, were felt to be unnecessary considering the approximate nature of the solution.

6. Conclusion

The evaluation of field measurements through the shear-beam theory, and the estimation of elastic material properties for a simplified elastic half-space analysis are thought to be sufficiently well determined to validate a comparison between field data and theory.

Soil-structure interaction is a complex phenomenon, and there is a scarcity of field data to help substantiate the varied and often complex analytical solutions to the problem.

As a first stab at the problem, the results of this comparison of field measurements with a highly simplified analytical solution have proved to be remarkably good.

VI-1-6. Longitudinal Vibration

Unfortunately the measurements recorded during the longitudinal shaking (unique in earth dam research) of the dam were not extensive. The following reasons were responsible:

1. Limitation of time; the test permit was only for about six weeks, and since the U-D shaking, the ambient vibration tests, and the popper tests had already taken about ten weeks (this was due to severe weather conditions such as rain and due to some technical difficulties), it was decided to end the test program after

minimal longitudinal testing.

2. At the end of the U-D shaking phase, one of the two shakers was malfunctioning and its repair needed at least a week. So it was decided to use only one shaker (at station E2) for the longitudinal shaking phase. As a result, the symmetric and antisymmetric longitudinal motions were impossible to distinguish, and detailed modal measurements were practically impossible to achieve.

Nonetheless, the response curves, the preliminary modes of about half of the dam crest and the Fourier amplitude spectra obtained from the ambient vibration in the longitudinal direction (see Sec. VI-2) helped in understanding, to some extent, the nature of the longitudinal vibration of the dam.

Table 7 summarizes all resonant frequencies of major peaks recorded at selected stations for the longitudinal shaking. Because only eight seismometers were used during this shaking, it is difficult to determine various complete modes of longitudinal vibrations corresponding to these resonant frequencies. However, Figs. 47a, b, c, and d show estimations of some of the resonating modes (from about 1.0 to 3.0 Hz) obtained during the longitudinal frequency sweeps. For modes above 3 Hz only the measured data points are presented with possible connective interpolations. (The solid lines connecting the data points in Fig. 47 are estimates of the modal configurations, while the dashed lines represent possible extrapolations.) Visual examination of the figures reveals the local magnification effect of the soil surrounding the shaker block; no correction was made in the longitudinal direction to get rid of this soil-block interaction. Again, if the two shakers had been working, it

would have been possible to distinguish between symmetric and antisymmetric mode shapes.

From Table 7 and Fig. 47 the following observations can be made:

There were many closely spaced natural frequencies in the longitudinal direction. Also, some longitudinal resonant frequencies were very close (even identical) to some of the upstream-downstream resonant frequencies; examples of these are:

L Frequency (Hz)	U Frequency (Hz)
1.675 (L2)	1.635 (S1)
1.850 (L3)	1.850 (R1)
2.275	2.270 (R2) and 2.300 (AS2)
2.625 (L6)	2.600 (R3) and 2.650 (AR2)
2.875 (L7)	2.920 (R4)
3.050 (L8)	3.100 (AS3)
3.150 (L9)	3.100 (AS3) and 3.150 (R5)
4.175	4.220 (AR3)
4.700 (L14)	4.700 (AS7) and 4.665 (S7)
4.875 (L15)	4.900 (AR4)

Frequencies separated by 0.05 Hz or less are defined as "close."

This proximity may suggest a strong coupling between the U-D and L vibrations, or it may suggest that due to both the eccentricity of the single shaker (it was not located on the longitudinal axis of the dam) and the fact that the dam is not symmetrical, the U-D modes containing significant longitudinal motions were excited.

Furthermore, some of the incomplete longitudinal mode shapes are similar to the longitudinal components of the three-dimensional motions recorded during the up-stream-downstream shaking; examples

Table 7

Resonant Frequencies (in Hz) Observed in the Longitudinal Direction

(Longitudinal Shaking - One Shaker)

Santa Felicia Earth Dam

Measurement Station								Representative Natural Frequency	Desig-nation
W2	W1	0	E1	E3	E4	E5	E7		
1.425	1.425	1.425	1.425	1.425	1.425	-	1.425	1.425	L1
1.675	1.675	1.675	1.675	1.675	1.675	-	1.600	1.675	L2
1.850	1.850	1.850	1.850	1.850	1.850	-	1.825	1.850	L3
1.975**	-	1.950	1.975	1.950*	1.950	-	1.950	1.950	L4
2.150**	-	2.125	2.175	2.150	2.150	-	2.150	2.155	L5
2.275	2.225	2.250**	2.225*	2.200**	2.325*	-	2.250**	2.275	Possible
2.450	2.450	2.400**	2.450*	2.425	2.375	-	2.425	2.425	Possible
2.625	2.625	2.650	2.650	2.600	2.625	-	2.625	2.625	L6
2.875	2.875	2.875	2.850	2.875	2.900	-	2.825	2.875	L7
-	-	3.050	3.025	3.025	-	-	-	3.050	L8
-	-	3.150	3.150	3.125	-	-	-	3.150	L9
-	-	3.225**	3.275*	3.225*	-	-	-	3.230	Possible
-	-	3.350	3.350	3.350	-	-	-	3.350	L10
-	-	3.475	3.475	3.475	-	-	-	3.480	L11
-	-	3.775	3.755	3.750	-	-	-	3.775	L12
-	-	4.000**	4.050**	4.025	-	-	-	4.025	Possible
-	-	4.175**	4.150**	4.200**	-	-	-	4.175	Possible
-	-	4.325	4.350	4.425	-	-	-	4.370	L13
4.700	4.700	4.700	4.700	4.675	-	4.700	-	4.700	L14
4.900	4.900*	4.850	4.900	4.925*	-	4.825*	-	4.875	L15
-	5.400	5.350	5.350	5.350	-	5.400	-	5.350	L16
-	5.600**	5.600	5.600**	5.600*	-	5.600	-	5.600	L17
5.900	5.900	5.900	5.850	5.900	-	5.900	-	5.900	L18

Most reliable data (no asterisk); Less reliable data (*); Least reliable data (**).

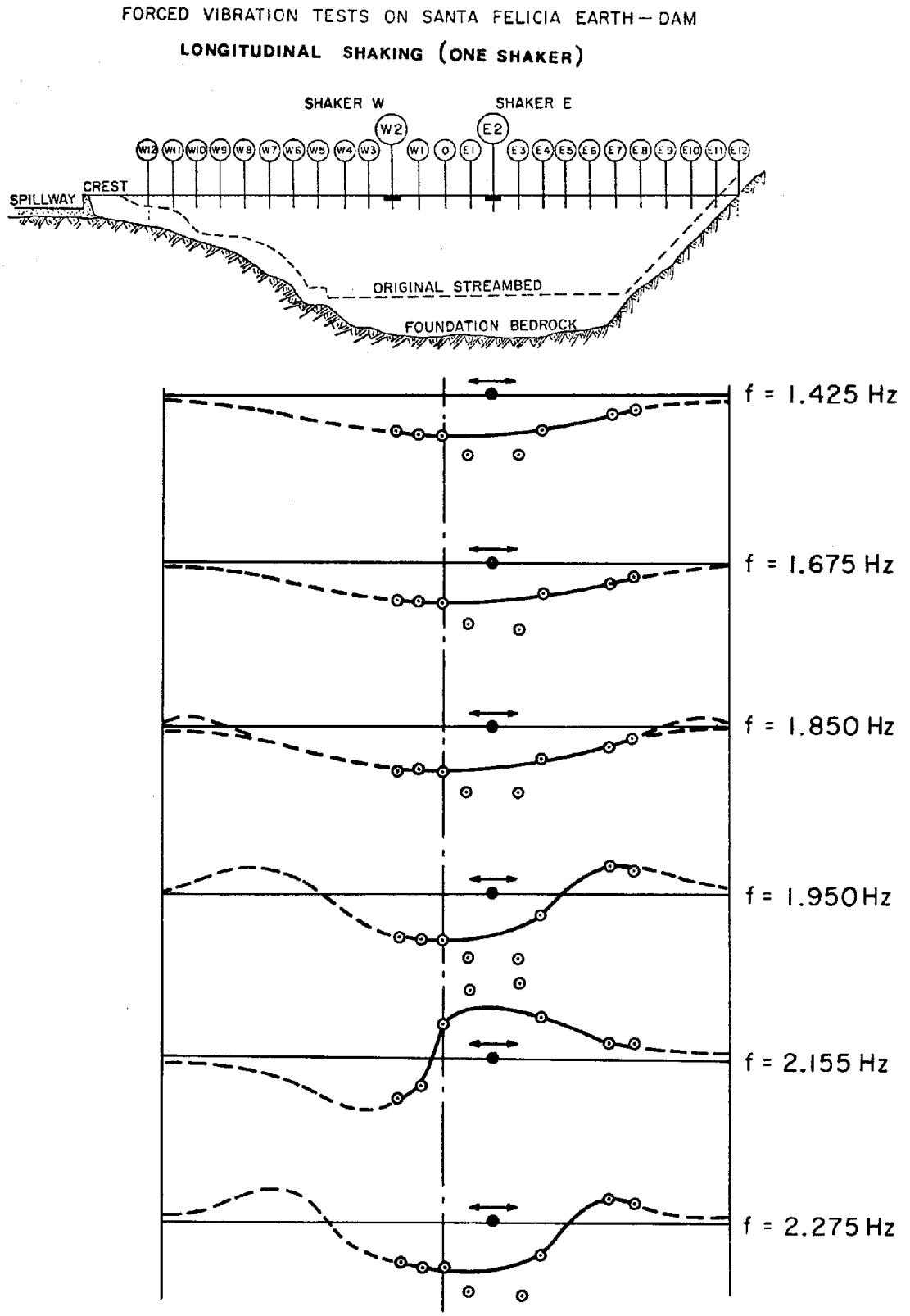

Fig. 47(a). Estimation of some of the resonating modes obtained during the longitudinal frequency sweeps.

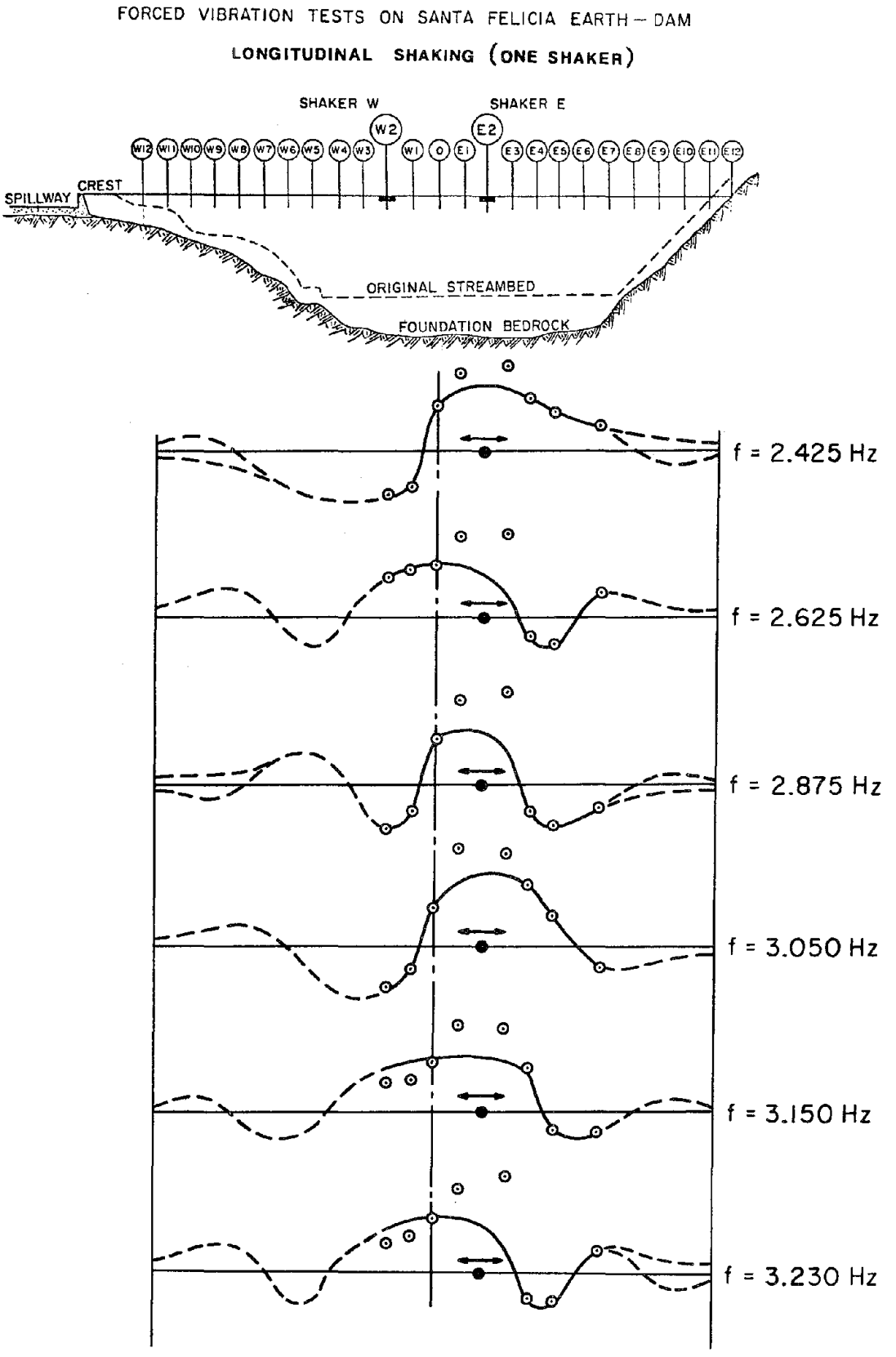

Fig. 47(b). Estimation of some of the resonating modes obtained during the longitudinal frequency sweeps.

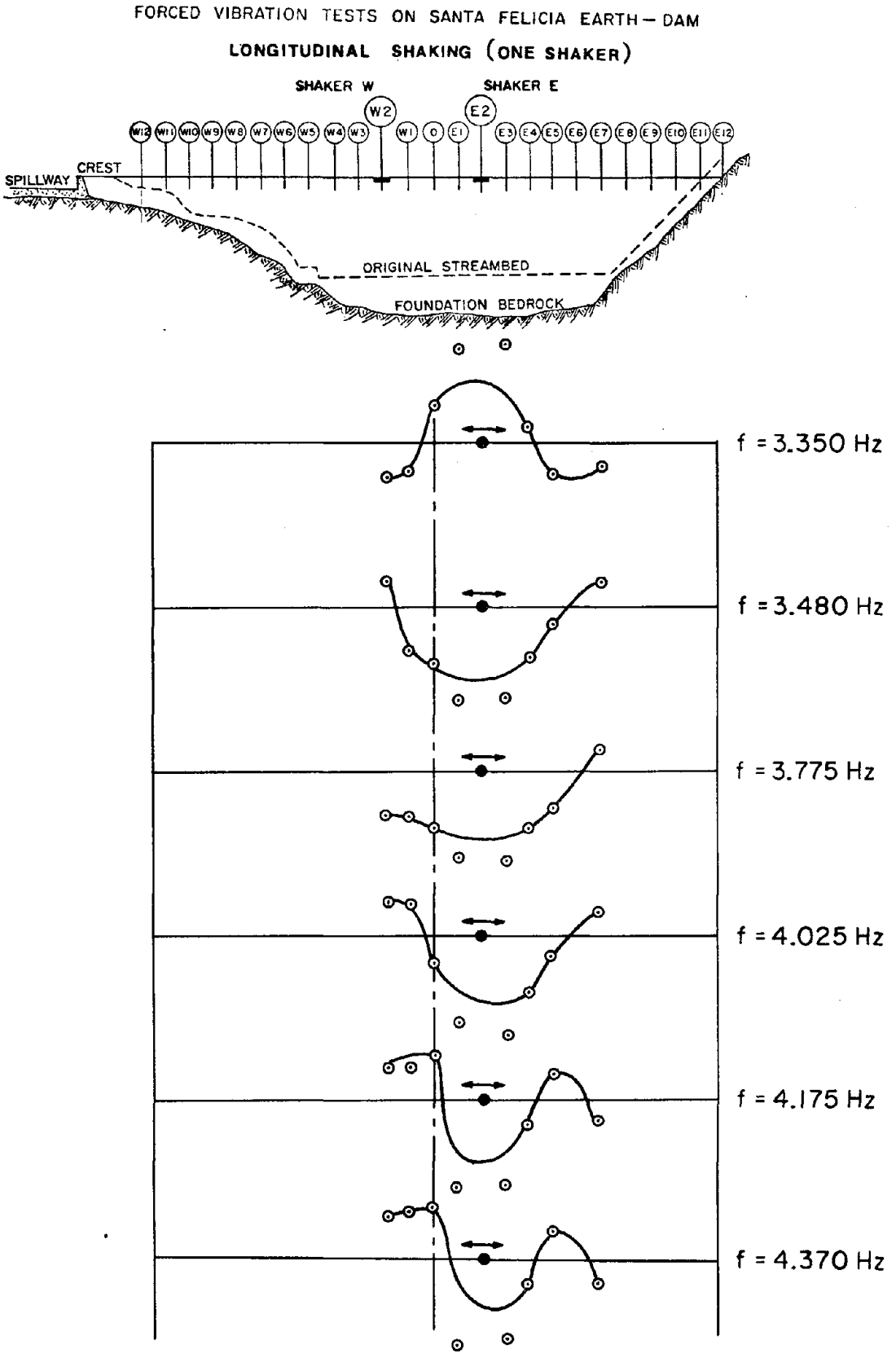

Fig. 47(c). Estimation of some of the incomplete (not covering all of the crest) resonating modes obtained during the longitudinal frequency sweeps.

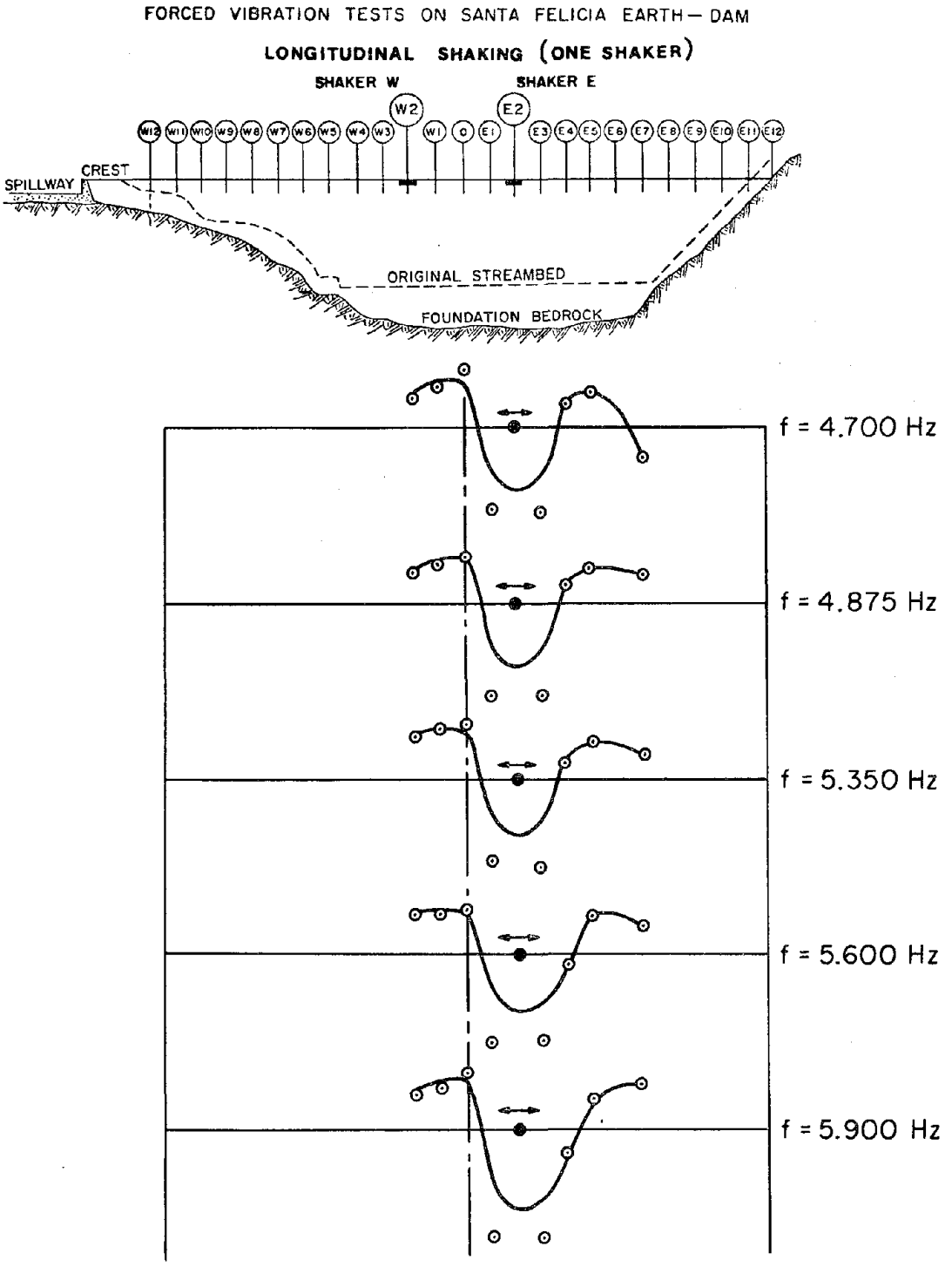

Fig. 47(c). Estimation of some of the incomplete (not covering all of the crest) resonating modes obtained during the longitudinal frequency sweeps.

of these are:

1.675 Hz (L2)	and	1.635 Hz (S1)
1.850 Hz (L3)	and	1.875 Hz (AS1)
1.950 Hz (L4)	and	2.100 Hz (S2)
2.275 Hz	and	2.300 Hz (AS2)
2.625 Hz	and	2.820 Hz (S3)
3.150 Hz	and	3.100 Hz (AS3)
3.775 Hz	and	3.540 Hz (S4), 3.600 Hz (AS4)

It is apparent from these observations that it was very difficult to tell from the data available whether a given mode was purely longitudinal, was associated with an upstream-downstream mode, or was a three-dimensional mode.

VI-2. Ambient Vibrations

VI-2-1. Fourier Amplitude Spectra

The unique and extensive collection of ambient vibration records on Santa Felicia Dam was used in this investigation to make various comparisons of the dam's dynamic characteristics, namely natural frequencies, mode shapes, and damping values when available. The collected data provided the basis for:

(1) Comparison of the Fourier Amplitude Spectra (FAS) from the different ambient tests with the response (resonance) curves from the forced vibration tests and, in addition, with the amplification spectra obtained from the two earthquake records (discussed in a later section).

(2) Comparison of the FAS obtained on different days, under different wind conditions, for different seismometer orientations and for different measurements stations; this allowed the stationarity of the

records to be examined. Stationarity implies that the structure is a linear and time-invariant system.

A collection of the most significant FAS obtained under different conditions is shown in Figs. 48 through 58. These figures have been chosen as best exemplifying the basic trends seen in all the analyses and comparisons. Additional FAS, which may also be of general interest, can be found in Appendix C (Figs. C-1 through C-9). The frequencies associated with the peaks in all the FAS are written along the horizontal axis. The frequency resolution (or the distance between any two discrete values) in all the FAS figures was 0.0073 Hz, which proved to be high resolution. The spectra were smoothed with one pass of a Hanning Window ($\frac{1}{4}, \frac{1}{2}, \frac{1}{4}$ weights). This smoothing facilitates, to some extent, selection of the natural frequencies and thus identification of the associated modes of vibration. Tables 8, 9, and 10 summarize the resonant (natural) frequencies for the dam which have been identified from the FAS (as well as cross-spectral functions) of the records taken during the ambient excitations in U-D, L, and V directions. Table 8 gives a summary of the average resonant frequencies (averaged over different stations in the same measurement run) of the U-D direction; these average values were considered to be representative of the data taken simultaneously from different seismometer stations. Although the differences of the frequency values in this table are small, they are distinct. Tables 9 and 10 illustrate the values obtained for individual stations for different days in both the longitudinal (L) and vertical (V) directions. The individual values of the stations in the U-D direction were not tabulated because they were numerous.

Identification of the different resonating modes (e.g., S1, AS1, R1, and AR1) was accomplished by the aid of the Digital Signal Processor (as mentioned previously); the results have already been presented in Figs. 48 through 58 and in Appendix C. For the sake of consistency, the modal identification in the figures and tables is accomplished by reference to symmetrical (S) and antisymmetrical (AS) shear mode shapes as well as rocking (R and AR) modes measured from the forced vibration tests, which have previously been presented and discussed. In addition, peaks designated by L and V correspond to modes dominated by longitudinal and vertical vibrational amplitudes, respectively.

By comparing the FAS obtained for different seismometer stations, directions, and measurement days on the dam, the following questions may be answered:

(1) How similar are the FAS obtained, simultaneously, on the same day for the same direction (U-D or L or V) at different stations?

(2) How similar are the FAS obtained from measurements on different days for the same seismometer direction and same station?

(3) How similar are the FAS obtained, simultaneously, for different directions of the seismometer at the same station and on the same day?

(4) How similar are the FAS obtained on the same day, for the same direction but at different hours (or different measurement runs)?

On the basis of the information contained in the FAS obtained for ambient vibrations shown in Figs. 48 through 58 and Tables 8, 9, and 10, the following interpretations (which contain answers to the above questions) may be made:

1. From the analysis of the forced vibration records, it was found that the differences between adjacent natural frequencies (symmetric, anti-symmetric, shear, or rocking modes of vibration in the upstream-downstream or longitudinal direction) were sometimes small; in some cases, frequencies of different type modes were almost identical. Therefore, during the ambient vibration spectral analysis, it was decided to use the high resolution of 0.0073 Hz despite some accompanying disadvantages. The primary disadvantage of high frequency resolution is that, consequently, the natural frequencies may not appear constant. It was felt that one smoothing pass of the FAS might compensate for this effect by helping to eliminate the clutter of nonresonant peaks which may surround a natural frequency, thus aiding in selection of the true resonance. Of course, actual resonant peaks may also be eliminated by this process, and so it is sometimes difficult to select the most appropriate resolution-versus-smoothing combination. In this analysis the procedure adopted gave fairly satisfactory results, although some modes were unfortunately lost.

2. The distribution of the energy imparted to the dam (or the FAS) by the wind, over the frequency range 0.0 to 6.0 Hz, appears to a varying degree unique for each day, and each seismometer direction (as shown in Figs. 48-58 and the figures of Appendix C). However, because peaks occurred at almost the same frequencies, the basic nature of the structural response (or energy transfer) must be similar for each day at this low level of ambient excitations.

3. The major spectral peaks of the FAS (or energy transfer) appear mainly to represent modal vibrations. However, spectral analysis indicated that the ambient vibrations contained a great deal of low frequency drift causing a build-up in the Fourier coefficients near the origin; i.e., there

is bias in the noise-level peaks near the origin as seen in Figs. 49, 50, 57, and 58 and in Figs. C-1, C-3, C-4, C-5, C-7, and C-9 of Appendix C. In addition, there was some non-structural low-frequency noise in the frequency range between 0.0 and about 1.0 Hz as in Figs. 48, 49, 50, 51, 55, and 58 and C-9. This nonstructural noise appears more strongly in recorded motions in the vertical direction (Figs. 49, 58, C-1, C-3, and C-5) than in the two horizontal directions; it also appears markedly in stations close to the end restraints (particularly close to the western spillway) and close to station W1 (Figs. C-1, C-3, C-4, C-6, and C-9). The source of this energy was probably the falling of water from the spillway to the stream which is about 200 ft deep (downstream), and also, possibly the electric generator (located close to station W1); finally, the interaction between the dam body and the end restraints (abutments) may have contributed to this low-frequency noise.

4. From a visual comparison of all of the FAS for the U-D direction (given in Figs. 48-58 and Appendix C), it appears that the dam did not have constant dynamic parameters at ambient levels of force. Even natural frequencies obtained from measurements made on the same day at the same station but at different hours changed slightly with time as shown in Figs. 49 and C-3, 50 and C-2, 51a and 51b, 51c and 51d, C-6a and C-7b, C-6b and C-7c, 55a and 56a, 56b and C-7a, 55c and 56c, 57a and C-8b, 58b and 58d, and finally C-9b and C-9d. All of these paired figures represent different measurement runs on the same day.

5. Nonetheless, the peaks of Fourier amplitude spectra obtained from seismometers positioned in the same direction (often the U-D direction) on the same day and at different stations can be correlated, to a great extent; in other words, most of these FAS contain peaks at common

frequencies. However, again, these spectral peaks are not always at exactly the same frequencies. One possible explanation for the variance of the frequencies at which peaks occur is that several modes of vibration were excited in varying degrees from one test (or station) to the other because of the variable air density and velocity and also because of different weights of water overflowing from the spillway. Also, the ambient vibrations were caused principally by wind loads which are randomly distributed over the surface of the structure. The shakers, on the other hand, input deterministic loads to the structure but at only two specific points. Of course, for a perfectly linear structure, natural frequencies are independent of loading; however, this structure, like most full-scale structures, is not linear. For this dam, the natural frequencies and modes of vibration are influenced by the point of application of the loading (as well as by its magnitude).

6. As mentioned previously, the dynamic characteristics of the dam are functions of the excitation level of the structure. Changes in frequency due to structural nonlinearity (this will be discussed later) are quite noticeable when comparing ambient with forced vibrations, but from one ambient level of excitation to another these changes are relatively very small (e.g., less than 10%). The ambient vibration mode shapes were determined (as were the forced vibration mode shapes) by dividing the spectral amplitude of the response at a given station by the (common) spectral amplitude of the simultaneously-recorded response at a reference station. In this way, an amplitude was obtained proportional to the mode shape at that station for a given frequency of vibration. Repeating this procedure for all stations where measurements were made, the mode shape

amplitudes were determined. These mode shapes were identical to those resulting from the forced vibration tests; so only the natural frequencies (which did vary with the level of excitation) of the ambient modes are presented in this report. To illustrate the modal amplitudes, examples of FAS at different stations for the same direction and which contain common spectral peaks are shown in Figs. 55, 56, and 57 and Figs. C-6, C-7, and C-8 of Appendix C.

7. Often the FAS obtained from the ambient levels of vibration appear to have common spectral peaks in the three orthogonal directions (U-D, L, and V); i.e., during the ambient vibration excitations the dam sometimes exhibited motion which dominated all three orthogonal directions, as seen in Figs. 48, 50, 54, and 58 and Figs. C-1, C-2, C-3, C-4, C-5, and C-9. In some instances, however, the FAS obtained for the two horizontal directions, U-D and L, although at a common position or measurement station, have almost no major spectral peaks in common, as seen in Figs. 49 and 52 and Figs. C-2 and C-4. The vertical component (V) in most cases shows a more complicated spectral pattern than the two horizontal components, exhibiting several major peaks in addition to those common to the horizontal directions, as seen clearly in Figs. 49 and 58 and Figs. C-2, C-4, and C-9.

8. To study the local effect of the shaker slab on the surrounding soils during the ambient excitations, the FAS of the slab and of nearby points on the dam's crest (from simultaneous recordings) were compared in Figs. 48d and C-1d, 51a and 51c, 51b and 51d, and 53a and 53b. The distribution of spectral peaks over the frequency range shown in these figures is generally identical, although there is some magnifi-

cation in the higher frequency range (3.0 to 5.0 Hz) from the shaker slab (or block), as shown in Figs. 51b and 51d.

9. Unlike the results obtained from the resonance (response) curves of the forced vibration, the FAS of the ambient vibration tests show an exceptionally clear picture of the upstream-downstream "shear" fundamental mode (S1) (Figs. 52, 53, 54, 55, 56, and 57). Although the values given in Table 8 for this fundamental frequency indicate nonconstant values, they support an average representative value of 1.614 Hz.

10. In some instances, lower U-D modes are very distinct, while higher U-D modes are not clearly discernible from other nearby (closely-spaced) modes as seen in Figs. 48, 51, and 54. In other instances, the opposite is true. In addition, in some instances, lower U-D modes are very distinct from those lower longitudinal and vertical modes, and in other instances lower U-D modes are not clearly distinguished from neighboring L and V modal amplitudes. Thus, this indicates that in the ambient vibration tests there were both strong modal coupling and interference.

11. From Table 8 (from ambient vibrations), it is evident that the dam has a slightly lower first symmetric, shear natural frequency in the U-D direction (about 1.614 Hz), than the one recorded from the forced vibration tests (1.635 Hz). A later section will be devoted completely to a comparison among all results: forced vibrations, ambient vibrations, popper vibrations, and earthquake responses. But it may be noted here that this frequency difference might suggest that the forces generated by wind (from 10-40 mph) on the dam's downstream face were larger than those generated by the shaking machines; in addition, the distribution of the forces was completely different in the two cases. An estimate of the wind

forces acting on the dam can be made by using the dynamic pressure expression (usually used for calculating wind loads on structures)

$$p = 0.00256\ C_s \cdot V^2 \quad (psf)$$

where C_s is the shape factor and V is the wind velocity in mph. Now, if we assume $C_s \simeq 1.0$ (a convenient assumption for the rectangular horizontal projection area of the downstream face) and assume an average velocity of 20 mph; then, the above expression gives p = 1.024 psf. The exposed effective area (horizontal projection) of the downstream face can be estimated to be 100 ft (depth) times 800 ft (average length); this value produces a total wind force of

$$F_w = 1.024 \times 100 \times 800 = 81{,}920.0 \text{ lbs}$$

If one assumes that the wind was not really perpendicular to the downstream face, then the above value can be reduced by, say, 40%; this gives a total wind force of 49,152 lbs, which is approximately five times larger than the average steady-state sinusoidal force. Thus the total amount of energy imparted to the dam by the wind was, very likely, greater than that produced by the shaking machines.

12. Clarity of the spectral peaks, as well as the values of the shear natural frequencies mentioned in the last point, appear to indicate a larger and differently distributed force caused by wind excitation than that caused by the shakers. Several natural frequencies, particularly those of rocking modes (R's and AR's) of the dam, have well-defined spectral peaks in the FAS of the ambient excitations; in contrast, the response curves of forced vibrations showed that for these rocking modes only the first few modes (R1, AR1, and R2) have well-defined peaks.

Table 8

Resonant Frequencies (Average from Different Days) from

Ambient Vibration Tests

(Santa Felicia Dam)

Upstream-Downstream Direction

Average Measured Frequency (Hz)							Average Measured Frequency (Hz) "7 days"
3-13-78	3-14-78	3-15-78	3-16-78	3-17-78	3-24-78	3-27-78	
1.620	1.621	1.586	1.619	1.603	1.620	1.626	1.614
1.753	1.779	1.792	1.773	1.745	1.787	1.780	1.773
1.934	1.884	1.924	1.835	1.916	1.881	1.924	1.900
2.025	2.020	2.030	1.978	-	2.035	2.044	2.022
2.130	2.130	2.097	2.044	2.050	2.111	2.119	2.097
2.224	2.244	2.168	2.161	2.225	2.237	2.229	2.213
2.368	2.350	2.395	2.333	2.377	2.367	2.320	2.359
2.591	2.611	2.549	2.540	2.587	2.568	2.500	2.564
2.680	2.693	2.680	2.645	2.632	2.699	2.646	2.675
2.900	2.809	2.783	-	2.842	2.869	2.859	2.844
3.010	2.942	2.903	-	3.038	2.970	2.989	2.975
3.091	3.230	3.128	-	3.190	3.214	3.135	3.165
3.157	3.348	3.230	-	3.289	3.105		3.226
-	3.606	3.474	-	3.480	3.539	3.582	3.536
-	3.745	3.641	-	3.515	3.704	3.669	3.665
-	3.943	3.853	-	3.847	3.866	3.830	3.868
-	4.146	4.136	-	4.124	4.181	-	4.147
-	4.241	4.197	-	4.243	4.204	-	4.221
-	4.360	4.282	-	4.339	4.325	-	4.327
-	4.472	4.398	-	4.433	4.476	-	4.445
-	4.594	4.516	-	-	-	-	4.555
-	4.695	4.656	-	4.636	4.598	-	4.646
-	4.780	4.749	-	4.804	4.790	-	4.781
-	-	-	-	-	4.973	-	4.973
-	-	-	-	-	5.140	-	5.140

Table 9

Resonant Frequencies (in Hz) from Ambient Vibration Tests
(Santa Felicia Earth Dam)

Longitudinal Direction

3-13-1978		3-14-1978				3-15-1978		3-16-1978			3-27-1978	
W1	W10	W1[a]	W1[b]	W5[a]	W5[b]	W1	W4	W1[a]	W1[b]	W5	W1	E4-D5
1.545	1.450	1.406	1.428	1.399	1.435	1.468	1.472	1.443	1.377	1.436	1.440	1.428
1.648	1.610	1.663	1.648	1.597	1.611	1.663	1.663	1.545	1.611	1.545	1.626	1.663
1.897	1.860	1.875	1.882	1.889	1.868	1.882	1.860	1.824	1.802	1.838	1.802	1.801
2.000	2.060	1.941	1.948	1.999	2.036	1.948	1.956	2.007	2.080	2.051	1.904	1.941
2.219	2.240	2.117	2.124	2.109	2.197	2.175	2.175	2.161	2.153	2.153	2.161	2.161
2.395	2.330	2.388	2.373	2.344	2.336	2.366	2.299	2.241	2.241	2.278	2.293	2.278
2.446	2.439	2.534	2.432	2.461	2.490	2.564	2.417	2.410	2.388	2.373	2.454	2.439
2.622	2.680	2.600	2.681	2.666	2.688	2.681	2.556	2.666	-	2.454	2.571	2.622
2.937	2.805	-	2.920	2.915	2.952	2.886	2.813	2.937	-		2.875	2.747
3.091	3.032	-	3.098	-	3.069	3.106	2.908	-	-		2.981	2.974
3.157	3.135	-	3.186	-	3.142	3.179	3.142	-	-		3.106	3.149
3.237	3.193	-	-	-	3.208	3.325	3.237	-	-		3.267	3.252
3.340	3.362	-	3.340	-	3.318	-	-	-	-		3.398	3.362
3.501	3.486	-	3.501	-	3.480	3.464	3.464	-	-		3.486	3.508
3.779	3.721	-	3.751	-	3.823	3.838	3.809	3.699	-		3.816	3.794
4.035	4.091	-	-	-	4.043	4.058	4.080				4.050	4.006
-	4.168	-	4.233	-	4.204	4.166	4.146				4.219	4.211
-	4.365	-	-	-	4.373	4.270	4.387				4.380	4.351
		-	-	-	4.644	4.636	4.753				4.658	4.666
		-	4.929	-	4.915	4.841	4.871				4.834	4.863

[a] and [b] were recorded at different hours on the same day.

Table 10

Resonant Frequencies (in Hz) From Ambient Vibration Tests
(Santa Felicia Earth Dam)
Vertical Direction

03-13-1978		03-14-1978				03-15-1978		03-16-1978			03-27-1978	
W1	W10	W1 (a)	W1 (b)	W5 (a)	W5 (b)	W1	W4	W1	W5 (a)	W5 (b)	W1	W4-D5
0.99	1.00	0.98	0.98	1.00	-	1.00	-	1.00	1.00	1.05	1.00	1.00
-	1.15	1.06	-	1.12	1.06	1.17	1.07	1.14	1.08	1.12	-	1.17
1.30	1.27	1.29	1.27	1.26	1.30	-	1.24	1.23	1.22	-	1.22	1.27
-	1.33	-	1.37	1.37	1.39	1.34	1.34	1.34	1.37	1.32	1.33	1.34
1.48	-	1.46	1.45	1.50	-	1.46	1.49	1.43	1.44	1.42	1.45	1.42
1.57	1.52	1.59	1.55	1.54	-	-	-	1.53	1.56	1.49	-	1.53
1.64	1.64	-	1.65	1.65	1.60	1.69	1.63	1.67	1.62	1.59	1.63	1.62
1.77	1.77	1.78	1.74	1.78	1.77	1.77	1.76	1.77	1.70	1.72	1.81	1.73
1.90	1.86	-	1.86	1.90	1.86	1.85	1.82	1.85	1.86	1.82	1.90	1.94
1.97	1.98	1.91	1.99	2.01	1.93	1.98	2.00	1.97	-	1.88	2.04	2.04
2.11	2.10	2.10	2.12	2.10	2.02	-	2.13	2.05	2.01	2.11	2.07	2.10
2.19	2.19	2.16	2.22	2.26	2.25	-	2.39	2.23	2.24	2.23	2.29	2.29
2.35	2.38	2.35	2.29	2.34	2.41	2.41	2.45	2.42	2.34	2.42	2.44	2.43
2.45	2.46	-	2.50	2.49	2.50	2.56	2.55	2.50	2.56	2.58	-	-
-	2.64	2.67	2.60	2.69	2.56	2.65	2.64	2.66	2.64	-	-	2.63
2.70	2.74	2.76	2.70	2.80	2.81	-	-	2.79	2.75	2.78	2.70	2.82
2.92	2.90		2.92		-	2.93	2.90	2.90	2.86	2.94	2.92	2.93
3.04	3.02		-		3.06	3.03	3.09		3.00	-	3.00	3.06
3.14	-		3.13		3.13	-	-		3.13	3.13	3.05	-
3.22	3.22		3.22		-	3.24	3.24		3.21	3.17	3.17	3.20
			3.35		3.38	-	3.36		3.34	3.36	3.25	3.40
			3.51		3.54	3.54	3.49		3.44	3.44		3.51
			3.61		3.66	-	3.66		3.65	3.56		3.66
			3.77		3.77	-	3.79		3.74	3.71		3.78
			3.87		3.88	3.87	-		3.87	3.85		3.92
			4.04		3.98	3.91	3.99					4.02
			-		4.18	4.18	4.13					
			4.25		4.26	4.29	4.27					4.29
			-		4.34	4.46	4.42					4.39
			4.62		4.67	-	4.67					4.64
			4.75		4.78	4.83	4.82					4.74
					4.86							

(a) and (b) were recorded at different hours on the same day.

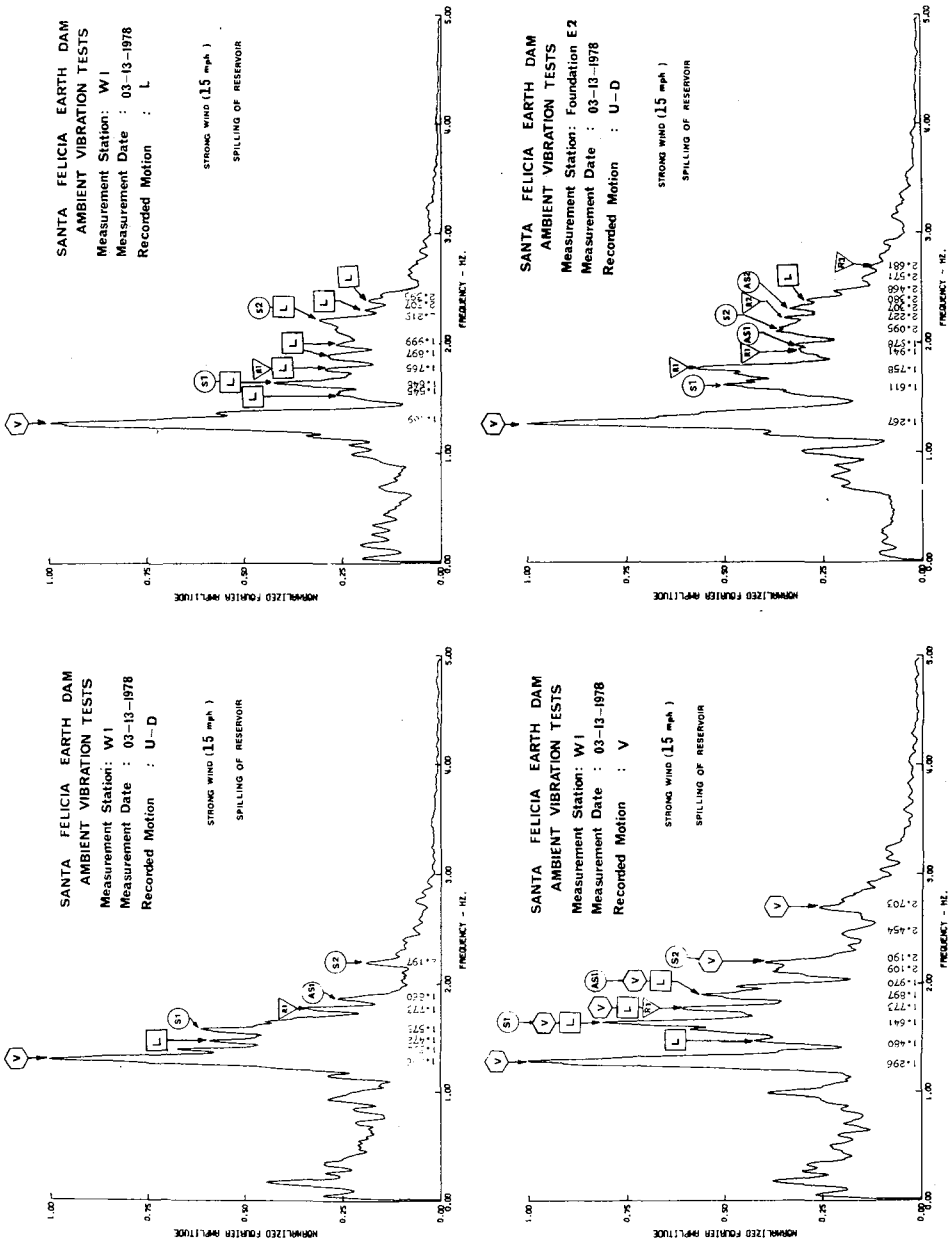

Fig. 48. Fourier amplitude spectra of the velocity proportional response of the three orthogonal directional motions recorded, simultaneously, at Station W1 as well as the upstream-downstream motion recorded at the east foundation on the crest of the dam. (L ≡ longitudinal, V ≡ vertical, S ≡ symmetric shear, AS ≡ antisymmetric shear, R ≡ symmetric rocking, and AR ≡ antisymmetric rocking modes of vibrations.)

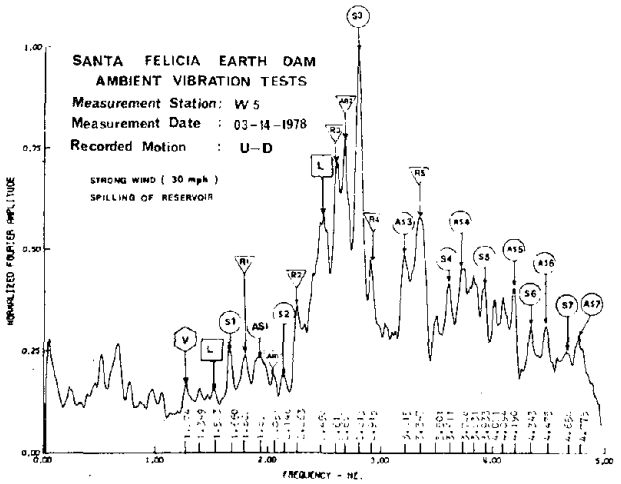

(a) Upstream-downstream direction

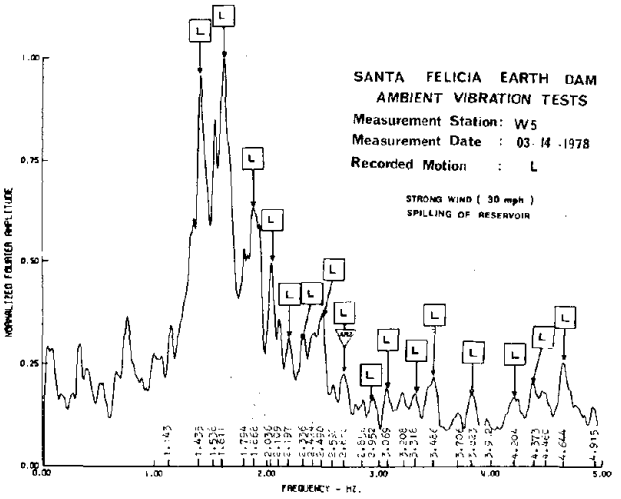

(b) Longitudinal direction

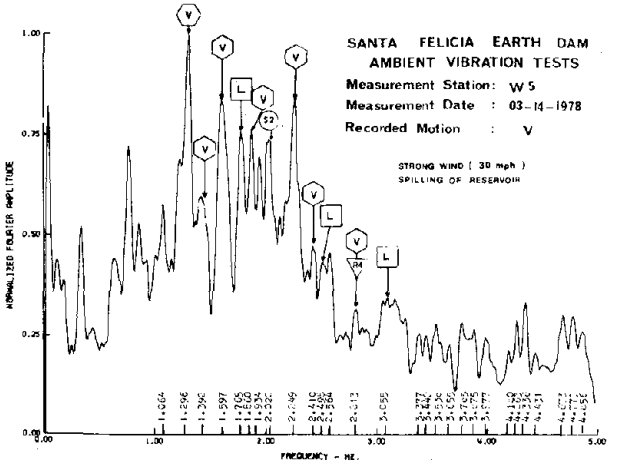

(c) Vertical direction

Note: in the three figures:
V ≡ vertical modes
L ≡ longitudinal modes
S ≡ symmetric shear modes
AS ≡ antisymmetric modes
R ≡ symmetric rocking modes
AR ≡ antisymmetric rocking modes

Fig. 49. Fourier amplitude spectra of the velocity proportional response of the three orthogonal directional motions recorded, simultaneously at Station W5 on the crest of the dam (5 Hz filtering).

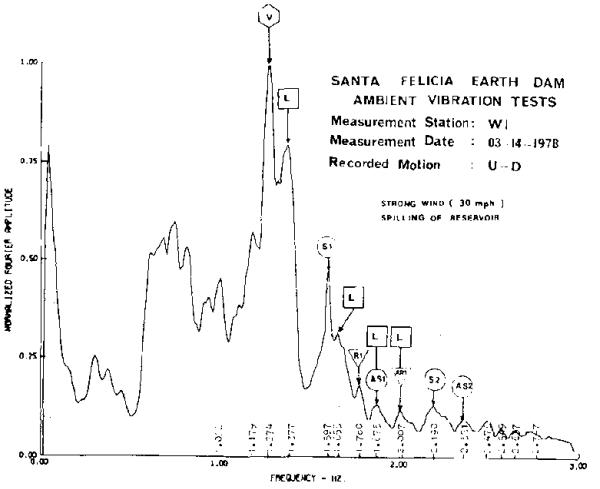

(a) Upstream-downstream direction

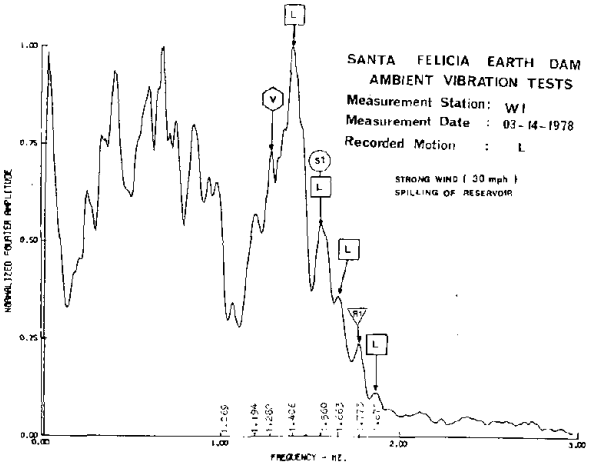

(b) Longitudinal direction

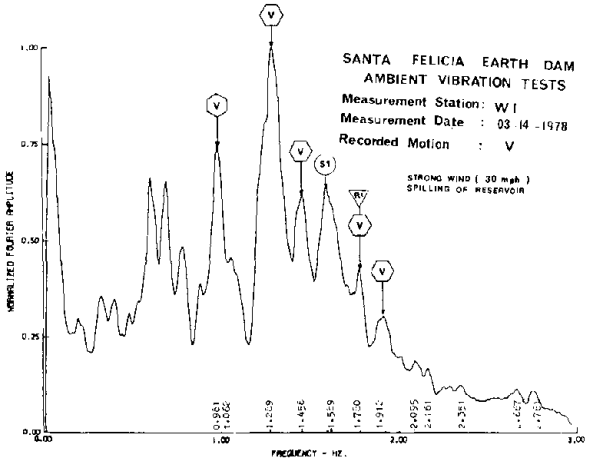

(c) Vertical direction

Note: in the three figures
V ≡ vertical modes
L ≡ longitudinal modes
S ≡ symmetric shear modes
AS ≡ antisymmetric shear modes
R ≡ symmetric rocking modes
AR ≡ antisymmetric rocking modes

Fig. 50. Fourier amplitude spectra of the velocity proportional response of the three orthogonal directional motions recorded, simultaneously at Station W1 on the crest of the dam (3 Hz filtering).

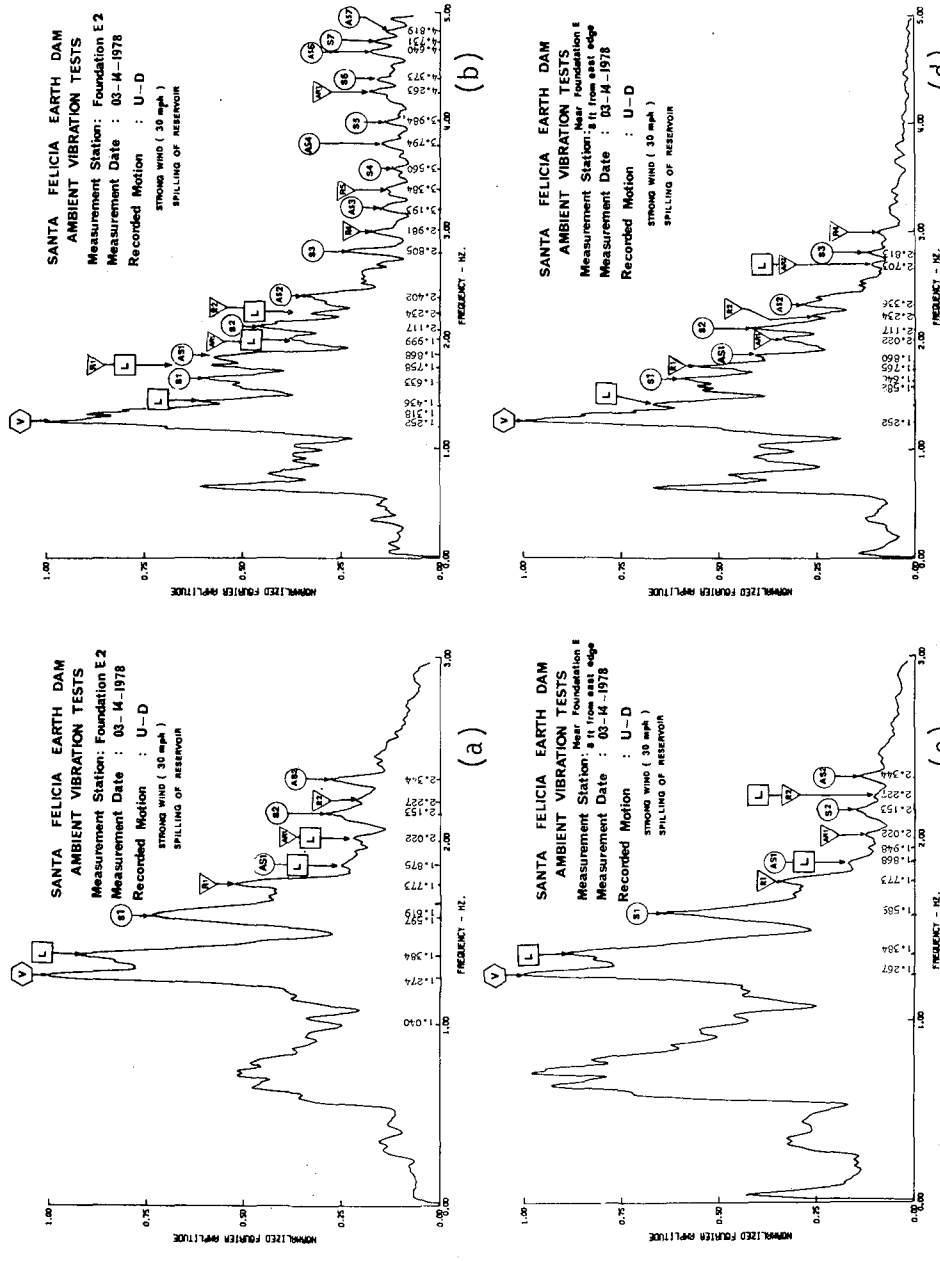

Fig. 51. Fourier amplitude spectra of the velocity proportional response of the upstream-downstream motion recorded; (a,c) simultaneously at the east foundation and nearby (5 Hz filtering or 3 Hz filtering), (b,c) at different hours (5 and 3 Hz filterings). L ≡ longitudinal, V ≡ vertical, S ≡ symmetric shear, AS ≡ anti-symmetric shear, R ≡ symmetric rocking, and AR ≡ antisymmetric rocking modes of vibrations.)

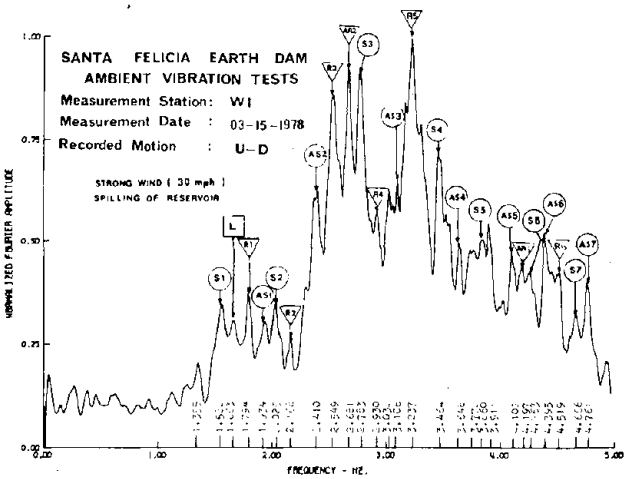

(a) Upstream-downstream direction

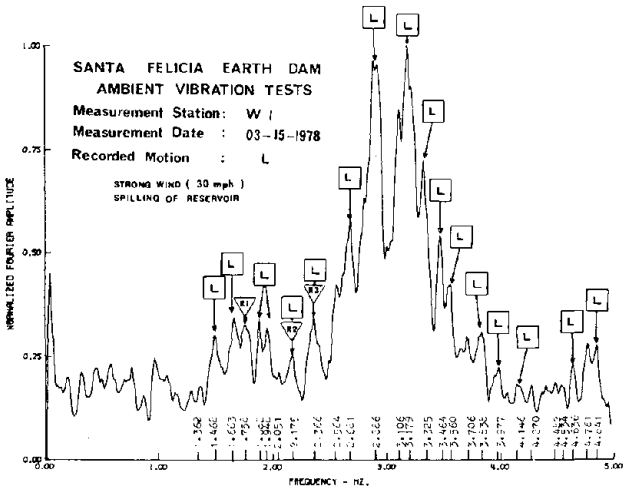

(b) Longitudinal direction

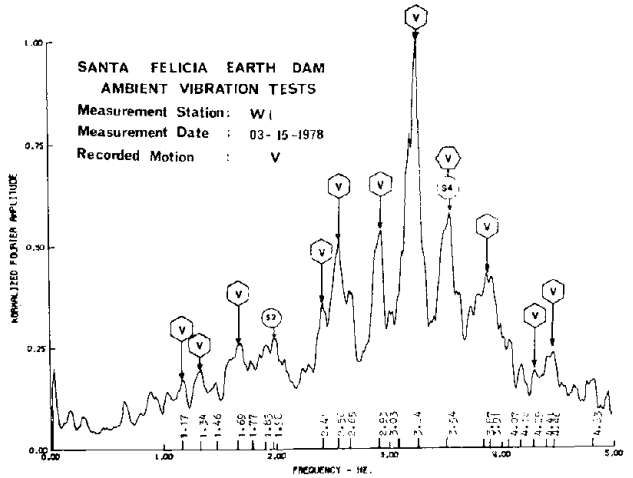

(c) Vertical direction

Note: in the three figures:
V vertical modes

Note: in the three figures:
V ≡ vertical modes
L ≡ longitudinal modes
S ≡ symmetric shear modes
AS ≡ antisymmetric shear modes
R ≡ symmetric rocking modes
AR ≡ antisymmetric rocking modes

Fig. 52. Fourier amplitude spectra of the velocity proportional response of the three orthogonal directional motions recorded, simultaneously, at Station W1 on the crest of the dam.

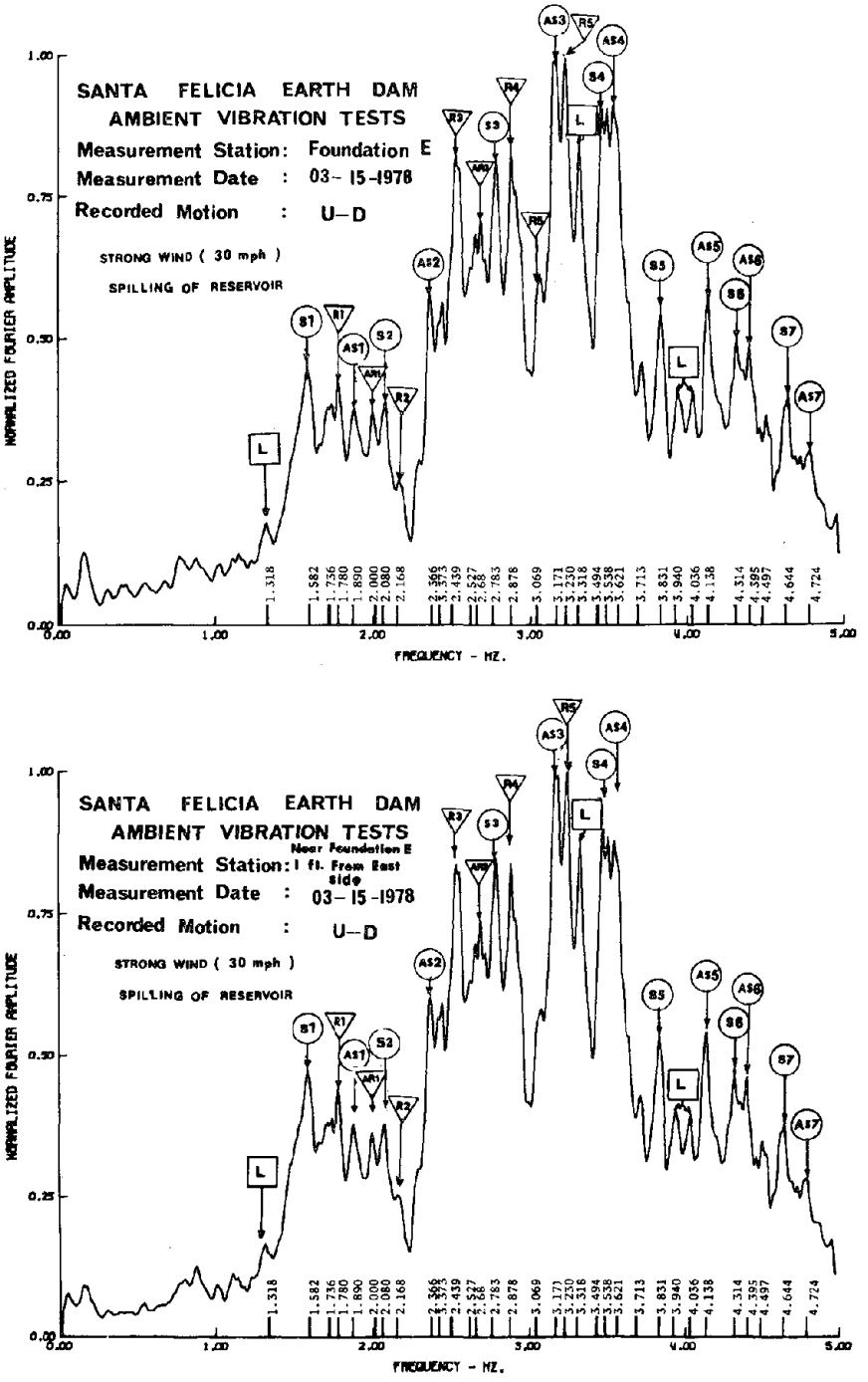

Fig. 53. Fourier amplitude spectra of the velocity proportional response of the upstream-downstream motion recorded, simultaneously, at the east foundation and at a nearby point on the crest of the dam. (L ≡ longitudinal, V ≡ vertical, S ≡ symmetric shear, AS ≡ antisymmetric shear, R ≡ symmetric rocking, and AR ≡ antisymmetric rocking modes of vibration.)

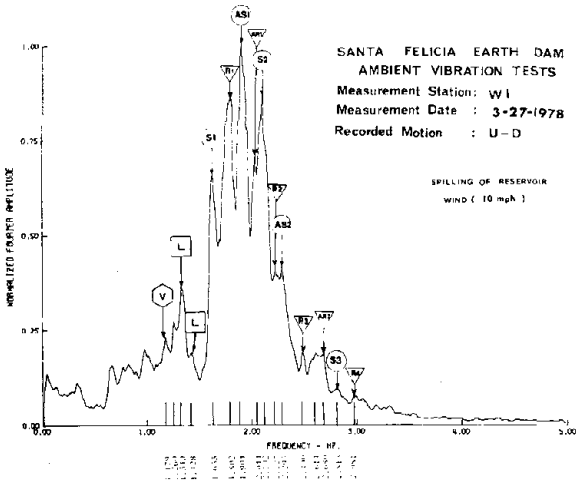

(a) Upstream-downstream direction

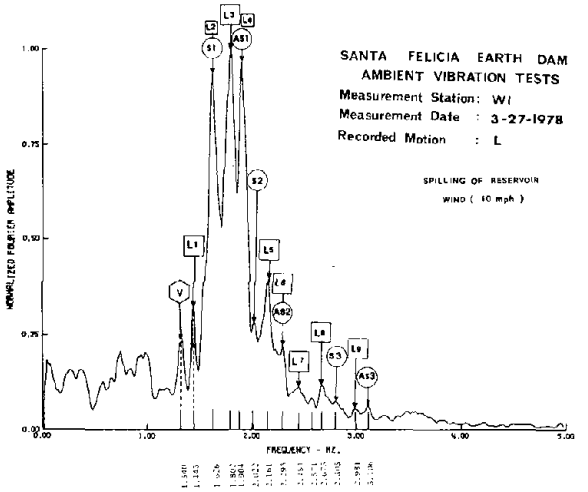

(b) Longitudinal direction

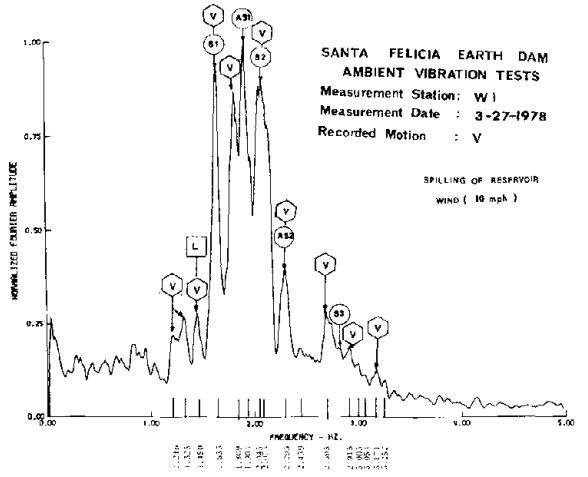

(c) Vertical direction

Note: in the three figures:
V ≡ vertical modes
L ≡ longitudinal modes
S ≡ symmetric shear modes
AS ≡ antisymmetric shear modes
R ≡ symmetric rocking modes
AR ≡ antisymmetric rocking modes

Fig. 54. Fourier amplitude spectra of the velocity proportional response of the three orthogonal directional motions recorded, simultaneously, at Station W1 on the crest of the dam.

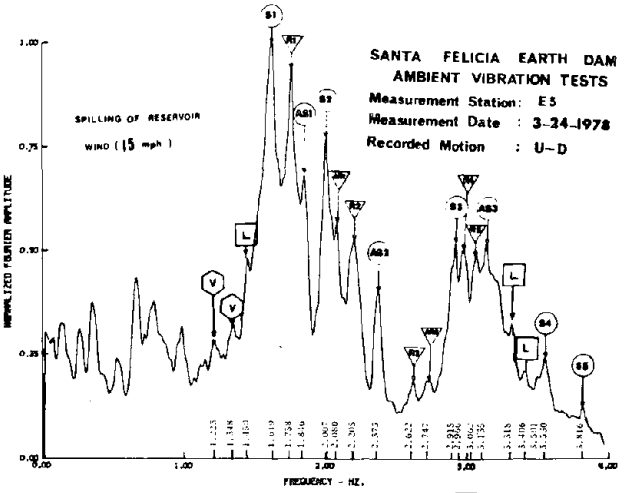

(a)

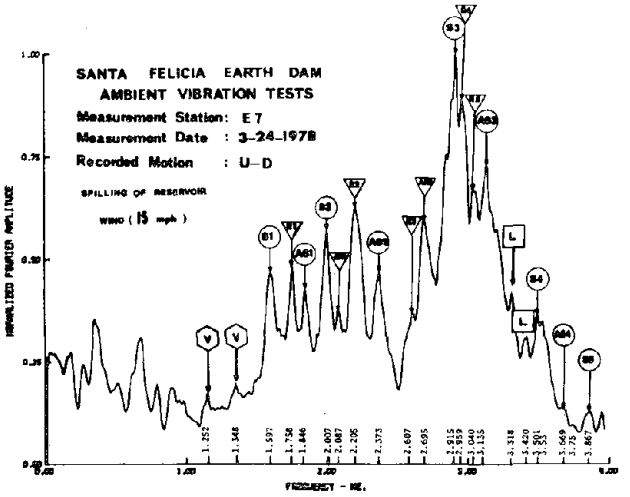

(b)

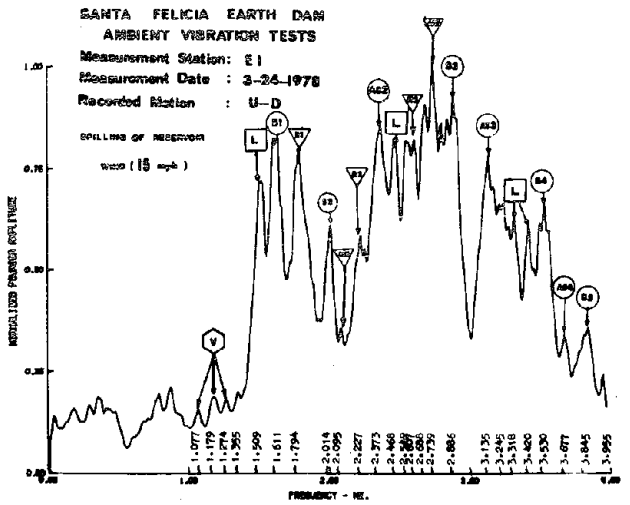

(c)

Note: in the three figures:
V ≡ vertical modes
L ≡ longitudinal modes
S ≡ symmetric shear modes
AS ≡ antisymmetric shear modes
R ≡ symmetric rocking modes
AR ≡ antisymmetric rocking modes

Fig. 55. Fourier amplitude spectra of the velocity proportional response of the upstream-downstream motion recorded, simultaneously, at Stations E5, E7 and E1 on the crest (4 Hz filtering).

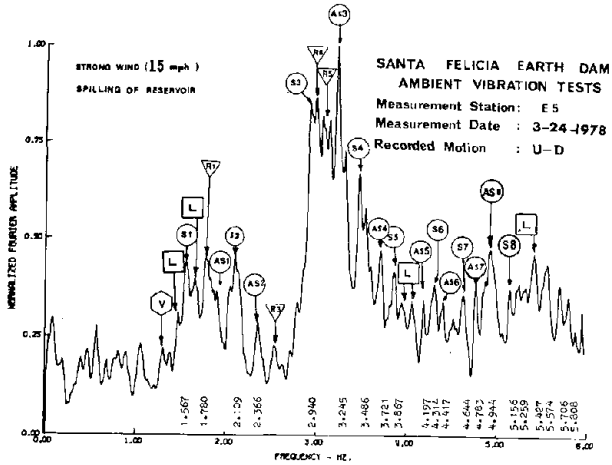

(a)

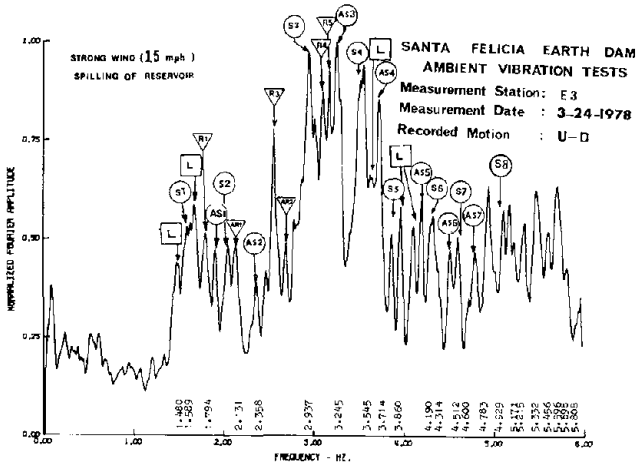

(b)

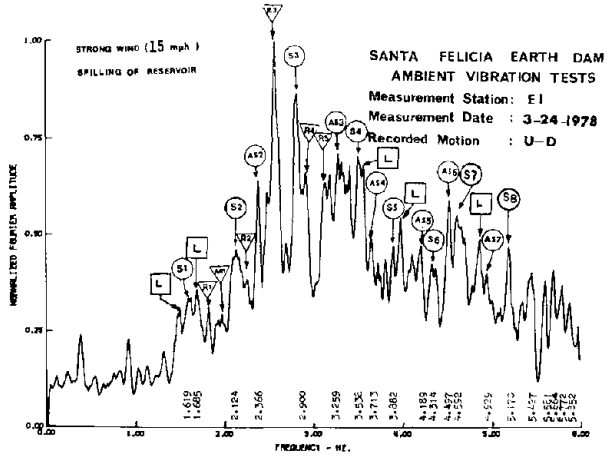

(c)

Note: in the three figures
V ≡ vertical modes
L ≡ longitudinal modes
S ≡ symmetric shear modes
AS ≡ antisymmetric shear modes
R ≡ symmetric rocking modes
AR ≡ antisymmetric rocking modes

Fig. 56. Fourier amplitude spectra of the velocity proportional response of the upstream-downstream motion recorded, simultaneously, at Stations E5, E3 and E1 on the crest (6 Hz filtering).

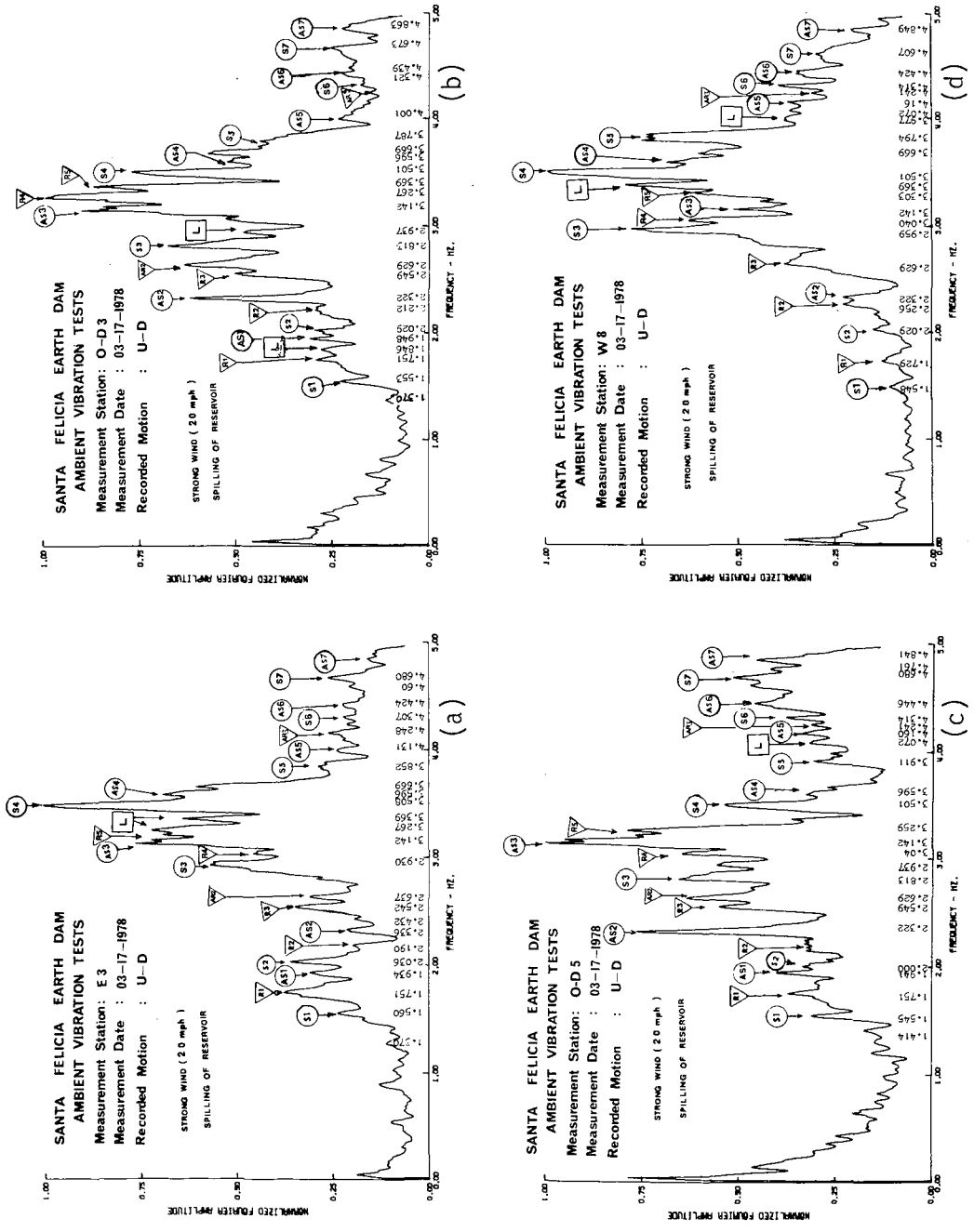

Fig. 57. Fourier amplitude spectra of the velocity proportional response of the upstream-downstream motion recorded, simultaneously, at Stations E3, O-D3, O-D5 and W8 (5 Hz filtering). (L ≡ longitudinal, V ≡ vertical, S ≡ symmetric shear, AS ≡ antisymmetric rocking modes of vibration.)

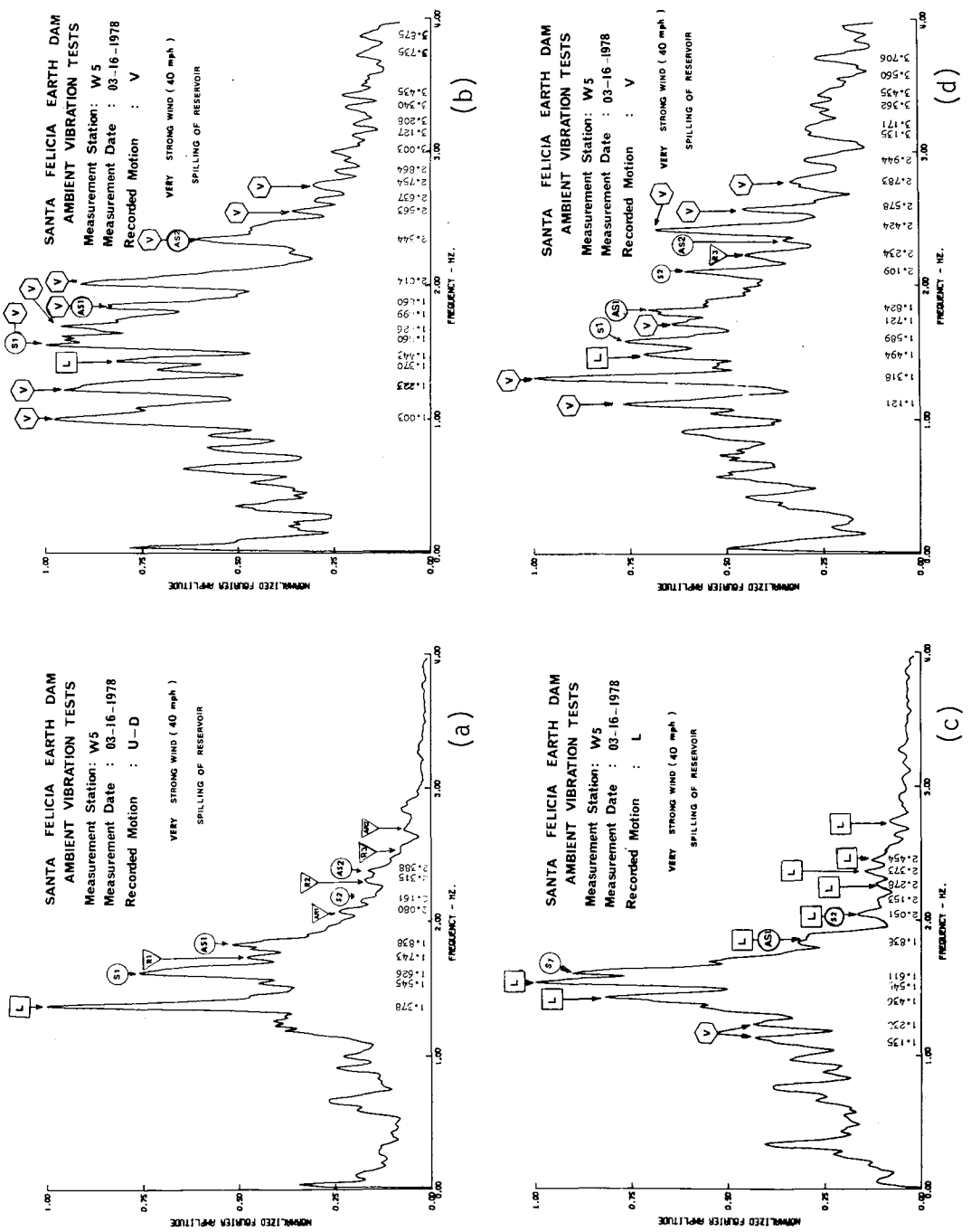

Fig. 58. Fourier amplitude spectra of the velocity proportional response of the three orthogonal directional motions recorded, simultaneously, at Station W5. (Note: The two vertical motions were recorded at different hours.)

VI-2-2. Damping Values from Fourier Amplitude Spectra

Estimated damping values from ambient vibration tests were obtained by the method of half-power bandwidth of the Fourier spectrum peaks. Unfortunately, several factors contribute to errors in computing damping values by this method. First, the vibration of the dam under different wind intensities is a nonstationary random process which can broaden the bandwidths of the individual response peaks and thus yield damping values that may be too high, Second, the presence of adjacent peaks in the spectrum due to closely spaced modal peaks (close proximity of two or more modes in the frequency domain) can cause difficulty in estimating damping values. Third, the smoothing process of the Fourier spectra could contribute to the overestimation of damping by diminishing the spectral peaks and broadening the bandwidth at the half-power points. Finally, for nonlinear structures such as earth dams, the width of the resonance peak can be influenced by the structural nonlinearities. In order to avoid this possible influence, damping or energy dissipation may also be calculated by the logarithmic decrement method applied to recordings of the damped free vibration of each mode; this proved to be, in the case of windy conditions, impractical. Calculation of the damping by this method was performed in the forced vibration tests (Section VI-1-4) and the results are compared to those from the ambient vibration tests later in this report.

Despite the difficulties in measuring bandwidths, a large number of individual peaks were adequately defined so that an estimate of half-point width was possible (as shown in Table 11). The modal damping values given in Table 11 were calculated by examining the width of each modal resonance as if these individual response peaks represented a linear model. The modal

damping terms have been uniformly rounded to the nearest 0.1% of critical damping. The values in Table 11 range from 2.3 to 3.6% of critical damping for the first symmetric U-D shear mode. Even for an earth dam, these are relatively large values of damping considering that they are determined from ambient level vibrations. In general, the damping values do not change greatly with a change in the ambient vibration level (see Table 11), and the damping values decrease when the order of the mode increases; i.e., higher modes have lower damping values.

VI-3. Popper Tests

By loading primarily the central portion (the region between stations W1 and E1) of the dam's upstream face and by placing the pressure wave source opposite the center line (as in Popper Test I), generally symmetric upstream-downstream modes can be excited. For the tests, it was intended to excite the first symmetric shear mode, S1, exclusive of all other modes; instead, the fourth symmetric shear mode, S4, of an average frequency equal to 3.268 Hz (f_4 = 3.540 Hz from the force vibration tests and f_4 = 3.665 Hz (average) from the ambient vibration tests) was excited, almost exclusive of all other modes as shown by the Fourier amplitude spectra (FAS) of the recorded time signal at the central measurement station 0 of Fig. 59. The frequency resolution was taken to be 0.0073 Hz, and the filtering frequency of the recorded signal was 10 Hz. A schematic diagram showing the excitation of the dam's 4th symmetric shear mode, as well as samples of the time traces recorded simultaneously when the Popper was opposite station 0 is shown in Fig. 60. The FAS of the other stations (E3, E8, and O-D5) of Fig. 59 show a narrow band of several spectral peaks of dominant excited resonating modes including S3, AS3, AS4, and S5, in

Table 11

Estimated Damping Ratios From the Fourier Amplitude Spectra of the Ambient Vibrations
in the Upstream-Downstream Direction
Santa Felicia Earth Dam

Mode	Average Measured Frequency (Hz) "7 days"	Average Measured Damping Ratio (Per cent)							Average Measured Damping Ratio "7 days"
		3-13-78 15 mph	3-14-78 30 mph	3-15-78 30 mph	3-16-78 40 mph	3-17-78 20 mph	3-24-78 15 mph	3-27-78 10 mph	
S1	1.614	2.3	3.3	3.6	3.2	2.8	3.0	2.6	2.97
R1	1.773	2.0	3.0	1.7	-	3.7	2.5	2.7	2.60
AS1	1.900	2.1	3.5	2.5	2.7	2.8	2.0	2.1	2.53
AR1	2.022	-	2.3	1.4	-	-	2.1	-	1.93
S2	2.097	1.7	2.5	2.4	2.2	3.0	2.2	2.5	2.36
R2	2.213	-	2.5	2.1	-	-	2.1	-	2.23
AS2	2.359	1.4	2.7	2.5	2.0	2.0	1.9	2.2	2.10
R3	2.564	1.4	1.4	2.5	2.0	1.9	1.8	1.6	1.80
AR2	2.675	-	1.5	1.9	-	2.1	1.8	1.9	1.84
S3	2.844	1.2	1.2	1.7	-	2.2	1.5	-	1.56
R4	2.975	-	1.4	2.1	-	2.3	1.5	-	1.83
AS3	3.165	-	1.7	-	-	2.7	1.6	-	2.00
R5	3.226	-	2.1	2.3	-	-	-	-	2.20
S4	3.536	-	1.3	1.6	-	1.4	1.7	-	1.50
AS4	3.665	-	1.3	1.0	-	-	1.1	-	1.13
S5	3.868	-	1.0	1.0	-	2.2	1.3	-	1.38
AS5	4.147	-	1.0	1.1	-	1.6	0.9	-	1.15
AR3	4.221	-	1.0	-	-	-	-	-	1.00
S6	4.327	-	0.9	-	-	1.6	1.2	-	1.23
AS6	4.445	-	0.8	-	-	1.7	1.1	-	1.20
R6	4.555	-	1.0	-	-	-	-	-	1.00
S7	4.646	-	0.7	1.0	-	1.0	1.1	-	0.95
AS7	4.781	-	0.9	0.8	-	0.8	1.0	-	0.88
AR4	4.973	-	-	-	-	-	-	-	-
S8	5.140	-	-	-	-	-	1.0	-	1.00

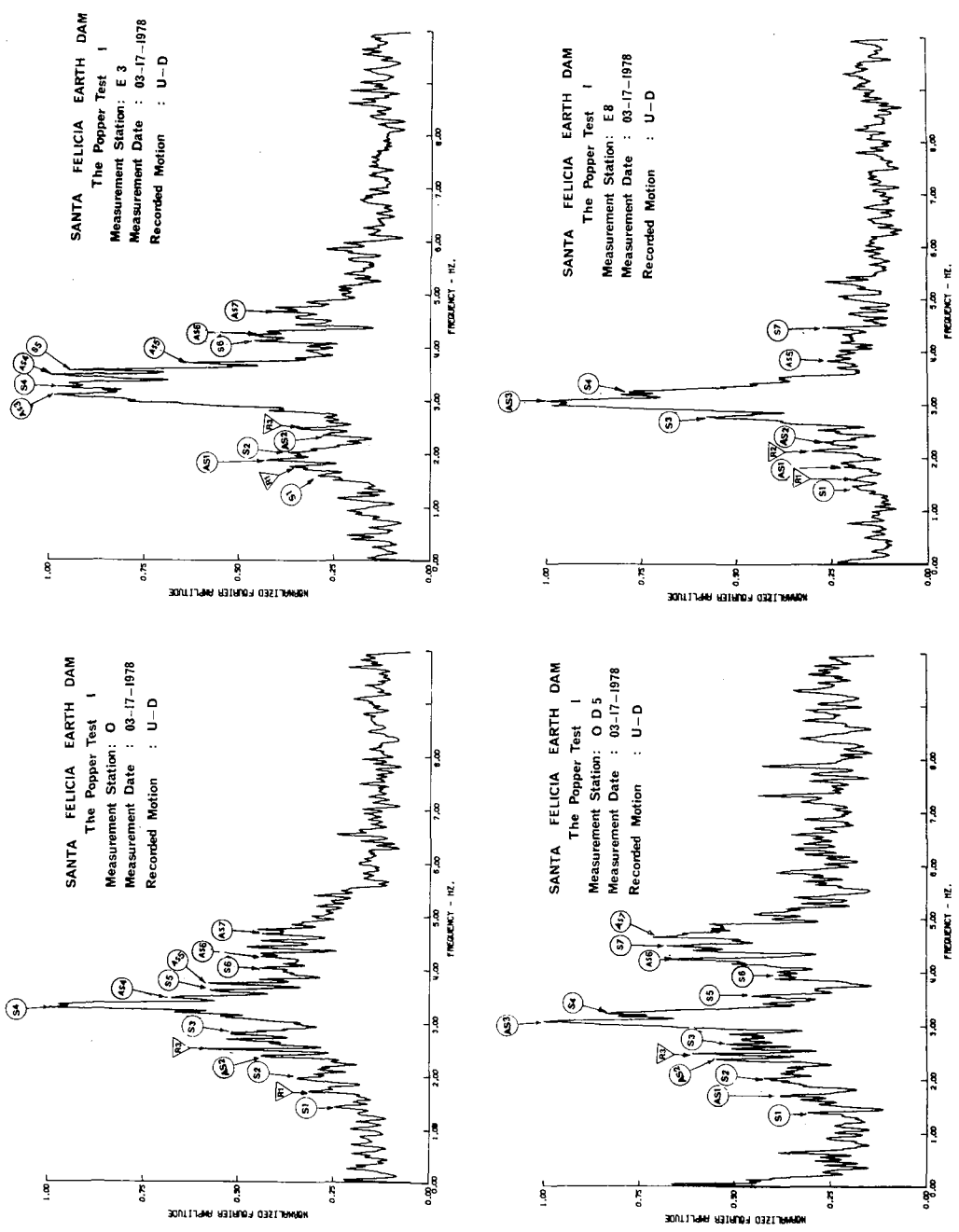

Fig. 59. Fourier amplitude spectra of the velocity proportional response of the upstream-downstream motion recorded simultaneously at Stations O, E3, O-D5 and E8 during Popper Test I.

addition to S4. Another set of sample time-traces recorded during Popper Test I is shown in Fig. 61.

Theoretically, to excite any mode exclusively, the distance from the source of the P-wave to the dam must be adjusted such that the pressure distribution would approximate the mode shape to be excited (Ref. 16). During Popper Test I, the source was placed relatively close to the dam (about 10 to 20 ft) in the central region, and it seems that the resulting wave-pressure distribution on the upstream face near the center line (between stations E6 and W6) was loaded more than, and in an opposite direction to, the area off to either side of station E6 and W6. However, neighboring, closely-spaced modes were excited as well (as mentioned above) because of the proximity of their resonant frequencies to that of S4 as well as because of the distribution of the pressure on the upstream face. Figure 62 shows the beating phenomenon, observed on the recorded time traces of the popper tests, which resulted from the proximity of modes.

Additional modes were excited by varying the location of the popper along a line perpendicular to the dam's longitudinal axis (Popper Test II) from 10 to about 50 ft from the dam. Figure 63 shows some of the time traces recorded during Popper Test II, while Fig. 64 shows the FAS of the recorded time signal. The frequency resolution was, again, 0.0073 Hz but the filtering frequency in the field was 5 Hz instead of 10 Hz. The appearance of the well-defined mode R5 high peak and the high contribution of modes AS4, AS3, R4, and S5 were evident when comparing the FAS of the stations of Fig. 59 to those of Fig. 64. One possible explanation of the strong appearance of mode R5 is the movement of the popper during this test; the previous apparent overlapping of R5 with S4 in Fig. 59 was

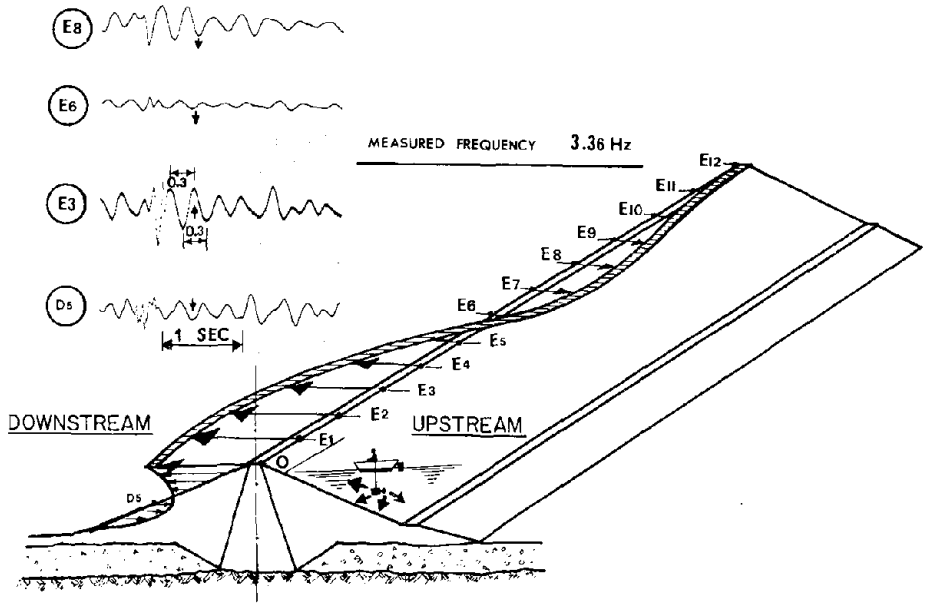

(a) Schematic diagram showing the excitation of the dams 4th symmetric shear mode, S4 (Popper opposite Dam's center line).

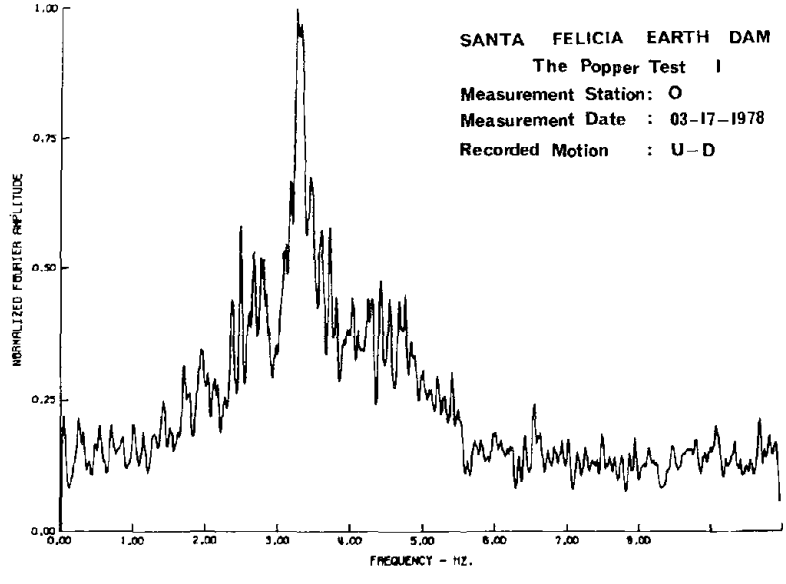

(b) Fourier amplitude spectrum of the velocity proportional response of the upstream-downstream motion during Popper Test I.

Fig. 60

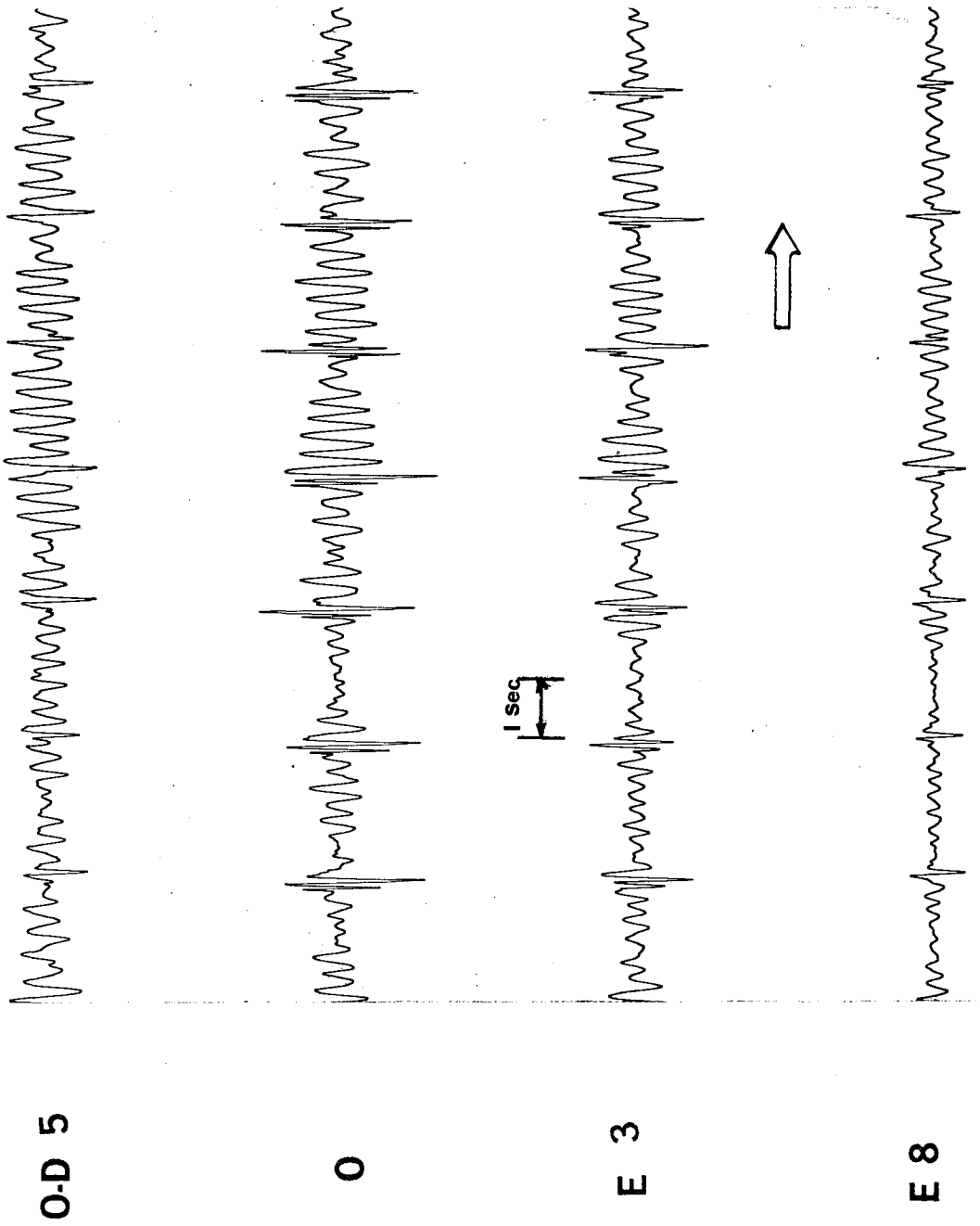

Fig. 61. Sample traces from the oscillograph recorder made simultaneously during Popper Test I at Stations O-D5, O, E3 and E8 in the upstream-downstream direction. (The repeated "pops" were at approximately two-second intervals.)

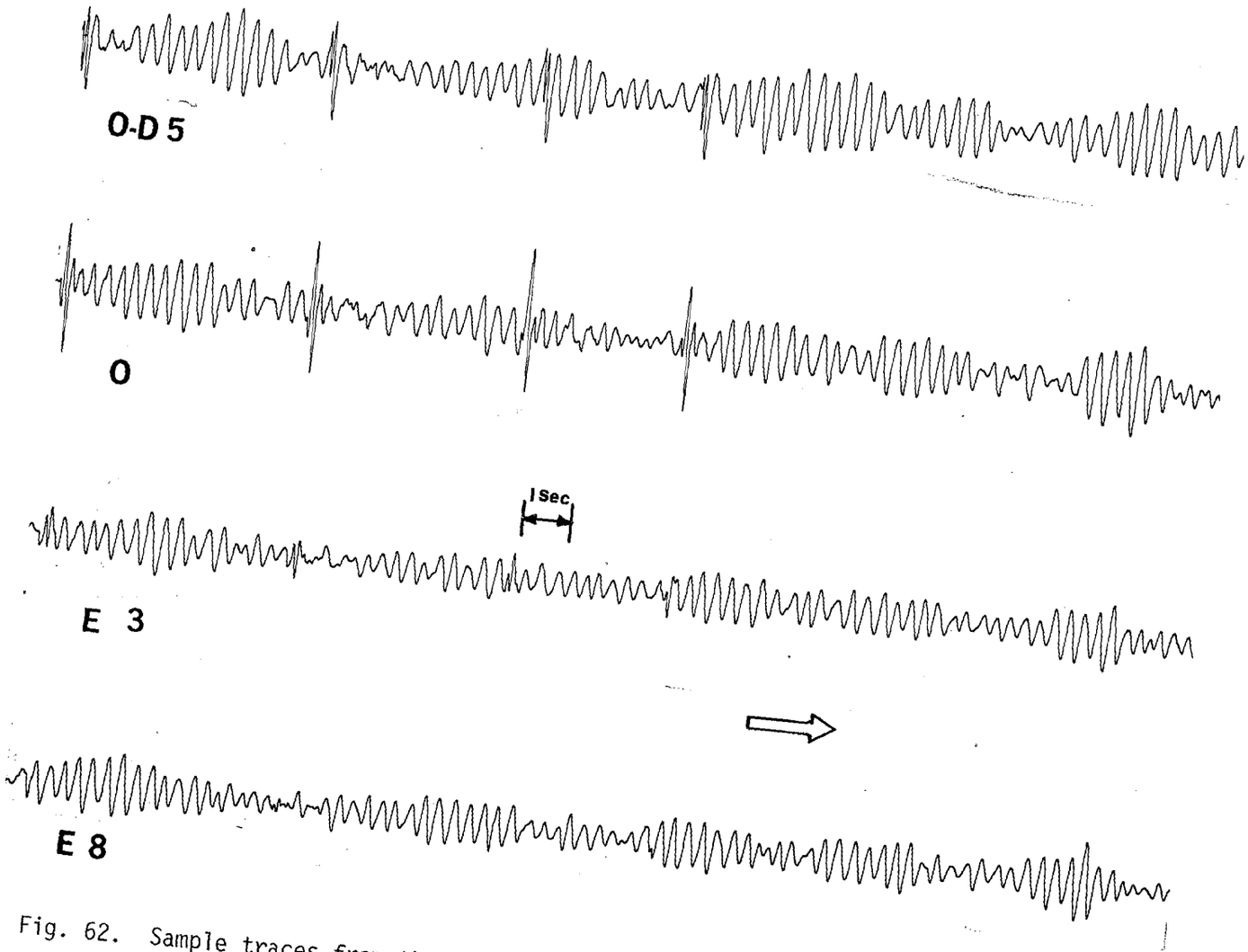

Fig. 62. Sample traces from the oscillograph recorder showing the beating phenomenon due to the proximity of the two modes S4 and R5 in the frequency domain.

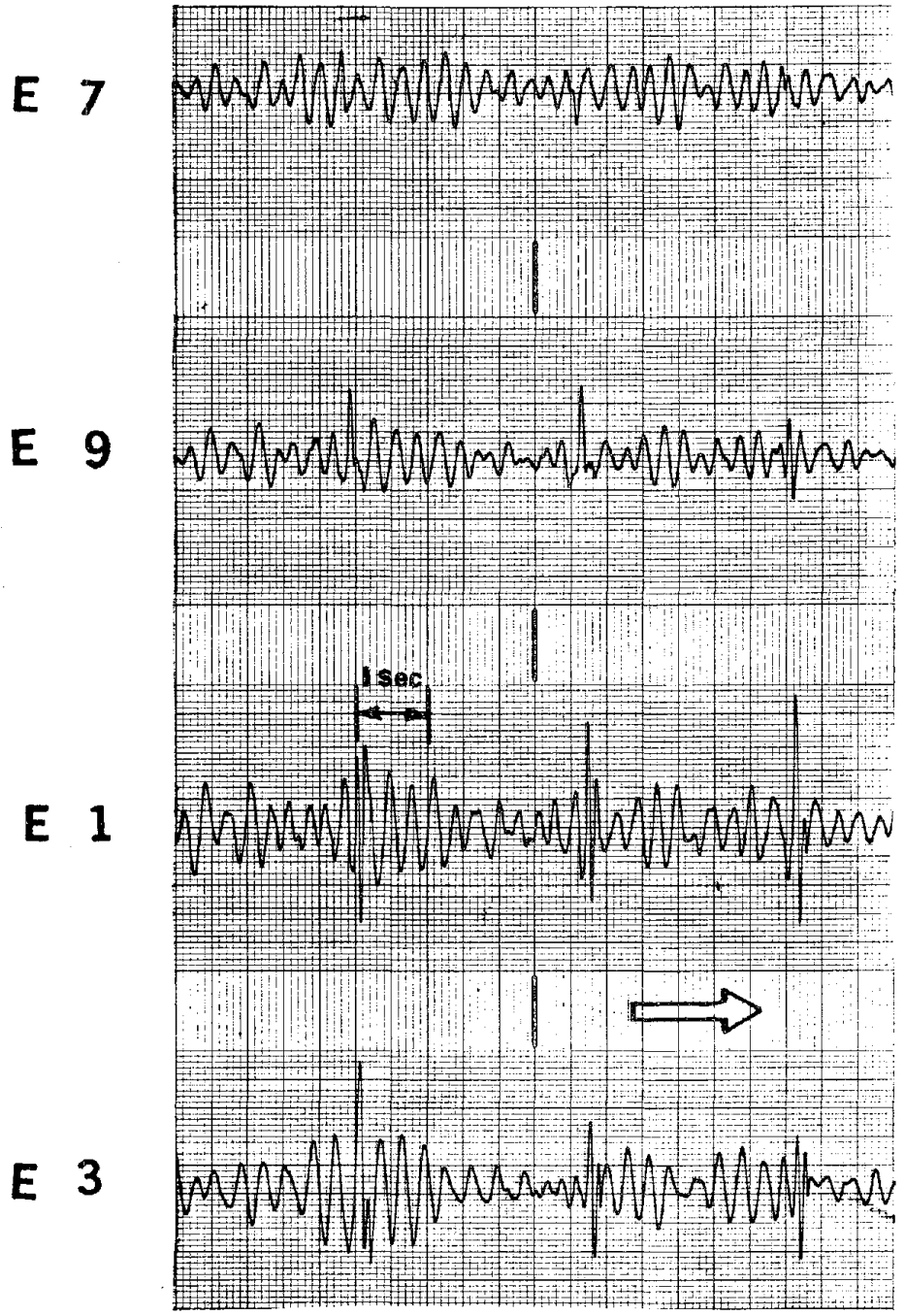

Fig. 63. Sample traces from the oscillograph recorder made simultaneously during Popper Test II at Stations E7, E9, E1 and E3 in the upstream-downstream direction.

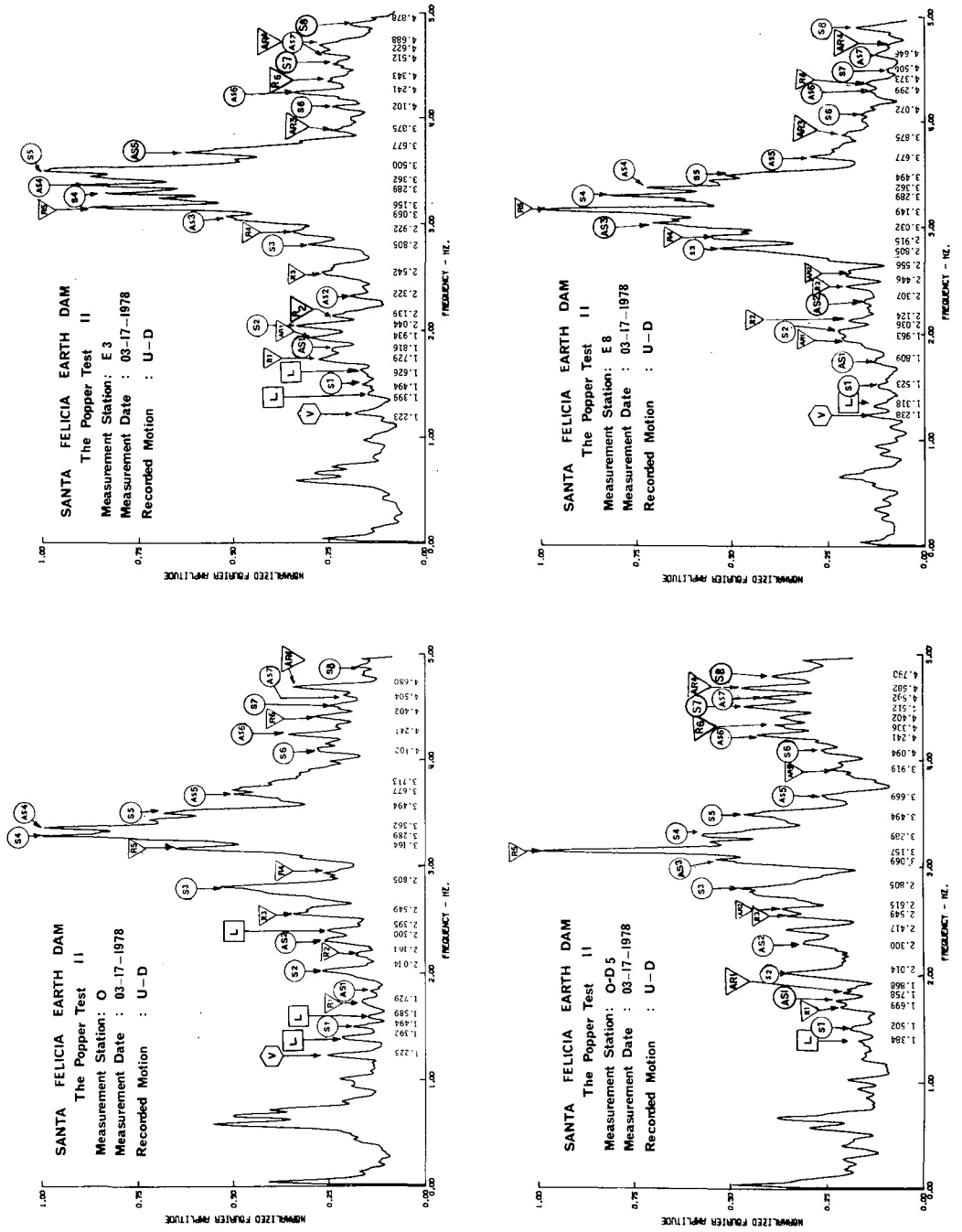

Fig. 64. Fourier amplitude spectra of the velocity proportional response of the upstream-downstream motion recorded simultaneously at Stations O, E3, O-D5 and E8 during Popper Test II.

thereby eliminated to some extent in Fig. 64.

In the subsequent test (Popper Test III), by varying the location of the Popper longitudinally along the dam crest, several modes were excited with each release of energy, particularly the antisymmetric modes which were obtained by placing the pressure wave source opposite the quarter-point. Figure 65 shows some of the time traces and Fig. 66 shows the FAS of four stations during Popper Test III; the FAS contain additional, clearer modes than those shown in Fig. 64 (for example, modes S1, R1, AS1, AS2, S6, AS6 were excited more effectively in Test III than in Test II). The results of Fig. 66 have the same frequency resolution as those of Figs. 59 and 64; however, although the filter used for Test II and Test III was the same (5 Hz), the results of Test III were smoothed with one more cycle of a Hanning Window ($\frac{1}{4}, \frac{1}{2}, \frac{1}{4}$ weights) than those of Test II (which had only one smoothing cycle).

In general, it seems that the symmetric shear mode S4 was profoundly excited during all three popper tests which may suggest that the pressure distribution on the upstream face was repeatedly approximating the S4 (or R5) modal configuration. Other possible explanations will be presented later after the results in the time domain are discussed.

Table 12 gives a summary of the resonant frequencies of the U-D direction from the popper tests (recorded at four different stations) while Table 13 contains the average resonant frequencies (averaged over different stations in the same run) as well as the total average over the three popper tests. Identification of the different resonating modes was accomplished with the aid of the digital signal processor (as mentioned previously).

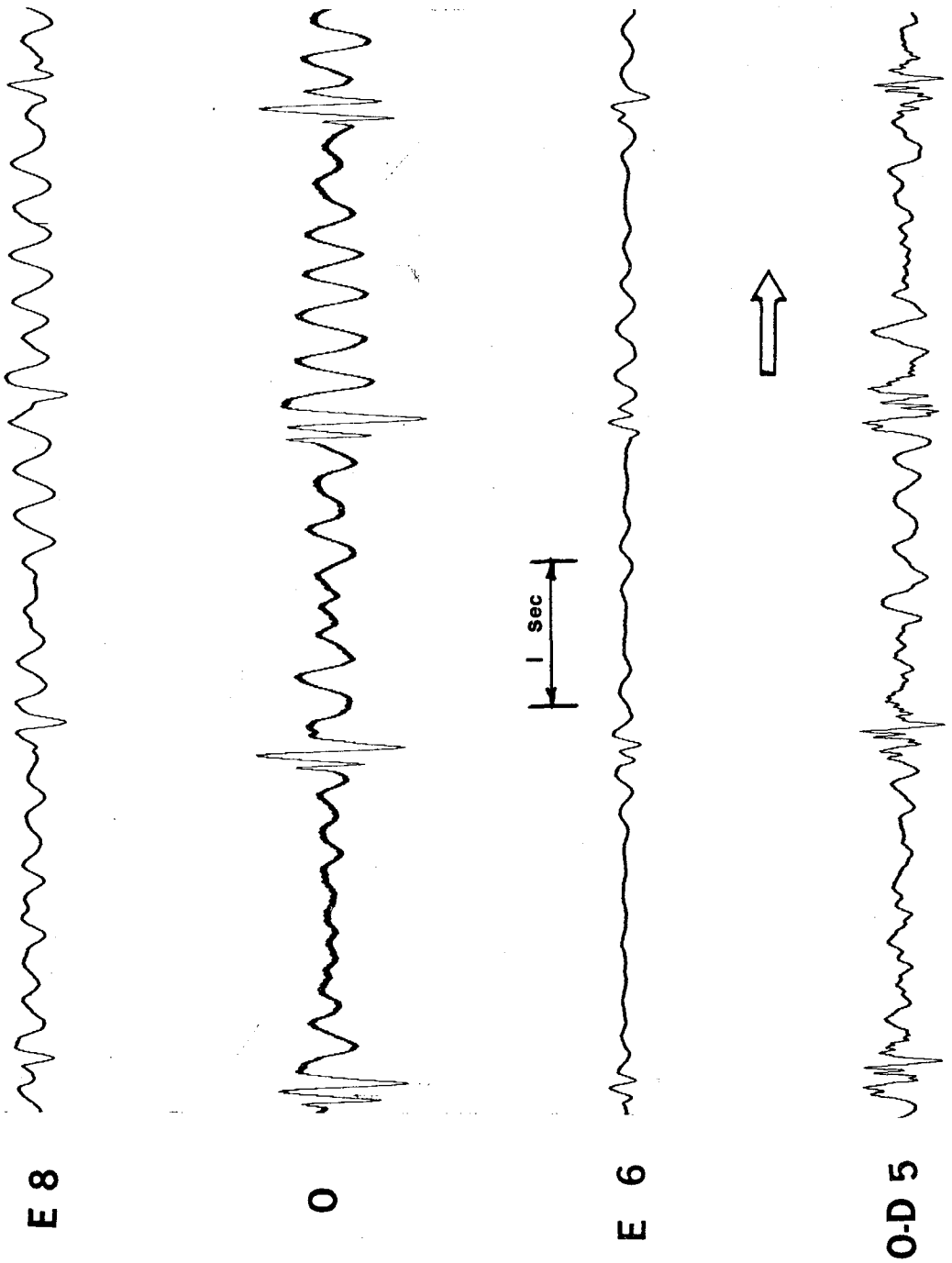

Fig. 65. Sample traces from the oscillograph recorder made simultaneously during Popper Test III at Stations E8, O, E6 and O-D5 in the upstream-downstream direction. (Popper was between Stations E1 and E2.)

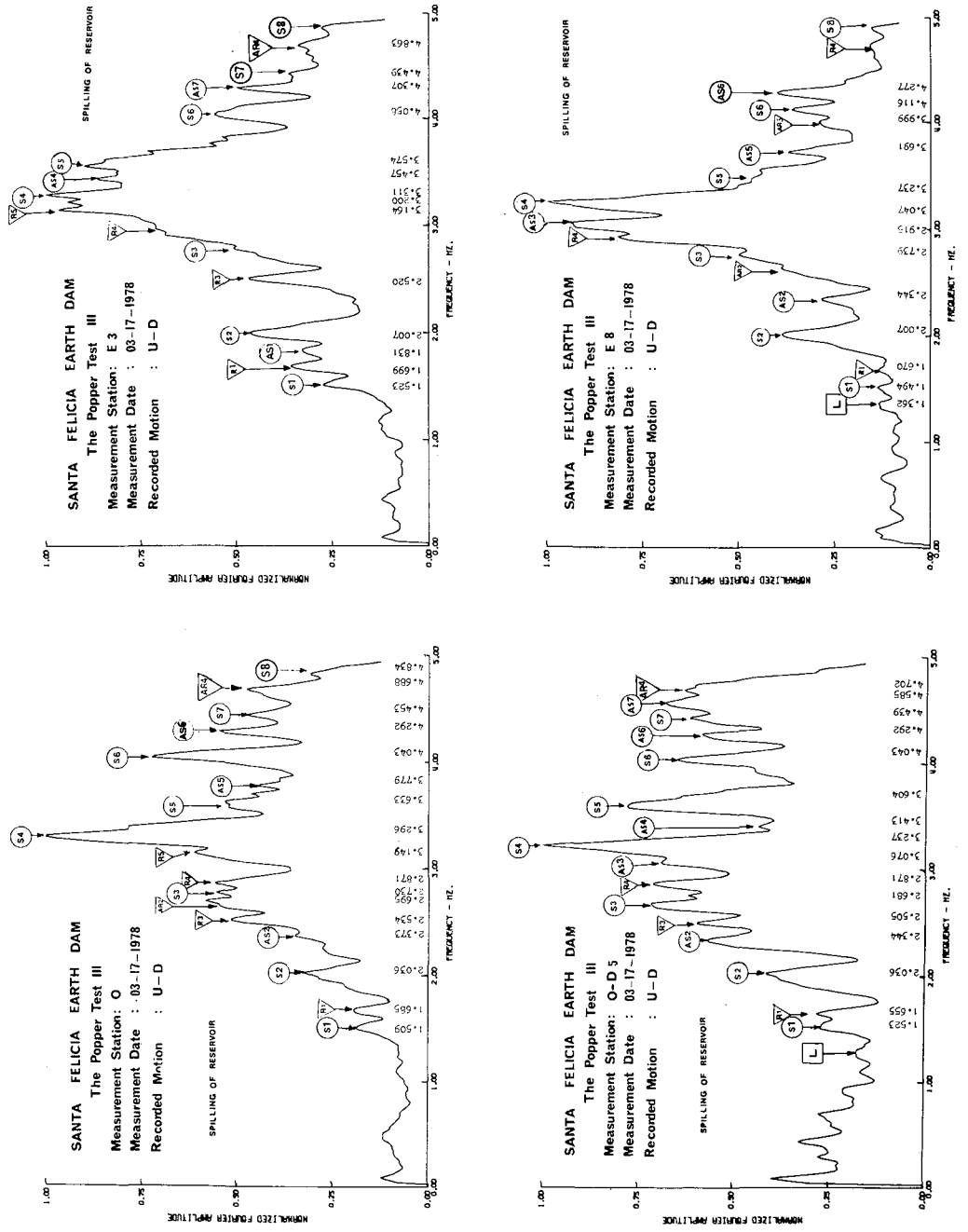

Fig. 66. Fourier amplitude spectra of the velocity proportional response of the upstream-downstream motion recorded simultaneously at Stations O, E3, O-D5 and E8 during Popper Test III.

Table 12

Resonant Frequencies (in Hz) from the Popper Tests
(Recorded at Different Stations in the Upstream-Downstream Direction)

Santa Felicia Earth Dam

Station \ Mode	Test I				Test II				Test III			
	0	0-D5	E3	E8	0	0-D5	E3	E8	0	0-D5	E3	E8
S1	1.516	1.545	1.509	1.480	1.494	1.502	1.494	1.523	1.509	1.523	1.523	1.494
R1	1.707	1.707	1.714	1.780	1.729	1.699	1.729	-	1.685	1.655	1.699	1.670
AS1	1.948	-	1.882	1.845	1.824	1.758	1.816	1.809	-	-	1.831	-
AR1	1.963	1.970	1.970	1.912	-	1.868	1.934	1.963	-	-	-	-
S2	2.036	2.124	2.022	2.065	2.014	2.014	2.044	2.036	2.036	2.036	2.007	2.007
R2	2.131	2.168	2.095	2.139	2.161	-	2.139	2.124	-	-	-	-
AS2	2.366	2.388	2.358	2.307	2.300	2.300	2.322	2.307	2.373	2.344	-	2.344
R3	2.490	2.483	2.483	2.498	2.549	2.549	2.542	2.446	2.534	2.505	2.520	-
AR2	2.673	2.666	2.607	2.688	-	2.615	-	2.593	2.695	-	-	2.622
S3	2.769	2.761	2.813	2.769	2.805	2.805	2.805	2.805	2.730	2.681	2.790	2.739
R4	2.989	2.849	2.989	2.988	2.922	-	2.922	2.915	2.871	2.871	2.930	2.915
AS3	3.113	3.091	3.106	3.062	-	3.069	3.069	3.032	-	3.076	-	3.047
R5	3.179	3.186	3.193	3.186	3.164	3.157	3.156	3.149	3.149	-	3.164	-
S4	3.259	3.237	3.259	3.230	3.289	3.289	3.289	3.289	3.296	3.237	3.311	3.237
AS4	3.450	3.420	3.479	3.494	3.362	-	3.362	3.362	-	3.413	3.457	-
S5	3.604	3.574	3.567	3.530	3.494	3.494	3.501	3.494	3.633	3.604	3.574	3.545
AS5	3.721	3.669	3.713	3.721	3.677	3.669	3.677	3.677	3.779	-	-	3.691
AR3	3.919	3.955	3.940	3.926	-	3.919	3.875	3.875	-	-	-	3.994
S6	4.109	4.021	4.131	4.109	4.102	4.094	4.102	4.072	4.043	4.043	4.058	4.116
AS6	4.241	4.248	4.233	4.197	4.241	4.241	4.241	4.299	4.292	4.292	4.307	4.277
R6	4.417	4.417	4.424	4.343	4.402	4.336	4.343	4.373	-	-	-	-
S7	4.541	4.504	4.556	4.468	4.504	4.512	4.512	4.504	4.453	4.439	4.439	-
AS7	4.680	4.673	4.680	4.614	4.607	4.592	4.622	4.644	-	4.585	-	4.629
AR4	4.753	4.746	4.750	4.731	4.680	4.680	4.688	4.724	4.688	4.702	4.702	4.731
S8	4.863	4.827	4.856	4.856	4.790	4.790	4.878	4.878	4.830	-	4.863	4.907

Table 13

Average Resonant Frequencies (in Hz) from the Popper Tests

Mode	Average Measured Frequencies from the Fourier Amplitude Spectra (Hz)			
	Test I	Test II	Test IV	Average
S1	1.513	1.503	1.512	1.509
R1	1.727	1.719	1.677	1.708
AS1	1.892	1.802	1.831	1.842
AR1	1.954	1.922	-	1.938
S2	2.062	2.027	2.022	2.037
R2	2.133	2.141	-	2.137
AS2	2.355	2.307	2.354	2.339
R3	2.489	2.522	2.520	2.510
AR2	2.659	2.604	2.659	2.641
S3	2.778	2.805	2.735	2.773
R4	2.954	2.920	2.897	2.924
AS3	3.093	3.057	3.062	3.071
R5	3.186	3.157	3.157	3.167
S4	3.246	3.289	3.270	3.268
AS4	3.457	3.362	3.435	3.418
S5	3.569	3.496	3.589	3.551
AS5	3.706	3.675	3.735	3.705
AR3	3.435	3.890	3.999	3.941
S6	4.093	4.093	4.065	4.084
AS6	4.230	4.256	4.242	4.259
R6	4.400	4.364	-	4.382
S7	4.517	4.507	4.444	4.489
AS7	4.662	4.616	4.607	4.628
AR4	4.745	4.693	4.706	4.715
S8	4.851	4.831	4.867	4.850

The recorded time traces of the popper tests on Santa Felicia earth dam were not clear enough to allow meaningful visual interpretation; the S4 (and perhaps the R5) mode shape, frequency, and damping value could be determined visually (see the time records of Figs. 60, 61, 62, 63, and 65). The S4 damping value, found to be 3.2 percent of critical damping, was determined using the logarithmic decrement method.

Some possible explanation of why the dam did not yield easily-interpreted data (other than S4 or R5 modes) from the time domain of the popper tests follows:

1. The upstream face is a sloped face (and not perpendicular to the propagation direction); it is also very rough (it consists of boulders), and thus does not allow a good transfer of energy from the water into the dam mass at a wide range of frequencies.
2. It is possible that the damping in the dam at the observed levels of response was too high to allow extended cyclic motions of low modes of vibrations.
3. It could also be that a relatively large distance from the crest of this massive structure is needed to effectively excite the lower modes or to generate a pressure distribution on the upstream face similar to some lower modes (such as the first symmetric shear mode S1).

Estimated damping values from Popper Tests II and III were obtained by the method of half-power bandwidth of the FAS and are shown in Table 14. Previous discussion of the reliability of the damping values from the ambient vibration tests can be applied to the damping values from the popper tests.

It is interesting to notice that the S4 modal damping value determined from the width of the modal peaks of the FAS and listed in Table 14 (ξ_4 = 2.83 percent of critical damping) is lower than that determined from the logarithmic decrement method (ξ_4 = 3.20 percent). The forced vibration tests showed the opposite results; however, the difference in the case of the popper tests was not as large as in that of the force vibration tests.

In conclusion, the popper test could be a more effective dynamic test of relatively large earth dams if more experimental studies could be done, particularly those emphasizing the relationships among the pressure-wave distribution on the upstream face, the distance of the source (or Popper) from the structure, the slope of the upstream face, the roughness of the upstream face, and the length of the dam crest. However, the spectral analysis of the recorded motions from this first trial of the popper test technique on the Santa Felicia earth dam provided information on the dynamic response characteristics of the dam, such as frequencies, modes, and damping values at this level of excitation, different from those due to forced vibrations, ambient vibrations, or earthquake shaking.

Table 14

Estimated Damping Ratios from the Fourier Amplitude Spectra of Popper Tests II and III (Upstream-Downstream Direction)

Santa Felicia Earth Dam

Mode	Popper Test II				Popper Test III				Average Measured Damping Ratio
	0	0-D5	E3	E8	0	0-D5	E3	E8	
S1	2.9	3.7	-	-	4.2	-	3.6	-	3.60
R1	-	-	-	-	3.3	-	3.2	-	3.25
AS1	-	-	-	-	-	-	-	-	-
AR1	-	-	2.6	-	-	-	-	-	2.60
S2	2.0	2.2	2.0	-	3.3	3.7	3.2	3.5	2.84
R2	-	-	-	-	-	-	-	-	-
AS2	2.0	2.2	1.0	-	-	3.4	-	3.2	2.36
R3	-	-	-	1.5	-	2.5	2.2	-	2.07
AR2	-	-	-	-	-	-	-	-	-
S3	1.8	-	1.8	1.6	-	2.6	-	-	1.95
R4	-	-	-	-	-	-	-	-	-
AS3	-	-	-	-	-	-	-	-	-
R5	1.1	1.0	1.0	1.1	-	-		-	1.05
S4	-	-	-	-	2.7	2.7	-	3.1	2.83
AS4	-	-	1.2	-	-	-	-	-	1.2
S5	-	-	-	-	-	2.4	-	-	2.4
AS5	-	1.4	1.4	-	-	-	-	1.8	1.53
AR3	-	-	-	-	-	-	-	-	-
S6	-	-	1.0	-	1.9	2.1	2.2	1.6	1.76
AS6	0.8	0.9	0.9	-	1.4	1.5	1.2	1.4	1.16
R6	1.1	-	-	-	-	-	-	-	1.10
S7	-	1.1	-	-	1.8	-	-	-	1.45
AS7	0.9	-	-	-	-	-	-	-	0.90
AR4	-	0.7	-	-	-	-	-	-	0.70
S8	-	1.0	-	-	-	-	-	-	1.00

VII. COMPARISON BETWEEN RESULTS OF FULL-SCALE DYNAMIC TESTS AND THOSE FROM THE DAM'S EARTHQUAKE RESPONSES

Tables 15, 16, and 17 contain summaries of comparisons made between resonant frequencies measured (in three orthogonal directions) in the dynamic tests and those determined from the spectral analysis of the dam's two earthquake responses (Ref. 2). The dam, instrumented with motion sensors that indicate its structural response as well as the input ground motion at the site, has been subjected to strong shaking during two earthquakes: the strong, 6.3 local Richter magnitude San Fernando earthquake of 1971, and a 1976 earthquake of magnitude 4.7. The records recovered from these two earthquakes provided usable information on the dam's dynamic properties such as natural frequencies, mode shapes, dynamic shear moduli, and damping factors (the latter two as functions of the induced dynamic strains). The spectral and time-history analyses of the dam's earthquake responses (Ref. 2) indicated that the structure responded primarily in its fundamental upstream-downstream shear mode with apparent natural frequency of 1.45 Hz (0.70 secs). However, the response in the longitudinal direction showed significant contribution from higher as well as lower modes; the vertical component indicated a very complex response. Furthermore, the earthquake response analysis indicated that a modern rolled-fill earth dam undergoes rather small relative displacements of its crest at a moderate intensity of shaking; the peak accelerations recorded during the 1971 earthquake were 0.22 g on the abutment and 0.21 g on the crest.

Table 15

Comparison Between Resonant Frequencies from Earthquake Records, Full-Scale Dynamic Tests and Existing Shear-Beam Theories (Santa Felicia Earth Dam)

Upstream-Downstream Direction

EARTHQUAKE RECORDS		2-D SHEAR-BEAM THEORY (Based on the Observed First Frequency 1.45 Hz)		FORCED VIBRATION TESTS						2-D SHEAR BEAM THEORY (Based on the Observed First Frequency 1.635 Hz)		AMBIENT VIBRATION MEASUREMENTS								THE POPPER TESTS			
				Symmetric Shaking			Antisymmetric Shaking					Average Measured Frequency (Hz) From the Fourier Amplitude Spectra								Average Measured Frequencies From the Fourier Amplitude Spectra (in Hz)			
San Fernando E.Q., 1971	Southern California E.Q., 1976	Mode n,r	Frequency $f_{n,r}$ (Hz)	Measured Frequency (Hz)	Designation	Remarks	Measured Frequency (Hz)	Designation	Remarks	Mode n,r	Frequency $f_{n,r}$ (Hz)	3-13-78	3-14-78	3-15-78	3-16-78	3-17-78	3-24-78	3-27-78	Average Measured Frequency (Hz) "7 days"	Test I	Test II	Test III	Average
Observed Frequency (Hz)	Observed Frequency (Hz)																						
1.44	1.46	1,1	1.45	1.635	S1(1,1)	Shear	-	-	-	1,1	1.635	1.620	1.621	1.586	1.619	1.603	1.620	1.626	1.614	1.513	1.503	1.512	1.509
-	1.66	-	-	1.850	R1	Rocking	-	-	-	-	-	1.753	1.779	1.792	1.773	1.745	1.787	1.780	1.773	1.727	1.719	1.677	1.708
1.81	1.86	1,2	1.67	-	-	-	1.875	AS1(1,2)	Shear	1,2	1.872	1.934	1.884	1.924	1.835	1.916	1.881	1.924	1.900	1.892	1.802	1.831	1.842
-	-	-	-	-	-	-	2.025	AR1	Rocking	-	-	2.025	2.020	2.030	1.978	-	2.035	2.044	2.022	1.954	1.922	-	1.938
2.03	2.08	1,3	1.95	2.100	S2(1,3)	Shear	-	-	-	1,3	2.209	2.130	2.130	2.097	2.044	2.050	2.111	2.119	2.097	2.062	2.027	2.027	2.037
-	-	-	-	2.270	R2	Rocking	-	-	-	-	-	2.224	2.244	2.168	2.161	2.225	2.237	2.229	2.213	2.133	2.141	-	2.137
2.27	2.25	1,4	2.32	-	-	-	2.300	AS2(1,4)	Shear	1,4	2.610	2.368	2.350	2.395	2.333	2.377	2.367	2.320	2.359	2.355	2.307	2.354	2.339
2.47	-	-	-	2.600	R3	Rocking	-	-	-	-	-	2.591	2.611	2.549	2.540	2.587	2.568	2.500	2.564	2.489	2.522	2.520	2.510
-	-	-	-	-	-	-	2.650	AR2	Rocking	-	-	2.680	2.693	2.680	2.695	2.632	2.699	2.646	2.675	2.659	2.604	2.659	2.641
2.88	2.75	1,5	2.71	2.840	S3(1,5)	Shear	-	-	-	1,5	3.048	2.900	2.809	2.783	-	2.842	2.869	2.859	2.844	2.778	2.805	2.735	2.773
-	-	-	-	2.920	R4	Rocking	-	-	-	-	-	3.010	2.942	2.903	-	3.038	2.970	2.989	2.975	2.954	2.920	2.897	2.924
3.10	3.13	1,6	3.11	-	-	-	3.100	AS3(1,6)	Shear	1,6	3.510	3.091	3.230	3.128	-	3.190	3.214	3.135	3.165	3.093	3.057	3.062	3.071
-	-	2,1	3.21	3.150	R5	Rocking	-	-	-	2,1	3.595	3.157	3.348	3.230	-	3.289	3.105	-	3.226	3.186	3.157	3.157	3.167
3.17	3.61	2,2	3.53	3.550	S4(2,3)	Shear	-	-	-	2,2	3.710	-	3.606	3.474	-	3.480	3.539	3.582	3.536	3.246	3.289	3.270	3.268
-	-	2,3	3.48	-	-	-	3.600	AS4(2,4)	Shear	2,3	3.891	-	3.745	3.641	-	3.515	3.704	3.669	3.665	3.457	3.362	3.435	3.418
-	-	1,7	3.54	3.870	S5(1,7)	Shear	-	-	-	1,7	3.987	-	3.943	3.853	-	3.847	3.866	3.830	3.868	3.569	3.496	3.589	3.551
3.93	3.81	2,4	3.68	-	-	-	4.100	AS5(1,8)	Shear	2,4	4.151	-	4.146	4.136	-	4.124	4.181	-	4.147	3.706	3.675	3.735	3.705
-	-	2,5	3.96	-	-	-	4.225	AR5	Rocking	2,5	4.421	-	4.241	4.197	-	4.243	4.204	-	4.221	3.935	3.890	3.999	3.941
-	-	1,8	3.97	4.300	S6(2,5)	Shear	-	-	-	1,8	4.476	-	4.360	4.282	-	4.339	4.325	-	4.327	4.093	4.093	4.065	4.084
4.25	4.00	2,6	4.25	-	-	-	4.420	AS6(2,6)	Shear	2,6	4.752	-	4.472	4.398	-	4.433	4.476	-	4.445	4.230	4.256	4.292	4.259
-	-	1,9	4.41	4.450	R6	Rocking	-	-	-	1,9	4.971	-	4.594	4.516	-	-	-	-	4.555	4.400	4.364	-	4.382
-	-	2,7	4.54	4.665	S7(1,9)	Shear	-	-	-	2,7	5.115	-	4.695	4.656	-	4.636	4.598	-	4.646	4.517	4.507	4.444	4.489
4.90	-	1,10	4.87	-	-	-	4.700	AS7(1,10)	Shear	1,10	5.470	-	4.780	4.749	-	4.804	4.790	-	4.781	4.662	4.616	4.607	4.628
-	-	2,8	4.90	-	-	-	4.900	AR4	Rocking	-	-	-	-	-	-	-	4.973	-	4.973	4.745	4.693	4.706	4.715
5.08	-	3,1	5.14	5.257	S8(2,7)	Shear	-	-	-	-	-	-	-	-	-	-	5.140	-	5.140	4.851	4.831	4.867	4.850
5.52	-	2,9	5.28	-	-	-	-	-	-	-	-	-	-	-	-	-	-	-	-	-	-	-	-

Table 16

Comparison Between Resonant Frequencies From Earthquake Records and Full-Scale Dynamic Tests (Santa Felicia Earth Dam) Longitudinal Direction

EARTHQUAKE RECORDS		FORCED VIBRATION TESTS		AMBIENT VIBRATION MEASUREMENTS					
San Fernando E.Q. 1971	Southern California E.Q. 1976	One Shaker Only		Measured Frequencies From the Fourier Amplitude Spectra (Hz)					Average Measured Frequency (Hz) "5 days"
Observed Frequency (Hz)	Observed Frequency (Hz)	Measured Frequency (Hz)	Remarks	3-13	3-14	3-15	3-16	3-27	
0.99	-	-	-	-	-	-	-	-	-
1.35	1.27	1.425	L1	1.498	1.417	1.470	1.410	1.434	1.446
1.70	1.66	1.675	L2	1.674	1.630	1.663	1.578	1.645	1.638
1.86	1.86	1.850	L3	1.881	1.879	1.871	1.813	1.802	1.849
-	-	1.950	L4	2.030	1.981	1.952	2.044	1.923	1.986
2.15	2.15	2.155	L5	2.230	2.151	2.175	2.157	2.161	2.175
2.32	-	2.275	Possible	2.363	2.360	2.333	2.241	2.286	2.317
-	-	2.425	Possible	2.443	2.479	2.491	2.399	2.447	2.452
-	2.64	2.625	L6	2.651	2.659	2.619	2.666	2.597	2.638
2.91	-	2.875	L7	2.871	2.929	2.850	2.937	2.811	2.880
-	-	3.050	L8	3.062	3.084	3.007	-	2.978	3.033
3.15	-	3.150	L9	3.146	3.164	3.161	-	3.128	3.150
-	3.22	3.230	Possible	3.212	3.208	3.237	-	3.260	3.229
-	-	3.350	L10	3.351	3.329	-	-	3.380	3.323
3.49	-	3.480	L11	3.494	3.491	3.464	-	3.497	3.487
3.85	3.71	3.775	L12	3.750	3.798	3.824	3.699	3.805	3.775
4.03	-	4.025	Possible	4.063	4.043	4.069	-	4.028	4.051
-	4.20	4.175	Possible	4.168	4.219	4.156	-	4.215	4.190
4.42	-	4.370	L13	4.365	4.373	4.329	-	4.366	4.358
-	4.59	4.700	L14	-	4.644	4.695	-	4.662	4.667
4.88	-	4.875	L15	-	4.922	4.856	-	4.849	4.876
5.44	-	5.350	L16	-	-	-	-	-	-
	5.57	5.600	L17	-	-	-	-	-	-
5.98	6.05	5.900	L18	-	-	-	-	-	-

Table 17

Comparison Between Resonant Frequencies From
Earthquake Records and Ambient Vibration Tests
(Santa Felicia Earth Dam)
Vertical Direction

EARTHQUAKE RECORDS		AMBIENT VIBRATION MEASUREMENTS					
San Fernando E.Q. 1971	Southern California E.Q. 1976	Measured Frequencies From the Fourier Amplitude Spectra (Hz)					Average Measured Frequency (Hz) "5 days"
Observed Frequency (Hz)	Observed Frequency (Hz)	03-13-1978	03-14-1978	03-15-1978	03-16-1978	03-27-1978	
		1.00	0.99	1.00	1.02	1.00	1.00
0.95	0.98	1.15	1.08	1.12	1.11	1.17	1.13
		1.29	1.28	1.24	1.23	1.25	1.26
		1.33	1.38	1.34	1.34	1.34	1.35
1.37	1.46	1.48	1.47	1.48	1.43	1.44	1.46
		1.55	1.56	-	1.53	1.53	1.54
		1.64	1.63	1.66	1.63	1.63	1.64
1.78	1.76	1.77	1.77	1.76	1.73	1.77	1.76
		1.88	1.87	1.84	1.84	1.92	1.87
		1.98	1.96	1.99	1.93	2.04	1.98
		2.11	2.09	2.13	2.06	2.09	2.10
2.20	2.25	2.19	2.22	2.39	2.23	2.29	2.26
		2.37	2.35	2.43	2.39	2.44	2.40
		2.45	2.50	2.56	2.55	-	2.52
2.34	2.64	2.64	2.63	2.65	2.65	2.63	2.64
		2.72	2.77	-	2.77	2.76	2.76
		2.91	2.92	2.92	2.90	2.93	2.92
2.91	3.03	3.03	3.06	3.06	3.00	3.03	3.04
		3.14	3.13	-	3.13	3.05	3.11
		3.22	3.22	3.24	3.19	3.19	3.21
3.20	3.22						
			3.37	3.36	3.35	3.33	3.35
			3.53	3.52	3.44	3.51	3.50
3.54	3.52						
			3.64	3.66	3.61	3.66	3.64
			3.77	3.79	3.73	3.78	3.77
3.64	3.71		3.88	3.87	3.86	3.92	3.88
			4.01	3.95		4.02	3.99
			4.18	4.16		-	4.17
3.93	4.10		4.26	4.28		4.29	4.28
			4.34	4.44		4.39	4.39
			4.65	4.67		4.64	4.65
4.59	-		4.77	-		4.74	4.76
			4.86	4.82			4.84

VII-1 Upstream-Downstream Direction

The results from the earthquake records and from the full-scale dynamic tests (including ambient, forced, and popper tests) were also compared with those estimated by using the 2-D shear-beam model. The results from the model were based upon substituting the value of the first measured (or determined) U-D resonant frequency from the forced vibration tests (or from earthquake records) into the frequency equation to obtain a representative value of the shear wave velocity from which the natural frequencies higher than the first were then calculated. The first frequency in the forced vibration case was 1.635 Hz; the results based on its use are shown in columns 11 and 12 of Table 15. The first frequency in the case of the earthquakes was 1.45 Hz, and the results are shown in columns 3 and 4. A frequency comparison between the calculated values and measured values from the forced vibration tests has already been discussed (in Section VI-1-3) and a comparison between the theory and the earthquake results can be found in Ref. 2.

Based on the results of Table 15 (enabling a comparison to be made between full-scale tests and earthquake responses) the following additional observations can be drawn:

1. By comparing the resonant frequency of the first U-D symmetric shear mode determined from various full-scale tests and that estimated from the response of the dam during the two earthquakes, it is seen that the natural period was longer during the earthquakes (f_1 = 1.45 Hz, or T_1 = 0.69 sec) than it was during the tests (forced: f_1 = 1.635 Hz, or T_1 = 0.61 sec; ambient: f_1 = 1.614 Hz, or T_1 = 0.62 sec; popper: f_1 = 1.509 Hz, or T_1 = 0.66 sec). The lengthening of the first symmetric shear

period during earthquakes by factors of 1.13 (as compared to forced tests), 1.12 (ambient, 1.04 (popper) corresponds to a decrease in overall stiffness by factors of 1.28, 1.25, and 1.08, respectively.

This behavior is typical of a softening dynamic system such as the soil of an earth dam which is known to be extremely nonlinear. However, in assessing this variability of the dam's dynamic characteristics one has to be very careful about concluding whether these changes in frequency are caused solely by a change of the stiffness due to different excitation levels of the dam material or by other factors as well. For example, this variability could be partially due to an increase in the vibrating mass of the dam caused by an increase in the level of the reservoir water, or it could be partly due to the nature of the dynamic excitations which varied greatly in their time-history characteristics, spatial distributions, and intensities.

During the full-scale measurements, the water level in the reservoir was at the same maximum (spilling) level throughout the tests; during the 1971 earthquake the reservoir level was quite high (according to the dam's caretaker) but not at its maximum level. The virtual additional mass could have had some effect, but it is believed that such effect would be very slight and probably unnoticeable (because of the massiveness of the structure and the flatness of the upstream face (Ref. 20). Thus, the data presented here seem to imply that changes in dynamic characteristics observed during the tests were mainly the result of the loss in stiffness due to the nonlinear behavior of the dam materials and less significantly due to the nature of the dynamic loadings.

Finally, comparison also indicates that, in exciting the first symmetric shear mode, S1, the force generated by the popper (at 1.509 Hz) was

more than that generated during the ambient and mechanical shaking tests. Unfortunately, there were no dynamic pressure transducers mounted on the upstream face to provide the order of magnitude of the popper forces.

2. During the two earthquakes, very few high modes (shear or rocking) were excited in the U-D direction (the response was primarily from the first mode), whereas, contrarily, the higher modes were excited efficiently and clearly by the three dynamic tests. In addition, the identification of some of the higher modes excited during the earthquakes was not reliable. As a result, it is difficult to make any reliable comparison based on a frequency-to-frequency analysis.

3. Looking at the frequencies of the first antisymmetric shear mode, AS1, (1.81 Hz "1971 earthquake", 1.86 Hz "1976 earthquake,) 1.875 Hz "forced," 1.900 Hz "ambient," and 1.842 Hz "popper"), it is seen that there is a maximum variance of only 5% which may suggest that the AS1 mode may not have been excited effectively by the two earthquakes (the participation factors of different modes excited during the two earthquakes are presented in Ref. 2). Other possible explanations of the similarity in these frequencies are: (i) the uniformity of ground shaking at the dam causing symmetric modes to be excited more effectively, and (ii) the location of the crest accelerograph in the central region of the crest (about 50 ft away from the crest midpoint), i.e., in a position more likely to pick up the dominant symmetric motions since this region represents nodes of antisymmetric modes.

4. Some of the lower U-D rocking modes were not excited during the shaking of the two earthquakes; examples of these modes are AR1, R2, AR2, and R4. Apparently the first rocking mode, R1, was excited during the

1976 earthquake (with frequency 1.66 Hz); this frequency was increased by 3% (1.708 Hz) during the popper tests, by 7% (1.773 Hz) during the ambient tests, and by 11% (1.850 Hz) during the forced vibration tests. The third symmetric rocking mode, R3, was excited during the 1971 earthquake at a frequency of 2.47 Hz compared to frequencies:

2.510 Hz (2% increase) from the popper tests,

2.565 Hz (4% increase) from the ambient tests,

2.600 Hz (5% increase) from the forced tests.

Finally, the resonant frequencies of the rocking modes AR1, R2, AR2 resulting from full-scale tests vary slightly from one type of test to another; the variation ranges from 1% to 5% as indicated by Table 15.

5. The frequencies of symmetric and antisymmetric shear modes, S2, AS2, and AS3, also vary slightly from the earthquake responses to the full-scale tests. However, the third symmetric shear mode, S3, was excited more strongly during the small earthquake of 1976 (frequency 2.71 Hz) than during the large earthquake of 1971 (frequency 2.88 Hz); the frequencies from the tests were 2.840 Hz, 2.844 Hz, and 2.773 from forced, ambient, and popper tests, respectively. This just demonstrates that greater shaking does not always excite all modes more strongly.

6. It is interesting to compare the frequencies of the fourth symmetric shear mode, S4, resulting from the different tests and the two earthquakes, since the mode associated with this frequency was excited very effectively by the popper test. The frequency determined from the 1971 earthquake response was 3.470 Hz, then it increased to 3.610 Hz from the 1976 earthquake response; the popper tests provided a frequency of 3.268 Hz, while the frequencies from the forced and ambient vibration

tests were 3.550 Hz and 3.536 Hz, respectively. Note that the popper test excited the S4 mode more strongly than even the strong earthquake. (For a discussion of this phenomenon see Section VI-3.) This observation is not a surprising one since the dam responded mainly in its fundamental symmetric shear mode during the two earthquakes; while during the popper test the dam was excited, exclusive of all other modes, in mode S4.

7. The dynamic shear moduli and damping factors of the dam's material were estimated from the measured responses (the hysteretic responses of the first symmetric shear mode) to the two earthquakes. Both dynamic properties were determined as functions of the induced dynamic strains (for more details see Ref. 2). The relationships between each dynamic property and the induced dynamic strain are illustrated by the semilog plots of Figs. 67 and 68 for the first 20 seconds of the 1971 earthquake and the first 6 seconds of the 1976 earthquake. It should be noted here that the estimation of the dam's dynamic soil properties was made from both the measured response and the existing 2-D shear beam theories.

In order to reveal any change in the dynamic properties of the dam, the estimated shear moduli and damping factors from the full-scale tests (discussed previously) are shown also on Figs. 67 and 68. In addition, Table 18 shows some of these dynamic properties associated with various levels of response. Both the figures and the table indicate that the dynamic properties of the dam's constituent materials estimated from low-strain full-scale tests are consistent with those determined from the relatively larger strains induced by the two earthquakes.

By interpolating and extrapolating the data of Figs. 67 and 68, Figs. 69 and 70, accordingly, are proposed to provide reasonable estimates

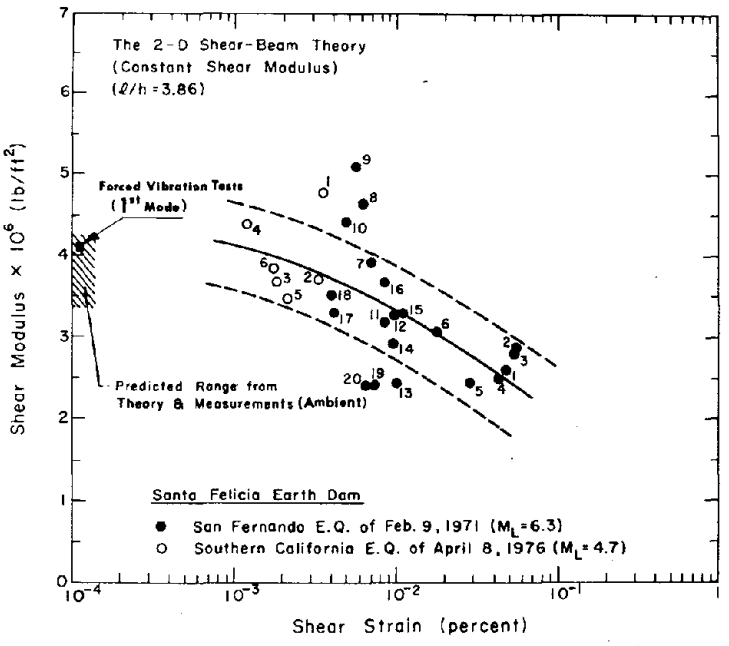
The 2-D Shear-Beam Theory
(Constant Shear Modulus)
(ℓ/h = 3.86)
Forced Vibration Tests
(1st Mode)
Predicted Range from
Theory & Measurements (Ambient)
Santa Felicia Earth Dam
San Fernando E.Q. of Feb. 9, 1971 (M_L = 6.3)
Southern California E.Q. of April 8, 1976 (M_L = 4.7)
Shear Modulus × 10^6 (lb/ft^2)
Shear Strain (percent)

Fig. 67

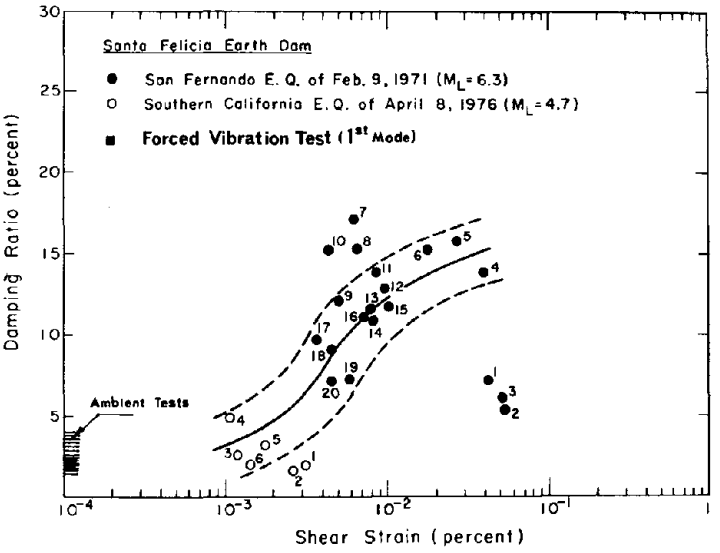
Santa Felicia Earth Dam
San Fernando E. Q. of Feb. 9, 1971 (M_L = 6.3)
Southern California E.Q. of April 8, 1976 (M_L = 4.7)
Forced Vibration Test (1st Mode)
Ambient Tests
Damping Ratio (percent)
Shear Strain (percent)

Fig. 68

Table 18

Comparison Between the Dynamic Properties (of an Earth Dam) Estimated From Earthquake Records and Those Determined From Full-Scale Dynamic Tests.

Source of Data (Different Levels of Excitation)	Upstream-Downstream Direction							Longitudinal Direction
	SYMMETRIC VIBRATION						ANTISYMMETRIC VIBRATION	Natural (First) Frequency
	First Shear Frequency	Estimated Shear Modulus	Estimated Shear Strain	Estimated Damping Factor	Max. Acceleration at the Crest	Max. Displacement at the Crest	First Shear Frequency	
1971 San Fernando Earthquake $M_L = 6.3$	1.440 Hz	Ranges from 2.4×10^6 lb/ft^2 to 4.5×10^6 lb/ft^2	Ranges from 0.4×10^{-2} % to 5.5×10^{-2} %	Ranges from 5.0% to 15.0%	20% g	13.30 mm	1.81 Hz	1.35 Hz
1976 Southern California Earthquake $M_L = 4.7$	1.460 Hz	Ranges from 3.4×10^6 lb/ft^2 to 4.8×10^6 lb/ft^2	Ranges from 0.10×10^{-2} to 0.40×10^{-2} %	Ranges from 1.5% to 5.0%	5% g	0.85 mm	1.86 Hz	1.27 Hz
Forced Vibration Tests (Mechanical Shaking)	1.635 Hz	4.10×10^6 lb/ft^2	0.716×10^{-5} %	3.0%	.0037% g	0.00336 mm	1.875 Hz	1.425 Hz
Ambient Vibration Tests (Wind and Spilling of the Reservoir)	Ranges from 1.570 Hz to 1.670 Hz	Ranges from 3.6×10^6 lb/ft^2 to 4.3×10^6 lb/ft^2	-	Ranges from 2.3 to 3.6%	-	-	Ranges from 1.85 Hz to 1.95 Hz	Ranges from 1.44 Hz to 1.48 Hz
Hydrodynamically Generated Force (Popper Tests)	Ranges from 1.50 Hz to 1.63 Hz	-	-	Ranges from 2.9% to 4.2%	-	-	Ranges from 1.76 Hz to 1.93 Hz	-

of the dynamic properties of the dam's constituent material; these estimates would be useful for any study of its upstream-downstream earthquake response characteristics. In addition, the variation of material properties with depth should be taken into account for any realistic dynamics study; the variation of the shear modulus of the dam material with depth is proposed in Fig. 71, which is based on an in situ wave velocity measurement (Fig. 72) as well as on the analysis of the two earthquake responses (Ref. 2). Figures 69, 70, and 71 should give a good guide to the material properties in the dynamic analysis of any earth dam composed predominantly of rolled-fill, essentially cohesionless material, with or without a relatively thin core.

VII-2. Longitudinal and Vertical Directions

With the exception of the first three longitudinal frequencies observed during the two earthquakes (at 1.35, 1.70, and 1.86 Hz), it is difficult to make any reliable comparison with the values of the resonant frequencies in the longitudinal direction resulting from the forced vibration tests and those resulting from various ambient vibration measurements, as indicated by Table 16. As was discussed previously, there are many closely-spaced frequencies in the longitudinal direction, and some of the longitudinal resonant frequencies are very close (even identical) to some of the U-D resonant frequencies which may suggest a strong coupling between the U-D and L vibrations.

The first longitudinal mode was apparently excited more strongly during the small (1976) earthquake (where f = 1.27 Hz) than during the large (1971) earthquake (where f = 1.35 Hz); the increase is about

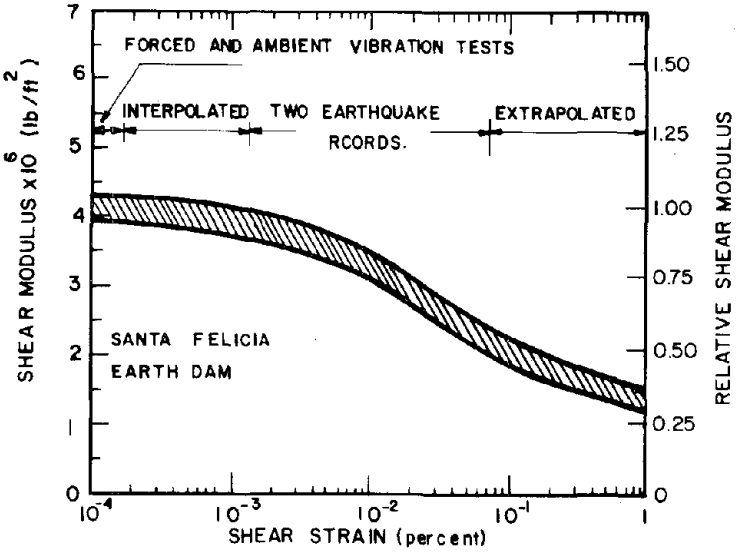
FORCED AND AMBIENT VIBRATION TESTS
INTERPOLATED TWO EARTHQUAKE RCORDS.
EXTRAPOLATED
SANTA FELICIA
EARTH DAM
SHEAR MODULUS x10^6 (lb/ft^2)
RELATIVE SHEAR MODULUS
SHEAR STRAIN (percent)

Fig. 71

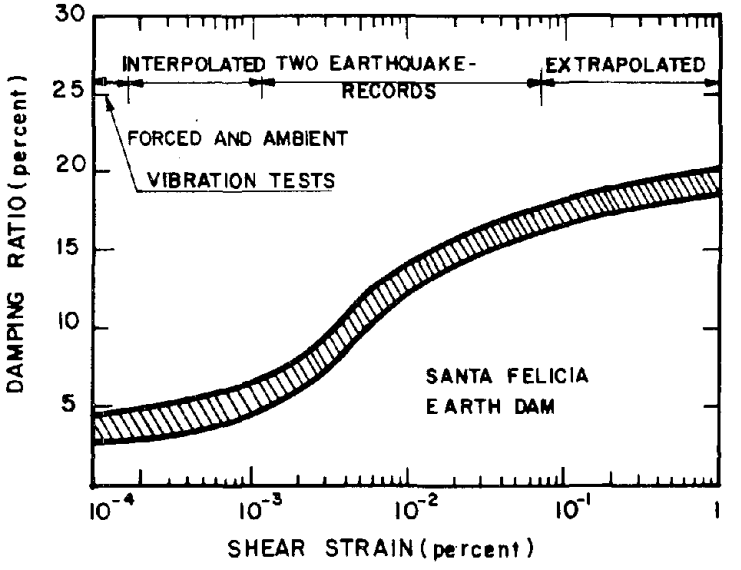
INTERPOLATED TWO EARTHQUAKE-RECORDS
EXTRAPOLATED
FORCED AND AMBIENT
VIBRATION TESTS
SANTA FELICIA
EARTH DAM
DAMPING RATIO (percent)
SHEAR STRAIN (percent)

Fig. 70

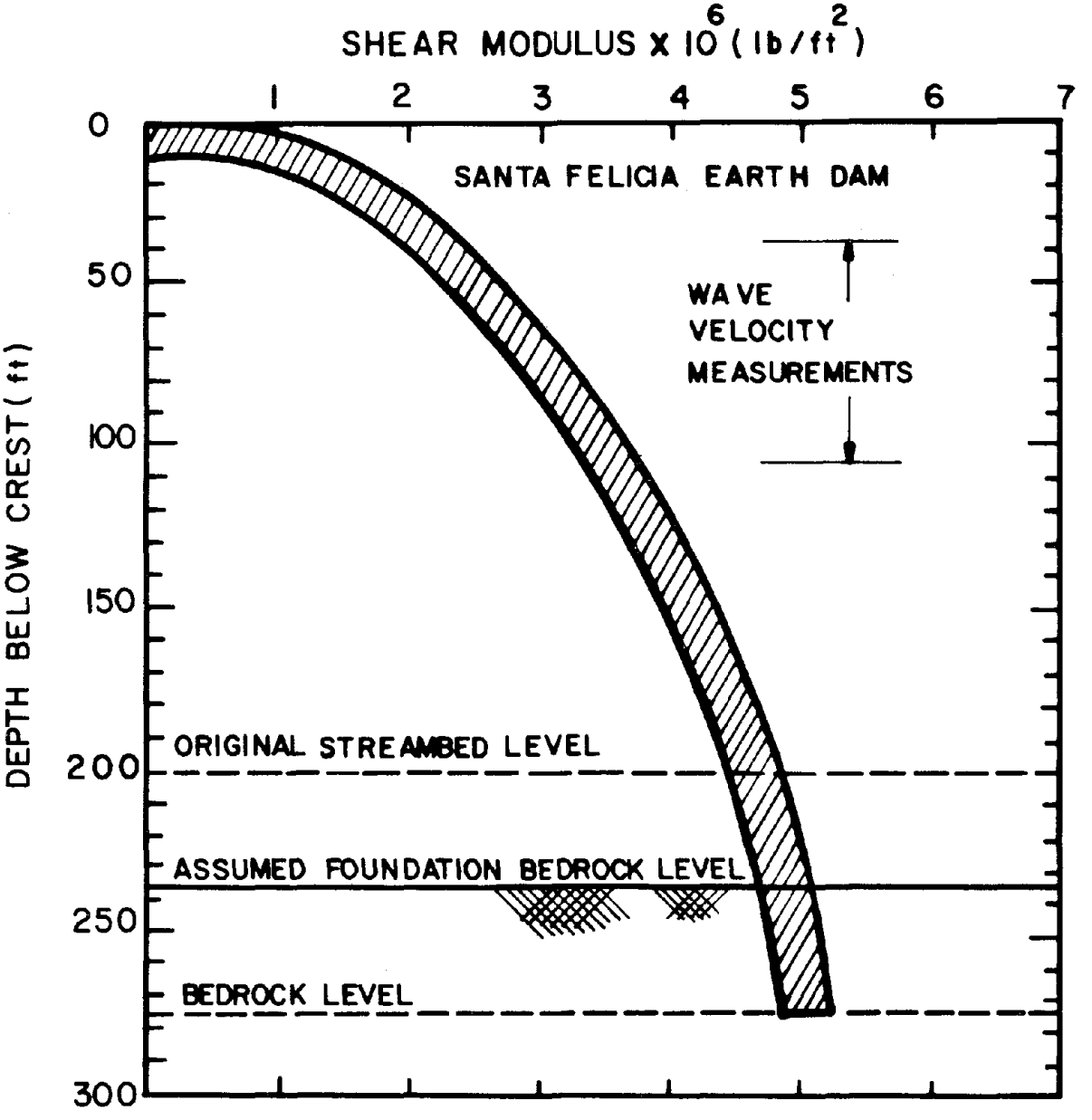
SHEAR MODULUS X 10^6 (lb/ft^2)
1
2
3
4
5
6
7
0
50
100
150
200
250
300
DEPTH BELOW CREST (ft)
SANTA FELICIA EARTH DAM
WAVE VELOCITY MEASUREMENTS
ORIGINAL STREAMBED LEVEL
ASSUMED FOUNDATION BEDROCK LEVEL
BEDROCK LEVEL

Fig. 71

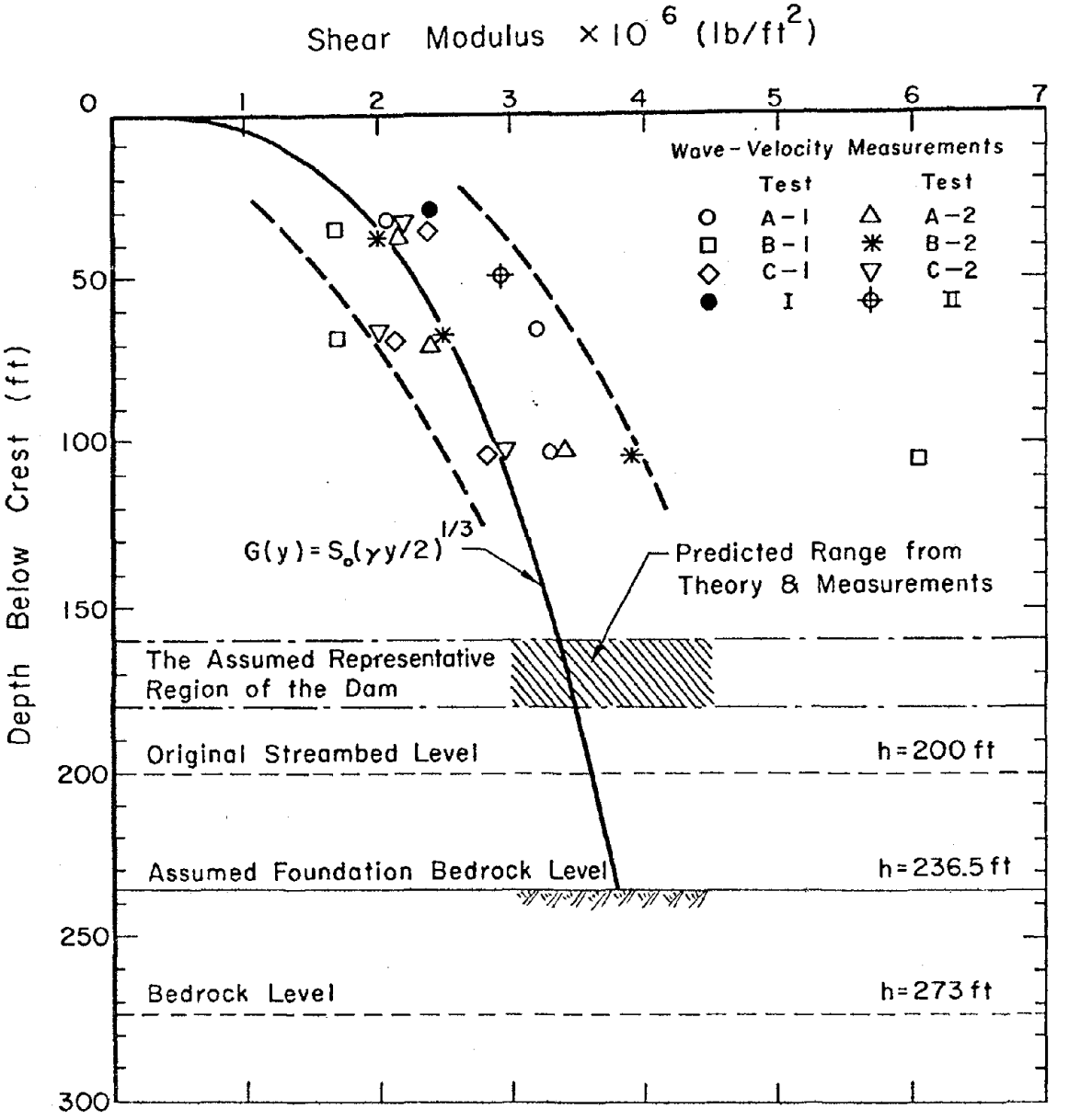
Shear Modulus $\times 10^6$ (lb/ft^2)
0
1
2
3
4
5
6
7
Depth Below Crest (ft)
50
100
150
200
250
300
Wave-Velocity Measurements
Test
Test
A-1
A-2
B-1
B-2
C-1
C-2
I
II
$G(y) = S_o(\gamma y/2)^{1/3}$
Predicted Range from Theory & Measurements
The Assumed Representative Region of the Dam
Original Streambed Level
h=200 ft
Assumed Foundation Bedrock Level
h=236.5 ft
Bedrock Level
h=273 ft

Fig. 72

6% which corresponds to a decrease in overall stiffness by a factor of 1.12. The frequency increased to 1.425 Hz when determined from the forced vibration tests (a 12% increase over the 1976 earthquake) and to an average value of 1.446 Hz (a 14% increase over the 1976 earthquake) as determined from the ambient tests. These increases of the first longitudinal frequency correspond to decreases in overall stiffness by factors of 1.25 and 1.30 for the forced and ambient tests, respectively. This behavior is similar to that observed for the upstream-downstream direction.

The situation for the vertical component is even more complicated as is seen from Table 17, where, while the comparison between the results of the two earthquakes is quite consistent, the comparison between the two earthquake results and those of the ambient vibration measurements is not consistent at all. The results of the ambient tests showed many, closely spaced resonant frequencies, while the results of the two earthquakes showed well-separated frequencies.

Finally, there is also substantial indication of modal coupling and interference between the three orthogonal directions; there were many frequencies with identical values measured in the three directions.

VII-3. Conclusions

It appears from the data available on the dam's responses and the above discussion that:

1. Analytical or finite element models are needed not only to represent the prototype realistically in both vertical and longitudinal directions, but also to include the coupling of the three directional motions (U-D, L, and V). These models should take into account the geometric variation of the dynamic properties as well as the material

degradation properties.

2. In order to get reliable information on any dam's three-dimensional behavior during an earthquake, more than two sets of strong-motion instruments should be deployed on and in the vicinity of the structure. Proper placement will yield information about the response of the dam, the nature of different modes of vibration, the coupling of these modes and the nature of the input ground motion. The following are suggestions for appropriate locations of the instruments; it should be noted that these suggestions assume an ideal set of circumstances and, thus, do not consider any economic limitations.

   a) A minimum set of 4 3-component accelerographs should be located on the crest and the downstream slope. One instrument whould be placed on the midpoint or the central region of the crest, a second on the midpoint (or lower than this point) of the downstream face, and a similar set of two accelerographs should be located on any given cross section between the crest midpoint and either of the two abutments. The records from these instruments would help to identify the different modes of vibration.

   b) A set of two instruments should be placed on the right and left abutments (crest level) of the dam in order to correlate the ground motions at the two sides and to evaluate any phase differences, as well as to compare the ground motion of the sides with that on the downstream foundation.

   c) A set of at least two instruments should be located in the downstream area. This set would provide information about the input ground motion and the uniformity of ground motion underneath the dam.

All of the instruments should be situated so as to record horizontal motions in the upstream-downstream, longitudinal and vertical directions. In addition, records from the instruments should be time-tied. Continuous digital tape recording with a several-second storage buffer is highly desirable, so that each record can be recovered in its entirety from the beginning of ground motion, after simultaneous triggering. Digital recording greatly eases data analysis.

VIII. SUMMARY AND EVALUATION

This investigation presents experimental measurements involving different levels of excitation and the corresponding analyses of a full-scale modern earth dam; also, a comparison between the low-strain response during the tests and the relatively high-strain response during two earthquakes is presented.

From the considerable amount of data contained in this report and the extensive analysis of both earthquake response records, the following conclusions may be drawn:

1. Existing, low-strain, mechanical vibration generators can be used effectively in earth dam tests but should be developed further to produce much larger oscillating forces (probably up to 100,000 lbs), particularly at low frequencies (perhaps from 0.3 Hz to 2.0 Hz) in order to most successfully carry out forced vibration tests on massive earth dams.
2. Some notable improvements in the testing program, added since most of the previous earth dam tests (Refs. 4, 12, 13, 15, and 17) were made, are:
   a) Measurement of the ambient vibrations of an earth dam for the first time. The results in this investigation lead to the conclusion that ambient studies of this massive structure can be beneficial. It is recommended that ambient vibration tests should be performed on important earth and concrete dams in areas susceptible to strong earthquake events in order to estimate roughly the structures' dynamic characteristics at this low level of excitation prior to any high-level seismic event.

b) Introduction of a new testing technique for earth dams, namely the popper test, that had previously proved very efficient in testing other types of dams such as arch dams. The results obtained via this new test proved to be very informative. For its use to be effective, the reservoir level has to be relatively high.

c) Longitudinal shaking of the dam, and determination of the dynamic properties in the longitudinal direction not only from the forced vibration tests, but also from the ambient vibration tests. The data obtained have great potential for future research.

d) Measurement of the three-dimensional response of the structure and the evidence of three-dimensional modal coupling and interference.

e) Availability of usable earthquake response records for the selected dam to compare with the full-scale low-level induced response measurements.

3. Full-scale tests at levels of excitation much lower than those experienced during the earthquakes have revealed substantial changes in the dynamic properties of the dam. The behavior is typical of softening dynamic systems involving soil, which is known to be extremely nonlinear, but has rarely been examined at full scale.

4. Dynamic properties of the dam's constituent materials, such as shear moduli and damping factors, estimated from low-strain full-scale tests and determined from the relatively larger strains induced by the two earthquakes are consistent with established shear moduli-induced strain and damping-induced strain curves. The lower levels of excitation involved in the ambient, forced, and popper tests gave dynamic properties which covered the lower range of induced strains in these

curves, while the strong ground motion during the earthquakes resulted in dynamic properties covering the intermediate and higher induced strains.

The losses in stiffness due to high strains have been attributed, for the most part, to the nonlinear behavior of the dam materials. An exact determination of the causes of these nonlinearities is almost impossible due to insufficient data on the influence of the foundation, the reservoir, and the pore pressure changes. These influences are complex and difficult to analyze accurately. Finally, the variations of these dynamic properties for this specific dam have been generalized to aid in developing analytical techniques to predict accurately the low- as well as high-strain level earthquake response for most modern earth dams.

5. Values of the observed resonant frequencies from low-strain forced vibration tests vary only slightly from those determined from the also low-strain ambient vibration and oppper tests. Also, it is noted that the observed resonant frequencies in the three orthogonal directions were very closely spaced, some being almost coincident.

6. The correspondence between resonant frequencies from full-scale tests and those estimated from the spectral analysis of the two earthquake records is reasonably good over the first few frequencies, but higher modes could not be reliably matched. A comparison of these first few frequencies revealed that the natural frequencies of the dam increased significantly during the full-scale tests in all three orthogonal directions (U-D, L, and V). Clearly, the dynamic characteristics of real structures are not actually constant as implied by linear shear-beam models.

7. During upstream-downstream shaking of the dam, the shear modes indicated significant longitudinal and vertical deformations. Vertical vibrations are important because they could weaken the cohesion of the dam's materials; longitudinal vibrations are also important because they could cause transverse cracks across the axis. Thus, mathematical (i.e., analytical or finite-element) models are needed to represent the prototype realistically in both longitudinal and vertical directions.
8. Existing shear-beam theories (low levels of strain), although in reasonably good agreement with predominantly shear-like modes, do not predict all the upstream-downstream motion-type modes, indicating the inadequacy of these theories for comprehensive earthquake response (high levels of strain) computations. The nonshear upstream-downstream modes are believed to be either rocking modes or indications of upstream-downstream motion associated with longitudinal or vertical vibrations.
9. It appears that precise field tests and more theoretical analyses over a wide range of strains are required to establish the nature of the dynamic response characteristics of earth dams. Despite the complexity of several factors influencing the response of the dam, it is believed that full-scale test studies will yield the information necessary to formulate accurate mathematical models. However, it is also desirable to reassess the installation and deployment of strong motion instrumentation on dams in order to provide more valuable, reliable, and information results for interpretation of the dynamic behavior of these structures.

10. With respect to investigations on the damping characteristics of the full-scale structure, further work is also needed to better understand the energy dissipation mechanism. Meaningful results require, again, that large force levels be generated by mechanical shakers. Results of such forced vibration studies will not only identify in what manner energy is actually dissipated at different levels of excitation, but will also help in understanding the complex soil-structure interaction problem. Better foundations will be required for large shaking machines to transmit the cyclic forces more effectively to the dam, and to minimize local interaction effects. Possibly a pile foundation will be needed to provide improved coupling.
11. Finally, it is believed that the analysis and the data presented here will provide information of practical, as well as academic, significance about the dynamic characteristics of earth dams and will promote further research in this area.

ACKNOWLEDGMENTS

This research was supported by grants from the National Science Foundation and the Earthquake Engineering Research Affiliates program at the California Institute of Technology.

The authors are grateful to Kinemetrics Inc. of Pasadena, California for providing one of the vibration exciting machines and some of the recording instruments and for maintaining these instruments during the tests. The authors are also grateful to the United Water Conservation District of Ventura County, California for giving permission to make the tests on Santa Felicia Dam. The assistance provided by R. Relles in operating and maintaining the instrumentation system, in conducting the tests, and also in reducing the data is greatly appreciated. Dr. D. Ostrom of Southern California Edison took an active interest in trying the popper tests, for the first time, on an earth dam. Appreciation is expressed to all persons and agencies who have contributed to the investigation, particularly to members of Caltech (both undergraduate and graduate students), for their time and effort.

Most of the data interpretation was carried out in the Department of Materials Engineering at the University of Illinois at Chicago Circle and in the Civil Engineering Department at Princeton University. The assistance provided by both departments is greatly appreciated.

Finally, the authors are indebted to Professors George Housner and Paul Jennings who provided great assistance and valuable suggestions in performing the tests.

REFERENCES

1. Abdel-Ghaffar, A. M. and Scott, R. F., "Experimental Investigation of the Dynamic Response Characteristics of an Earth Dam," Proceedings, U.S. National Conference on Earthquake Engineering, Stanford University, Palo Alto, California, August 1979, pp.
2. Abdel-Ghaffar, A. M., and Scott, R. F., "An Investigation of the Dynamic Characteristics of an Earth Dam," Earthquake Engineering Research Laboratory. Report No. EERL 78-02, California Institute of Technology, Pasadena, California, August 1978.
3. Ambraseys, N. N., "On the Shear Response of a Two-Dimensional Wedge Subjected to an Arbitrary Disturbance," Bull. Seismological Society of America, Vol. 50, January 1960, pp. 45-56.
4. Calcialti, F., Castoldi, A., Vanelli, M., and Mazzieri, C., "In Site Tests for the Determination of the Dynamic Characteristics of Some Italian Dams," Proceedings Sixth World Conference on Earthquake Engineering, New Delhi, India, Jan. 1977, Part 9, pp. 9-119 to 9-124.
5. Chopra, A. K., Dibaj, M., Clough, R. W., Penzen, J., and Seed, H. B., "Earthquake Analysis of Earth Dams," Proceedings Fourth World Conference on Earthquake Engineering, Santiago, Chile, Jan. 1969.
6. Foutch, D. A., "A study of the Vibrational Characteristics of Two Multistory Buildings," Earthquake Engineering Research Laboratory, Report No. EERL 76-03, California Institute of Technology, Pasadena, California, Sept. 1976.
7. Hudson, D. E., "A New Vibration Exciter for Dynamic Test of Full-Scale Structures," Earthquake Engineering Research Laboratory, California Institute of Technology, Pasadena, California, 1961.

8. Hudson, D. E., "Synchronized Vibration Generators for Dynamic Tests of Full Scale Structures," Earthquake Engineering Research Laboratory, California Institute of Technology, Pasadena, California, 1972.

9. Hudson, D. E., "Resonance Testing of Full-Scale Structures, Journal of Engineering Mechanics Division, Proceedings ASCE, Vol. 90, EM3, 1964, pp. 1-19.

10. Hudson, D. E., "Dynamic Tests of Full-Scale Structures," in "Earthquake Engineering", edited by R. L. Wiegel, Englewood Cliffs, N.J.: Prentice-Hall, Inc., 1970, pp. 127-149.

11. Jennings, P. C., Matthiesen, R. B., and Hoerner, J. B., "Forced Vibration of a 22-Story Steel Frame Building," Earthquake Engineering Research Laboratory, Report EERL 71-01, California Institute of Technology, Pasadena, California, February 1971.

12. Keightley, W. O., "Vibration Tests of Structures," Earthquake Engineering Research Laboratory, California Institute of Technology, Pasadena, California, July 1963.

13. Keightley, W. O., "A Dynamic Investigation of Bouquet Canyon Dam," Earthquake Engineering Research Laboratory, California Institute Technology, Pasadena, California, Sept. 1964.

14. Keightley, W. O., "Vibrational Characteristics of an Earth Dam," Bulletin of the Seismological Society of America, Vol. 56, No. 6, Dec. 1966, pp. 1207-1226.

15. Martin, G. R., "The Response of Earth Dams to Earthquakes," Ph.D. Thesis, 1965, Civil Engineering Department, University of California, Berkeley, California.

16. Ostrom, D. K. and Kelly, T. A., "Method for Dynamic Testing of Dams," Power Division, Proceedings ASCE, Vol. 103, no. PO1, July 1977, pp. 27-36.

17. Paskalov, T. A., Petrovski, J. T, Jurukovski, D. V., and Taskovski, B. M., "Forced Vibration Full-Scale Tests on Earth-Fill and Rock-Fill Dams," Proceedings Sixth World Conference on Earthquake Engineering, New Delhi, India, Part 9, Jan. 1977, pp. 9-125 to 9-130.

18. Scott, R. F. and Abdel-Ghaffar, A. M., "Forced Vibration Tests of an Earth Dam," International Journal of Water, Power, and Dam Construction, London, England, Oct. 1978, pp. 41-45.

19. Luco, J. and Westmann, A., "Dynamic Response of Circular Footings," Journal of Eng. Mechanics Division, ASCE, Oct. 1971.

20. Chwang, A. T. and Housner, G. W., "Hydrodynamic pressures on Sloping Dams During Earthquakes. Part 1. Momentum Method," J. Fluid Mechanics (1978), Vol. 87, Part 2, pp. 335-341.

APPENDICES

Appendix A

Response Curves of Upstream-Downstream and Longitudinal Shaking

(Note: In all the figures of the Appendix, the following symbols were used:

S ≡ symmetric shear modes

AS ≡ antisymmetric shear modes

R ≡ symmetric rocking modes

AR ≡ antisymmetric rocking modes

L ≡ longitudinal modes.)

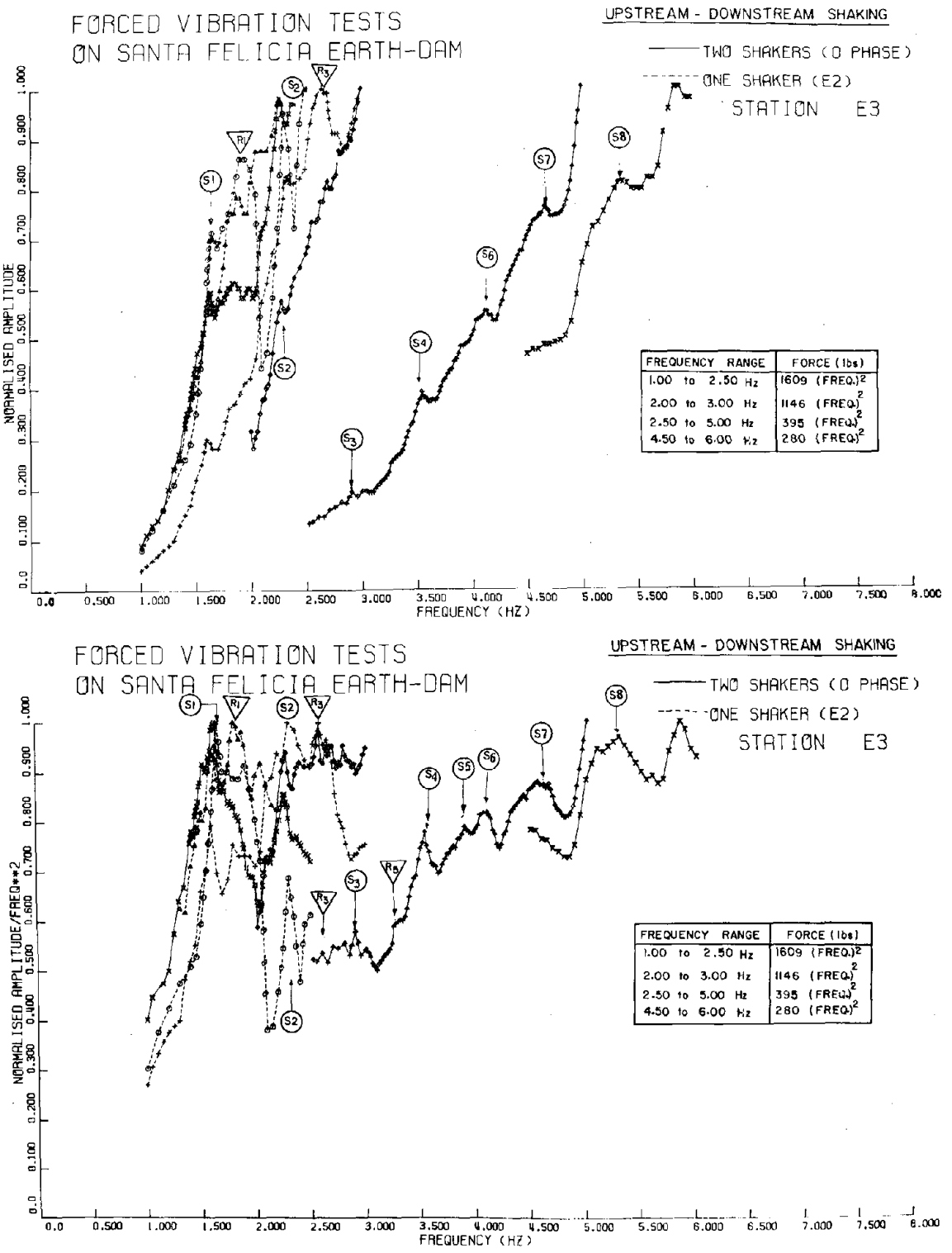

Fig. A-1. Response curves of symmetric upstream-downstream shaking (seismometer at Station E3).

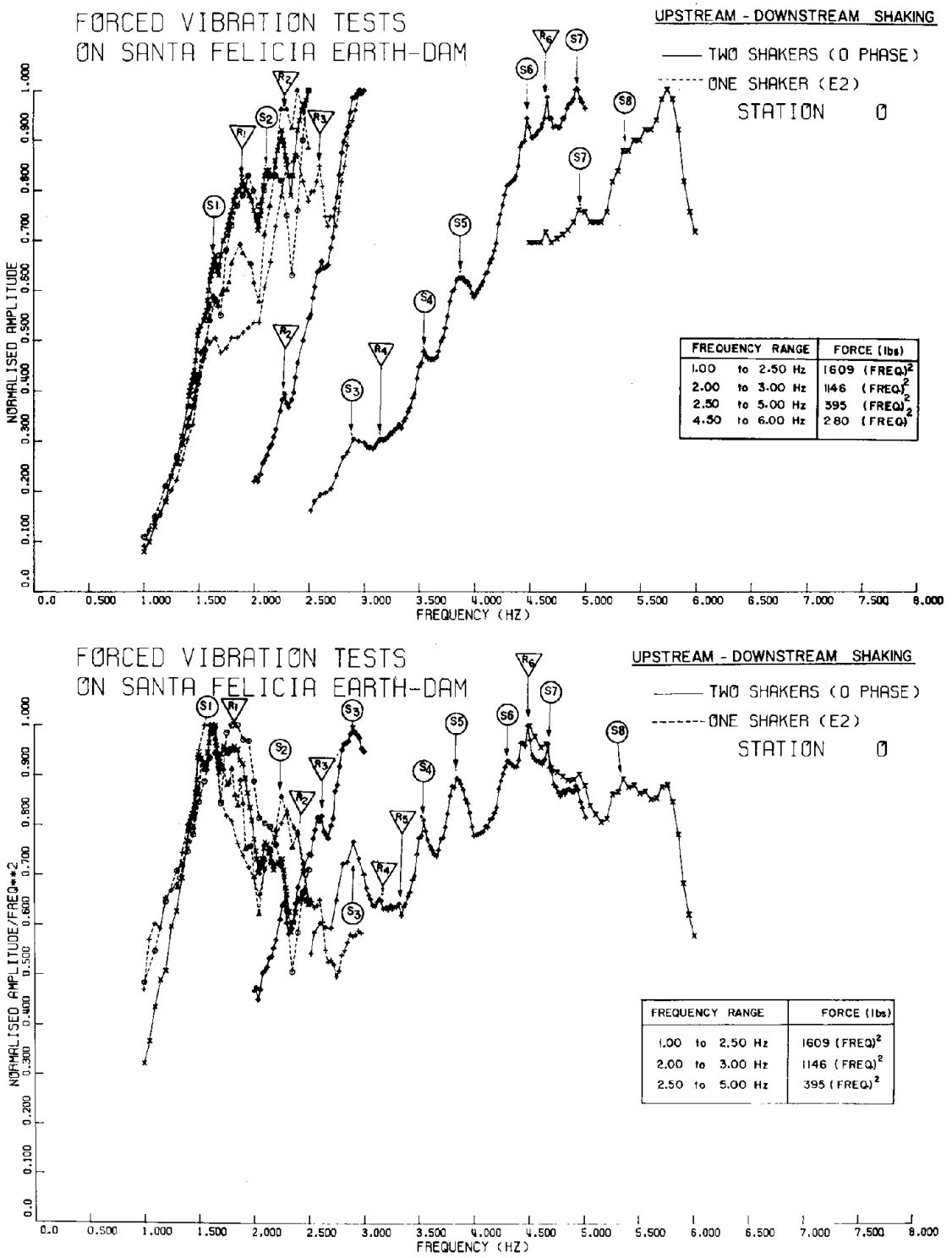

Fig. A-2. Response curves of symmetric upstream-downstream shaking (seismometer at Station 0).

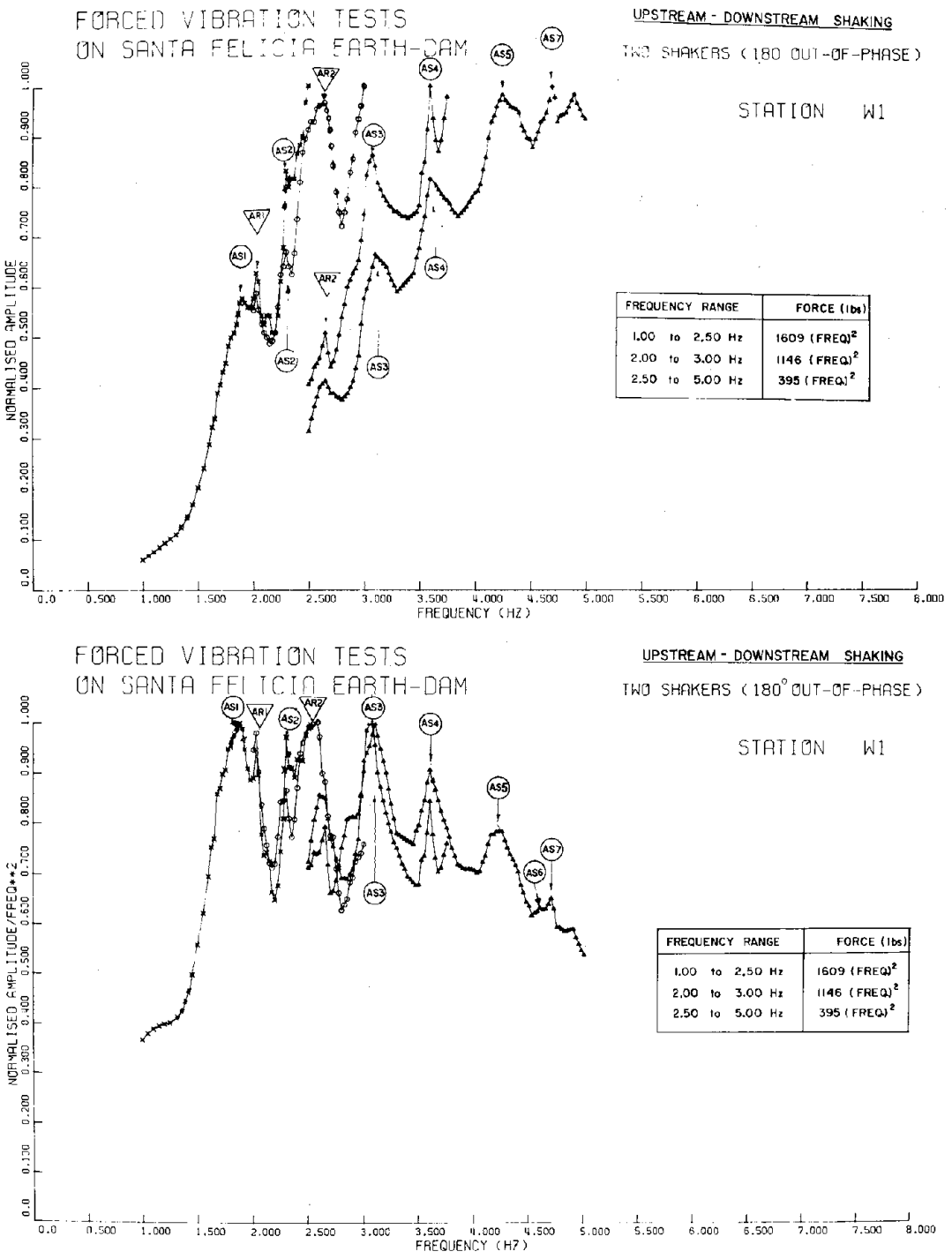

Fig. A-3. Response curves of antisymmetric upstream-downstream shaking (seismometer at Station W1).

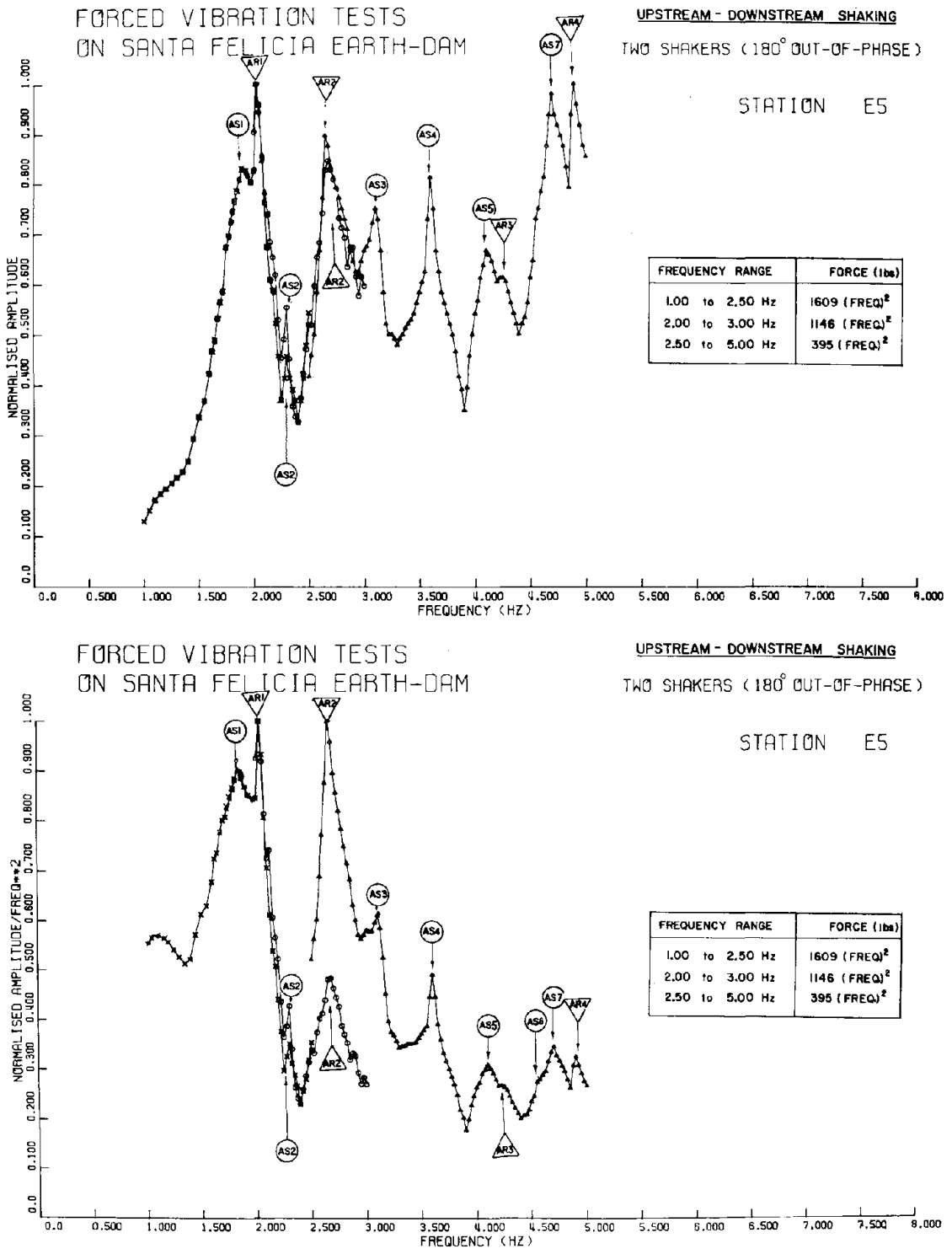

Fig. A-4. Response curves of antisymmetric upstream-downstream shaking (seismometer at Station E5).

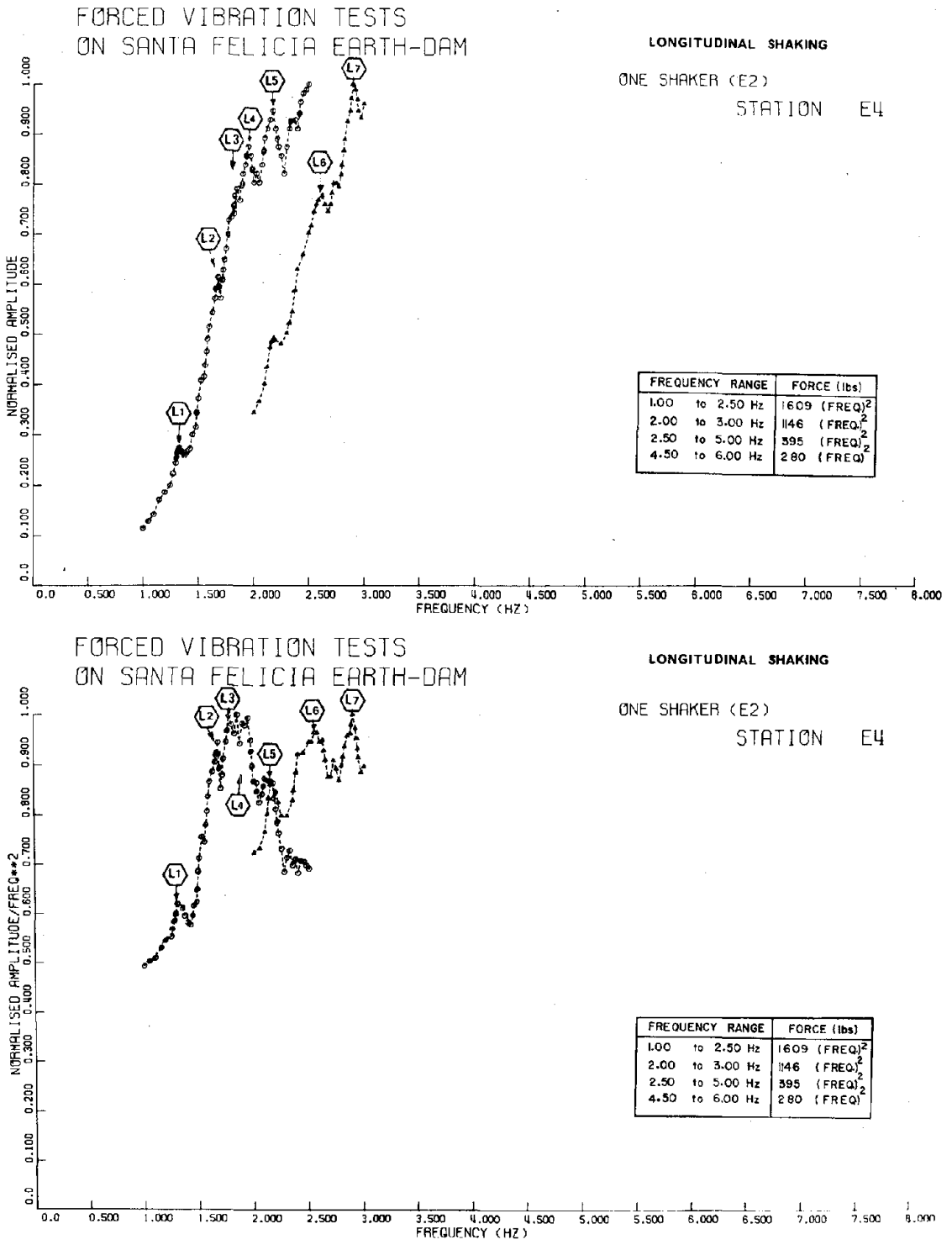

Fig. A-5. Response curves of longidutinal shaking (seismometer at Station E4).

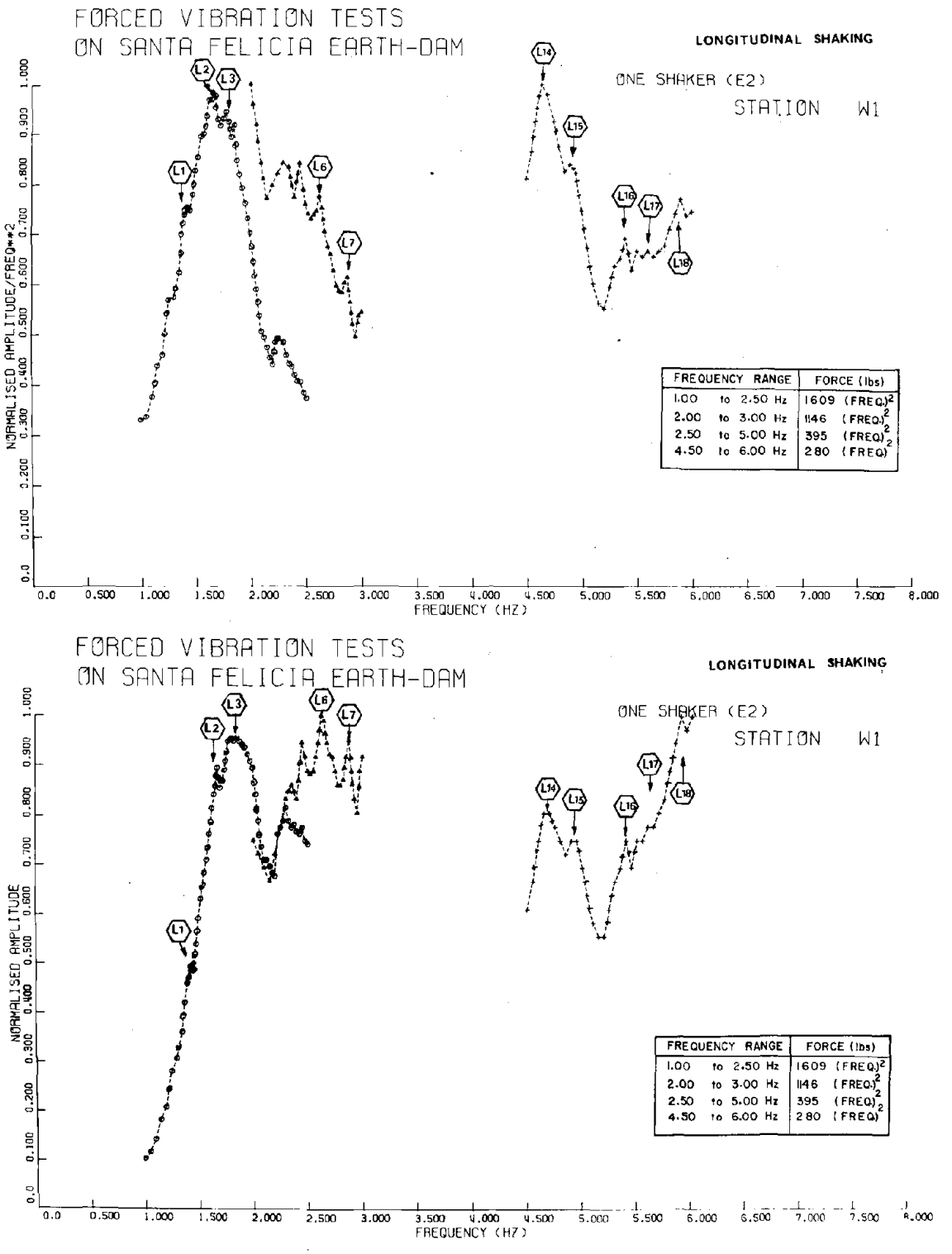

Fig. A-6. Response curves of longitudinal shaking (seismometer at Station W1).

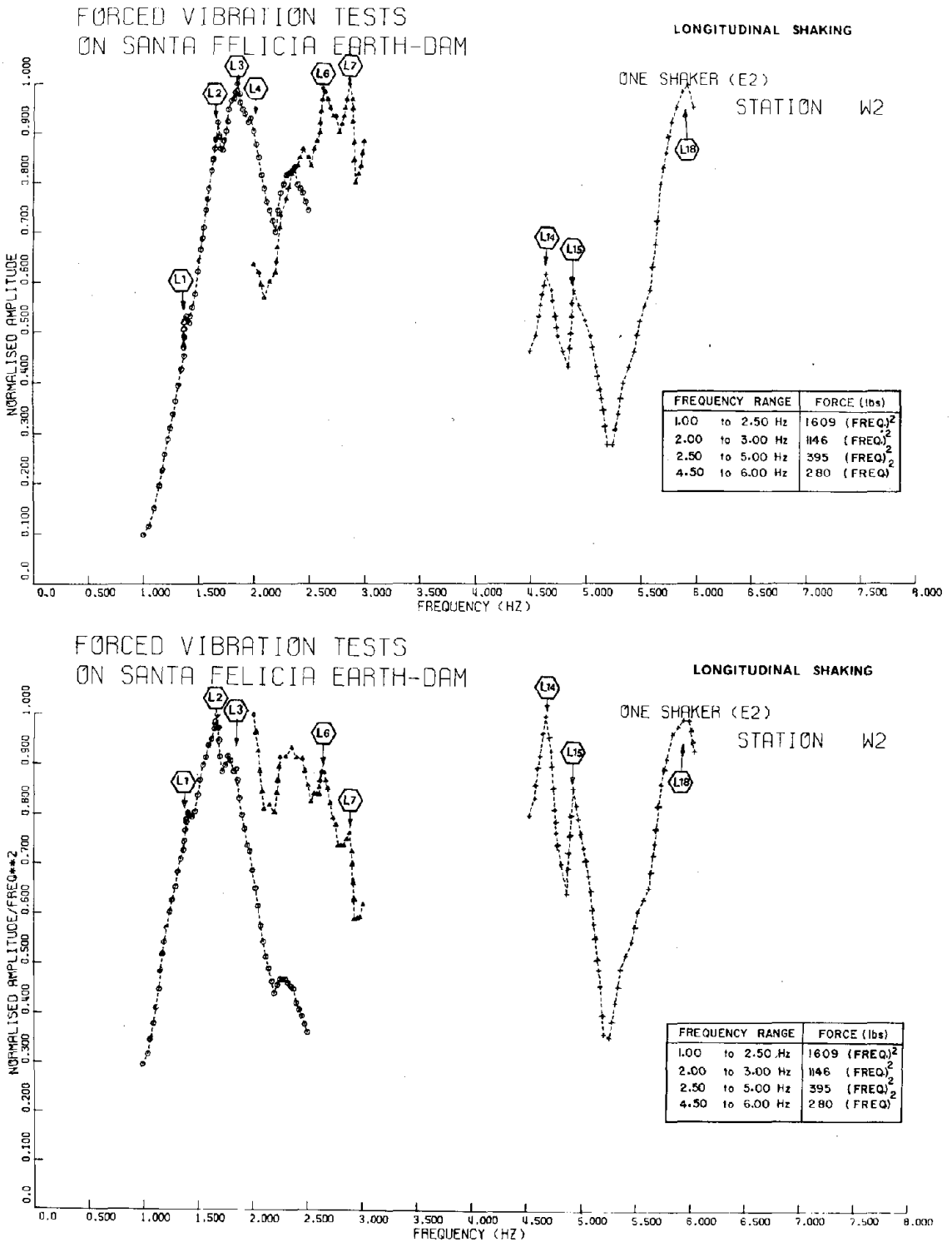

Fig. A-7. Response curves of longitudinal shaking (seismometer at Station W2).

Appendix B

Estimation of Displacements and Shear Strains Induced by Steady-State Vibration Using the 2-D Shear-Beam Theory

To make an estimate of the amplitude of the modal displacements and of the magnitude of shear strains induced during the steady-state excitation of the first symmetric shear mode, the equation of motion (using the 2-D shear-beam theory and assuming constant shear modulus) can be written as (see Fig. B-1)

$$m(y)\frac{\partial^2 u}{\partial t^2} + c\frac{\partial u}{\partial t} - \alpha G\left(y\frac{\partial^2 u}{\partial y^2} + y\frac{\partial^2 u}{\partial z^2} + \frac{\partial u}{\partial y}\right)$$

$$= P_o[\delta(y,z-\ell_1) + \delta(y,z-\ell_2)]\sin\omega_f t \qquad \text{(B-1)}$$

where $m(y)$ is the mass at a depth $y(=\rho\alpha y)$, c is the damping constant, $u(y,z,t)$ is the horizontal displacement of the dam, G is the shear modulus, α is a geometric property of the dam, P_o is the amplitude of the applied force per shaker, δ is the delta function, and ω_f is the frequency of the steady-state forced vibration.

Using the generalized coordinates and the principle of mode superposition, one can write

$$u(y,z,t) = \sum_{r=1}^{\infty}\sum_{n=1}^{\infty} \sin\frac{r\pi z}{\ell}\cdot J_o\left(\beta_n\frac{y}{h}\right)\cdot q_{n,r}(t) \qquad \text{(B-2)}$$

where $q_{n,r}(t)$ is the generalized displacement of the $(n,r)^{th}$ mode of vibration.

Substituting Eq. (B-2) in Eq. (B-1) and using the orthogonality properties of the mode shapes gives

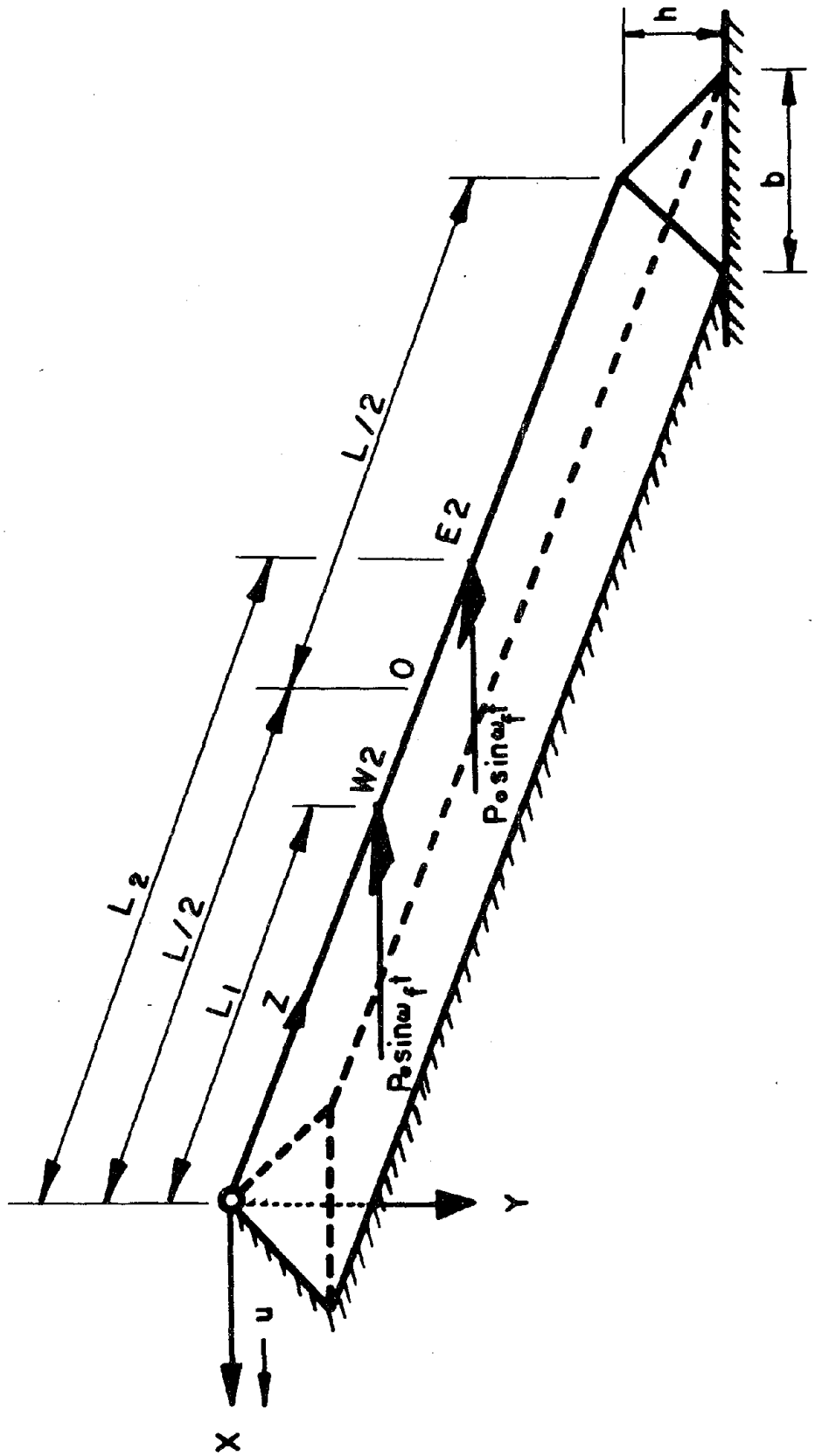

Fig. B-1. Forced vibration analysis using the 2-D shear-beam theory.

$$\ddot{q}_{n,r}(t) + 2\omega_{n,r}\,\xi_{n,r}\,\dot{q}_{n,r}(t) + \omega_{n,r}^2\,q_{n,r}(t) = \frac{P_{n,r}}{M_{n,r}}\sin\omega_f t \qquad \text{(B-3)}$$

where $M_{n,r}$ is the generalized mass in the $(n,r)^{th}$ mode; it is given by

$$M_{n,r} = \int_0^h \int_0^\ell \sin^2\frac{r\pi z}{\ell}\, J_o^2(\beta_n \frac{y}{h})\, m(y)\, dy\, dz = \frac{\alpha\rho\ell h^2}{4}\, J_1^2(\beta_n) \qquad \text{(B-4)}$$

and $\xi_{n,r}$ is the damping ratio in the $(n,r)^{th}$ mode. $P_{n,r}$ is the generalized amplitude of the applied force in the $(n,r)^{th}$ mode and is given by

$$P_{n,r} = P_o \int_0^h \int_0^\ell \phi_{n,r}(y,z)[\delta(y,z-\ell_1) + \delta(y,z-\ell_2)]\, dy\, dz$$

$$= P_o(\sin\frac{r\pi\ell_1}{\ell} + \sin\frac{r\pi\ell_2}{\ell})$$

$$= 2P_o \sin\frac{r\pi\ell_1}{\ell} \quad \text{for symmetric vibration, i.e., } r = 1,3,5 \qquad \text{(B-5)}$$

Note that $\phi_{n,r}$ is the $(n,r)^{th}$ mode shape (Eq. 2 in the text).

The steady-state response of the first symmetric shear mode at midpoint of the dam's crest is given by

$$q_{1,1}(t) = u_{1,1}(0,\frac{\ell}{2},t) = \frac{P_{1,1}}{M_{1,1}\omega_{1,1}^2}\,\frac{1}{2\xi_{1,r}}\sin(\omega_{1,1}t - \frac{\pi}{2}) \qquad \text{(B-6)}$$

where it was assumed that resonance occurs when $\omega_f = \omega_{1,1}$ and that the phase between the excitation and the response is equal to 90°.

The magnitude and distribution of shear strains in the $(n,r)^{th}$ mode, along the y-axis (Fig. B-1), are given by

$$\gamma_{n,r}(y,z,t) = \frac{\partial u_{n,r}}{\partial y} = \frac{\beta_n}{h}\, J_1(\beta_n \frac{y}{h})\, \sin\frac{r\pi z}{\ell}\, q_{n,r}(t) \qquad \text{(B-7)}$$

Therefore, multiplying numerator and denominator by $\omega_{n,r}$ (Eq. 1 in the text) and using Eq. (B-6), one can obtain

$$|\gamma_{n,r}| = \left\{ \frac{8J_1(\beta_n \frac{y}{h}) \sin(\frac{r\pi z}{\ell})}{\pi[\beta_n^2 + (\frac{r\pi h}{\ell})^2]J_1(\beta_n)} \right\} \frac{\pi\beta_n P_o \sin \frac{r\pi\ell_1}{\ell}}{hv_s^2 \rho\ell\alpha J_1(\beta_n)} \cdot \frac{1}{2\xi_{n,r}}, \quad r = 1,3,5,\cdots \tag{B-8}$$

or

$$\gamma_{n,r} = \Phi_{n,r} \frac{\pi\beta_n P_o \sin \frac{r\pi\ell_1}{\ell}}{\alpha\rho\ell h v_s^2 J_1(\beta_n)} \cdot \frac{1}{2\xi_{n,r}} \sin(\omega_{n,r}t - \psi_{n,r}) \tag{B-9}$$

where the function $\Phi_{n,r}(y,z)$ is defined through Eq. (B-8); it expresses the the modal participation and distribution of shear strain (see Ref. 2); $\psi_{n,r}$ is the phase between the excitation and the response of the $(n,r)^{th}$ mode.

The maximum shear strain associated with the first mode occurs at about 0.70 to 0.75 the depth of the dam (measured from the crest), where the value of the modal participation factor $\Phi_{1,1}$ is equal to 0.47. Therefore, the maximum shear strain associated with the first symmetric shear mode at the central region of the dam is given by

$$\gamma_{1,1}\Big|_{max} = 0.47 \frac{\pi\beta_1 P_o \sin \frac{\pi\ell_1}{\ell}}{\alpha\rho\ell h v_s^2 J_1(\beta_1)} \cdot \frac{1}{2\xi_{1,1}} \tag{B-10}$$

The following values are used in computations for Santa Felicia Dam using the 2-D shear-beam analysis:

1. Physical properties of the dam

ℓ = 912.5 ft , h = 236.5 ft

α = 4.3 , ρ = 4.03 lb.sec^{2}ft^{-4}

2. Measured quantities

$$\omega_{1,1} = 2\pi \times 1.635 = 10.273 \text{ rad/sec (which gives } v_s = 957 \text{ ft/sec)}$$

$$\xi_{1,1} = 3\%$$

$$P_o = 2{,}151 \text{ lbs/shaker (for the first symmetric mode)}$$

3. Other constants

$$\beta_1 = 2.4048$$

$$J_1(\beta_1) = 0.519$$

Now, substitution of these values in Eq. (B-4) gives

$$M_{1,1} = 5.9479 \times 10^{7} \text{ lb.sec}^2\text{ft}^{-1} \text{ (slug)}$$

Substituting the above values in Eqs. (B-6) and (B-10), the following steady-state displacement amplitude and shear strain for the first observed symmetric mode are given by

$$q_{1,1}\Big|_{max} = 114.22 \times 10^{-7} \text{ ft} = 1.370 \times 10^{-4} \text{ in} = 0.003358 \text{ mm}$$

$$\gamma_{1,1}\Big|_{max} = 0.7161 \times 10^{-5} \text{ (percent)}$$

when the dam is driven by the two shaking machines.

Appendix C

Fourier Amplitude Spectra from Ambient Vibration Tests

(Note: In all the figures of this appendix, the following symbols were used:

S ≡ symmetric shear modes

AS ≡ antisymmetric shear modes

R ≡ symmetric rocking modes

AR ≡ antisymmetric rocking modes

L ≡ longitudinal modes

V vertical modes.)

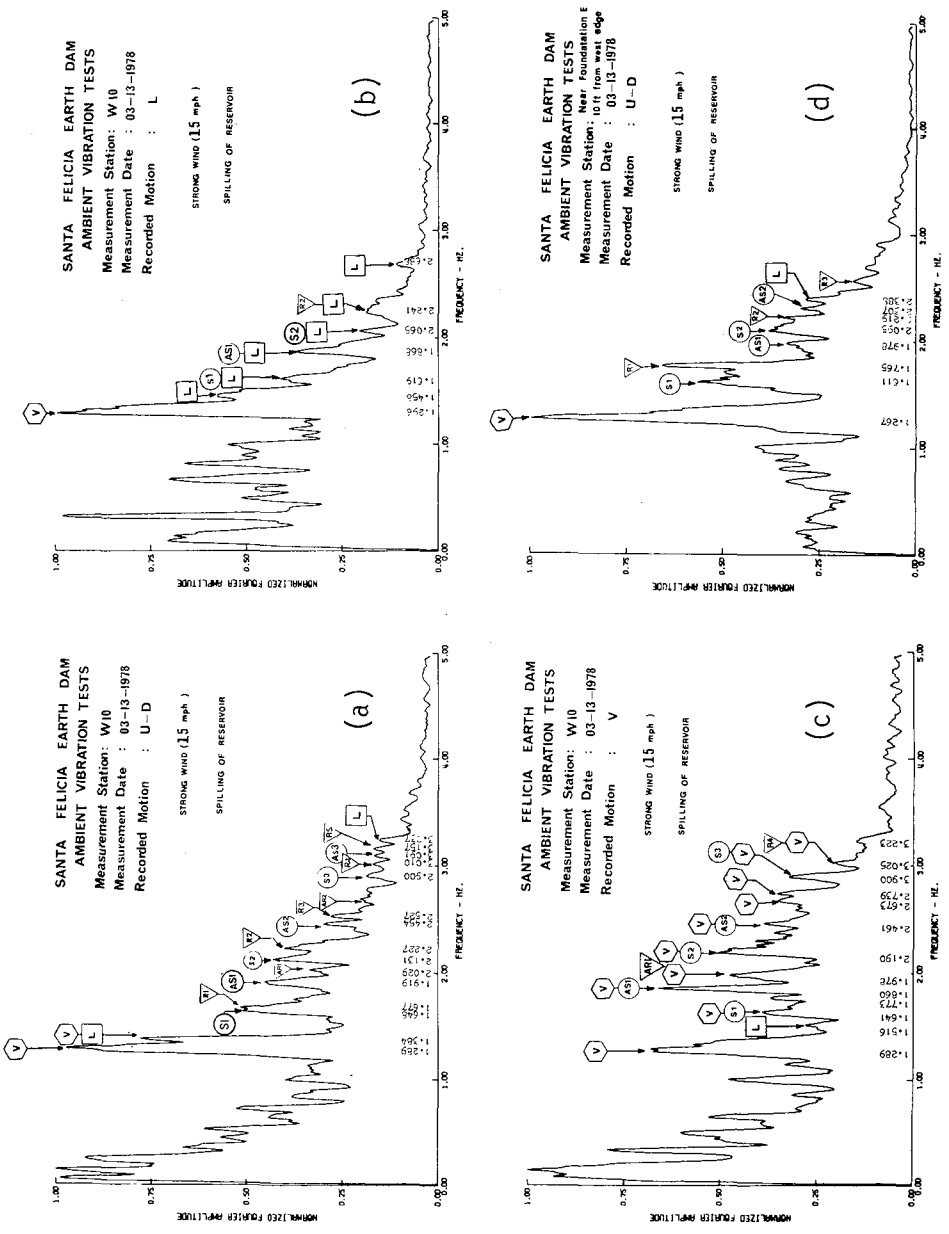

Fig. C-1. Fourier amplitude spectra of the velocity proportional response of the three orthogonal directional motions recorded, simultaneously, at Station W10 as well as the upstream-downstream motion recorded near the east foundation on the crest of the dam.

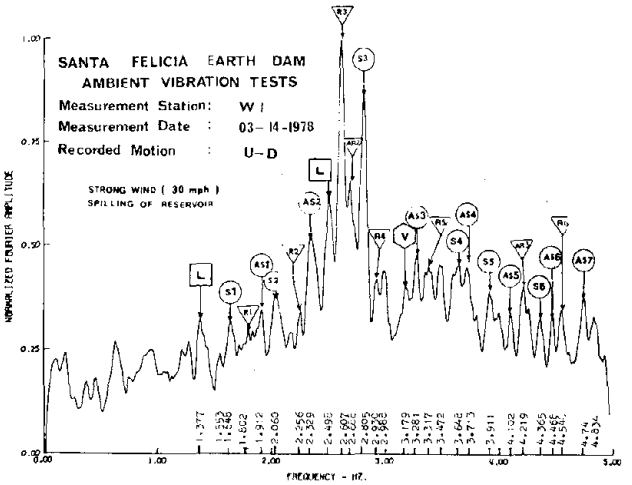

(a) Upstream-downstream direction

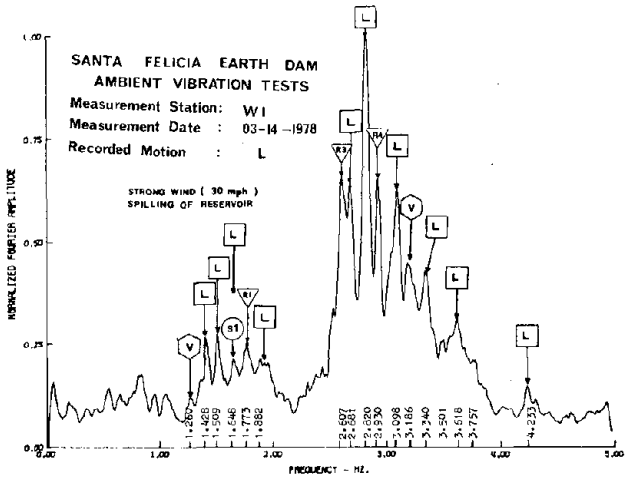

(b) Longitudinal direction

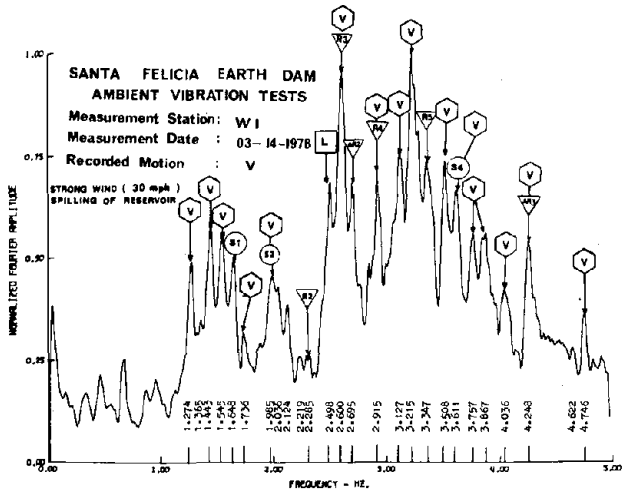

(c) Vertical direction

Fig. C-2. Fourier amplitude spectra of the velocity proportional response of the three orthogonal directional motions recorded, simultaneously, at Station W5 on the crest of the dam (5 Hz filtering).

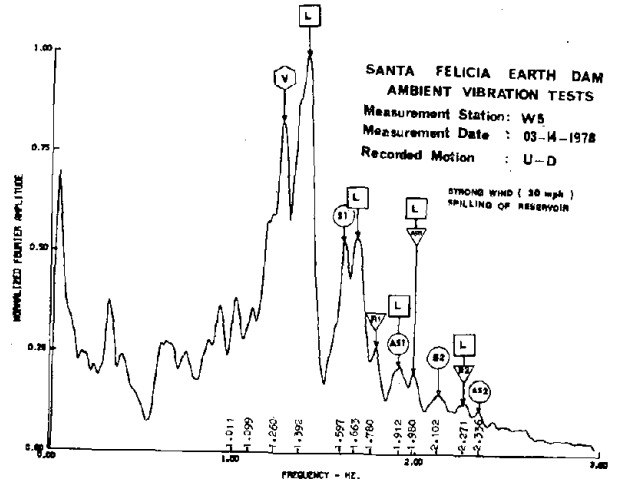

(a) Upstream-downstream direction

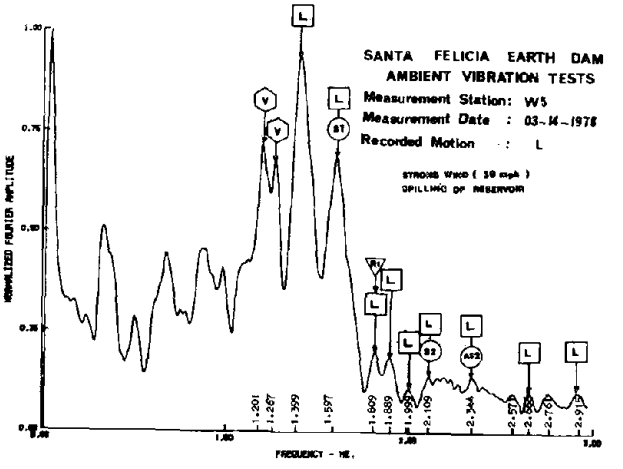

(b) Longitudinal direction

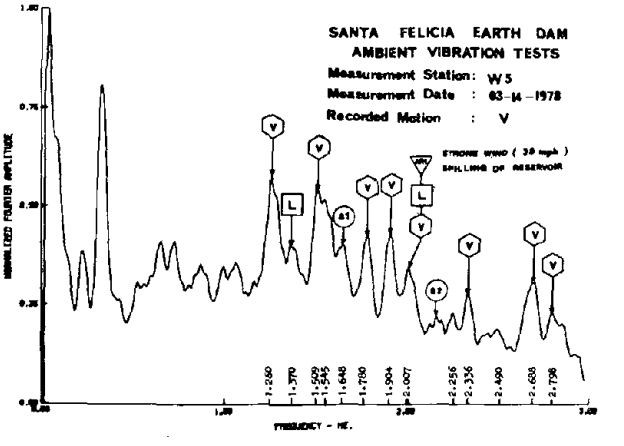

(c) Vertical direction

Fig. C-3. Fourier amplitude spectra of the velocity proportional response of the three orthogonal directional motions recorded, simultaneously, at Station W5 on the crest of the dam (3 Hz filtering).

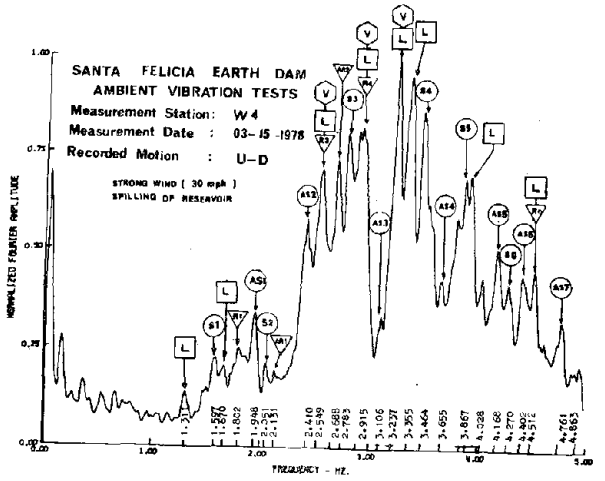

(a) Upstream-downstream direction

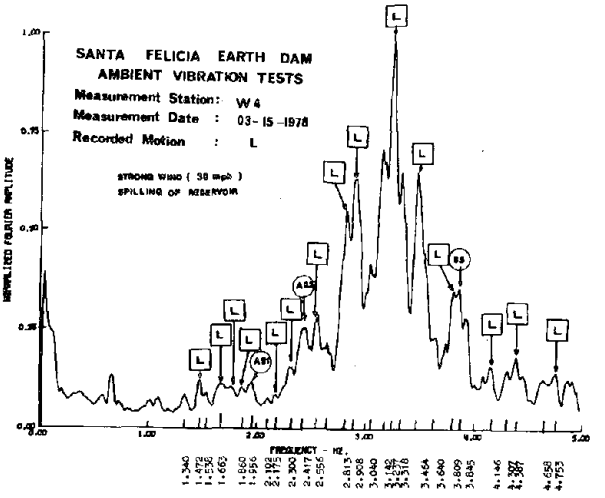

(b) Longitudinal direction

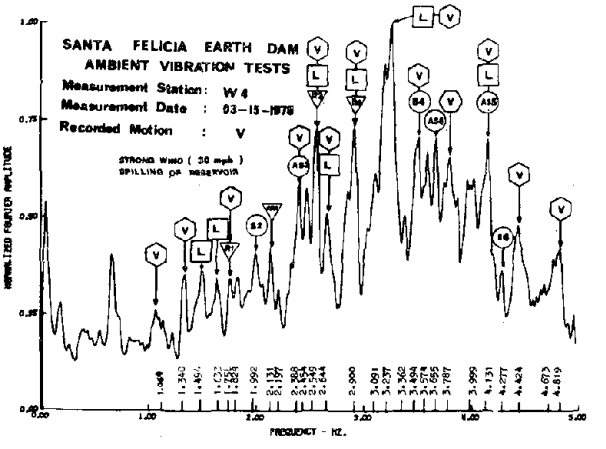

(c) Vertical direction

Fig. C-4. Fourier amplitude spectra of the velocity proportional response of the three orthogonal directional motions recorded, simultaneously, at Station W4 on the crest of the dam.

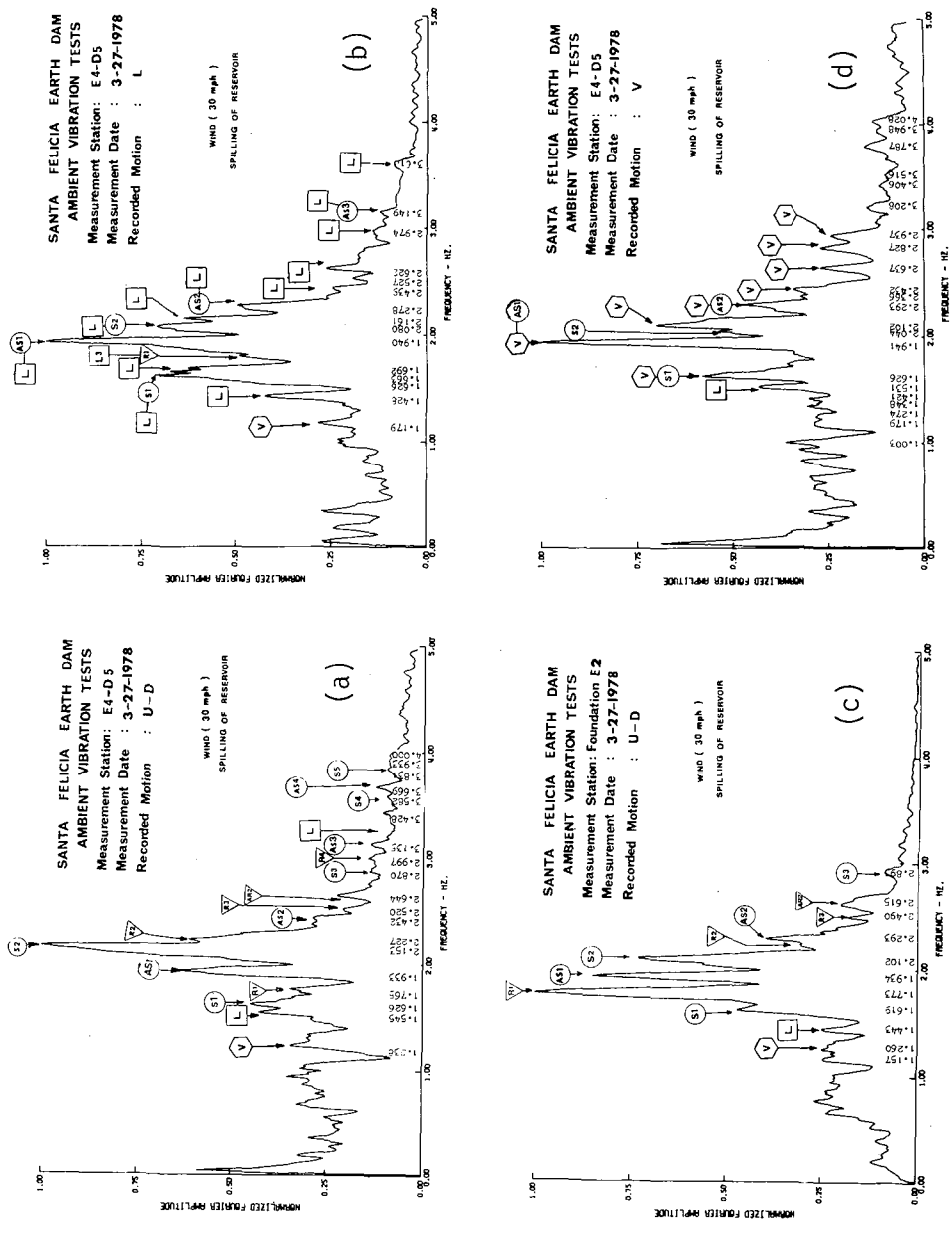

Fig. C-5. Fourier amplitude spectra of the velocity proportional response of the three orthogonal directional motions recorded, simultaneously, at Station E4-D5 (on the downstream face) as well as the upstream-downstream motion recorded at the east foundation (Station E2) on the crest of the dam.

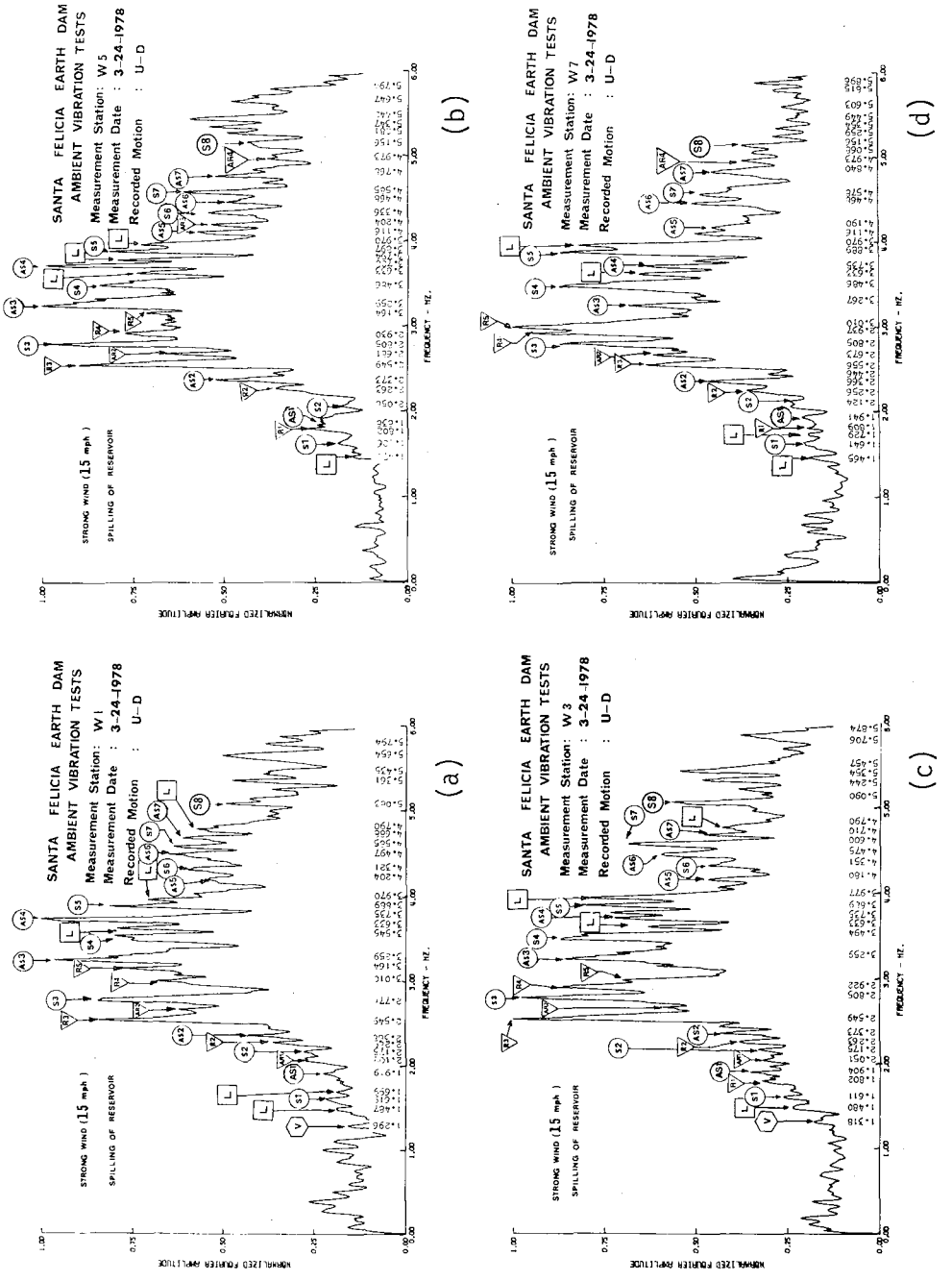

Fig. C-6. Fourier amplitude spectra of the velocity proportional response of the upstream-downstream motion recorded, simultaneously, at Stations W1, W5, W3 and W7 on the crest (6 Hz filtering).

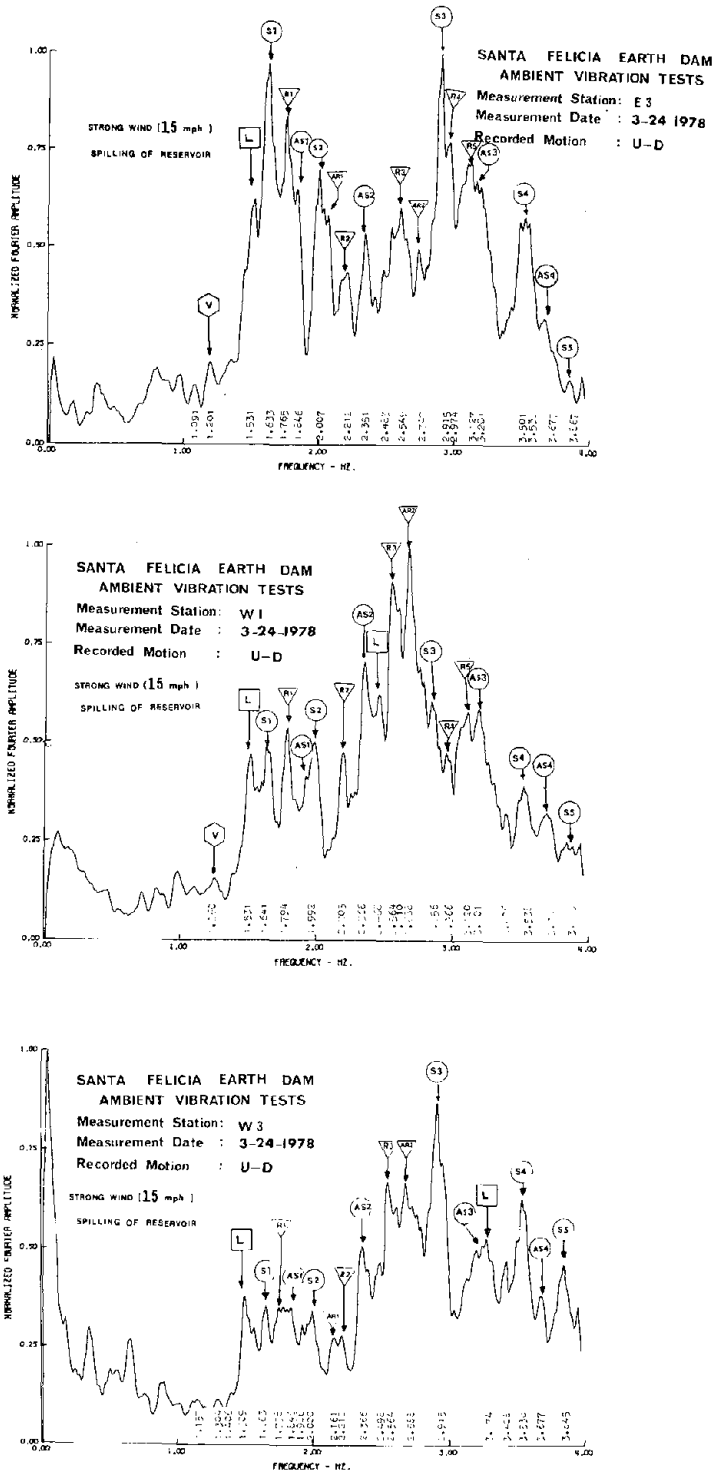

Fig. C-7. Fourier amplitude spectra of the velocity proportional response of the upstream-downstream motion recorded, simultaneously, at Stations E3, W1 and W3 on the crest (4 Hz filtering).

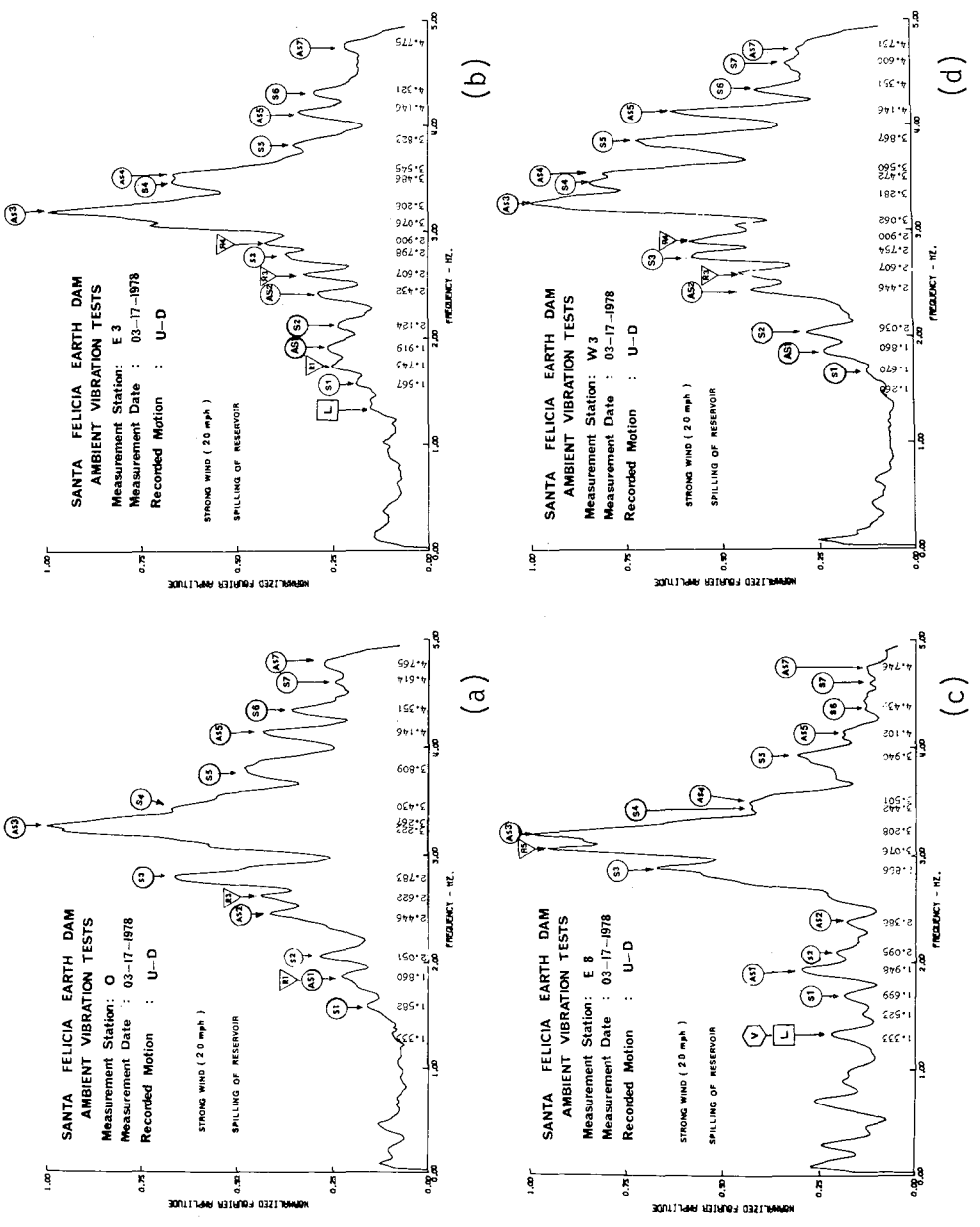

Fig. C-8. Fourier amplitude spectra of the velocity proportional response of the upstream-downstream motion recorded, simultaneously, at Stations O, E3, E8 and W3 on the crest (5 Hz filtering).

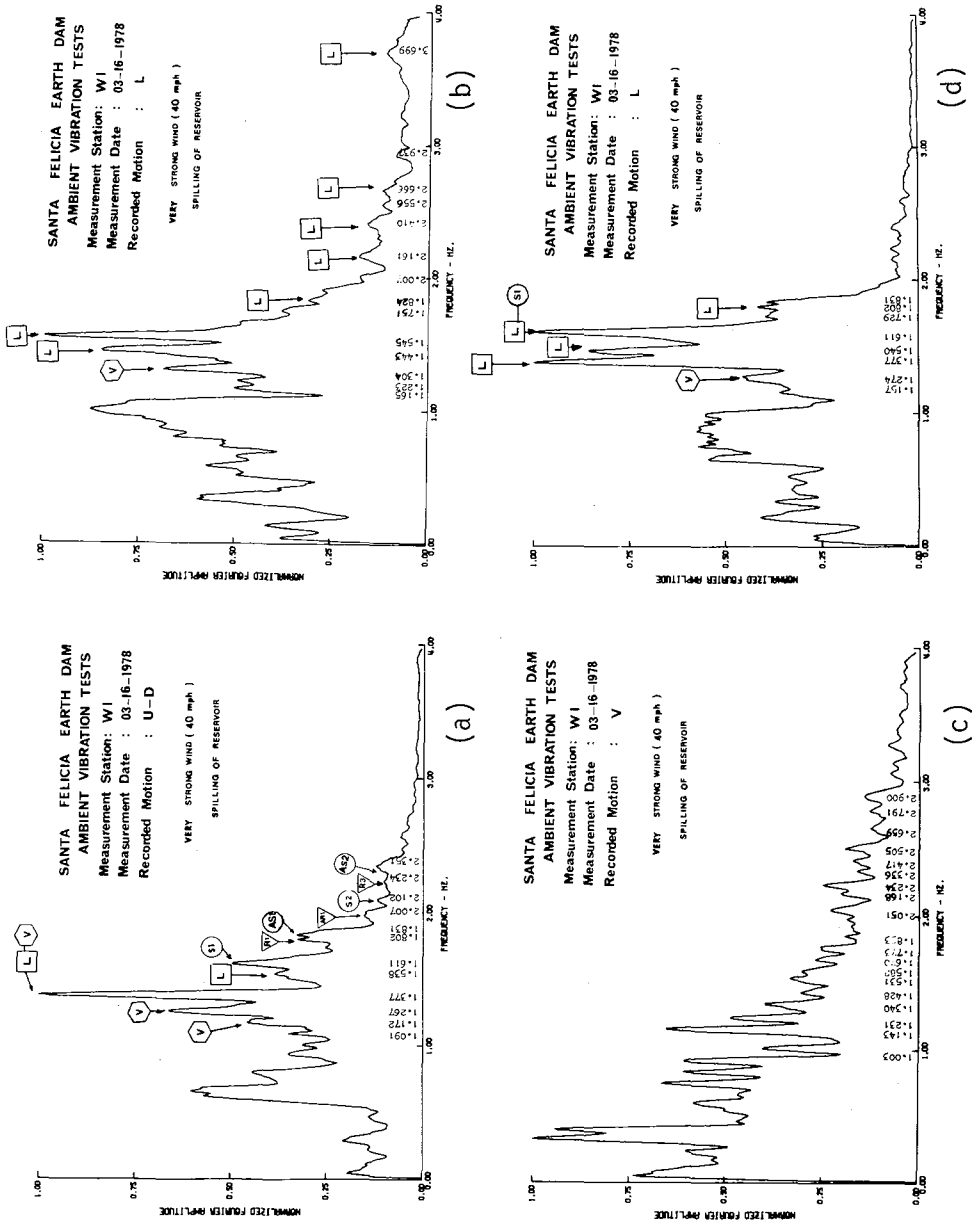

Fig. C-9. Fourier amplitude spectra of the velocity proportional response of the three orthogonal directional motions recorded, simultaneously, at Station W1. (Note: The two longitudinal motions were recorded at different hours.)